Establishing and using the new Tet system to study Parkinson's disease in mice

Dissertation with the aim of achieving a doctoral degree at the Faculty of
Mathematics, Informatics and Natural Sciences
Department of Biology
of Universität Hamburg

Submitted by
Helia Aboutalebi
Hamburg, Germany

Evaluation committee:

PD. Dr. Edgar Kramer (Supervisor)

Prof. Dr. Christian Lohr (Co-supervisor)

Date of disputation: 06 December 2016

Declaration on oath

I hereby declare, an oath, that I have written the present dissertation by my own and have not used other than acknowledged resources and aids.

Hamburg, date   06.12.2016   **signature**   Aboutalebi

Acknowledgments

The work presented in this thesis was performed in the laboratory of Dr. Edgar Kramer, at the Centre for Molecular Neurobiology Hamburg (ZMNH), Hamburg, Germany.

Table of Contents

Abstract

Parkinson's disease (PD) represents a major clinical challenge since it is the second most common neurodegenerative disease after Alzheimer's disease. PD affects primarily aging individuals which is a rapidly growing group of people in the world. The development of an efficient therapeutic treatment to prevent the PD causing loss of midbrain dopaminergic (DA) neurons and their innervations remains the biggest challenge in the field. Several gene mutations have been characterized to lead to PD such as different mutations or triplications of the gene encoding α-synuclein. Further research is needed to understand the etiology of PD and to develop a proper treatment to enhance in the long run the quality of life for people with PD. The lack of good animal models which mimic the pathology and symptoms of PD might be one reason why there is so far no treatment available to stop the progression of the disease or even to cure PD. Therefore, tetracycline-regulated transgenic mice (tet-off and tet-on system) expressing one of tetracycline-dependent transactivator -tTA or the reverse rtTA-, under the control of the tyrosine hydroxylase (TH) gene promoter have been established. Here the data about the specificity and inducibility of these different mouse lines using a transgenic and a viral reporter system has been reported. The TH-tTA and TH-rtTA mice have been successfully used to overexpress different transgenes to label and trace DA neurons and to challenge them in a PD-related manner. The TH-tTA and TH-rtTA mice turned out to be a versatile tool to introduce gene expression changes and to visualize the DA system *in vivo* and *in vitro*.

Taking advantage of the TH-tTA mice, an inducible and DA neuron specific α-synuclein transgenic PD mouse model (TH-tTA/tetO-A53T) has been established. Importantly, in these mice an age-dependent neurodegeneration of all midbrain DA neurons, spreading of α-synuclein accumulation to neighboring cells, reduced mitochondrial complex I activity and an impairment of both autophagy and Akt/mTOR signaling have been found which most likely induces the observed DA cell death phenotype. Next, overexpression of α-synuclein in DA neurons and in addition deletion of the glia cell line-derived neurotrophic factor (GDNF) receptor Ret in the same cells (TH-tTA/LC1/Retlox/tetO-A53T) has been done. These mice show a more pronounced degeneration phenotype suggesting a synergistic effect of both alterations and a neuroprotective effect of Ret in the α-synuclein overexpression scenario. This is an important finding since clinical trials using GDNF in PD patients did not so far show efficacy despite GDNF's promising neuroprotection and regeneration effect in PD

animal models. Recent data from rats with viral overexpression of α-synuclein suggested that high amounts of α-synuclein can downregulate the transcription factor Nurr1 and its target Ret and thereby might make DA neurons also in PD patients unresponsive to GDNF. Our more physiological PD mouse model supports the notion that Ret signaling also takes place under conditions of α-synuclein accumulation so that GDNF still holds promise to be beneficial also in PD patients.

Abstrakt

Parkinson-Krankheit (PD) stellt als die zweithäufigste neurodegenerative Erkrankung nach der Alzheimer-Krankheit eine große klinische Herausforderung dar. PD betrifft in erster Linie alte Personen, deren Anzahl in den nächsten Jahren auf der Erde stark zunehmen wird. Die Entwicklung einer effizienten therapeutischen Behandlung um PD Patienten vor dem Verlust an dopaminergen (DA) Neuronen im Mittelhirn und deren striatalen Innervation zu bewahren bleibt die größte Herausforderung in diesem Feld. Mehrere Genveränderungen wurden charakterisiert die zu PD führen können wie z.B. verschiedene Mutationen oder die Triplikation des Gens für α-Synuclein. Weitere Forschung ist notwendig, um die Ätiologie von PD zu verstehen und eine angemessene Behandlung zu entwickeln, die langfristig die Lebensqualität der Menschen mit PD verbessern hilft.

Der Mangel an guten Tiermodellen, die die Pathologie und Symptome von PD nachstellen ist ein Grund dafür, warum es bisher keine Behandlung von PD gibt die das Fortschreiten der Krankheit stoppt oder heilen könnte. Wir haben deshalb Tetracyclin-regulierte transgene Mäuse - Tet-Off und Tet-On-Mäuse – etabliert, die einen Tetracyclin-abhängigen Transaktivator (tTA oder reverses rtTA) jeweils unter der Kontrolle des Tyrosin-Hydroxylase (TH) Genpromotor expremieren. Hier stellen wir die Daten zur Spezifität und Induzierbarkeit dieser verschiedenen Mauslinien vor, die wir mit Hilfe von transgenen und viralen Reportersystemenermittelt haben. Die TH-tTA und TH-rtTA Mäuse wurden erfolgreich eingesetzt, um verschiedenen Transgene zu überexprimieren, um DA Neuron anzufärben und deren Axonenverlauf nachzuverfolgen sowie diese PD induzierenden Reizen auszusetzen. Die TH-tTA und TH-rtTA Mäuse erwies sich als ein vielseitiges Werkzeug, um Genexpressionveränderungen einzuführen und um das DA-System in vivo und in vitro zu visualisieren.

Unter Verwendung der TH-tTA-Mäusen haben wirein induzierbares und DA Neuron-spezifischen α-Synuklein transgenes PD Mausmodell kreiert (TH-tTA/tetO-A53T). Interessanterweise zeigen diese Mäusen eine altersabhängige Neurodegeneration derDA Mittelhirnneurone, eine Ausbreitung der α-Synuklein-Akkumulation in benachbarten Zellenn, eine reduzierte mitochondriale Komplex I-Aktivität und eine Verminderung der Autophagie und der Akt/mTOR Signaltransduktion, die höchstwahrscheinlich zusammen den beobachteten DA Zelletod induzieren. Als Nächstes haben wir α-Synuklein in DA

Neuronen überexpremiert und in den gleichen Zellen den Ret Rezeptor, den Rezeptor für den Glia cell line-derived neurotrophic factors (GDNF) herausgenommen (TH-tTA/LC1/Retlox /tetO-A53T).

Diese Mäuse zeigen einen ausgeprägteren Degenerationsphänotyp, der auf eine synergistische Wirkung beider Veränderungen und eine neuroprotektive Wirkung von Ret im α-Synuklein-Überexpression Szenario hindeutet. Dies ist eine wichtige Erkenntnis, da klinische Studien mit GDNF an PD Patienten bisher keine durchschlagende Wirkung gezeigt haben trotz der vielversprechenden neuroprotektiven und regenerativen Effekte von GDNF in verschiedenen PD Tiermodellen. Jüngste Daten von Ratten weisen darauf hin, dass virale Überexpression α-Synuklein die Expression des Transkriptionsfaktors Nurr1 und seines Zielgenes Ret herunterregulieren kann und damit möglicherweise DA Neurone von PD Patiente nicht mehr auf GDNF ansprechen. Unserphysiologischeres PD-Maus-Modell unterstützen die Ansicht, dass Ret-Signaltransduktion auch unterBedingungen stattfinden kann in denenα-Synuklein-akkumuliertwomit GDNF weiterhin ein vielversprechender Kandidate bleibt der möglicherweise auch PD Patienten helfen könnte.

1. Introduction

1.1 Dopaminergic system

In early 1960s a histofluorescence method for visualization of catecholamines and serotonin based on the exposure of freeze-dried tissue to formaldehyde vapor was developed by Falck, Hillarp and coworkers allowing converting of dopamine and noradrenaline to isoquinoline molecules that emitted yellowgreen fluorescence in the microscope (Falck *et al*., 1962; Carlsson *et al*., 1962; Anders Björklund and Dunnett, 2007). Using the newly introduced method for specific labeling of dopaminergic (DA) system has helped to study neurotransmitter system in the brain to make it one of the best known, and most completely mapped systems in the brain (Anders Björklund and Dunnett, 2007). However, the heterogeneity of DA neurons in the ventral midbrain has still not allowed a complete connectivity map and a method to precisely predict where each cell might connect to (Ungless and Grace, 2012; Lammel *et al*., 2012; Bourdy and Barrot, 2012; Jhou *et al*., 2013; Volman *et al*., 2013; Beier *et al*., 2015; Lerner *et al*., 2015; Hoglinger *et al*., 2015). The brain DA system plays a key role in the control of locomotion, working memory, learning, cognition, and emotion (Nieoullon and Coquerel, 2003; Benturquia *et al*., 2008; Rasheed and Alghasham, 2012) and involved in various neurological and mental/psychiatric disorders including schizophrenia, drug addiction and Parkinson's disease (Benturquia *et al*., 2008; Sarkar *et al*., 2010; Kramer and Liss, 2015). Hence, it is one of the most studied subjects and a major target for drug designing in the treatment of neurological diseases (Rasheed and Alghasham, 2012).

1.1.1 Physiology of the dopaminergic system

Dopamine containing neurons (dopaminergic neurons) comprise less than 1% of all neurons and are present in the ventral mesodiencephalon of the mammalian central nervous system. The reported numbers of DA neurons varies from 20,000-30,000 in the mouse to 400,000–600,000 in the human brain (left and right side together) and they are distributed from the mesencephalon to the olfactory bulb (German *et al*.,1983; Pakkenberg *et al*.,1991; Blum, 1998; Anders Björklund and Dunnett, 2007; Hegarty *et al*., 2013).

The developmental of adult midbrain DA (mDA) neurons is marked by the influence of distinct extrinsic and intrinsic factors. Extracellular signaling proteins include sonic hedgehog (Shh), fibroblast growth factor (FGF8), transforming growth factor-β (TGF-β), GFLs (GDNF), Wnt1 and Wnt5a as well as transcriptional factors such as Nurr1, Lmx1a/Lmx1b, Pitx3 and others that are involved in the specification of early progenitor cells to DA neurons (Smidt and Burbach, 2007). The first detailed study of DA neurons goes back to the early 1960s when for the first time the formaldehyde histofluorescence method was used and resulted in the identification of the two primary catecholamines (CAs): noradrenaline (NA) and dopamine (DA) (Carlsson *et al*., 1962). Soon after, the distribution of CA and serotonin-containing neurons in the rat brain was described (Dahlström *et al*., 1964) and seventeen groups of CA cells (A1–A17) and three groups of adrenaline-containing cell (C1-C3) were identified (Hökfelt *et al*., 1984). Nine major CA groups are dopaminergic cell groups distinguished by tyrosine hydroxylase (TH) staining (A8-A16 as presented schematically in sagittal view of the rat brain in Figure 1.1) (Anders Björklund and Dunnett, 2007). mDA neurons are the most prominent cell groups which are located in the retrorubral field (RRF) (A8), substantia nigra pars compacta (SNpc) (A9) and ventral tegmental area (VTA) (A10). DA neurons differ in their morphology, connectivity, molecular markers and patterns of forebrain projections. Based on mentioned features, the mDA neurons divided into a dorsal and a ventral tier (Björklund and Dunnett, 2007).

The dorsal tier is formed by cells located in the dorsal part of the VTA and SN. They are round shaped, calbindin-positive and expressing low level of DA transporter (DAT) and are innervating the matrix compartment of the ventral striatum (Figure 1.2 B and C) (Gerfen *et al*., 1987; Lynd-Balta and Haber, 1994; Bentivoglio and Morelli, 2005; Björklund and Dunnett, 2007). The ventral tier consists out of the ventral parts of the VTA and SN with angular, densely packed cells which are calbindin-negative but GIRK2 and DCC positive and expressing high level of DAT (Figure 1.2 A and C) (Gerfen *et al*., 1987; Prensa and Parent, 2001; Björklund and Dunnett, 2007). To briefly summarize the two major connections of the mDA, the mesostriatal pathway connects the ventral tier of the SN and some VTA DA neurons with the dorsal striatum and is important for the control of voluntary movement. The mesocorticolimbic pathway projects from the VTA, the dorsal tier of the SN and the RRF to the ventral striatum (including the nucleus accumbens, olfactory tubercle, septum, amygdala, habenula, hippocampus and cortex) and is involved in cognitive, rewarding/aversive and emotion-based behavior (Figure 1.3) (Kramer and Liss, 2015). The cells of the retrorubral field

innervating ventral striatal, limbic and cortical areas. Therefore, DA neurons of SNpc and VTA comprise distinct neuronal subpopulations with different physiological functions which are still not completely understood.
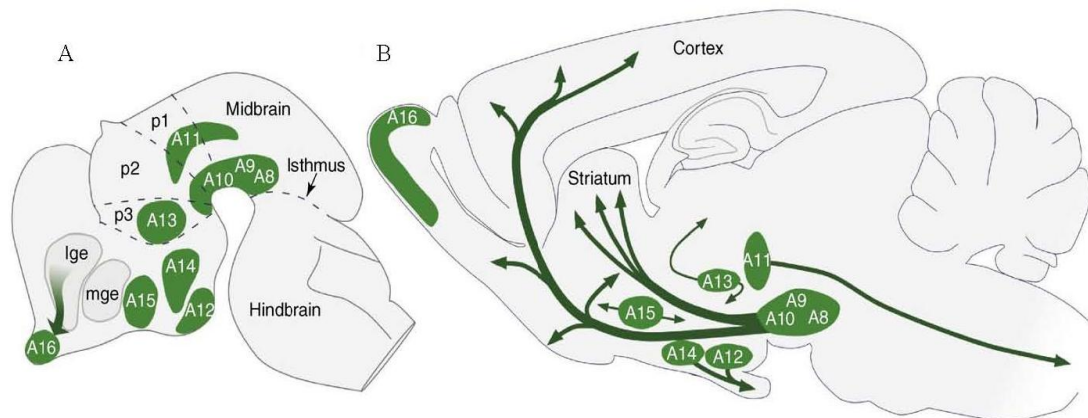
Figure 1.1 A sagittal view of distribution of nine distinctive dopaminergic neuron cell groups in the developing (A) and adult (B) rodent brain.

> The numbering of the cell groups, from A8 to A16 referred to: A8 retrorubral field , A9 substantia nigra pars compacta, A10 ventral tegmental area , A11 posterior thalamus, A12 arcuate nucleus, A13 mammillothalamic tract, A14 periventricular nucleus, A15 the preoptic area and rostral hypothalamus , A16 olfactory bulb (Björklund and Dunnett, 2007).
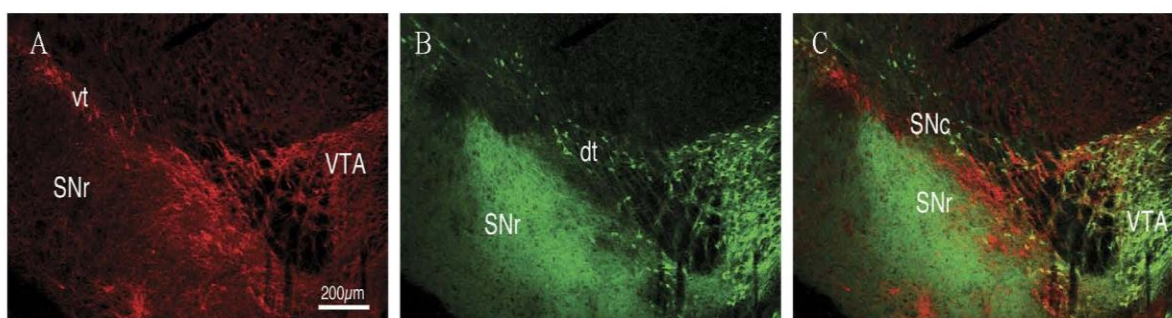
Figure 1.2 Dorsal and ventral tier dopaminergic neurons in adult rat

> The SN and VTA DA neurons in a dorsal (dt) and a ventral tier (vt), distinguished on the basis of their expression of the ion channel protein GIRK2 (red) (A and C) and calbindin (green) (B and C) (Björklund and Dunnett, 2007).
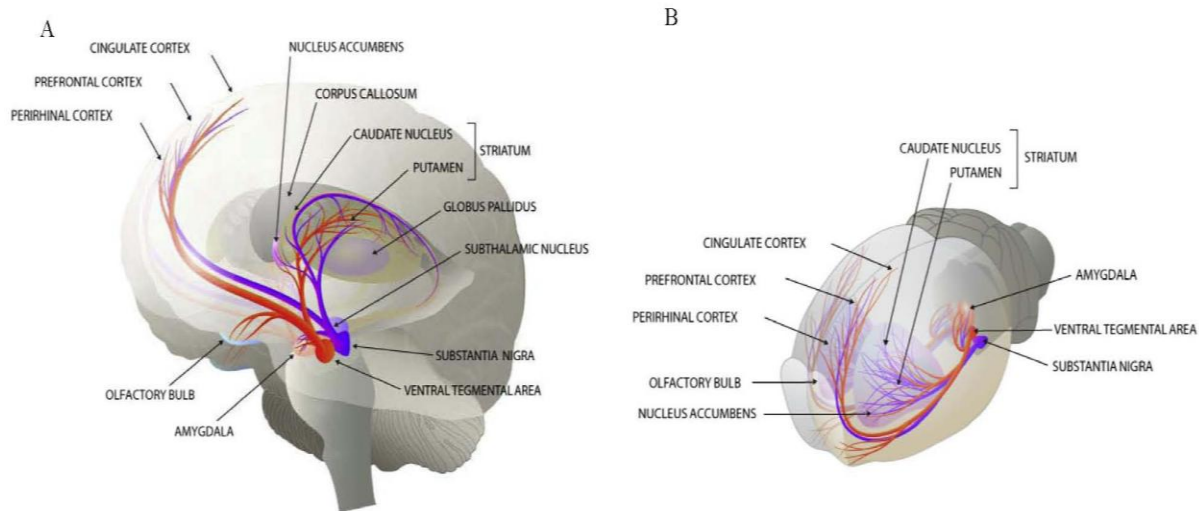
Figure 1.3 dopaminergic pathway systems

The mDA system in human brain (A) an adult mouse (B) in the sagittal view (Kramer and Liss, 2015).

1.1.2 Dopamine synthesis and TH

Dopamine (DA) is a neurotransmitter that is produced in the SN, VTA, and hypothalamus and plays multiple functions in the brain such as modulation of behavior and cognition, working memory, learning, motivation, punishment and reward, voluntary movement, inhibition of prolactin production inhibition, dreaming and sleeping, mood and attention. Therefore, DA dysfunction is involved in health and disease (Calabresi *et al*., 2007; Hugo Juárez Olguín *et al*., 2016).

There are two pathways for DA including reward and motor function. In the reward pathway, DA produces in VTA cell bodies and releases into the nucleus accumbens and prefrontal cortex (Slaney *et al*., 2013; Hugo Juárez Olguín *et al*., 2016). Differently, in the motor function pathway DA produces in SN cell bodies and releases into the striatum (Calabresi *et al*., 2007; Hugo Juárez Olguín *et al*., 2016). The biosynthesis of DA arises by action of the enzyme TH in the cytoplasm (Figure 1.4). In dopamine synthesis pathway L-tyrosine is converted to L-dihydroxyphenlyalanine (L-DOPA) by TH. L-DOPA is then converted to DA by DOPA decarboxylase which is an aromatic L-amino acid decarboxylase (AADC). DA acts as a precursor in the synthesis of other catecholamines such as norepinephrine (noradrenalin) and epinephrine (adrenalin).

Catalytic action of DA β-hydroxylase in the presence of L-ascorbic acid and molecular oxygen (O_2) results in norepinephrine synthesis which is an intermediate product to synthesis epinephrine by the enzyme phenylethanolamine N-methyltransferase with S-adenosyl-L-methionine (SAMe)(Hugo Juárez Olguín *et al*., 2016).
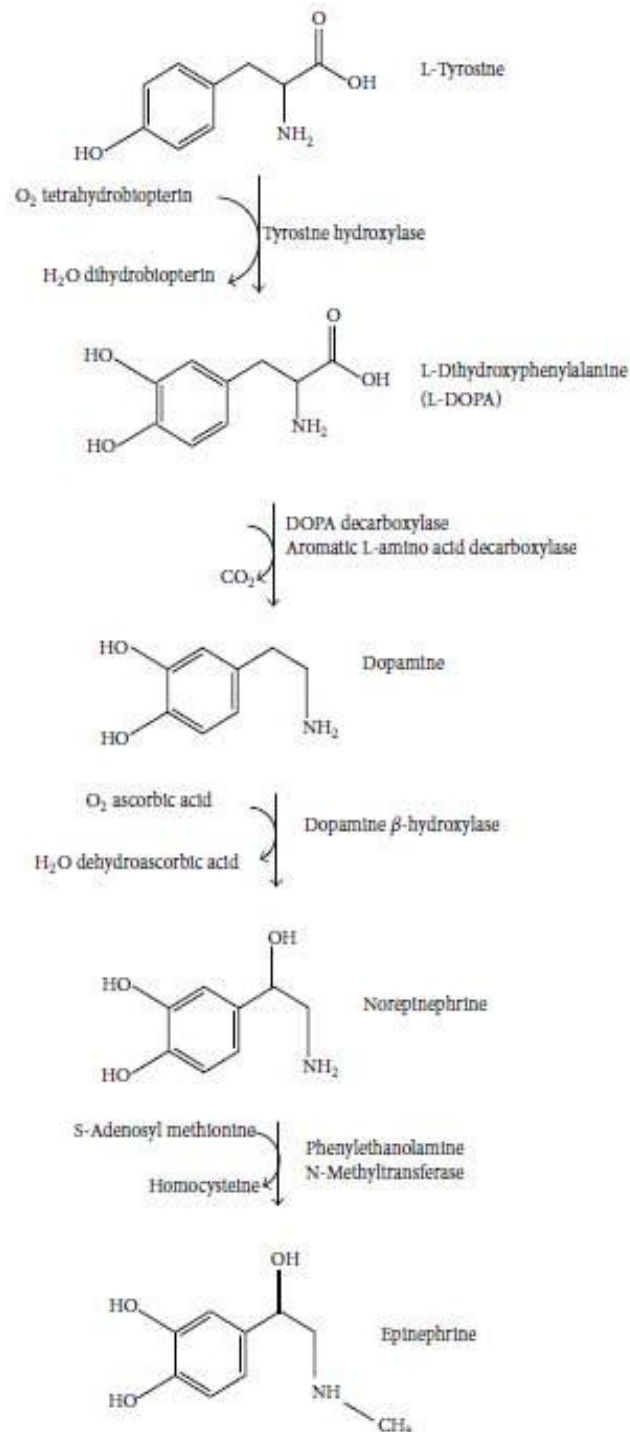
Figure 1.4 catecholamine biosynthesis

During the DA synthesis pathway L-tyrosine is converted to L-dihydroxyphenlyalanine (L-DOPA) by TH. L-DOPA is then converted to DA by DOPA decarboxylase which is an aromatic L-amino acid decarboxylase (AADC). DA acts as a precursor in the synthesis of other catecholamines such as norepinephrine and epinephrine. Catalytic action of DA β-hydroxylase in the presence of L-ascorbic acid and molecular oxygen (O_2) result in Norepinephrine synthesis which is a precursor to produce epinephrine by the enzyme phenylethanolamine N-methyltransferase with S-adenosyl-L-methionine (SAMe)(Hugo Juárez Olguín *et al*., 2016).

After the synthesis of DA, it is packaged into presynaptic vesicles by the action of vesicular monoamine transporter 2 (VMAT2) and forms DA filled vesicles which can fuse to presynaptic membrane to release DA in to the synaptic cleft in response to an action potential. The released DA binds to the postsynaptic D1R (D1 receptor subtype) and D2R (D2 receptor subtype) for further signal transduction. Unused synaptic DA is taken up again into the cytosol by presynaptic cells through the actions of either high-affinity DA transporters (DAT= a sodium-coupled symporter protein responsible for modulating the concentration of extraneuronal DA in the brain) or low-affinity plasma membrane monoamine transporters and restored in vesicles by VMAT2 (Schmitt *et al*., 2013; Chen *et al*., 2015).

Degradation of excess intracellular DA is carried out by catechol-O-methyl transferase (COMT) and two monoamine oxidase (MAO) isoforms: isoform MAO-A and MAO-B. MAO metabolizes dopamine to 3,4-dihydroxyphenylacetaldehyde (DOPAL), which is then degraded by aldehyde dehydrogenase (ALDH) to a nontoxic and diffusible metabolite 3,4-dihydroxyphenylacetic acid (DOPAC). Catechol-O-methyl-transferase (COMT) in the synapse converts the diffused DOPAC to the final end product of DA metabolism which is homovanillic acid (HVA) (Figure 1.5) (López-Pérez *et al*., 2015). Another pathway for the metabolism of DA involves the degradation of excess DA in the synapse. In this pathway DA can be converted to 3-methoxytyramine (3-MT) by COMT. The 3-MT then is reduced by MAO to corresponding aldehyde and then by ALDH to HVA and eliminated in the urine (Figure 1.5) (Hugo Juárez Olguín *et al*., 2016).
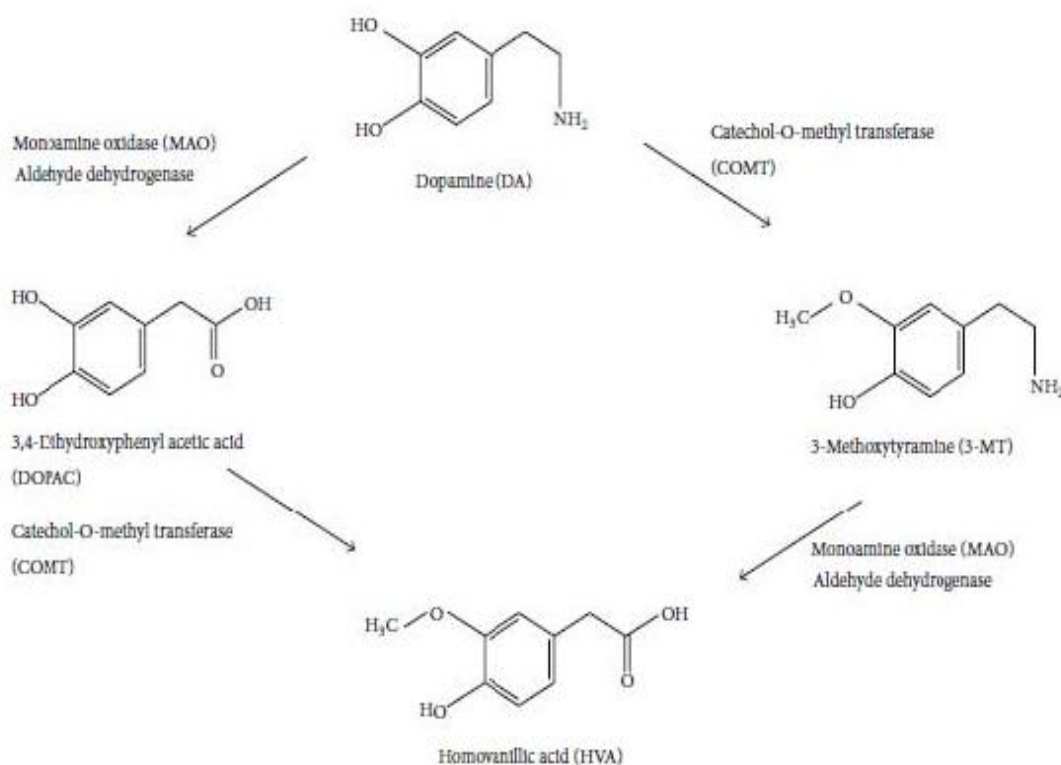
Figure 1.5 Dopamine metabolism

(Hugo Juárez Olguín *et al*., 2016)

TH is a rate-limiting enzyme that belongs to the family of aromatic amino acid hydroxylases (AAAHs). Its amino terminal ~150 amino acids make up a regulatory domain that is involved in regulating the enzyme's activity and control access of substrates to the active site. TH activity regulations include phosphorylation by multiple kinases at 4 different serine residues, and dephosphorylation by 2 phosphatases. TH modification in the presence of nitric oxide results in nitration of tyrosine residues and the glutathionylation of cysteine residues (Daubner *et al*., 2011). At E10.5 of mouse development TH expression in the brain starts (Suri *et al*., 1993) which is regulated by some transcription factors such as Nurr1 and Pitx3 (Abeliovich and Hammond, 2007). In adult mice TH protein expression becomes more restricted and is no longer detectable in some regions such as interneurons of the cortex (Satoh and Suzuki, 1990; Asmus *et al*., 2008), deeper layers of the olfactory bulb (Min *et al*., 1994), mesospiny neurons in the striatum (Masuda *et al*., 2011) and Purkinje cells of the cerebellum (Fujii *et al*., 1994) though they still continue to express TH mRNA (Baker *et al*., 2003a).

1.1.3 Dopaminergic system and neurophsychatric disorders

Dysfunction of DA pathways and DA levels play an important role in the pathogenesis of neurological and psychiatric disorders including Parkinson's disease (PD), schizophrenia (SZ), amphetamine and cocaine addiction and depressive disorders (Rasheed and Alghasham, 2012).

SZ is a mental disorder and one of the most common health problems in the world (Craenenbroeck *et al*., 2006). SZ is associated with subtle differences in brain structures which commonly occur in the frontal lobes, hippocampus and temporal lobes (Kircher *et al*., 2006), reduced function of the NMDA glutamate receptor (Konradi and Heckers, 2003), hyperactivity of DA transmission (Laruelle *et al*.,1996) and excessive activation of D2 receptors (Jones and Pilowsky, 2002). The accidental finding that phenothiazine drugs, which block DA function, could reduce psychotic symptoms of SZ, increased the attention for alterations in DA function in SZ. This hypothesis is also supported by the fact that amphetamines, which trigger the release of DA, may worsen the psychotic symptoms in schizophrenia (Laruelle *et al*., 1996). Atypical antipsychotic drugs such as clozapine and risperidone, which are antagonists of the DA receptors and block DA synaptic signaling can be used to treat the psychotic symptoms of SZ (Jones and Pilowsky, 2002; Barry *et al*., 2012).

Addiction is primarily a chronic disease of the brain reward system and occurs over time from chronically high level exposure to an addictive stimulus such as morphine or cocaine (Nestler, 2013). DA is responsible for the pleasurable feelings associated with rewards and addictive behaviors. Addiction is considered as a consequence of the continued need to elicit enhanced DA concentrations in the mesolimbic pathway (Adinoff, 2004). Substances of abuse including alcohol, caffeine, amphetamine, and cocaine increase the extracellular concentration of mesolimbic DA in reward pathway. Cocaine and amphetamines increase the DA concentration in the synapse and the time interval that DA remains at the postsynaptic receptor site (Adinoff, 2004). Using cocaine results in a DA deficit state (Dackis and Gold, 1985; Koob and Moal, 2001; Volkow *et al*., 2002), in a cocaine crash (i.e., depression) and a biological demand for more cocaine to refill the depleted DA stores (Adinoff, 2004). Attempts to treat cocaine addiction by activating DA receptors with DA agonists such as pergolide (Malcolm *et al*., 2000) or amantadine (Soares *et al*., 2001; Shoptaw *et al*., 2002) have not been successful (Stine *et al*., 1995). For the successful treatment of many addicted

individuals a variety of pharmacologic interventions according to specific relapse characteristics, genotype, and addiction severity are required (Adinoff, 2004).

1.2 Parkinson's disease

PD is a disease of the DA system. It is the second most common progressive neurodegenerative disorder at higher ages (>50) and affects approximately seven million people in the world (Yao *et al*., 2013). It is characterized by motor and non-motor symptoms. PD has been recognized since 1817 when the physician James Parkinson described it for the first time in his monograph "Essay on the Shaking Palsy" (Kempster *et al*., 2007). It is a chronic progressive neurodegenerative disorder. Sometimes it is called "paralysis agitans," because of the uncontrolled shaking often observed in older PD patients. Juvenile PD is uncommon but that can appear also in younger patients under the age of 40 (Beitz, 2014). There are also parkinsonian like syndromes such as corticobasal degeneration (CBD), dementia with Lewy bodies (DLB), progressive supranuclear palsy (PSP) and multiple system atrophy (MSA) (Beitz, 2014). In PD the amount of DA secreting cells is greatly reduced due to the cell death in the SNpc leading to a reduced innervation of the oculo-motor, associative, limbic, orbitofrontal and motor circuit which results in movement symptoms. DA acts to facilitate the release of inhibition in the basal ganglia on motor systems, thereby high levels of DA promote motor activity, whereas low levels of DA, like in PD, demand greater exertions of effort for movement (Obeso *et al*., 2008). The hypokinesia (reduction in motor output) due to the DA depletion can be compensated to some extent by application of levadopa (L-Dopa a precursor of DA synthesis), MAO-B inhibitors and DA receptor agonists to reduce dyskinesias (Heinz Reichmann, 2016). However, these drugs only can help to improve the early symptoms of the disease since these medications become ineffective with the progression of the disease and continued neuronal loss. Until now, there is no cure known for PD.

Prevalence and incidences of PD are higher for men (1.5 times more) compared to women in regard to age (Nerius *et al*., 2015). The prevalence of PD is low before age 60 and increases with age reaching a maximum at the age of 80-84 years. At higher ages between 85 and 89, the prevalence declines again (Nerius *et al*., 2015).

Around 90% increase in PD patients for Europe, USA, and Canada from 2010 to 2050 is expected in the future through ageing of the population (Bach *et al*., 2011). PD

reduces life expectancy (Louis *et al*., 1997; Hely *et al*., 1999; Elbaz *et al*., 2003; de Lau *et al*., 2005), quality of life for patients and relatives (Hobson *et al*., 1999; Schrag *et al*., 2000) and leads to substantial social and economic burdens (Whetten-Goldstein *et al*., 1997; Huse *et al*., 2005; Nerius *et al*., 2015).

1.2.1 Pathophysiology of Parkinson's disease

Degeneration or loss of the DA neurons in the SNpc and the development of Lewy bodies (LBs) and Lewy neurites (LNs) in DA neurons are pathological hallmarks of PD (MacPhee and Stewart, 2001; Beitz, 2014). Loss of DA neurons in SNpc results in marked impairment of motor control like tremor, bradykinesia, rigidity and postural instability. Cognitive changes, behavioral/neuropsychiatric changes autonomic nervous system failure, sensory and sleep disturbances are non-motor symptoms (Jain, 2011).

It might take two decades or more from the onset of PD until the first symptoms are observed (Gazewood *et al*., 2013). By the time these symptoms occur, about 60-70 percent of the neurons in the SNpc are already gone (Postuma *et al*., 2010; Jankovic *et al*., 2016; Beitz, 2014). Over the time, with progression of the disease, the latter symptoms appear (Chou, 2016) and currently there is no available therapy to slow, stop or cure the disease (Lew, 2007; Beitz, 2014).

1.2.2 Classification and genetic principles of Parkinson's disease

There are two types of PD, the sporadic/idiopathic form and the familial form (Dauer *et al*., 2003). The familial form is due to genetic causes and this accounts for only around 10% of patients with family history. The majority of PD cases are sporadic for which the causes remain unclear. But it is likely a complex interaction of environmental and genetic factors leading to the disease. For example toxins such as 1-methyl 4-phenyl 1, 2, 3, 6-tetrahydropyridine (MPTP) can induce PD (Dauer *et al*., 2003; Klein and Westenberger, 2012).

Up to now, PD genetics involved 18 chromosomal loci termed as PARK and numbered in chronological order of their identification (PARK1, PARK2, etc.). The most famous ones linked to heritable, monogenic PD are SNCA (PARK1=4) and LRRK2 (PARK8), which are responsible for autosomal dominant PD forms, and mutations in Parkin

(PARK2), PINK1 (PARK6), DJ-1 (PARK7), and ATP13A2 (PARK9) are responsible for autosomal recessive (AR) PD forms (Klein and Westenberger, 2012).

These mutations in genes encoding proteins expressed in the central nervous system play a role in DA neuronal death. The SNCA gene encodes a small protein called α-synuclein which becomes abnormal, self-aggregates and becomes a major constituent of LBs (Jankovic *et al*., 2016). In PD the ubiquitin - proteasome system responsible for breaking down proteins can also be impaired. In addition, abnormal oxidative stress through reactive oxygen species and mitochondrial dysfunction has been implicated in PD (Jankovic *et al*., 2016; Beitz, 2014).

1.3 α-synuclein and synucleinophaties

1.3.1 The structure and function of α-synuclein

α-synuclein is a small 140 amino acid protein encoded by the SNCA gene. α-synuclein can bind to negatively charged lipids such as phospholipids on the cell membrane and can form α-helical structures or under unfavorable conditions β-sheets structures. α-synuclein has three defined regions: (1) The amino terminus (residuals 1–60) which play a role in forming α-helical structures on membrane binding, (2) a NAC or non-Ab component which is the central hydrophobic region (61-95) and confers the β-sheet potential, and (3) a highly negatively charged carboxyl terminus that is prone to be unstructured (Figure 1.6) (Maroteaux and Scheller 1991; Ueda *et al*., 1993; Maroteaux *et al*., 1988; Stefanis, 2012).
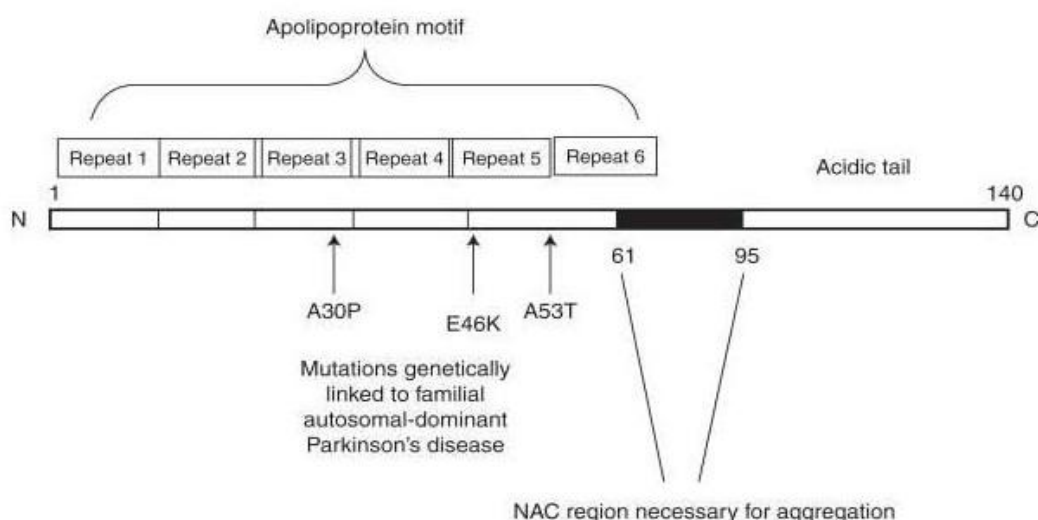
Figure 1.6. Schemtic structure of α-synuclein (Stefanis, 2012)

α-synuclein is a member of the protein family synuclein. The other two members are β-synuclein and γ-synuclein. A distinct feature of α-synuclein is the NAC region which sets it apart from the other two proteins (George, 2002; Stefanis, 2012). All synucleins are ubiquitously expressed but enriched in the central nervous system in neurons and glia cells (Maroteaux *et al*., 1988; Mori *et al*., 2002a and b). They localize in neurons under physiological conditions to the presynaptic terminals. In human brains α-synuclein comprises 1% of total cytosolic protein (Kahle, 2008). Its expression is induced during neuronal development (Withers *et al*., 1997; Kholodilov *et al*., 1999; Murphy *et al*., 2000; Rideout *et al*., 2003) and its level is modulated in conditions that alter plasticity or due to injury (George *et al*., 1995; Kholodilov *et al*., 1999; Vila *et al*., 2000; Stefanis, 2012).

Mice lacking α-synuclein showed an enhanced DA release in the striatum but not a severe neurological phenotype (Abeliovich *et al*., 2000). Consistently, triple αβγ-synuclein knockout mice showed alterations in synaptic structure and transmission, age-dependent neuronal dysfunction, as well as diminished survival (Greten-Harrison *et al*., 2010; Anwar *et al*., 2011). These data suggest a putative role of α-synuclein in regulating or mediating synaptic functions as well as DA synaptic release and homeostasis (Yavich *et al*., 2004). Moreover, α-synuclein can bind to the SNARE complex protein VAMP2 (vesicle associated membrane protein 2), thereby α-synuclein might control neurotransmitter release (Burre *et al*., 2010).

α-synuclein may also regulate or modulate many different physiological processes, but its exact function still remains unclear (Surguchov, 2008).

1.3.2 α-synucleinopathies

Under certain circumstances α-synuclein has the ability to generate β-amyloid in parallel to β-sheet structures. Wildtype and mutated α-synuclein can form amyloid-like fibrils on prolonged incubation in solution and is consequently a unified pathogenetic basis for PD (Conway *et al*., 2000). These fibrils form the basis of the mature LBs and LNs present in synucleinopathies. These forms of α-synuclein have initially soluble oligomeric, spherical, ring and string-like characteristics and gradually become insoluble and coalesce into fibrils (Emmanouilidou *et al*., 2010a; Stefanis, 2012). This mature fibrils formed by the unfolded protein termed aggregates and is a main pathogenic feature of α-synuclein and a hallmark of α-synucleinopathies including PD (Tofaris and Spillantini, 2007; Dickson, 2012). α-synuclein aggregation might be

induced by increased protein levels generated by increased expression or reduced degradation which might be due to mutations, truncation and posttranscriptional modifications (Stefanis, 2012). There are three point mutations linked to PD: A30P, E46K and A53T (Kruger *et al*., 1998; Polymeropoulos, 1997; Zarranz *et al*., 2004).

The G209A substitution mutation in the SNCA gene results in an A53T amino acid change and autosomal dominant PD. Other point mutations in SNCA, leading to A30P and E46K amino acid changes, are also associated with autosomal-dominant PD (Kruger *et al*., 1998; Zarranz *et al*., 2004).

Duplication and triplications of the SNCA locus in separate families with an autosomal-dominant inheritance pattern have also been identified (Singleton *et al*., 2003), which lead to higher protein levels (Miller *et al*., 2004).

Misfolded α-synuclein can propagate in a prion-like manner through cell to cell transmission and lead to aggregation also in previously healthy cells (Angot *et al*., 2012; Costanzo and Zurzolo, 2013; Olanow and Brundin, 2013). Other defined toxicity mechanisms of α-synuclein rather than aggregation itself might be disruption of Golgi-ER trafficking, rupture of cell membranes and DA leakage due to pore structure formation, inhibition of axonal transport and protein turnover via ubiquitin-proteasomal or chaperon-mediated autophagy system, and mitochondria dysfunction (Surguchov, 2008).

1.4 Neurotrophic GDNF-Ret system

Neurotrophic factors (NTFs) are important secreted proteins for development and maintenance of the nervous system and the most potent mediators of neuronal survival (Aron and Klein, 2011; Kramer and Liss, 2015) which regulates the number of neurons, synaptogenesis, neurite branching, adult synaptic plasticity and maturation of electrophysiological properties (Sariola and Saarma, 2003). There are four families comprising most neurotrophic factors including: (1) the glial cell-line derived neurotrophic factor family ligands (GFLs), (2) the neurotrophins (NTs) (3) the neuropoietic cytokines and (4) the CDNF/MANF family of ligands (Deister and Schmidt, 2006; Lindholm and Saarma, 2010). NTs and GFLs acts mainly through their receptor tyrosine kinases (Airaksinen and Saarma, 2002).

1.4.1 Glial cell line-derived neurotrophic factor (GDNF)

Glial cell line-derived neurotrophic factor (GDNF) - a member from GFLs - was identified as a survival factor for mDA neurons in 1993 (Lin *et al*., 1993) and subsequently as an important neurotrophic factor for spinal motoneurons (Henderson *et al*., 1994) and central noradrenergic neurons (Arenas *et al*., 1995).

Survival of mDA neurons and motoneurons is supported by GDNF and three other members of GFLs including persephin (PSPN), artemin (ARTN), and neurturin (NRTN). In particular survival of neurons and regulating the differentiation of many peripheral neurons like sympathetic, parasympathetic, sensory and enteric neurons is mediated by GDNF, NRTN and ARTN (Airaksinen *et al*., 1999; Manié *et al*., 2001; Airaksinen and Saarma, 2002). Kidney development and spermatogonial differentiation are also dependent on GDNF function (Saarma and Sariola, 1999; Airaksinen and Saarma, 2002).

GFLs have different binding affinities to glycosyl phosphatidylinositol (GPI)-linked ligand-binding subunit known as GDNF family receptor α (GFRα) including GFRα1, GFRα2, GFRα3 and GFRα4. They are the high affinity receptors for GDNF, NRTN, ARTN and PSPN, respectively. The receptor tyrosine kinase Ret (Rearranged during transfection) is the common and canonical signaling receptor for all GFLs.

Binding of GFLs to two GFRα receptors lead to a high-affinity complex which can recruit two molecules of Ret and trigger transphosphorylation of specific tyrosine residues in the intracellular domain of Ret and leading to activation of downstream intracellular signaling cascade (Figure 1.7) (Airaksinen and Saarma, 2002; Sariola and Saarma, 2003).

Additional data indicate that GDNF, GFRα1 and Ret signaling can be enhanced by heparan sulphate glycosaminoglycans (such as syndecans and glypicans) (Barnett *et al*., 2002; Tanaka *et al*., 2002) to induce axonal growth and scattering of epithelial cells (Barnett *et al*., 2002). But high concentrations of GDNF activate Ret even in cells depleted of surface heparin sulphates, thus GDNF can be locally concentrated by heparan sulphate proteoglycans at the plasma membrane (Barnett *et al*., 2002). Studies on GDNF signaling have revealed the widespread expression of GFRα proteins in many tissues and areas of the nervous system such as in the forebrain, cortex and inner ear without coexpression of Ret (Trupp *et al*., 1997; Kokaia *et al*., 1999; Ylikoski *et al*., 1999), suggesting GDNF signaling events independent of Ret. Activation of Src and Met through Ret-independent GDNF signaling might be mediated by heparin sulphate

proteoglycans and neural cell adhesion molecule (NCAM) (Sariola and Saarma, 2003), Integrins and N-cadherin (Kramer and Liss, 2015).
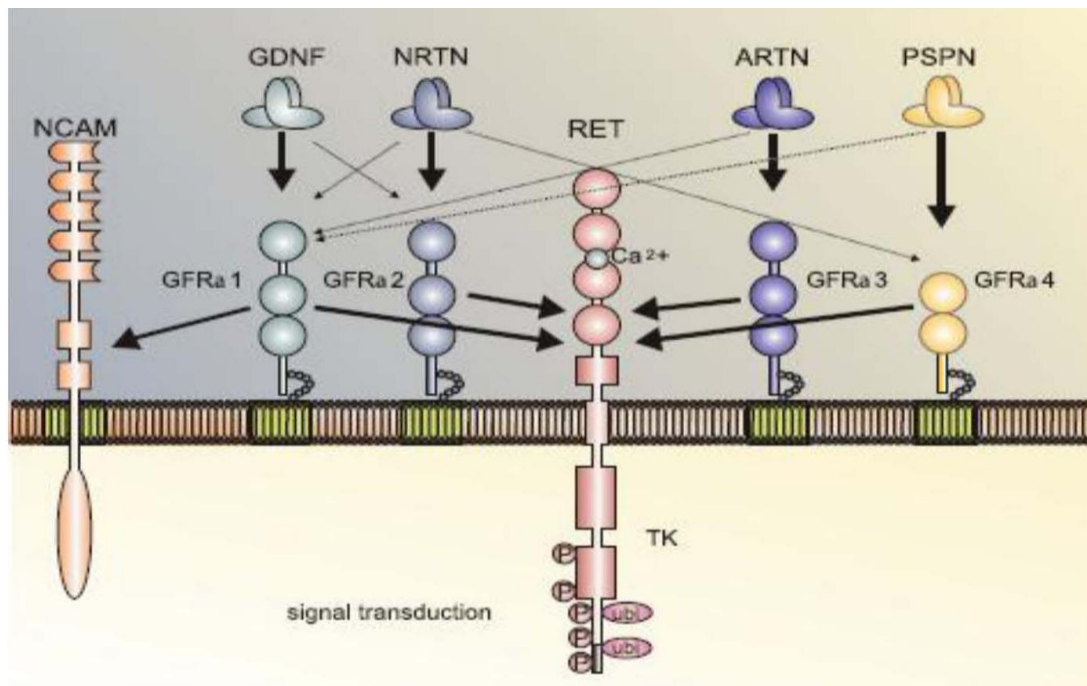
Figure 1.7 GDNF intracellular signaling

A GDNF dimer with two molecules of GFRα1 forms a complex and dimerizes with two molecules of Ret leading to transphosphorylation of their tyrosine kinase domains. All GFLs activate Ret tyrosine kinase through GFRα1-4 receptors. GDNF can also activate alternative GDNF receptors, e.g. NCAM (Kramer and Liss, 2015).

NCAM can function as an alternative signaling receptor for GDNF (Paratcha *et al*., 2003). When GFRα1 protein is present GDNF can bind with high affinity to p140NCAM and activates the Src-like kinase Fyn and focal adhesion kinase FAK in the cytoplasm (Paratcha *et al*., 2003). GDNF stimulates axonal growth in hippocampal and cortical neurons and Schwann cell migration by binding to NCAM and independent of Ret (Sariola and Saarma, 2003). The function of the alternative GDNF receptors in DA neurons is not completely understood (Kramer and Liss, 2015).

1.4.2 GDNF receptor tyrosine kinase Ret

Rearranged during transfection (Ret) is the canonical receptor for GFLs including: GDNF, PSPN, ARTN and NRTN (Sariola and Saarma, 2003; Wang, 2013). Ret belongs to the Receptor tyrosine kinases (RTKs) which is the second largest family of transmembrane receptors and important to control many cell functions such as: cell cycle, proliferation, differentiation, migration, metabolism and survival (Schlessinger, 2000; Gschwind *et al*., 2004; Lemmon and Schlessinger, 2010). The activation of Ret by GFLs is facilitated by the co-receptor GFRα (Airaksinen *et al*., 1999). The gene encoding Ret was identified in 1985 as a proto-oncogene that can be activated by DNA rearrangements (Takahashi *et al*., 1985). It was shown in mice that kidney development, spermatogenesis, and regulation of thyroid function as well as development of the sympathetic, parasympathetic and enteric nervous systems requires Ret function (Schuchardt *et al*., 1994; Durbec *et al*., 1996a; Meng *et al*., 2000; Jain *et al*., 2004). As in mice also in humans the Ret receptor is expressed in different neuron populations including central motor, dopaminergic, noradrenergic, peripheral enteric, sympathetic and sensory neurons. Outside the central nervous system (CNS) Ret is for example expressed in branching ureteric bud during embryogenesis and in differentiating spermatogenia cells (Pachnis *et al*., 1993; Meng *et al*., 2000; Wang, 2013). Ret gain and loss of function mutations are associated with different diseases (Takahashi, 2001; Santoro *et al*., 2004a; Arighi *et al*., 2005). Ret loss of function mutations in neural crest during development can lead to Hirschsprung disease (Arighi *et al*., 2005), whereas Ret gain of function mutations are associated with familial and sporadic cancer in neuroendocrine organs including papillary thyroid carcinoma, medullary thyroid carcinoma and multiple endocrine neoplasias type 2A (MEN2A) and 2B (MEN2B) (Santoro *et al*., 2004b). Increased numbers of DA neurons and more dopamine and DA innervation of the striatum has been shown in knock-in mice containing the constitutive active allele of Ret (MEN2B) (Mijatovic *et al*., 2007). Conversely, a mild progressive loss of DA neurons in the SN and their striatal innervations was observed in aged Ret knockout mice (Kramer *et al*., 2007).

The Ret protein can be divided in three domains: extracellular, intracellular and transmembrane helical region. Ret's N-terminal extracellular domain (ECD) is comprised of four cadherin-like domains (CLD1–CLD4) and a membrane-proximal cysteine-rich domain (CRD) (Anders *et al*., 2001). Ret intracellular structure consists of

a juxtamembrane domain, a tyrosine kinase domain and a C-terminal tail (Knowles *et al.*, 2006; Wang, 2013).

Several intracellular signaling cascades are activated by Ret through three pathways: (1) The MAP kinase pathway which is involved in ureteric branching during nephrogenesis (Fisher *et al.*, 2001), neurite outgrowth in the nervous system and neuronal survival (Kaplan and Miller, 2000). (2) The phosphoinositide 3-kinase (PI3K) pathway which is important for neuronal survival and neurite outgrowth (Sariola and Saarma, 2003). (3) The phospholipase Cγ (PLC-γ) pathway which modulates the intracellular level of Ca^{2+} ions by increasing the level of inositol (1, 4, 5) - trisphosphate (Sariola and Saarma, 2003).

Ret is mostly phosphorylated upon GFL binding at tyrosine residues Tyr905, Tyr1015, Tyr1062 and Tyr1096 and specifically at serine residues Ser696 after the elevation of cyclic AMP levels which is important for GDNF-induced Rac activation and lamellipodia formation (Fukuda *et al.*, 2002). Additional phosphorylated tyrosine residues are Tyr687, Tyr752, Tyr806, Tyr809, Tyr826, Tyr900, Tyr928, Tyr981 but their roles are unclear until now (Sariola and Saarma, 2003; Kramer and Liss, 2015). It has been shown *in vitro* and *in vivo* that in sympathetic neurons Ret phosphorylation levels increases with postnatal age (Sariola and Saarma, 2003).

There are three isoforms for Ret reported Ret9, Ret43 and Ret51, which differ only in their C-termini. Ret9 (The short isoform) and Ret51 (The long isoform) regulates different signaling (Tsui-Pierchala *et al.*, 2002a). Ret51, interact with the ubiquitin ligase Cbl for faster turnover and with the adaptor Crkl to produce sustained activation of Erk1 and Erk2 (R. P. Scott, PhD thesis, 2002). Nerve growth factor (NGF) increases Ret51 phosphorylation independently of either GFLs or GFRα co-receptors (Tsui-Pierchala *et al.*, 2002b).

Studies on Ret-null mutation mice showed that mice lacking the long isoform are normal, whereas mice lacking the short isoform have kidney abnormalities and enteric aganglionosis in mice. Only the Ret9 isoform can rescue the Ret knockout phenotype (de Graaf *et al.*, 2001; Sariola and Saarma, 2003).

1.4.3 Orphan nuclear receptor Nurr1

The orphan nuclear receptor Nurr1 (also known as NR4A2) is a developmental transcription factor and belongs to the family of ligand-activated transcription factors. Nurr1 function as a ligand-independent nuclear receptor while despite most other

nuclear receptors, it lacks a hydrophobic pocket for ligand binding (Wang *et al*., 2003; Baker *et al*., 2003b). Nurr1 binds as a monomer or homodimer to specific DNA binding sites or as a heterodimer with retinoid X receptor (RXR) that are robustly activated by RXR ligands, therefore, Nurr1 acts as a constitutively active transcription factor (Perlmann and Jansson., 1995). Nurr1 also enhances Ret expression (Zetterstrom *et al*., 1997; Wallen *et al*., 2001; Galleguillos *et al*., 2010).

Nurr1 is expressed in the ventral midbrain at embryonic day 10.5 in mice, exactly the day they start to express TH and AADC (aromatic amino acid carboxylase) (Decressac *et al*., 2003), hence it should be associated with DA neuron function (Smidt and Burbach, 2007). In this regard, genetic deletion of Nurr1 in newborn homozygous Nurr1-deficient (Nurr1$^{-/-}$) mice showed that development of mDA neurons is impaired and mDA neurons are absent (Zetterstrom *et al*., 1997). Importantly, DA neurons of heterozygous Nurr1-deficient (Nurr1$^{+/-}$) mice showed increased susceptibility to toxic stress conditions like exposure to the mitochondrial toxin MPTP, the drug metamphetamine and the proteasome inhibitor lactacystin (Le *et al*., 1999; Pan *et al*., 2008; Luo *et al*., 2010), as well as progressive nigrostriatal dysfunction in aged Nurr1$^{+/-}$ mice (Jiang *et al*., 2005).

Nurr1 is not only important for the development of DA neurons but also expressed postnatally which is important for maintenance of these cells. The evidence comes from studies on late developmental Nurr1 knockout mice showing loss of SN DA neuron cell bodies and reduced striatal innervations and dopamine levels (Kadkhodaei *et al*., 2009). The deletion of Nurr1 in adult DA neurons resulted in reduced DA neuron markers in the ventral midbrain and striatum and striatal dopamine with impaired motor behavior (Kadkhodaei *et al*., 2013). These data demonstrate that Nurr1 deletion in adult mice leads to early PD like phenotype.

Further studies indicate that 90% of genes encode proteins involved in oxidative phosphorylation are downregulated in Nurr1-deficient DA neurons, suggesting an important role of Nurr1 in sustaining sufficient respiratory activity in these neurons and therefore mitochondrial dysfunction as a main consequence of Nurr1 downregulation (Decressac *et al*., 2003).

Finally, Nurr1 has a role in anti-inflammatory pathway in microglia and astrocytes that protects DA neurons from inflammation induced death (Deleidi and Gasser, 2013).

1.4.4 Nurr1, Ret and GDNF in Parkinson's disease

Studies on Ret and Nurr1 conditional knockout mice revealed progressive pathological changes that are similar to early stages of PD (Kramer *et al*., 2007; Pascual *et al*., 2008; Kadkhodaei *et al*., 2013), and hence indicate the important role of the Ret-Nurr1 pathway in maintenance of nigral DA neuron integrity and their function. For GDNF the picture is more complicated since conditional GDNF knockout mice have been described to have no alterations to a dramatic loss of mDA neurons during adulthood (Pascual *et al*., 2008; Kopra *et al*., 2015). However, in animal models of PD GDNF has been shown to provide a neuroprotective effect (Kramer and Liss, 2015). GDNF provides a neuroprotective effect against 6-hydroxydopamine (6-OHDA) and 1-methyl-4-phenylpyridinium (MPP$^+$) toxicity in neuronal cell cultures (Lin *et al*., 1993; Hou *et al*., 1996; Eggert *et al*., 1999) and in toxin-based rodent and primate models of PD (Sauer *et al*., 1995; Tomac *et al*., 1995; Gash *et al*., 1996; Choi-Lundberg *et al*., 1997; Kirik *et al*., 2000a; Grondin *et al*., 2002). Based on the beneficial effect of GDNF on the DA system in cell culture and animal experiments, GDNF was test in clinical trials on PD patients. GDNF was either injected into the cerebroventricular system, or into the putamen (Gill *et al*., 2003; Nutt *et al*., 2003; Lang *et al*., 2006) in patients with advanced PD. In the beginning GDNF was provided as purified protein and later trials also used GDNF encoded in an adeno-associated virus (AAV) (Marks *et al*., 2010; Bartus *et al*., 2011). Besides GDNF also another member of the GDNF family, NRTN, has been tested.

However, so far all these human trials did not showing efficacy of GDNF family members in PD patients (Domanskyi *et al*., 2015). Some patients have shown a positive response and elevated DA activity at the site of injection (Tan *et al*., 2003) and in one single case elevated TH immunoreactivity (Gill *et al*., 2003). However, other patients fail to respond to GDNF therapy and in some cases the placebo effect in the controls was as strong as the GDNF effect. Technical issues might be considered as an explanation such as low biological activity of the used proteins, inefficient delivery of the protein to the target issue, and too advanced PD patients with too few DA cells left on which GDNF family members can act. Physiological issues might also be considered and are pushed forward mainly by the laboratory of Anders Björklund at Lund University, Sweden, as an explanation why GDNF therapy of PD patients might not be able to work. They show in a rat PD model that viral overexpression of GDNF in the SN or in the striatum was not protective against viral overexpression of human wildtype

α-synuclein in the SN (Lo Bianco *et al*., 2004; Decressac *et al*., 2011, Decressac *et al*., 2012). In this model, Nurr1 and its downstream target Ret, were found to be transcriptionally downregulated by α-synuclein accumulation. Overexpression of Nurr1 prevented the α-synuclein overexpression-induced neurodegeneration and the downregulation of the Ret protein levels. GDNF induced survival response in mDA neurons (Decressac *et al*., 2012). How far these data are relevant under more physiological conditions in PD patients is not completely clear since so far no (Hofer and Harry, 2011) or only mild (Decressac *et al*., 2012) reductions of Ret mRNA and protein levels were found in the SN of PD patients (Kramer and Liss, 2015), although downregulation of Nurr1 in DA neurons has been described to be associated with the intracellular pathology in both synucleinopathies and tauopathies (Chu *et al*., 2006). Lin and colleagues show in a transgenic mouse model overexpressing the A53T mutant form of α-synuclein in DA neurons under the control of a PITX3 locus driven tet-system that already the presence of the transgenic constructs (with and without DOX) leads to a reduction of TH, DAT, Nurr1 and Ret protein levels in one month old mice and a DA neurodegneratation phenotype and that at two weeks of age Nurr1 mRNA levels were not altered, although TH, DAT, Ret and VMAT2 mRNA levels were already significantly reduced (Lin *et al*., 2012). This paper only partially supports the direct link between α-synuclein accumulation and reduced Nurr1 and Ret expression, and more observations are needed to clarify this issue. Taken together, it remains an open question how far α-synuclein, Nurr1 and GDNF/Ret signaling are influencing each other and how far the therapeutic treatment of PD patients with GDNF family members can be successfully achieved.

1.5 Tet-system

Gene activation and inactivation has been achieved in different cell types in animals using the bacterially-derived tet-controlled inducible systems (Gossen and Bujard, 1992; Gossen *et al*., 1995; Gossen and Bujard, 2002). Tet promoters (tet-off) are activated by the tetracycline transactivator (tTA) (Gossen and Bujard, 1992) and inactivated by tetracycline or its derivatives such as doxycycline (DOX). The reverse tetracycline transactivator (rtTA) in tet-on system is a complementary genetic model for rapid gene activation by addition of DOX (Zhu *et al*., 2007). Switching gene expression ''on'' and ''off'' using tet-systems is of extreme importance in understanding the function of genes especially in the adult nervous system (Zhu *et al*., 2007).

The tet system is commonly used for expression of recombinant genes and is derived from the Tn10 tetracycline-resistance operon in E.coli (Gossen and Bujard, 1992). The fusion of this tet repressor (Tn10-derived E. coli tetR) with the carboxy-terminal activating domain of virion protein 16 of herpes simplex virus has generated a tTA which binds specifically to tet operator sequences (tetO) in the promoter of the resistance gene tetA that can be regulated by tetracycline or its more stable derivate DOX (Gossen and Bujard, 1992). In many tet-off systems there are seven copies of tetO sequences with a human cytomegalovirus hCMV promoter called tetracycline response element (TRE). Naming of TRE is due to the responding of binding the tetracycline transactivator protein tTA by increased expression of the gene or genes downstream of its promoter. In the presence of tetracycline or DOX in the tet-off system expression of TRE-controlled genes can be repressed because tTA cannot bind to TRE. A reverse functioning tet-system in the opposite fashion of response to DOX (rtTA) has been stablished that is active with DOX, and rtTA can bind to tetO and expression is induced (Gossen *et al*., 1995). The tet-on system shows faster responsiveness compared to tet-off, and is therefore, preferable for some special studies. To optimize the tet-off and tet-on systems, TRE and tTA and rtTA proteins were subjected to several modifications (Baron *et al*., 1997; Urlinger *et al*., 2000; Zhou *et al*., 2006; Loew *et al*., 2010). To control gene expression and deletion, the tet-system can be combined with the Cre-lox system (Schoenig, 2002) and might be a good system to manipulate genes to study PD after their developmental roles have been fulfilled.

1.5.1 Using tet-system to study Parkinson's disease

Although PD does not naturally develop in any animals, the development and use of PD animal models has increased our knowledge about the pathogenesis of PD. The first animal models were established with toxins that inhibit mitochondrial function and create reactive oxygen species leading to nigrostriatal DA lesions such as 6-OHDA, MPTP, paraquat or rotenone (Greenamyre *et al*., 2003; Bov´e *et al*., 2005; Fornai *et al*., 2005; Terzioglu and Galter, 2008). Although these toxins can lead to behavioral alterations in animals, they do not recapitulate all clinical symptoms and pathologies observed in human PD patients (Terzioglu and Galter, 2008). While these models are used to find out the etiology of PD and to test the efficacy of therapeutic agents, the results coming from these toxin models so far did not translate successfully in clinical trials. This is most likely because of their acute nature which is completely different

from the insidious progression of PD observed in patients (Waldmeier *et al*., 2006; Lane and Dunnett, 2008). A good model to study PD should present different specific aspects of the disease including: (1) specific and age dependent neurodegeneration of SN DA neurons, (2) development of protein aggregations (LBs and LNs), and (3) physiological changes including reduced dopamine levels and motor behavioral alterations. To address this issue, animal models were generated carrying one or several genetic mutations found in PD patients. The mouse as a model system of PD has the advantage of established genetic manipulation techniques and a strong genetic, anatomical and physiological similarity to humans. Like in humans also in mice more than 60% of DA neurons and 80% of the striatal innervation have to be lost before motor symptoms appear (Cheng *et al*., 2010). But the short life span of mice of maximal three years and some physiological differences in the DA systems, such as the lack of neuromelanine, might still generate some limitations in modeling PD in mice.

Recently, transgenic mouse models expressing mutated α-synuclein (A30P and /or A53T) under the control of the TH promoter in CA neurons have been developed (Thiruchelvam and Powers, 2004), though, none of them could mimic the complete pathology of PD including LB aggregation, progression of neuronal loss and impaired locomotive function (Potashkin, 2011).

To facilitate the development and analysis of PD mouse models a regulatable genetic system is a big advantage that would allow to introduce and to follow alterations over time ad libitum. In the past only a few systems like that were published and showed quite some limitations especially in the case of efforts to generate a model for PD expressing mutant variants of α-synuclein with enhanced levels of DA neurodegeneration (Chesselet, 2008; Daher *et al*., 2009a; Lin *et al*., 2009; Nuber *et al*., 2008) even with combination of the other PD related proteins like parkin (von Coelln *et al*., 2006; Stichel *et al*., 2007) or DJ-1(Ramsey *et al*., 2010) failed.

Therefore, our laboratory generated transgenic mice using the tet-system which express the tTA and rtTA controlled by promoter elements of the TH gene to target CA and more specific mDA neurons. The aim was to use these mice (1) to express and delete genes of interests in a regulated fashion allowing to switch on and off genes at a specific time in DA neurons (to distinguish gene function during development, adulthood and aging), (2) to *in vivo* image the DA system over time (bioluminescence and fluorescence imaging), (3) to trace individual DA neurons (unique labeling of single neurons), and (4) to improve the *in vitro* quantification of DA neurons (replacing stereology).

Parts of this work are already documented in the PhD thesis of Karsten Tillack which is summarized below, but several aspects remained unresolved and were followed up and completed in the work presented here.

1.5.2 Generation and basic characterization of TH-tTA and TH-rtTA mice for gene manipulation and *in vivo* imaging

TH-tTA and TH-rtTA mouse lines were generated using the TH promoter enabling temporally controlled gene manipulation specifically in DA neurons and were characterized for basic expression patterns (Tillack *et al*., 2015).

New approaches to visualize and analyze the DA system were evaluated. Optical *in vivo* imaging was successfully used in TH-tTA mice and viral vector mediated overexpression of fluorescent mCherry protein in DA neurons could be directly detected in the striatum of living mice and was used to follow DA neurodegeneration in the striatum over time *in vivo* (Tillack *et al*., 2015).

The three fluorescent markers RGB expression was applied for single cell tracing. Karsten Tillack established Brainbow founders with the combination of Brainbow mice and DOX-controlled expression of Cre in the TH-tTA mice to label cells and axons with different fluorescent colors which were not successful. Therefore, he used an alternative approach using rAAV vector based multicolor labeling. rAAVs with Cre induced expression of fluorescent proteins mCherry, Venus and mTFP1 (Red, Green, Blue; RGB method) were generated and administered through stereotactic injection into the midbrain of mouse. The RGB labeling worked in both DAT-Cre and TH-tTA/LC1 mice since many neurons showed distinct color expression (Figure 1.8 A and B). However, due to labeling of almost all DA neurons of the ventral midbrain of DAT-Cre mice, using TH-tTA/LC1 mice with transient DOX treatment had a benefit because of limited Cre activity. This resulted in sparse labeling of DA neurons in the midbrain (Figure 1.8 B).
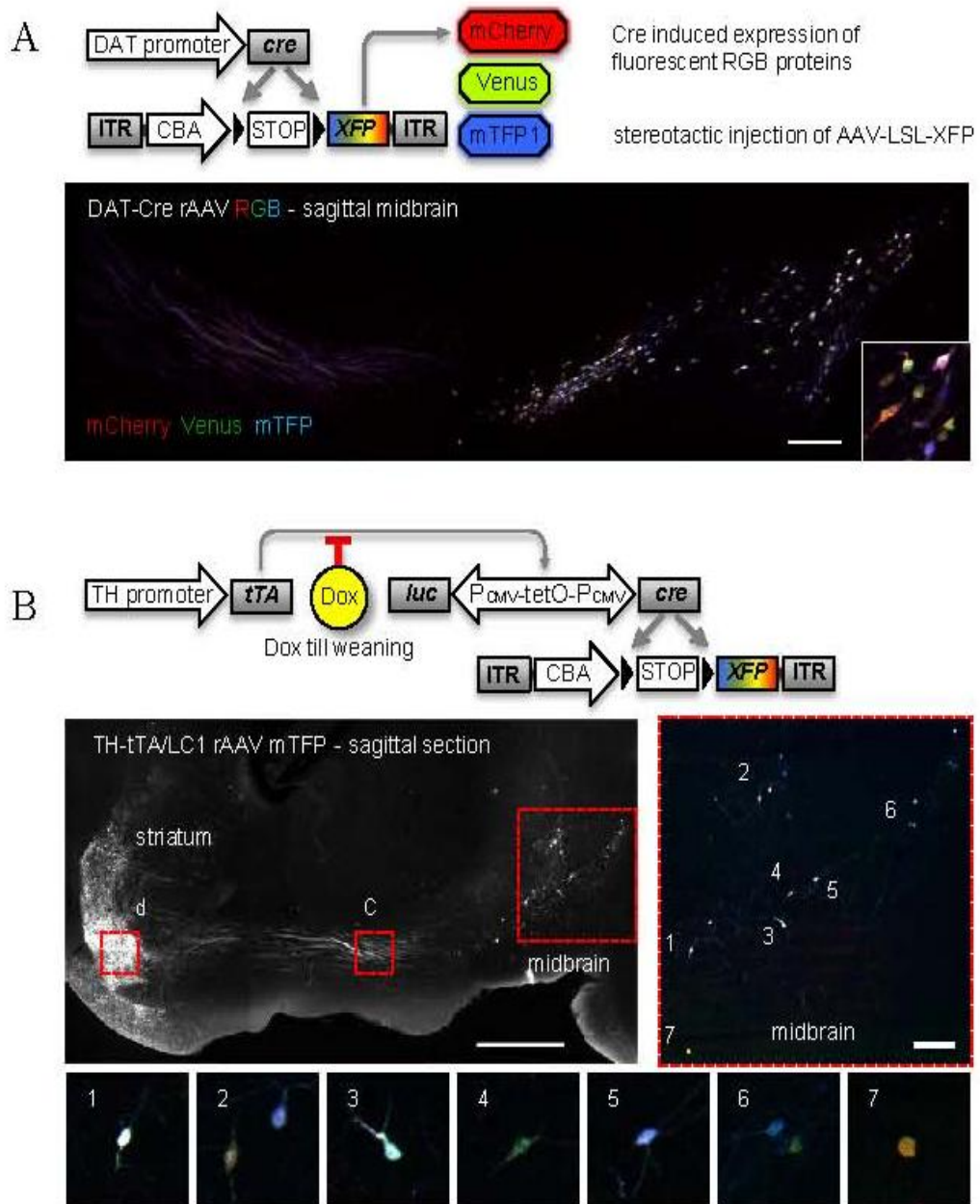
Figure 1.8 Cre-mediated multicolor labeling of individual DA cells *in vivo* after injection of AAV-LSL-XFP encoding different fluorescent proteins in DA neuron specific Cre mice

(A) Confocal image of merged signals of mCherry, Venus and mTFP in sagittal midbrain of Dat-Cre mouse after stereotactic injection of AAV-LSL-XFP mix. (B) Confocal image of mTFP signal showing mainly the mesolimbic DA pathway after stereotactic injection of AAV-LSL-XFP mix into midbrain of TH-tTA/LC1 mice with transient DOX treatment until age of four weeks. Zoom in of mDA cell soma. Individual cells with different color labeling are depicted in 1-7 (Tillack thesis, 2013).

In addition, TH-tTA mice were used to investigate the effect of embryonic compensation in neurotrophic Ret receptor mutant mice by deleting Ret in DA neurons selectively in adult mice (Figure 1.9). No increased neurodegeneration was detected in the mouse indicating that early embryonic compensation does not explain the different level of neurodegeneration in Ret receptor and Ret ligand GDNF mutant mice.

Next, the new mouse model was used to delete the Ret receptor and at the same time to overexpress human Parkinson´s disease related α-synuclein specifically in DA neurons (TH-tTA/tetO-synA53T). Transgenic α-synuclein expression pattern in TH-tTA/tetO-synA53T mice was analyzed by specific human α-synuclein immunostaining and the pattern was comparable with induced β-galactosidase expression in TH-tTA/LC1/R26R mice (Figure 1.10 B). Targeting efficiency of synA53T transgenic expression was 76% and the level of transgenic α-synuclein protein expression was 2 fold in 3 month old mice (Figure 1.10 C and D). At an age of 3 month, TH-tTA/tetO-synA53T mice showed no atypical behavior and no cell loss in the SNpc, VTA and striatum. To investigate the neurodegeneration in TH-tTA/LC1/Retlox/tetO-synA53T mice like in TH-tTA/LC1/Retlox mice, 1 year old TH-tTA/tetO-synA53T, TH-tTA/LC1/Retlox mice, TH-tTA/LC1/Retlox/tetO-synA53T and control mice analyzed histologically (Figure 1.11). A loss in TH positive neurons of 15 % in the SNpc and 25 % in the VTA (Figure 1.11 A and C) and an additional loss of DA innervations (Figure 1.11 B and D) was found in the dorsal and ventral striatum of TH-tTA/LC1/Retlox/tetO-synA53T mice. Also, increase in the level of dopamine metabolite DOPAC in TH-tTA/tetO-synA53T and TH-tTA/LC1/Retlox/tetO-synA53T mice was observed (Figure 1.11 E).

This enhanced neurodegeneration in 1 year old double mutant mice indicates that loss of neurotrophic support in DA neurons increases susceptibility for α-synuclein toxicity (Figure 1.11).
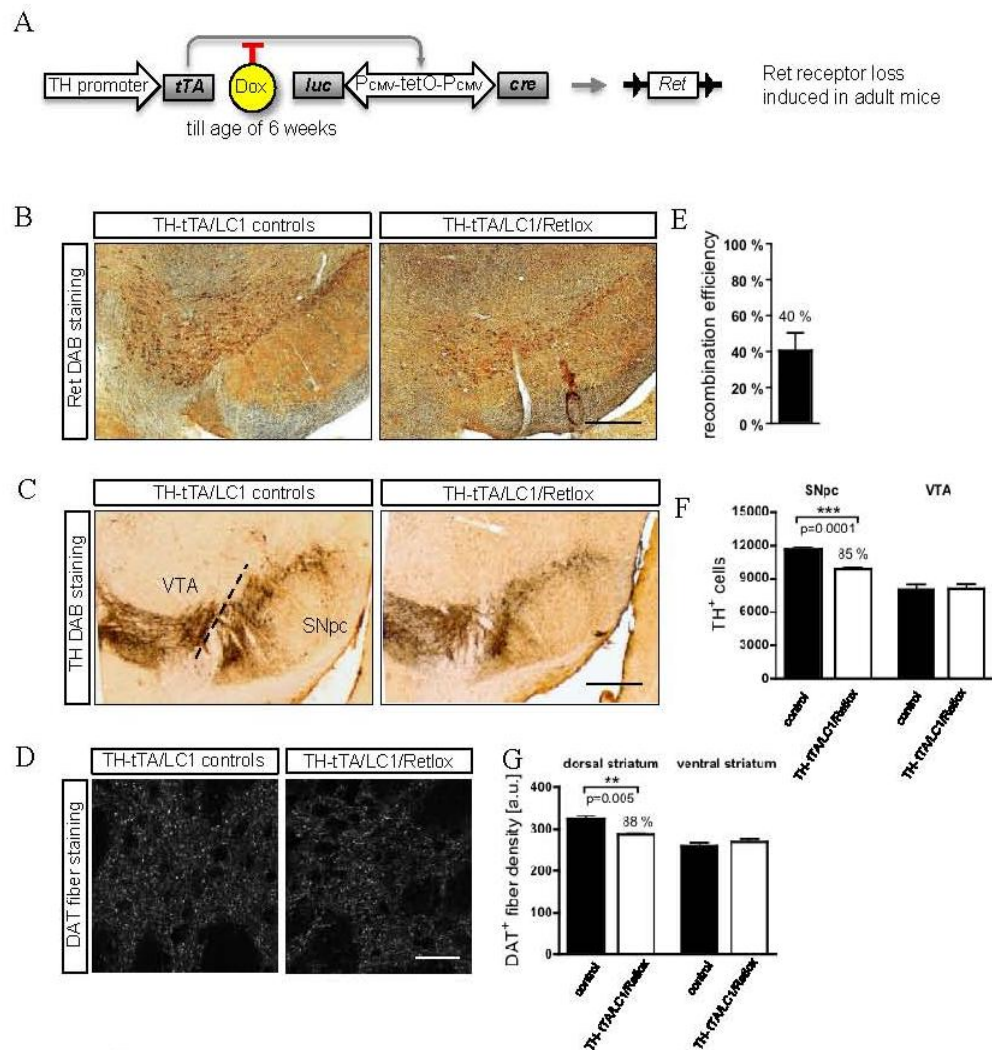
Figure 1.9 Loss of DA cells and innervation in aged mice with induced deletion of Ret receptor during adulthood

(A) Genetic scheme of induced Ret loss in TH-tTA/LC1/Retlox mice at an age of 6 weeks. (B) Immunohistochemical staining against Ret receptor in midbrain coronal sections of two year old control mice and TH-tTA/LC1/Retlox mutants. Mice had been treated with DOX until age of 6 weeks (C) Coronal midbrain sections of two year old control and THtTA/LC1/Retlox mutant mice stained for TH to visualize DA neurons in the SNpc and VTA and (D) DAT to visualize fibers in the dorsal and ventral striatum. (E) Ret positive cells in 3 different sections per mouse were counted in THtTA/LC1/Retlox mice. Percentage of less Ret positive cells in mutant mice was considered as recombination efficiency for Ret. n=3; mean + s.e.m. (F) Stereological quantification of TH positive cells in the VTA and SN. mean + s.e.m., n=5, ***p<0.001, Student´s t-test. (G) Relative density of DAT positive fibers in the dorsal and ventral striatum. mean + s.e.m., n=4, **p<0.01, Student´s t-test. Scale bars: 200 μm (B-C), 10 μm (D). (Tillack thesis, 2013).
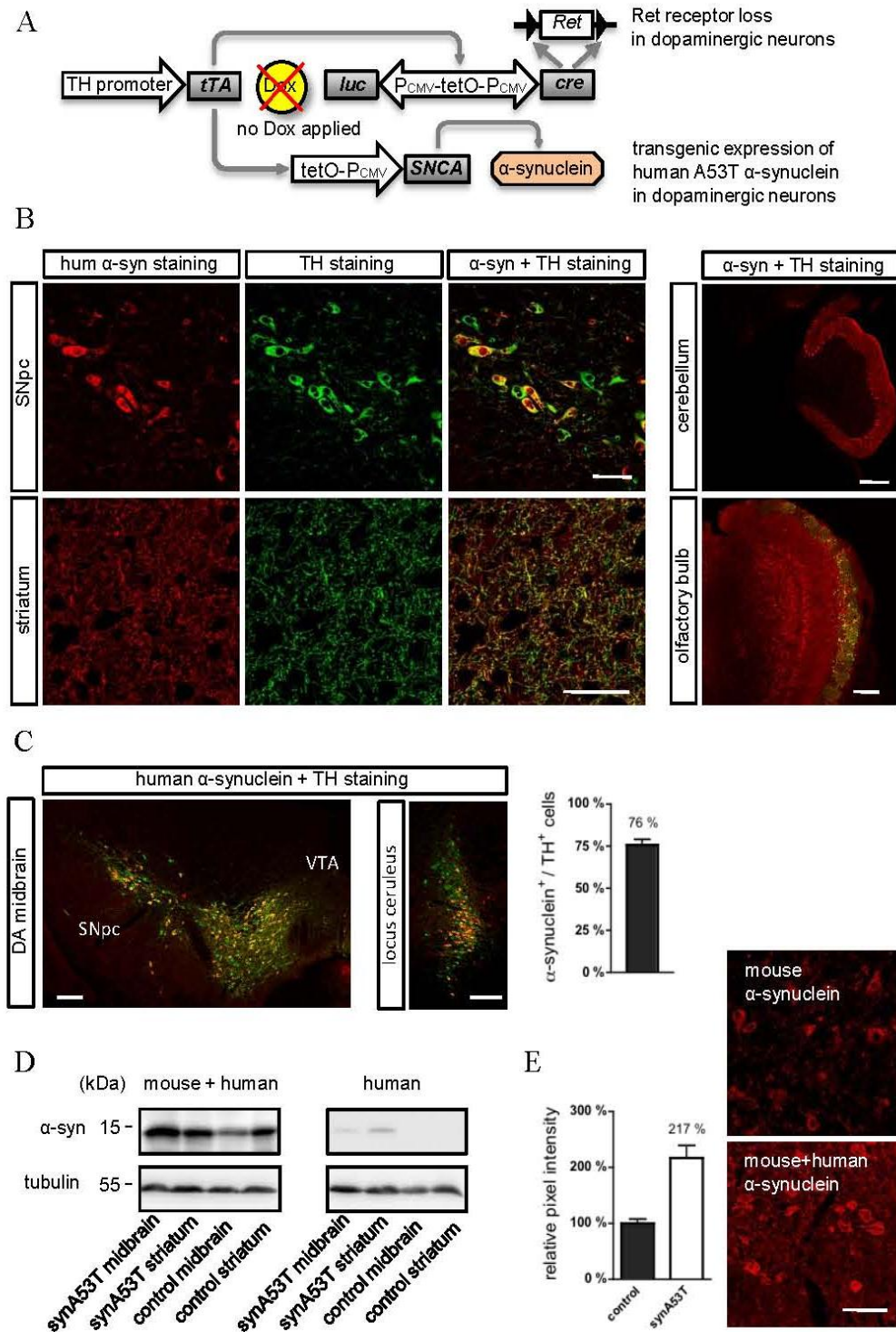
Figure 1.10 Expression of human α-synuclein A53T mutant protein in DA neurons of TH-tTA/tetO-synA53T mice

(A) Scheme of TH-tTA/LC1/Retlox/tetO-synA53T mice without DOX. (B-C) Confocal fluorescent pictures of human α-synuclein A53T expression in coronal mouse brain

sections stained for TH and for human α-synuclein protein. (C) Quantification of α-synuclein and TH double positive cells in the midbrain to estimate efficiency of transgenic expression. n=3; mean + s.e.m. (D) Western blot analysis of transgenic α-synuclein expression in midbrain and striatum tissue of control and transgenic TH-tTA/tetO-synA53T 3 month old mice. Antibodies recognizing endogenous mouse and transgenic human α-synuclein or antibodies recognizing only human α-synuclein were used together with an antibody against α-tubulin as loading control. (E) Quantification of human transgenic α-synuclein expression relative to endogenous mouse α-synuclein expression by measuring and comparing relative pixel intensity of α-synuclein fluorescent staining using an antibody detecting both endogenous mouse and transgenic human protein. Cells per mouse > 200; n=3; mean + s.e.m. Scale bars: 20 μm (B (SNpc, striatum), E) and 200 μm (B (cerebellum, olfactory bulb), C) (Tillack thesis, 2013).
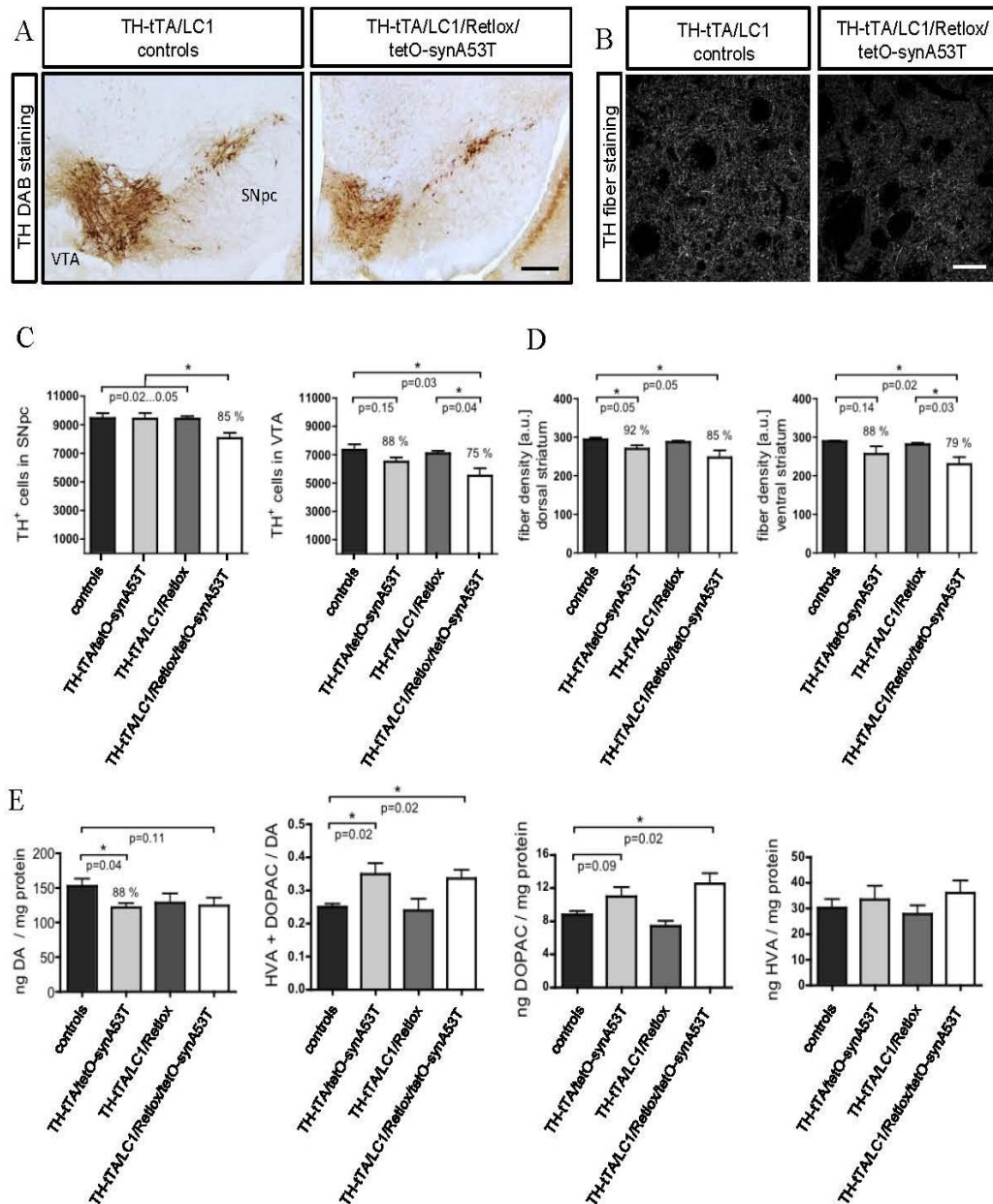
Figure 1.11 Alterations in one year old mice with DA neuron-specific Ret deletion and/or human A53T α-synuclein overexpression.

(A) Coronal midbrain sections of control, TH-tTA/tetO-synA53T, TH-tTA/LC1/Retlox and TH-tTA/LC1/Retlox/tetO-synA53T mice stained for TH to visualize DA neurons in the SNpc and the VTA. Scale bar: 200 μm. (B) Confocal fluorescent images of striatal sections of control, TH-tTA/tetO-synA53T, TH-tTA/LC1/Retlox and TH-tTA/LC1/Retlox/tetO-synA53T mice stained for TH to visualize DA fibers in dorsal striatum. Scale bar: 20 μm. (C-D) Stereological quantification of TH positive cells in the SNpc and VTA (C) and relative density of TH positive fibers in the dorsal and ventral striatum (D) of control, TH-tTA/tetO-synA53T, TH-tTA/LC1/Retlox and TH-

tTA/LC1/Retlox/tetO-synA53T mice. mean + s.e.m., n=4, *p<0.05, Oneway ANOVA. (E) Dopamine (DA) and DA metabolites in striatal brain lysates measured by HPLC. dihydroxyphenylalanine (DOPAC), homovanillic acid (HVA), mean + s.e.m., n=5, *p<0.05, Students t-test (Tillack thesis, 2013).

2. Aims

The aim of this study was to complete the characterization of the newly developed TH-tTA and TH-rtTA mouse lines specific for the DA system and to evaluate their use as mentioned above for (1) expression and deletion genes of interests in a regulated fashion allowing to switch on and off genes at a specific time in DA neurons (to distinguish gene function during development, adulthood and aging), (2) *in vivo* imaging of the DA system over time (bioluminescence and fluorescence imaging), and (3) tracing individual DA neurons (unique labeling of single neurons)

Specific Aims:

1. To evaluate the newly generated TH-tTA and TH-rtTA mouse lines for specificity, inducibility and efficacy by crossing them with LC1 and ROSA26 receptor mice and staining DA neurons.

2. To examine the inducibility in TH-rtTA mice in addition with an LC1 independent procedure using an alternative tet-responsive construct - a recombinant adeno-associated viral vector (rAAV) encoding a Venus fluorescent protein marker – to overcome the possible LC1 silencing without DOX.

3. To establish a simple mouse model with reduced number of DA neurons by generating and characterizing TH-tTA/LC1/R26dt-a mice.

4. To optimize the procedure for single DA cell tracing techniques using the TH-tTA and TH-rtTA mice by comparing different procedures.

5. To develop and test a novel bioluminescence substrate to improve the resolution and sensitivity of the *in vivo* bioluminescence imaging with the TH-tTA and TH-rtTA mice.

6. To establish a novel PD mouse model by genetically deleting the Ret receptor and overexpressing α-synuclein and analyze possible synergistic effects. The three hallmarks of a good PD animal model will be assessed – SN DA neuron specific degeneration, protein aggregation and physiological alterations – as well as the molecular mechanisms which lead to the neurodegeneration process, such

as alterations in mitochondrial function, autophagy, and cell signaling events. α-synuclein spreading will also be investigated as a possible age-dependent neurodegenerative propagation mechanism.

3. Materials and Methods

A. Materials

3.1 Laboratory equipment

Table 3.1

Equipment	Manufacturer
Spectrophotometer ND-1000	NanoDrop Technologies
Tabletop centrifuge 5810R	Eppendorf GmbH
Centrifuge 5417R	Eppendorf GmbH
Centrifuge J2-21 M/E, rotors Ja-14; Ja-20	Beckman Coulter GmbH
Ultracentrifuge TL-100, rotor TLA100.3	Beckman Coulter GmbH
PCR PTC-250	MJ Research, Inc.
Agagel Maxi gel electrophoresis	Biometra
E.A.S.Y WIN 32 gel documentation	Intas Science Imaging Instruments GmbH
PH Meter 522	Wissenschaftlich-Technische Werkstatten GmbH
Stereo microscope SZX16 with DP72 camera	Olympus.
Axio Imager.M1	Carl Zeiss Corp.
Confocal microscope system TCS SP2	Leica
In Vivo Imaging System IVIS 200	PerkinElmer
Confocal microscope LSM 700	Zeiss
TRANS-BlotR SD semi-dry transfer cell	Bio-Rad Laboratories
KT 50 micro ultrasonic cell disrupter	KONTES
Cryostat LEICA CM3050S	Leica Microsystems GmbH
Thermofixer comfort heating block	Eppendorf GmbH
UltiMate 3000 HPLC	Dionex - Germany, Idstein
Micropump Injectomate	Neurostar
Mini-PROTEANR II-Electrophoresis-System	Bio-Rad Laboratories GmbH
Rotating laboratory roller mixer RM5	Hecht Assistent
Stereotaxic apparatus model 2006	David Kopf Instruments
Non-puncture ear bars and incisor adapter #922	David Kopf Instruments
Heating plate ATC1000	World Precision Instruments
Dissection microscope SZ51	Olympus
Dental drill IH-300	NSK
Glass puller P-97	Sutter Instruments
Orbital platform shaker Certomat TC3	B. Braun Biotech International
Peristaltic pump Minipuls	Gilson
Glass bead sterilizer	Fine Scientific Tools

Equipment	Manufacturer
Image Reader LAS-4000	GE Healthcare
C18 reverse-phase HR-80 column	ESA, Bedford, MA
HPLC electrochemical detector electrodes, model 5011 / 5020	ESA, Bedford, MA
Scale BA 200	Sartorius AG
Ultrascale AE 240	Mettler - Toledo GmbH

3.2 Chemical substances

Table 3.2

Substance	Company	Order number
2-mercaptoethanol	Sigma-Aldrich	M3148
3,4-dihydroxybenzylamine	Aldrich	358781
Acrylamid	Roth	3029.1
Agarose	BIOzym	840040
Ampicilin	Carl Roth	K 029.3
Ammonium Persulfate (APS)	Appli Chem	2941
Bone Wax	WPI	501771
Bovine serum albumine	PAA Laboratories	K45-001
Complete™ Protease Inhibitor Cocktail Tablets	Roche	11697498001
Coumaric acid	Carl Roth	9908.1
D-luciferine	Promega	E1601
DAPI	Mol Probes	D-21490
Dibenzyle ether	Sigma-Aldrich	108014-1KG
Diaminobenzidine (DAB)	Sigma Aldrich	D4418-50set
Disodiumhydrogen phosphate	Carl Roth	4984.1
DMEM w/GlutaMAX™ I, Glucose w/o Na Pyr	Invitrogen	61965026
DMSO	Carl Roth	19941
dNTP Set, 100mM Solutions	Fermentas	R0186
Doxycycline (Dox)	Sigma Aldrich	D1822
EDTA	Applied Biosystems	AM9260G
EGTA	Roth	3054.2
Eosin G	Merck	1.15935
Ethidiumbromide	Carl Roth	7870.1
Ethylene glycol	Sigma Aldrich	E9129
Eukitt	Fluka	03989

Substance	Company	Order number
Fuoromount G	Southern Biotech	0100-01
Glutaraldehyde	Fluka	49629
Glycerol	Carl Roth	3783.2
HCL 37 %	Carl Roth	X942.2
HEPES	Appli Chem	A3268.0250
Hydrochloric acid	Sigma Aldrich	H9892
Hydrogen peroxide	Merck	1.07209
Kanamycin	Carl Roth	T832.2
Luminol	Carl Roth	4203.1
Magnesium chloride	Carl Roth	2189.1
Orthovanadate	Sigma-Aldrich	S6508-50G
Paraformaldehyde	Appl Chem	A3813.1000
Penicillin-Streptomycin	Invitrogen	15140122
Pepsin	Appli Chem	A4289
perchloric acid	Appli Chem	A0539
Ponceau S solution	Sigma-Aldrich	P-7170-1l
Potassium chloride	Carl Roth	6781.1
Potassium dihydrogen phophate	Merck	1.12034
Sodium dodecyl sulfate	Carl Roth	5136.1
Sodium hydroxide	Carl Roth	P031.2
Succrose	Carl Roth	9097.1
TEMED	Carl Roth	9351.1
Tetrahydrofuran Tissue-Tek® O.C.T.™	Sigma-Aldrich SAKURA Inc.	186562-1L 4583
Tris(hydroxymethyl)aminomethane Triton X-100	Merck Carl Roth	108382 3051.2
Trypsin-EDTA Tween20	Invitrogen Carl Roth	25300054 9127.1
X-gal Xylene cyanol dye solution	Carl Roth Sigma-Aldrich	2315.3 B3269

3.3 Pharmaceutical substances

Table 3.3

Substance	Company
Isoflurane (pure liquid)	Baxter Deutschland GmbH
Betadine (Povidone-iodine)	Provet AG
Temgesic inj. Solution (300 μg/ml buprenorphine)	RB Pharmaceuticals Ltd.
Rimadyl inj Solution (50 mg/ml carprofen)	Pfizer Animal Health Inc
Baytril inj. Solution 10 % (100 mg/ml enrofloxacine)	Bayer Vital GmbH

Substance	Company
Rompun inj. Solution 2 % (20 mg/ml xylazine)	Bayer Vital GmbH
Ketamin Gräub inj. Solution (100 mg/ml ketamine)	Albrecht GmbH

3.4 Buffers and Solutions with constituents

Table 3.4

Buffer / Solutions	Constituents
1X (0.1 M) PBS	10 mM Na2HPO4; 2 mM KH2PO4; 0.137 M NaCl; 2.7 mM KCl; pH 7.4
1X (0.1 M) TBS (TBS-T)	50 mM Tris pH 7.4; 150 mM NaCl (+ 0.1 % (v/v) Tween20)
Tail lysis buffer	A: 5 M NaOH; 0.5 M EDTA / B: 1 M Tris-HCl pH 5.0
10X PCR buffer	1M KCl; 1M Tris HCl pH 9.0; 1M MgCl2
Annealing buffer	100 mM NaCl; 50 mM HEPES 50 mM pH 7.4
TE buffer	10 mM Tris pH 8.0; 1 mM EDTA 1
DNA loading buffer	3 % (w/v) Ficoll Type 400; 0.05 % (w/v) bromophenol blue; 0.05 % (w/v) xylene cyanol FF
50X TAE buffer	2 M Tris pH 7.8; 0.5 M NaOAc; 50 mM EDTA
HPLC lysis buffer	0.1M perchloric acid; 0.5 mM EDTA; 100 ng/ml 3,4-dihydroxybenzylamine (internal standard)
Western Blot lysis buffer	50 mM Tris-Hcl pH 7.5; 150 mM NaCl; 0.5 % Triton X-100; 10 mM NaPPi; 20 mM NaF; 1 mM Orthovanadate; Complete™ mini protease inhibitor cocktail (Roche)
5X Western Blot loading	125 mM Tris-HCl pH 6.8; 20 % (v/v) glycerol; 4 % (w/v) SDS; 0.02 % (w/v) bromophenol blue;
Buffer	5 % (v/v) 2-mercaptoethanol
Western Blot transfer buffer	20 mM Tris; 150 mM glycerine; 0.1 % (w/v) SDS; 20 % (v/v) methanol
Western Blot ECL solution	0.1 M Tris pH 8.5; 3 μl of 30 % H2O2; 50 μl of 250 mM luminol(DMSO); 25 μl 90 mM coumaric acid(DMSO)
Mounting medium	Celvol®205 125 g/L; glycerol 25 % (v/v); in 0.1 M PBS pH 7.4
Cryoprotection solution	30 % glycerol (v/v); 30 % ethylene glycol (v/v); in 0.1 M PBS pH 7.4

3.5 Molecular biological kits and enzymes

Table 3.5

Kits and enzymes	Company	Order number
EndoFree Plasmid Maxi Kit	Qiagen	12362
Pierce™ BCA protein assay kit	Thermo Scientific	23225
Complex I Enzyme Activity Microplate assay	Abcam	ab109721
ATP(Colorimetric/Fluorometric) Assay	Abcam	ab83355

3.6 Antibodies and other consumables

Table 3.6 Primary Antibodies

Antibody	Company	Order number	Host	Clonality	Working dilution	Used for
α-synuclein	Santa Cruz Biotechnology	sc-69977	mouse	monoclonal	1:500	IHC, WB
α-synuclein	Santa Cruz Biotechnology	Sc-7011	rabbit	polyclonal	1:100	IHC
α-tubulin	Sigma-Aldrich	T-9026	mouse	monoclonal	1:1000	WB
β-actin	Santa Cruz Biotechnology	Sc-130657	rabbit	polyclonal	1:1000	WB
Akt	Cell Signaling Technology	4691	rabbit	monoclonal	1:1000	WB
AMPK	abcam	Ab131512	rabbit	polyclonal	1:1000	WB
ATG9A	abcam	Ab108338	rabbit	monoclonal	1:1000	WB
DAT	Millipore	MAB369	rat	monoclonal	1:500	WB
GDNF	R & D Systems	AF212NA	goat	polyclonal	1:500	WB
GFAP	Dako	Z0334	rabbit	polyclonal	1:250	IHC
GFRα1	Santa Cruz Biotechnology	Sc-10716	rabbit	polyclonal	1:500	WB
GFRα2	Santa Cruz Biotechnology	Sc-7136	goat	polyclonal	1:500	WB
GIRK2	Millipore	AB5200	rabbit	polyclonal	1:200	WB
Hsc-70	abcam	ab19136	rat	monoclonal	1:10000	WB
Human α-synuclein	Santa Cruz Biotechnology	Sc-58480	mouse	monoclonal	1:500	IHC, WB
Human α-synuclein(15G7)	A.G.Scientific	S1114	rat	monoclonal	1:100	IHC
Iba1	Wako	019-19741	rabbit	polyclonal	1:200	IHC
LAMP2A	abcam	ab18528	rabbit	polyclonal	1:1000	WB
LC3	Novus Biologicals	NB100-2220	rabbit	polyclonal	1:2000	WB
NCAM	Millipore	AB5032	rabbit	polyclonal	1:500	WB
NDUF10	Santa Cruz Biotechnology	sc-292084	rabbit	polyclonal	1:1000	WB
NDUFB8	Abcam	Ab192878	rabbit	monoclonal	1:1000	WB
Nurr1	Santa Cruz Biotechnology	Sc-991	rabbit	polyclonal	1:500	WB
N-Cadherin	Hybridoma bank USA	MNCD2	rat	monoclonal	1:1000	WB
OPTN	proteintech	10837-1-AP	rabbit	polyclonal	1:1000	WB

Antibody	Company	Order number	Host	Clonality	Working dilution	Used for
p62	Enzo Life Sciences	BMLPW9860	rabbit	polyclonal	1:1000	WB
Parkin	Santa Cruz Biotechnology	sc-32282	mouse	monoclonal	1:500	WB
PINK	abcam	Ab23707	rabbit	polyclonal	1:1000	WB
Phospho-S6 (S235/236)	Cell Signaling Technology	2211	rabbit	monoclonal	1:1000	WB
Phospho-Akt (Ser 473)	Cell Signaling Technology	4051	mouse	monoclonal	1:1000	WB
Phospho-AMPKalpha(Thr172)	Merk Millipore	07-681	rabbit	polyclonal	1:1000	WB
Phospho-Ret(Tyr 1062)	Santa Cruz Biotechnology	Sc-1062	rabbit	polyclonal	1:250	WB
Phospho-mTOR(ser2448)(D9C2)	Cell Signaling Technology	5536	rabbit	monoclonal	1:1000	WB
Phospho-mTOR(ser2481)	Cell Signaling Technology	2974	rabbit	polyclonal	1:1000	WB
Phospho-ULK1	Cell Signaling Technology	6888	rabbit	polyclonal	1:1000	WB
Phospho α-synuclein	Wako	014-20281	mouse	monoclonal	1:1000	IHC
RTP801	Millipore	ABN483	rabbit	polyclonal	1:1000	WB
Syndecan 3	abcam	AB155952	rabbit	monoclonal	1:1000	WB
S6	Cell Signaling Technology	2317	mouse	monoclonal	1:1000	WB
TH	Acris	22941	mouse	monoclonal	1:1000	IHC, WB
TOM20	Santa Cruz Biotechnology	Sc-11415	rabbit	polyclonal	1:500	WB
TOM40	Santa Cruz Biotechnology	Sc-11414	rabbit	polyclonal	1:500	WB
mTOR	Cell Signaling Technology	2972	rabbit	polyclonal	1:1000	WB
ULK1	Cell Signaling Technology	8054	rabbit	monoclonal	1:1000	WB

Table 3.7 Secondary Antibodies

Antibody	Company	Order number	host	Working dilution	Used for
goat anti-rabbit IgG Alexa Fluor® 488	Invitrogen	A11008	rabbit	1:400	IHF
goat anti-mouse IgG Alexa Fluor® 488	Invitrogen	A11001	mouse	1:400	IHF
goat anti-rabbit IgG Alexa Fluor® 647	Invitrogen	A21244	rabbit	1:400	IHF
goat anti-mouse IgG Alexa Fluor® 647	Invitrogen	A21235	mouse	1:400	IHF
strepavidine Alexa Fluor® 488 conjugate	Invitrogen	S11223	-	1:400	IHF
strepavidine Alexa Fluor® 647 conjugate	Invitrogen	S-21374	-	1:400	IHF
horse anti-mouse IgG biotinylated	Linaris	BA-2001	mouse	1:200	IHC IHF WB
horse anti-rabbit IgG biotinylated	Linaris	BA-1100	rabbit	1:200	IHC IHF WB
goat anti-rat IgG biotinylated; mouse adsorbed	Linaris	BA-9401	rat	1:200	IHC IHF WB
Vectastain ABC-HRP Standard (streptavidin-peroxidase)	Linaris	PK-4000	-	1:200	IHC IHF WB

3.7 Consumables/lab ware

Table 3.8

Product	Company	Order number
Whatmann blotting paper	Hassa	3030-917
Amicon Ultra-15 Filter Unit, 30kD membrane for HPLC loading	Millipore	UFC903024
Agrafe Reflex Wound Clip 7 mm	WPI	500344
Syringe, 75 RN, no needle	VWR	HAMI7634-01

Product	Company	Order number
RN Compression Fitting 1mm	VWR	HAMI55750-01
PVDF membrane	Amersham	RPN 303F
Dako Pen, Liquid Repellent stick	Dako	S200230
Homogenizer Glass Dual Size 20	Fisher Scientific	3121999
PTFE Pistil Size 20	Fisher Scientific	3122124
tissue sample corers	Fine Scientific Tools	18035-01/02
Borsilicate glass capillaries: OD 1 mm; ID 0.86 mm; with filament	Science Products GmbH	GB100-8P
24 well plates; flat bottom; cell culture grade	Sarstedt	83.1836
Petri dishes; 10 cm, cell culture grade	Sarstedt	83.1802
Peel-A-Way® Embedding Mold (Square - S22)	Polysciences	18646A
Microfuge Tube; 1.5ml	Beckman	357448
Object slides Superfrost Plus	Roth	H867.1
96 well PCR plate	4titude	4ti-0750B
8-strip tubes+caps	4titude	4ti-0780

3.8 DNA oligonucleotides and PCR primers

Table 3.9

Genotype	TM [°C]	Bandsize	Primer name	Sequence in 5'- 3' orientation
TH-tTA/ TH-rtTA	67	333mutant	gTH2f	AGAACTCGGGACCACCAGCTTG
			gTH2r	CACTTTAGCCCCGTCGCGATG
LC1(Cre)	67	500mutant	CreA	GCCTGCATTACCGGTCGATGCAACGA
			CreB	GTGGCAGATGGCGCGGCAACACCATT
			Dat3	GCCGCATAACCAGTGAAACAGC
R26-R	58	600wt/300m	Rosa1	AAAGTCGCTCTGAGTTGTTAT
			Rosa2	GCGAAGAGTTTGTCCTCAACC
			Rosa3	GGAGCGGGAGAAATGGATATG
R26-DT-A	55	580wt/320m	Rosa1	AAAGTCGCTCTGAGTTGTTAT
			SpliAcB	CATCAAGGAAACCCTGGACTACTG
			Rosa3	GGAGCGGGAGAAATGGATATG

Genotype	TM [°C]	Bandsize	Primer name	Sequence in 5'- 3' orientation
Ret floxed	62	300wt/350m	Retgeno5	CCAACAGTAGCGTCTGTGTAACCCC
			Retgeno7	GCAGTCTCTCCATGGACATGGTAGCC
Ret rec	62	400m	Retgeno6	CGAGTAGAGAATGGACTGCCATCTCCC
			Ret3E	ATGAGCCTATGGGGGGGTGGGCAC
tetO-synA53T	60	450m	synA	ATGGATGTATTCATGAAAGG
			synB	TTAGGCTTCAGGTTCGTAG

3.9 Transgenic mouse lines

Table 3.10

Name	Type	Description	Reference
TH-tTA	transgenic	TH(ms) promoter driven Tet-Off tTA expression in CA neurons	Tillack, 2015
TH-rtTA	transgenic	TH(ms) promoter driven Tet-On rtTA expression in CA neurons	Tillack, 2015
LC1	transgenic	luciferase and Cre expression by Tet responsive promoter	Schoenig, 2002
R26-R	knock-in Chr.6	Cre inducible expression of β-galactosidase from *rosa26* locus	Soriano, 1999
R26-DT-A	knock-in Chr.6	Cre inducible expression of diphtheria toxin-A from *rosa26*	Brockschnieder, 2006
Ret floxed	knock-in Chr.6	loxP conditional allels for neurotrophic receptor Ret	Kramer, 2006
tetO-synA53T	transgenic	hum α-synuclein A53T expres-sed by Tet responsive promoter	Lin, 2010

B. Methods

3.10 DNA techniques

3.10.1 Plasmid DNA preparation and propagation

Plasmids containing adeno-associated viral genome derived sequences were transformed and propagated in Escherichia coli SURE1 cells (Table 3.11). The reason to use these bacteria is that they are more suitable than conventional bacteria as they show much reduced likelihood for recombination events, which occur especially often in plasmids with repetitive sequences such as AAV terminal repeats. Other plasmids were amplified in DH5-α.

Table 3.11 Competent *E.coli* strains

Strain	Genotype	Company
SURE1	e14-(McrA-) Δ(mcrCB-hsdSMR-mrr)171 endA1 gyrA96 thi-1	Stratagene
DH5-α	supE44 relA1 lac recB recJ sbcC umuC::Tn5 (Kanr) uvrC [F-proAB lacIqZΔM15 Tn10 (Tetr)]. F- φ80dlacZΔM15 Δ(lacZYA-argF) U169 recA1 endA1 hsdR17(rk-, mk+) phoA Invitrogen supE44 λ-thi-1 gyrA96 relA1	Invitrogen

5 μl of Escherichia coli SURE1 bacterial glycerol stocks were picked and spread out onto LB agar plates. 50 μg/ml antibiotics (ampicillin) attenuated growth of un-transfected bacteria and plates were incubated for 12-16 hours overnight. For small scale plasmid preparation, single colonies were picked with autoclaved wooden toothpicks and transferred to 12 ml incubation tubes containing 5 ml LB medium with appropriate antibiotics (ampicillin) (50 μg/ml) and incubated overnight with constant shaking (140 rpm). A day after, 0.5 ml of bacteria suspension was mixed with 0.5 ml sterile glycerol and stored in cryo-tubes at -80 °C as glycerol stocks. Next, 4 ml of remaining cultures were pelleted with a tabletop centrifuge (4 °C; 10 min; max. speed) and plasmid DNA was extracted using Macherey Nagel's NucleoSpin Plasmid (250) Kit as stated in the manual. In the applied DNA extraction kits the use of alkaline cell lysis is followed by adsorption of DNA onto silica-gel membrane. The adsorbed DNA is then

washed and eluted from the membrane. For large scale plasmid preparations, 200 ml LB medium with respective antibiotics were inoculated with 2 ml of preparatory culture and grown overnight. Cultures were then pelleted in a JA-14 rotor (Beckmann, 4 °C; 10 min; 5000 g) and plasmid DNA was extracted using the QIAprep Spin MaxiPrep Kit according to the manufacturers' protocol. During extraction, all centrifugation steps were carried out in a JA-20 rotor (Beckmann, 4 °C; 20 min; 12000 g) and pelleted plasmid DNA was re-dissolved in 200 µl NE buffer (Table 3.5). DNA concentrations were measured with a NanoDrop spectrophotometer and all plasmid stock solutions were diluted to 0.5 µg/µl in TE buffer. Working DNA samples were stored at -20 °C. Glycerol stocks were kept at -80 °C.

3.10.2 DNA transformation

For transformation of ligated plasmid DNA, an aliquot of 100 µl chemical competent cells was thawed on ice and incubated with up to 10 µl of ligation mix on ice for about 20 min. Next, transformation mix was heat shocked at 42 °C for 90 seconds in a water bath and then transferred immediately onto ice. 600 µl of pre-warmed LB medium were added and the transformation was incubated for 1 hour at 37 °C for expression of the plasmid encoded resistance genes. 50 µl of transformation mix were directly transferred to a LB plate containing kanamycin (50 µg/ml) or ampicillin (100 µg/ml). The remaining fraction was centrifuged at 2000 g in a tabletop centrifuge for 5 min. Supernatant was discarded and the re-suspended pellet was spread onto a second LB plate to get a sufficient number of colonies even in case of very low transformation rates. All plates were incubated overnight at 37 °C.

3.10.3 Agarose gel electrophoresis

PCR genotyping samples were loaded on 1–2 % (w/v) agarose gels. The agarose concentration was chosen according to the size of the respective DNA fragments. To produce a gel, agarose was weighed and dissolved in TAE buffer (Table 3.4) by boiling in a microwave. To visualize the DNA, 0.5 µg/ml ethidiumbromide was incorporated into the gel. The sample together with the respective volume of 10x DNA loading buffer was loaded onto the gel. Electrophoresis was performed with an electric field strength of 180 Volt for about 30 min. The images were taken using the E.A.S.Y WIN 32 gel documentation system (Table 3.1).

3.11 Cell culture techniques

3.11.1 Adeno-associated virus production

Production of recombinant Adeno-associated virus serotype 5 (rAAV5) was done by Dr. Ingke Braren according to the standard operating procedure of the Vector Core Facility at the UKE. Briefly, viral particles were generated in HEK 293T cells after transient transfection (polyethylenimine, 25 kDa linear) of the helper plasmid pDP5rs (Prof. Kleinschmidt, DKFZ) and the transfer plasmid encoding the sequence of interest flanked by the inverted terminal repeats. After 2-3 days, cells were harvested and lysed by freeze-thawing cycles, and then nucleic acids were removed by BenzonaseR digestion. Supernatants containing the rAAV5 particles were concentrated and purified by iodixanol-gradient ultracentrifugation and further ultrafiltration was done using Amicon Ultra-4 centrifugal filter units with 50 kDa cut-off. Final rAAV vector solution in PBS-MK was aliquoted and stored at -80 °C freezer until use. To determine the titer of rAAV5 particles in the final solution, quantitative real-time PCR was performed to calculate viral vector genomes per ml (vg/ml). Typical viral vector genome titers used for *in vivo* transductions in this study were 10^{13} vg/ml.

3.11.2 Cell cultures and RNA interference

The cell culture part has been done by Eva Dürholt a PhD student from Konstanze Winklhofer's lab. Briefly, SH-SY5Y (human neuroblastoma cells; ATCC® CRL-2266™) cells were cultivated in DMEM supplemented with 15% FCS (life technologies, #31330095) and maintained at 37°C, 5% CO_2. For RNAi intereference, cells were reversely transfected with the siRNA oligo human Ret or human α-synuclein A53T using Lipofectamine RNAiMAX (life technologies, #18324-012). 3 to 5 h post-transfection medium was changed for α-synuclein A53T and Ret knock-down cells respectively. 48 h after transfection for α-synuclein A53T and 72 h after transfection for Ret knock-down, cells were washed twice with PBS and fix with 3.7% PFA in PBS for 10 min at room temperature followed by four times wash with PBS. The cells were mounted onto glass slides using mounting media with DAPI and confocal Imaging was performed.

3.12 Transgenic mouse lines

3.12.1 Animal housing

All animal experiments were performed in accordance with the German Animal Welfare Act and approved by the local authorities of the city state Hamburg and the animal care committee of the University Medical Center Hamburg-Eppendorf (UKE). Mice were housed in the mouse facility of UKE under constant conditions at 22 °C and 40-50% humidity in a 12 h light / dark cycle with free access to food and water. All routine mouse work, like cage change, supply of water and food, breedings, weanings, collection of biopsies and marking of mice was handled by the animal care takers of the UKE mouse facility.

3.12.2 Mouse lines and genotyping

All transgenic mouse lines used in this study (Table 3.10) were maintained on a C57BL/6J inbred strain background. Before employing mice in the experiments new transgenic mouse lines generated by pronucleus injection with a C57BL/6/CBA mixed background were crossed for at least 4 generations with C57BL/6J mice. During the first week of life, mouse tail biopsies were taken by animal care taker and sent to us for genotyping of transgenic mouse lines via PCR. Genomic DNA for genotyping was released from tissue by alkaline cell lysis. In this procedure, 100 µl of tail lysis buffer A were added to every sample in a 96-well plate and heated for 20 min at 95 °C in a PCR machine, followed by vortexing vigorously. The routine was repeated until tissue was sufficiently dissolved. To neutralize and stabilize the DNA solution, samples were briefly spinned down and 100 µl of tail lysis buffer B were added to each well which were afterward mixed and centrifuged at full speed for several minutes (5810R centrifuge; Eppendorf) to pelletize remaining cell debris and hairs. For immediate use tail DNA samples were kept at 4 °C and later stored at -20 °C. Genotyping PCR was carried out with a master-mix which was prepared using homemade Taq DNA polymerase enzyme and 2 µl of genomic DNA template per reaction. The PCR master-mix prepared as below (for 50 µL):

1 μL each of the reverse and forward primers (30 μM), (Table 3.9)

5 μL of 10X TAQ buffer (1X)

5 μL of dNTPs mix (10 μM),

1 μL Taq DNA polymerase,

36 μL distilled water and

2 μL from the DNA solution

Sequence specific primers and PCR conditions for each transgene are listed in Table 3.9. Ret receptor conditional alleles were tested for recombination events during germline transmission via an additional PCR. Amplified DNA was analyzed by agarose gel electrophoresis.

3.12.3 Doxycycline administration

DOX was administered to mice via drinking water (2 mg/ml) plus 5 % sucrose to mask the bitter taste; protected from light, renewed twice a week) to induce gene expression in the TH-rtTA system and via food pellets (200 mg/kg) to suppress gene expression in the TH-tTA system, respectively. For DOX treatment during embryogenesis, parental mice received DOX already 1 week previous to mating start.

3.12.4 Stereotactic injections

The surgery area was disinfected by whipping with 70 % ethanol and surgical tools were sterilized by immersion in disinfectant and by using a glass bead sterilizer before starting the procedure. The appropriate doses of analgesia and antibiotics were calculated based on the weight of the mice. Mice received preemptive analgesia by subcutaneous injection of buprenorphin (0.05 mg per kg body weight), 30 minutes before surgery. 4 % isofluran in pure oxygen was induced as general anesthesia of mice and maintained with 1.5 % isofluran during surgery procedure. In addition anesthetized mice received an antibiotic treatment by subcutaneous injection of enrofloxacin (7.5 mg per kg body weight) and subcutaneous injection of the non-steroidal anti-inflammatory analgesia carprofen (5 mg per kg bodyweight). Optionally, treatment with carprofen was prolonged after operation by injection every 24 hours. Mice were placed in the

stereotactic apparatus and head fixed using non-puncture ear bars and an incisor adapter (David Kopf Instruments 2006 #922). The body temperature of animal was measured with a rectal probe and maintained at 37 °C using a heating plate (ATC1000 WPI). The fur on the skull was shaved and skin was disinfected using povidone-iodine (Betadine). Subsequently, Lubricant eye ointment was applied to prevent corneal drying during the surgery. Checking the lack of responses to footpad and tail pinching was done before and during the operation to be ensured about surgical anesthesia. A small midline incision was applied in the scalp and skull was exposed and cleaned. Z coordinates of bregma and lambda were measured using a dissection microscope (Olympus SZ51), and equalized by adjusting the head position. Dividing the distance of bregma and lambda by the standard distance 4.2 mm of the mouse brain atlas (George Paxinos and Keith B.J. Franklin, Academic Press, 2005) was calculated as correction factor to adjust coordinates for injections to the actual skull size. Using a dental drill (NSK IH-300), a small craniotomy was drilled above the area of the substantia nigra and the dura was carefully perforated using a 30 gauge injection needle. The surface of the skull was kept moist with sterile PBS. For injections, thin-walled borat glass pipettes were used which have been made by Sutter Instruments. For that, glass pipettes were pulled on a P-97 (Sutter Instruments: Heat=530 Pull=255 Vel=255 P=300), broken back using a razor blade to a length of 4.3 mm and a tip opening of approximately 25 μm and back-filled with mineral oil and attached to a 10 μl syringe (Hamilton). Using an automated micropump (Injectomate Neurostar) virus solution was soaked up and injection pipette was slowly and carefully lowered to the desired coordinates for stereotactic injection in the substantia nigra: bregma: -3.15 mm, lateral: 1.2 mm, ventral: 4.2 mm. A volume of 1 μl virus solution was injected at a rate of 0.2 μl per minute into the substantia nigra region. To avoid backflow of virus, injection pipette was left in place for additional 5 minutes before slowly withdrawing. Craniotomy was sealed with bone wax (World Precision Instruments) and using the wound clips the scalp sutured and then sterilized by applying povidone-iodine. Mice were removed from stereotact and transferred back to the home cage. Mice were kept warm on a heating pad until fully recovered from anesthesia and water-soaked chow was provided for them.

3.12.5 Tissue preparation

Mice were transcardially perfused with fixative to prepare tissue for histological analysis. First, mice were deeply anesthetized by intraperitoneal injection of a mixture

of ketamine and xylazine (120 mg/kg and 12 mg/kg, respectively), which was ensured by the absence of any nociceptive responses to tail and toe-pinching. A lateral incision was made just beneath the rib cage and the thorax was opened by carefully cutting the diaphragm and along both sides of the rib cage towards the collarbone to get free access to the heart. A 30 gauge needle was inserted into the posterior end of the left ventricle of the heart and hold in place with a small clamp and then an incision was made at the right atrium to allow outflow of the blood. Using a peristaltic pump at a flow rate of 2.5 ml/min blood was washed out with 50 ml of ice-cold PBS. Before fixation, a small tail biopsy was taken to allow re-genotyping of the mice. For fixing, mice were perfused with 50 ml of ice-cold 4 % PFA in PBS. To remove the brain, the head of the mice was cut off and skin and muscle tissue was taken out to expose the skull. Using fine scissors, the skull was cut sagittally along the midline suture, starting from the cerebellum towards the olfactory bulbs and to prevent damage to the brain the scissors were carefully slid along the inner surface of the skull. Another cut was made rostral to the olfactory bulbs to free them from the inner nose tissue. Using forceps, the skull was carefully pulled off and opened along the midline and brain was gently freed cutting all nervous connections along the ventral surface of the brain. After removing, brains were collected in 15 ml falcon tubes and post-fixed with 4 % PFA over night at 4 °C while gently rocking. Brains were washed and stored in PBS at 4 °C until further used for histological analysis or transferred to 15% and 30% sucrose for egg embedding procedure after sinking in sucrose. For X-gal staining, transgenic mice expressing β-galactosidase were perfused and post-fixed with 2 % PFA to better preserve enzyme activity. To prepare unfixed tissue for biochemical analysis, mice were killed by cervical dislocation and brains were quickly dissected and were transferred into wells of a 12-well plate floating in liquid nitrogen for fast freezing. A small piece of tail as biopsy was taken from dead mice to allow re-genotyping of the mice. Plates with frozen brains were stored at -80 °C until being further used for dopamine measurements or western blot.

3.13 Biochemical analyses

3.13.1 Preparation of tissue lysates

To get striatum tissue samples, a 2 mm coronal slice from frozen mouse brain was cut on dry ice using razor blades at approximate coordinates bregma -0.5 to 1.5 mm.

Striatum was punched out with 2 mm inner diameter tissue sample corers (FST #18035-02). Ventral midbrain tissue from substantia nigra was punched out with 1 mm inner diameter corers (FST #18035-01) from 1.5 mm coronal brain slices at approximate coordinates bregma -3.8 to -2.3 mm. To prepare tissue lysate for western blot analysis, tissue of both hemispheres was transferred into a glass douncer with 200 µl western blot lysis buffer and pestled 30 times on ice with 10 minutes break after each 10 strokes. Homogenized lysates were spinned at 13000 g in a table top centrifuge at 4 °C for 10 min to pelletize insoluble components. Supernatants were aliquoted and stored at -80 °C or immediately used for western blot analyses and to determine protein concentrations. Tissue from punched striatum for HPLC measurements was homogenized like western blot samples using HPLC-lysis buffer. Lysates were cleared by ultra-centrifugation at 48000 g for 30 min. Supernatants were used for HPLC measurements, while pellets were used to determine protein concentrations. For that, pellets were dried and re-dissolved in 200 µl western blot lysis buffer by applying sonication.

3.13.2 Determination of protein concentration

Protein concentrations of tissue lysates were determined using the Pierce™ BCA protein assay kit (Thermo Scientific #23225) according to manufacturer´s instructions. 10 µl of diluted sample was mixed with 80µl BCA working reagent in a 96-well plate. Plate was incubated for 20 min at 37 °C and absorbance was measured at 565 nm using an absorbance plate reader (BioTek). BSA standards with concentrations ranging from 0-10 µg/µl were measured and a standard curve was prepared. All samples were measured in triplicates. For HPLC samples, the volume of the re-dissolved protein pellet was measured and multiplied with the protein concentration to get the total protein content of the homogenized tissue.

3.13.3 Dopamine measurements by HPLC

The concentrations of monoamines and its metabolites were measured by reversed phase HPLC with electrochemical detection. For that, dissected mouse striatal tissue was homogenized in 0.1 M perchloric acid containing 0.5 mM disodium EDTA and 100 ng/mL, 3,4-dihydroxybenzylamine (internal standard) and then centrifuged at 50,000 g for 30 min. Pellets obtained were re-suspended in 200 µL neutralizing buffer (lysis buffer used for Western blotting) for protein determination using BCA (as described in

3.4.2). The supernatants after filtering through a 0.22 µM PVDF membrane were subjected to HPLC electrochemical detection system analysis using the method of Yang and Beal (Yang and Beal 2011) with some modifications. 3,4 dihydrobenzylamine (100 ng/mL lysate buffer) was used as internal standard and flow rate of the mobile phase was set to 1.2 mL/min. A 20µl of samples were injected onto a C18 reverse-phase HR-80 column (ESA, Bedford, MA). Chromatograms of monoamines and its metabolites were recorded by electrochemical detectors (coulometric electrodes, ESA model 5011 / 5020) applying following potentials: Conditioning cell +10 mV; Analytical cell channel 1 +50 mV / channel 2 +360 mV. The retention times of the measured metabolites were: DOPAC (3.80 min), 3,4-dihydroxybenzylamine (4.25 min), dopamine (6.88 min) and HVA (10.30 min). Amount of monoamines and its metabolites were calculated from peak area and normalized with the peak areas of internal standard to obtain the total amount DA and its metabolites present in the injected sample volume and the final values were represented as nanogram per milligram of striatal protein.

3.13.4 SDS-PAGE and Immuno blot

Sodium dodecyl sulfate polyacrylamide gel electrophoresis (SDS-PAGE) was applied for separating proteins according to their molecular weight. Using a Hoefer SE 600/400 16-cm system with 1.5 mm spacers and Teflon combs, 10 % (w/v) acrylamide mini gels and 4% stacking gels were prepared according to the following scheme:

	separating gel 10 %	stacking gel 4 %
autoclaved, distilled water	4.05 ml	3.05 ml
acrylamide 30 %	3.3 ml	0.65 ml
Tris 1.5 M pH 8.8, 0.4 % SDS	2.6 ml	
Tris 0.5 M pH 6.8		1.3 ml
APS10%	50 μl	50 μl
TEMED	5 μl	5 μl
total volume	10 ml	5 ml

Samples with 20-100 μg protein were mixed with equal volumes of protein loading buffer and heated for 5 min at 95 °C before being loaded into the wells of the gel. A well was loaded with pre-stained protein molecular weight standard (in kDa). PAGE

was performed at 110 V for approximately 2 h until bromphenol blue tracking dye has reached the bottom of the separating gel.

After protein separation by SDS-PAGE, proteins were transferred onto PDVF membranes. For western blotting, PDVF-membranes were activated in methanol for 5 min and transferred to blotting buffer together with 6 Whatmann blotting papers. Blot was assembled in the following way: 3 sheets of blotting paper, gel with membrane on top, 3 sheets of blotting paper. Western blot was carried out in a semi dry transfer cell device with 1 mA/cm2 (for 1 blot: ~0.12 A) for 1 h. Efficiency of protein transfer was confirmed by reversible staining of the membrane with Ponceau S. Membranes were blocked in blocking solution (5% BSA powder in TBS-T) for 1 h at room temperature while gently rocking on a horizontal shaker. Next, membranes were transferred onto the inner surface of 50 ml plastic falcon tubes and incubated with 10 ml of primary antibody (Table 3.6) diluted in blocking solution on a rolling mixer at 4 °C over night. After incubation in primary antibody, the membrane was washed 5 times with 50 ml TBS-T for 5 min with constant agitation on a horizontal shaker. Horse radish peroxidase (HRP)-conjugated secondary antibody (Table 3.7) diluted in blocking solution was applied to the membrane. After incubation for 1 h at room temperature in 50 ml falcon tubes on a rolling mixer, the membrane was washed 5 times in TBS-T again followed by one time in distilled water. Immunodetection was achieved by incubating the membrane fro 1-2 min in ECL solution. Chemiluminescent signals were detected with an Image Reader LAS-4000 system according to manufacturer´s instructions. The chemiluminescent signals were saved as pictures by the image reader at pre-determined time points and later quantified using the Image Studio Lite (from LI-COR).

3.13.5 Measurement of Cellular ATP Levels in mouse brain tissue

Punched SN tissue samples from mouse brain were homogenized in 200 μL of pre-cooled ATP assay buffer provided in the kit (ATP Assay Kit - Abcam) using Teflon Dounce. Small volume of the homogenate was used for protein concentration determination using BCA kit (as described in 3.4.2.1). The rest of the homogenate was centrifuged at 14000g for 15 min and 50 μL of the supernatant was used to perform fluorometric ATP assay according to the kit manufacturer's instructions.

3.13.6 Mitochondrial enrichment and Complex I activity from SN tissue samples

Punched SN tissue samples were homogenized in 1 ml pre-cooled homogenization buffer containing 320 mM sucrose, 5 mM Tris pH-7.4, 2 mM EGTA along with appropriate amounts of protease inhibitor cocktail (Roche). After ten strokes with Teflon dounce, the lysates were centrifuged for 3 min at 2000g to remove nuclei and other cell particles. Supernatants were collected and centrifuged for 10 min at 12,000g to pellet mitochondria and synaptosomes. The crude pellet was resuspended in 1 ml of homogenization buffer containing 0.02% w/v of digitonin to disrupt synaptosomal membranes and release trapped mitochondria (Palacino *et al*., 2004). The re-suspended samples were centrifuged for 10 min at 12,000g to pellet mitochondria, which were again re-suspended in 100 µl of the homogenization buffer, and protein content was determined by BCA assay (as described in 3.4.2). Complex I enzyme activity assay was performed using the complex I enzyme activity microplate assay kit (Abcam) according to the manufacturer's instruction with 30 µg protein from the enriched mitochondrial preparations.

3.14 Histological methods

3.14.1 Tissue embedding and sectioning

For cryo-sectioning, perfused mouse brains were incubated in 15% sucrose and subsequently in 30 % sucrose at 4 °C until saturated. Brains were cut sagittally along the midline and the two left and right hemispheres were embedded separately. Tissue was frozen on dry ice either in egg yolk or in TissueTekR O.C.T.™. For egg yolk embedding, 10 % (v/v) sucrose was dissolved in egg yolk by stirring over night at 4 °C. Polymerization and hardening was initiated by adding 5 % (v/v) glutaraldehyde on ice and the mixture was immediately used for embedding of tissue. Embedded tissues were stored at -80 °C until further processed. Egg yolk embedded brains were cut into 30 µm coronal or sagittal sections and collected free floating as serial sections in a 24-well plate in cryoprotection solution. Plates with sections were stored at -20 °C freezer. In contrast, brains in TissueTekR O.C.T.™ were cut on a cryostat into 20 µm coronal sections and directly mounted on SuperFrost slides.

3.14.2 β-galactosidase staining

To stain for β-galactosidase activity, sections were first incubated in 0.5 % EGTA (v/v), 20 mM MgCl2 solution in PBS at room temperature for 15 min and sub-sequentially washed 3 times in washing buffer (2.5 mM MgCl2, 0.02 % (v/v) Tween 20 in PBS) for 15 min each at room temperature. Sections were stained in X-gal solution in dark at 37°C for 1 h to overnight depending on the level of β-galactosidase activity. Chromatic reaction was stopped by incubation the sections in 4 % PFA on ice for 10 min, followed by washing 3 times in PBS for 15 min at room temperature. Sections were either mounted or further used for co-staining with TH antibody.

3.14.3 Immunohistological staining

All immunohistological stainings were performed using free floating sections, besides striatal fiber immunofluorescent staining which was done with mounted sections to better preserve fiber histology during staining procedure. In general, all stainings were performed according to the following procedure: Sections were first blocked for 1-2 h in 5 % BSA, 0.3 % Triton X-100 in TBS in room temperature, then incubated with first antibody (Table 3.6) diluted in 2 % BSA, 0.1 %Triton X-100 in TBS at 4 °C overnight. Sections were washed three times in TBS for 15 min and incubated in secondary antibody (Table 3.7) diluted in 2 % BSA, 0.1 %Triton X-100 in TBS at 4 °C overnight, again washed three times in TBS for 15 min. stained sections were mounted in aqueous mounting medium (CelvolR205), or in case of immunofluorescent stainings, with anti-fading reagent (Fluoromount G), or with mounting medium containing 45% acrylic resin and 55% xylenes (Eukitt) for Nissl staining. To increase sensitivity of stainings, biotinylated secondary antibodies (Table 3.7) combined with avidin-biotin complex (ABC) horseradish peroxidase Vector kit (Table 3.7) or streptavidin-coupled fluorochroms (Table 3.7) were used according to manufacturer´s instructions, and horseradish peroxidase reaction was applied for chromatically staining with diaminobenzidine. For Ret staining, prior to immunodetection of Ret receptor, enzymatic antigen retrieval was performed. Sections and antigen retrieval solution (1 mg/ml pepsin in 0.2 N HCl) were heated to 37 °C in a water bath and warmed sections were incubated in enzyme solution for 3 min, then washed 3 times for 5 min with cold TBS to rinse off the enzyme and stop the reaction.

3.15 Imaging techniques

3.15.1 Microscopy

Transmitted light images were acquired using a SZX16 stereo microscope equipped with a DP72 camera and cellSens Entry 1.4.1 imaging software (Olympus). DAB stained sections and fluorescent samples were imaged with an epifluorescent upright microscope Axio Imager.M1 (Zeiss, Goettingen, Germany) equipped with an automated stage (Ludl MAC 6000 system) and a Hamamatsu camera C8484 using fluorescent filter sets 1; 10; 15; 46 and 47 and Axiovision software 4.8. Multicolor images of brainbow samples and for co-localization studies were obtained with a Leica TCS SP2 confocal microscope system and 10x (0.3 NA) and 63x (oil 1.32 NA) objectives or Zeiss LSM 700 Confocal microscope system with 10x (0.25 NA) and 40x (oil 1.3 NA) objectives. Confocal images with multiple fluorophores were acquired sequentially by using a 458-nm Argon laser line for mTFP and Cerulean, a 488-nm Argon line for EGFP and Alexa 488, a 514-nm Argon line for EYFP and Venus or a 561-nm photodiode laser for DsRed, tdTomato, mCherry and Alexa 555. Image stack were maximally projected and contrast and intensity levels were uniformly adjusted using ImageJ (NIH).

3.15.2 Fluorescence and bioluminescence *in vivo* imaging

Bioluminescence imaging was performed by using the *In Vivo* Imaging System IVIS 200 and Living ImageR 3.2 software (Caliper Life Science) according to manufacturer´s instructions. Mice were anesthetized by isofluran inhalation and the fur of the head was removed by applying hair removal cream (Veet) and a shaver. Before image acquisition, a photographic image was taken to set the position of the mice inside the detection chamber. For bioluminescence imaging, mice were intraperitoneally inoculated with 200 µl (10 µl per g of bodyweight) of an aqueous solution of D-luciferin (15 mg/ml; 150 mg per kg of bodyweight). Images were acquired every 5 min during 20 min period, routinely starting 5 min after luciferin administration with automatic binning. Maximum of luminescence signal of all images was considered for quantifications. Bioluminescence image signals were displayed in units of photon radiance (photons/sec/cm2/sr).

3.16 Quantifications and statistics

3.16.1 Fluorescence intensity measurements

To correlate protein expression levels in tissue with fluorescence intensities, and for co-localization studies, immunofluorescent stainings was performed using at least 3 coronal sections representing different parts of the regions of interest of 3 different mice per genotype. Grayscale images were acquired and fluorescence intensities were measured as mean pixel intensities using ImageJ (NIH) program. To measure pixel numbers in of individual cells in each image, the image was duplicated and one copy was converted to a binary mask via thresholding. The binary image was redirected to the original grayscale image and mean pixel intensities were measured using the "Analyze Particles" function. The average Intensities of all cells and sections were obtained to compare mice with different genotype. For co-localization studies, at least 150 cells were counted from each mouse using the cell counter plugin in the imageJ program (NIH).

3.16.2 Fiber density measurement

The measurements of striatal fiber density were performed as described by Kowsky and colleagues (2007). Confocal pictures of TH immunofluorescent stainings were taken using 6 sections equally distributed between bregma +1.10 and −0.10 mm. For every section, three pictures in the dorsal striatum and two pictures in the ventral striatum were acquired. In order to automatically delineate the fibers and to increase the signal-to-noise ratio, the images were first thresholded and then quantified with an automatic counting-grid macro implemented in the Metamorph software (Molecular Devices, Sunnyvale, California, United States).

3.16.3 Quantification of cell populations

Stereological countings were performed with the optical fractionator method of the StereoInvestigator software (MicroBrightField, Williston, Vermont, United States) on 30 μm coronal serial sections analyzing every sixth section for the SNpc and VTA. Counting was done blinded for genotype, using an oil immersion 63x objective, a counting frame of 50 x 50 μm, and a grid size of 100 x 100 μm. To assess specificity

and efficiency of transgene expression, cell countings were performed on at least 3 representative sections per mouse, either by hand or by applying a binary mask and the "Analyze Particles" function in ImageJ (NIH).

3.16.4 Quantification of soma size

TH immunostained coronal sections of mouse brain were analyzed using a bright field microscope with a 63x objective. All the cells in the SNpc and VTA regions were selected using optical fractionator work flow and soma size was determined using the 'nucleator' probe in the StereoInvestigator software (MicroBrightField, Williston, Vermont, United States). The experiments were done blinded to the genotype of each animal (4 different genotypes).

3.16.5 Astrocyte and microglial density quantifications

Every sixth section of 30 μm thick coronal brain sections from the striatum and the midbrain was used to determine the density of astrocytes (immunostained for GFAP) or microglial cells (immunostained for Iba1) in the dorsal striatum and SNpc respectively. For each section, the area containing labeled cells was counted using optical fractionator work flow of the StereoInvestigator software. For Iba1 cell types at least 100 cells per section were counted in the trace area and distinguished by its different type. The average from all sections in each mice used for final statistics.

3.16.6 Statistical analysis

Data are expressed as mean+/-s.e.m. The statistical analyses were performed with GraphPad Prism 5.0 (GraphPad Software) using two-tailed, unpaired Student´s t-test or ANOVA, followed by Tukey's post hoc test to compare group means. In all analyses a p-value of smaller than 0.05 was considered statistically significant.

4. Results

4.1 Establishment of new TH-tet mouse lines specific for dopaminergic system

4.1.1 Characterization of new TH-tTA and TH-rtTA mouse lines

The newly generated TH-tTA and TH-rtTA transgenic mice (Tillack thesis, 2013; Tillack *et al*., 2015) were crossed with LC1 mice (Schonig *et al*., 2002) and Rosa26R reporter mice (Soriano *et al*., 1999) for characterization. First the characterization of the TH-tTA mouse lines has been done. In these triple-transgenic TH-tTA/LC1/Rosa26R mice, tyrosine hydroxylase promoter drives expression of the tetracycline-controlled transactivator (tTA). tTA specifically binds to the tetOperon (tetO) sequence, which can be prevented by tetracycline or its derivatives such as doxycycline (DOX). The presence of DOX prevents the binding of tTA to tetO, thereby inactivating the expression system and termed as ''TH-tet off''.

In the absence of DOX, the transactivator binds to the tetOperon on the LC1 transgene and leads to activation of a bidirectional tetO promotor which drives expression of luciferase (L) which can be used for non-invasive bioluminescence *in vivo* imaging and expression of cre (C) which can be used for inducible gene recombination or gene expression. The Cre recombinase triggers the deletion of a floxed transcriptional termination cassette in the R26R transgene and activates LacZ gene expression. The LacZ gene encoded β-galactosidase enzyme converts the X-gal substrate into a blue precipitate (Figure 4.1A). Thus, cells expressing lacZ can be easily visualized by a blue colored staining and β-galactosidase activity in mDA neurons can be detected. Specificity and inducibility of lacZ reporter gene expression was analyzed in triple-transgenic TH-tTA/LC1/R26R mice to characterize the founders. Adult mice without any DOX treatment at the age of 12 weeks from different founders were characterized using X-gal staining. Accordingly, β-galactosidase enzyme expression was active during development and adulthood of the mice and staining on mouse brain tissues showed β-galactosidase activity in four TH-tTA founders (Founders 1-4) (Figures 4.1B and 4.2A) out of nine and the rest didn't show any staining. X-gal staining detected in DA cells of the SNpc, VTA, olfactory bulb, retrorubral field and noradrenergic cells of the locus coeruleus (LC) (Tillack thesis, 2013; Tillack *et*

al., 2015) with similar expression pattern in all four founders. As a result of early expression of endogenous TH enzyme at embryonic day E10.5, X-gal staining was not only obvious in CA neurons, but also in other regions such as cerebellum, striatum, pons, hippocampus, thalamus and cortex (Tillack thesis, 2013; Tillack *et al*., 2015).
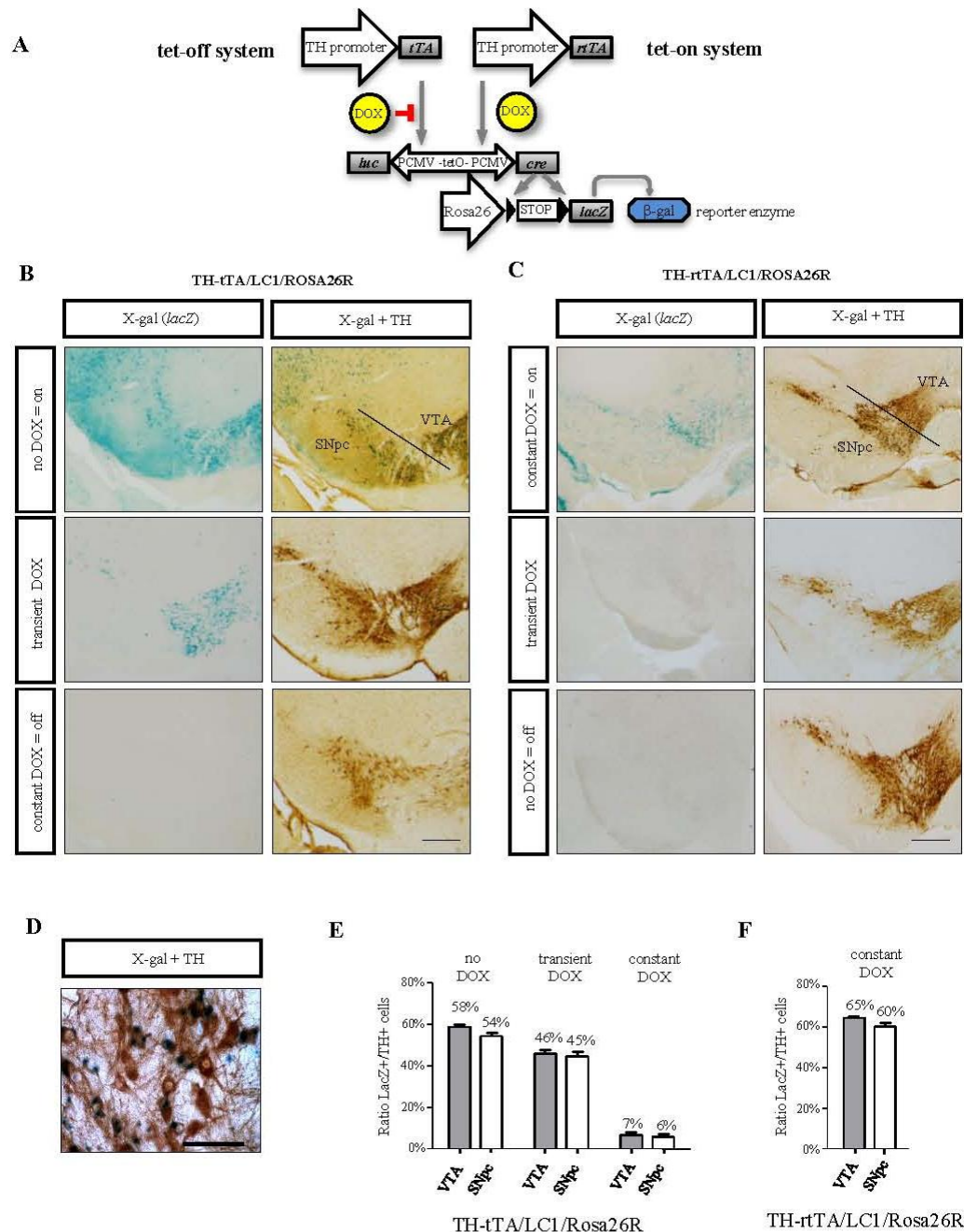
Figure 4.1 Specificity, inducibility and efficacy of gene expression in TH-tTA/LC1/Rosa26R and TH-rtTA/LC1/Rosa26R mice

(A) Genetic scheme of DOX-regulated reporter gene expression in TH-tTA and TH-rtTA mice crossed with LC1 and Rosa26R reporter mice. (B and C) Coronal midbrain sections with SNpc and VTA DA neurons of TH-tTA/LC1/Rosa26R (B) and TH-rtTA/LC1/Rosa26R (C) mice raised without and with DOX or transiently with DOX to have the system switched off during development (TH-tTA mice treated with DOX during pre- and postnatal development till 6 weeks of age; TH-rtTA mice raised without DOX) and on during analysis (TH-tTA mice from the age of 6 weeks without Dox; TH-rtTA mice from the age of 6 weeks with DOX). Sections were stained for β-galactosidase activity with X-gal to visualize cells with activated tet-system. Adjacent sections were X-gal stained and co-stained with TH antibodies and DAB substrate (brown) to mark DA neurons. (D) Zoom in picture of TH and lacZ double positive cells in the SNpc. (E and F) Quantification of TH and lacZ double positive cells (LacZ+TH+) in the SNpc and VTA to estimate recombination efficacy in DA neurons (TH+) of animals treated constantly (constant DOX), transiently (transient DOX) or without DOX (no DOX) in the TH-tTA (E) and TH-rtTA mice (F). (n = 3, data are represented as mean +/- s.e.m., Scale bars: 500 µm (B and C), 50 µm (D) (partially provided by Karsten Tillack).

Characterization of the TH-rtTA mutant mice was done according to the same paradigm applied to TH-tTA founders using X-gal staining (Figures 4.1C and 4.3A). The difference between TH-rtTA and TH-tTA mice is reverse DNA binding properties in response to DOX and it binds to tetO sequences only in the presence of DOX. Therefore, to switch on the tet-system in TH-rtTA founders, mice obtained DOX in the food or water. To obtain mice in which the systems are constantly switched on also during development, not only the mice were kept constantly on DOX but also their parents received DOX food before and during pregnancy. A broad expression of β-galactosidase in the SNpc and VTA (Figures 4.1C and 4.3A), as well as in the hippocampus, striatum, cerebellum and olfactory bulb with similar expression pattern in all five founders were observed (Tillack thesis, 2013; Tillack *et al*., 2015).

To test the regulation of the TH-tet system in TH-tTA mice, first TH-tTA/LC1/Rosa26R mice were fed constantly with food containing DOX (200 mg/kg) to switch the system off and the mice showed only a few X-gal positive cells (Figures 4.1B and 4.2A).
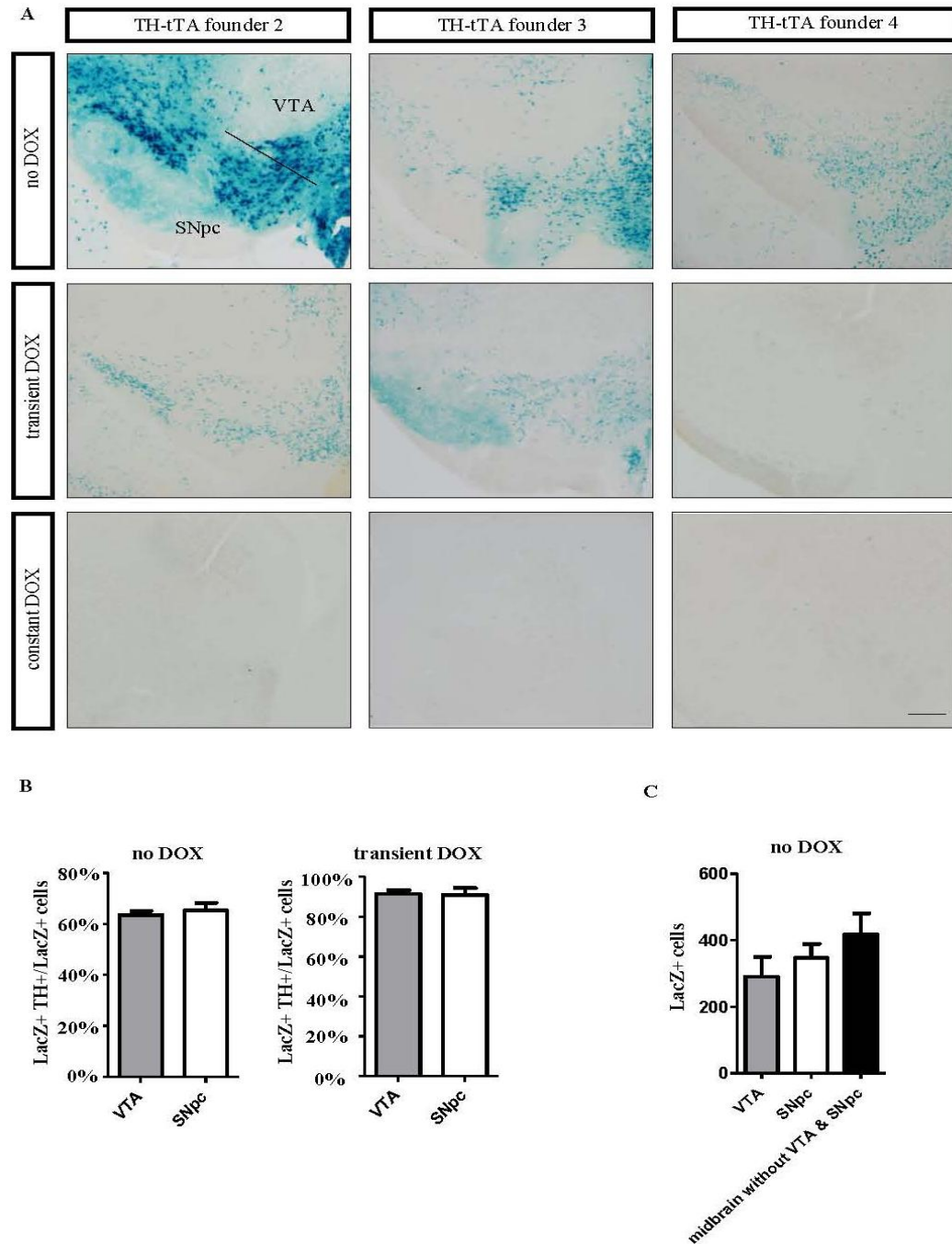
Figure 4.2 Specificity, inducibility and efficacy of gene expression in additional TH-tTA founders after crossing them with LC1 and Rosa26R mice

(A) Coronal midbrain brain sections with SNpc and VTA DA neurons of TH-tTA/LC1/Rosa26R for founders 2, 3, and 4, respectively. Mice were raised without (no) DOX, with (constant) DOX or with DOX until the age of 6 weeks followed by 6 weeks without (transient) DOX. Sections were stained for β-galactosidase activity with X-gal to

visualize cells with activated tTA, LC1 and ROSA26 locus. Scale bars: 500 µm. (B) Ratio of lacZ and TH double positive cells to all lacZ positive cells in the SNpc and VTA in TH-tTA/LC1/Rosa26R without or transient DOX treatment as indicated. (C) lacZ positive cells in the VTA, SNpc and ventral midbrain without VTA and SNpc in non DOX treated TH-tTA/LC1/Rosa26R mice (n = 3, data are represented as mean +/- s.e.m.) (partially provided by Karsten Tillack).

This suggests that the TH-tet system could be efficiently blocked in TH-tTA mice by applying DOX with little leakage in DA neurons and other cells. Second, TH-tTA/LC1/Rosa26R mice were transiently treated with DOX food until weaning and evaluated after 6 weeks without DOX. In these mice β-galactosidase expression was detected and showed a successful specific activation in the midbrain DA neurons (Figures 4.1B and 4.2A). To evaluate tet-system inducibility in TH-rtTA founders, TH-rtTA/LC1/Rosa26R mice were first raised on DOX and showed intensive β-galactosidase staining (Figure 4.1 C). Next, we raised them without DOX and the mice started to receive DOX food at the age of 6 weeks to induce expression of the β-galactosidase reporter enzyme. Surprisingly, no β-galactosidase activity was observed in SNpc and VTA or other brain regions. Similar results were observed when mice treated completely without DOX (Figures 4.1C and 4.3A).

To test the specificity of expression in TH-tTA and TH-rtTA mice, X-gal stained sections were co-stained with TH antibody to quantify the double positive cells. The percentage of X-gal/TH positive cells in TH-tTA/LC1/Rosa26R mice without DOX treatment was in average 54% in SNpc and 58% in VTA, whereas this percentage in transiently treated mice with DOX food was 45% for SNpc and 46% for VTA (Figure 4.1E). The same procedure in the TH-rtTA/LC1/Rosa26R mice showed 60% specificity for SNpc and 65% for VTA (Figure 4.1F). These results suggest an incomplete targeting of mDA neurons in the TH-tTA and TH-rtTA mice.

In TH-tTA/LC1/Rosa26R mice raised without DOX and TH-rtTA/LC1/Rosa26R mice raised with DOX, around 60% of X-gal positive cells in SNpc and VTA were also positive for TH (Figures 4.2B and 4.3B), whereas, in transiently treated TH-tTA/LC1/Rosa26R mice with DOX, most of the X-gal stained cells (around 90%) co-localized with TH, suggesting a more DA system specific targeting during adulthood (Figure 4.2B). The observed X-gal positive/TH negative cells during adult specific activation are most likely

due to cells expressing TH mRNA without TH protein and thereby activation also the TH promoter in the TH-tTA and TH-rtTA constructs, while activation during development targets in addition cells that activate the TH promoter only during development and not in adulthood (Figures 4.2B, 4.2C, 4.3B and 4.3C).
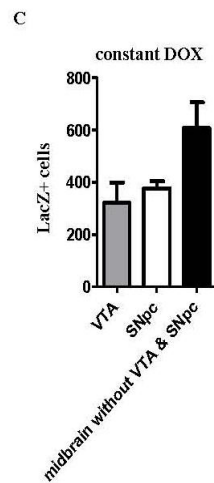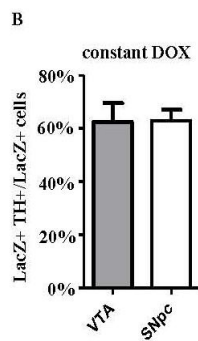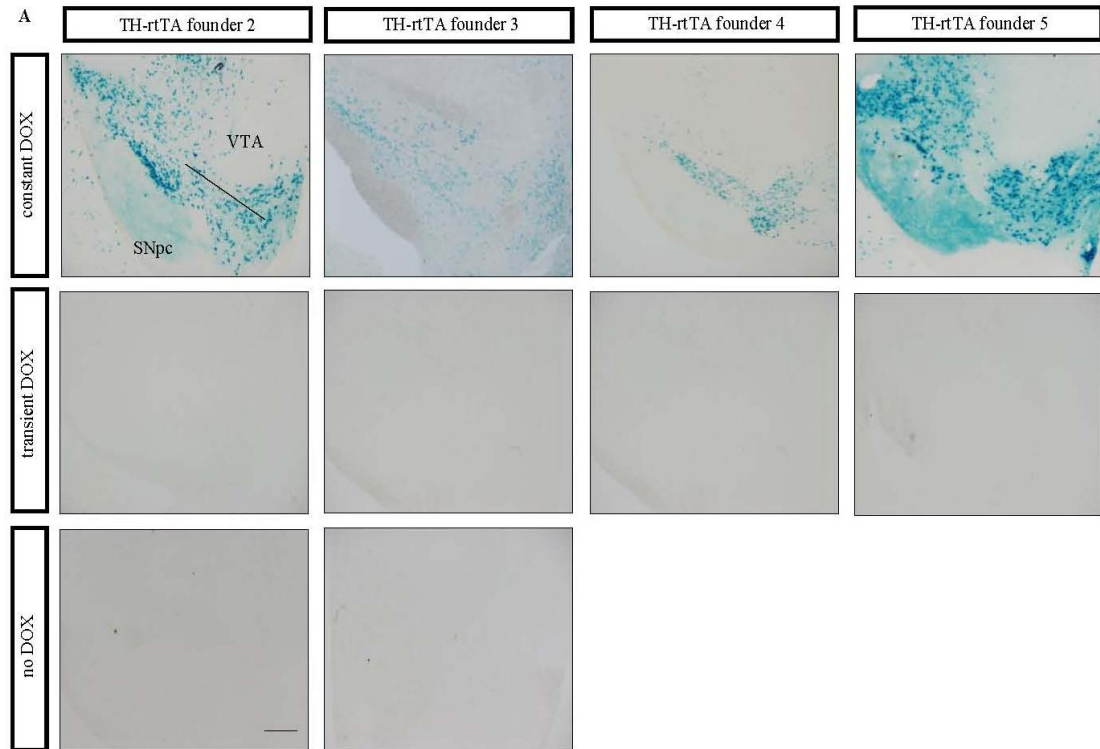
Figure 4.3 Specificity, inducibility and efficacy of gene expression in additional TH-rtTA founders after crossing them with LC1 and Rosa26R mice

(A) Coronal midbrain brain sections with SNpc and VTA DA neurons of TH-rtTA/LC1/Rosa26R for founders 2, 3, 4, and 5, respectively. Mice were raised with (constant) DOX, without (no) DOX, or transiently without DOX until the age of 6 weeks followed by 6 weeks with (transient) DOX. Sections were stained for β-galactosidase activity with X-gal to visualize cells with activated rtTA, LC1 and ROSA26 locus. Scale bars: 500 µm. (B) Ratio of lacZ and TH double positive cells to all lacZ positive cells in the SNpc and VTA in TH-rtTA/LC1/Rosa26R with constant DOX treatment. (C) lacZ positive cells in the VTA, SNpc and ventral midbrain without VTA and SNpc in constantly DOX treated TH-rtTA/LC1/Rosa26R mice (n = 3, data are represented as mean +/- s.e.m.) (partially provided by Karsten Tillack).

4.1.2 Genetic silencing of the LC1 and its independent targeting of adult DA neurons in TH-tTA and TH-rtTA mice

The lack of expression in adult TH-rtTA/LC1/Rosa26R mice after DOX treatment during development and reduced number of X-gal positive cells in transiently DOX-treated mice, might be due to epigenetic silencing of the LC1 transgene during development that cannot be re-activated later again (Zhu *et al*., 2007; Oyer *et al*., 2009).

An AAV vector encoding the fluorescent protein Venus under the control of the tetO promoter (AAV-tetO-Venus) was generated to circumvent the possible genetic silencing of the LC1 construct in TH-rtTA/LC1 mice. AAV-tetO-Venus DNA construct was tested in HEK293-T cells co-transfected with a tTA expression vector and found a DOX-dependent expression of Venus (Tillack thesis, 2013; Tillack *et al*., 2015). After AAV-tetO-Venus virus production, stereotactic injection was performed in the SN of adult DOX-treated TH-rtTA mice and non-DOX treated TH-tTA mice (Figure 4.4). Five weeks after injections, mDA neurons of the relative mice were investigated for Venus expression using TH staining.

Quantification of DA neurons in TH-tTA mice showed 67% and 27% Venus positive cells in non-DOX treated mice and mice started to be treated with DOX 10 days before injection, respectively (Figures 4.4A, 4.4B, 4.4E and 4.5A). In TH-rtTA mice treated with DOX 73% of DA neurons were expressing Venus, while no DOX treated ones expressed only 23% of Venus (Figures 4.4C-4.4E and 4.5B). In control non-transgenic mice, only 5% of TH positive cells were also positive for Venus (Figures 4.4E and 4.5C), which can be explained with auto-activation or leakiness of the tetO promoter in the AAV-tetO-Venus as seen

already in transfected HEK293-T cells (Tillack *et al.*, 2015). Therefore, inducing the TH-rtTA construct in TH-rtTA mice with a transient postnatal DOX treatment is possible and silencing of the LC1 construct in the non-DOX treated TH-rtTA/LC1/Rosa26R mice seems to be the problem. In summary, TH-tTA and TH-rtTA mouse lines allow a regulated gene expression during adulthood that can be achieved by injecting a virus encoding a tetO regulated gene.
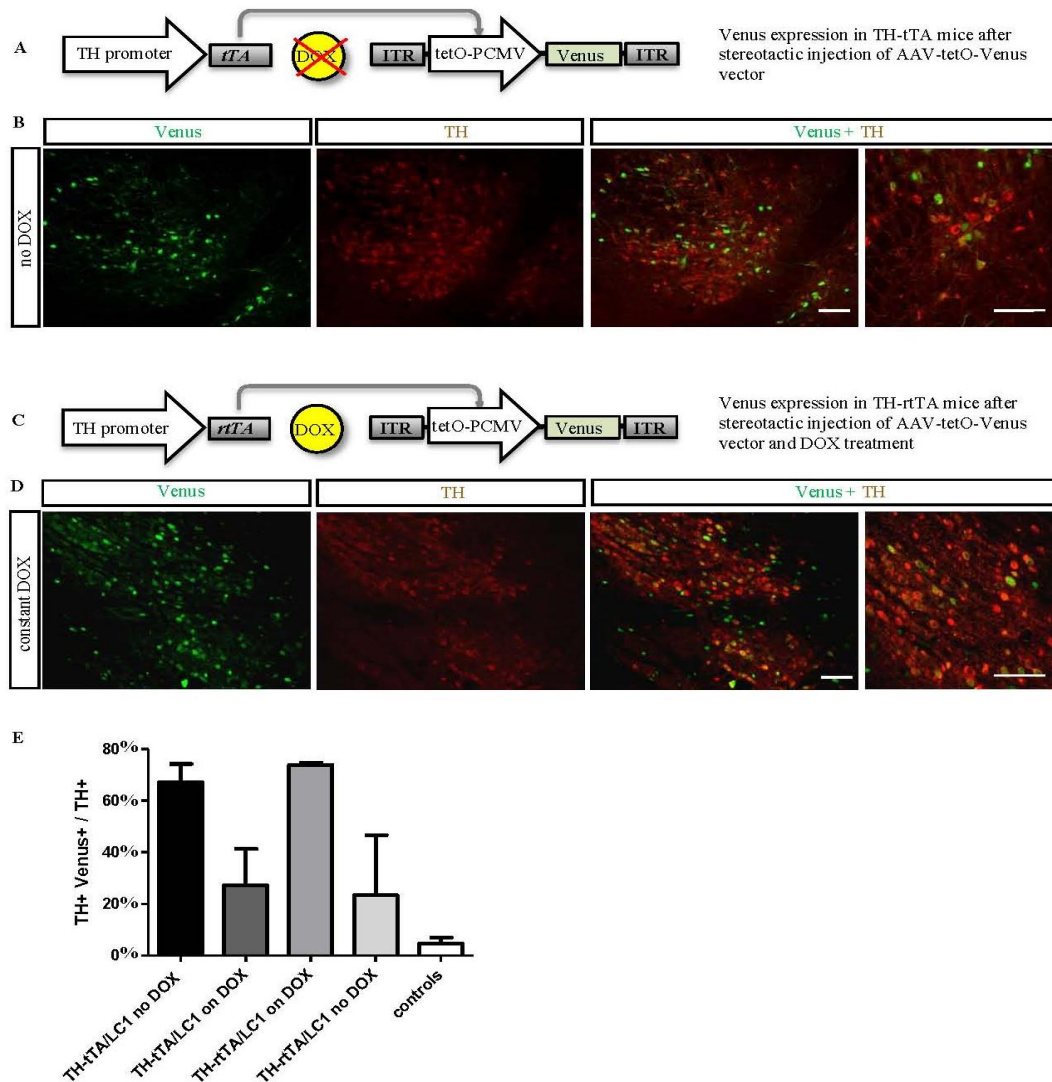
Figure 4.4 Cre independent adult gene expression in DA neurons of TH-tTA and TH-rtTA mice using a AAV-tetO-Venus vector

(A) Scheme of fluorescent DA neuron labeling in non-DOX treated TH-tTA mice stereotactically injected with AAV-tetO-Venus vector in the ventral midbrain. (B) Confocal fluorescent pictures of Venus expression (green) in DA neurons co-stained for TH (red) in the SNpc of sagittal TH-tTA mouse brain sections. (C) Scheme of fluorescent DA neuron

labeling in DOX-treated TH-rtTA mice stereotactically injected with AAV-tetO-Venus vector in the ventral midbrain. (D) Confocal fluorescent pictures of Venus expression in DA neurons co-stained for TH in the SNpc of sagittal TH-rtTA mouse brain sections. (E) Quantification reveals that in the on-state 67% and 73% and in the off-state 27% and 23% of TH+ cells are also Venus-positive in TH-tTA and TH-rtTA mice, respectively. In non-transgenic mice (controls) only 5% of TH+ cells were also Venus-positive. (n = 3-5, data are represented as mean +/- s.e.m., Scale bars: 250µm and in high magnification picture 50 µm).
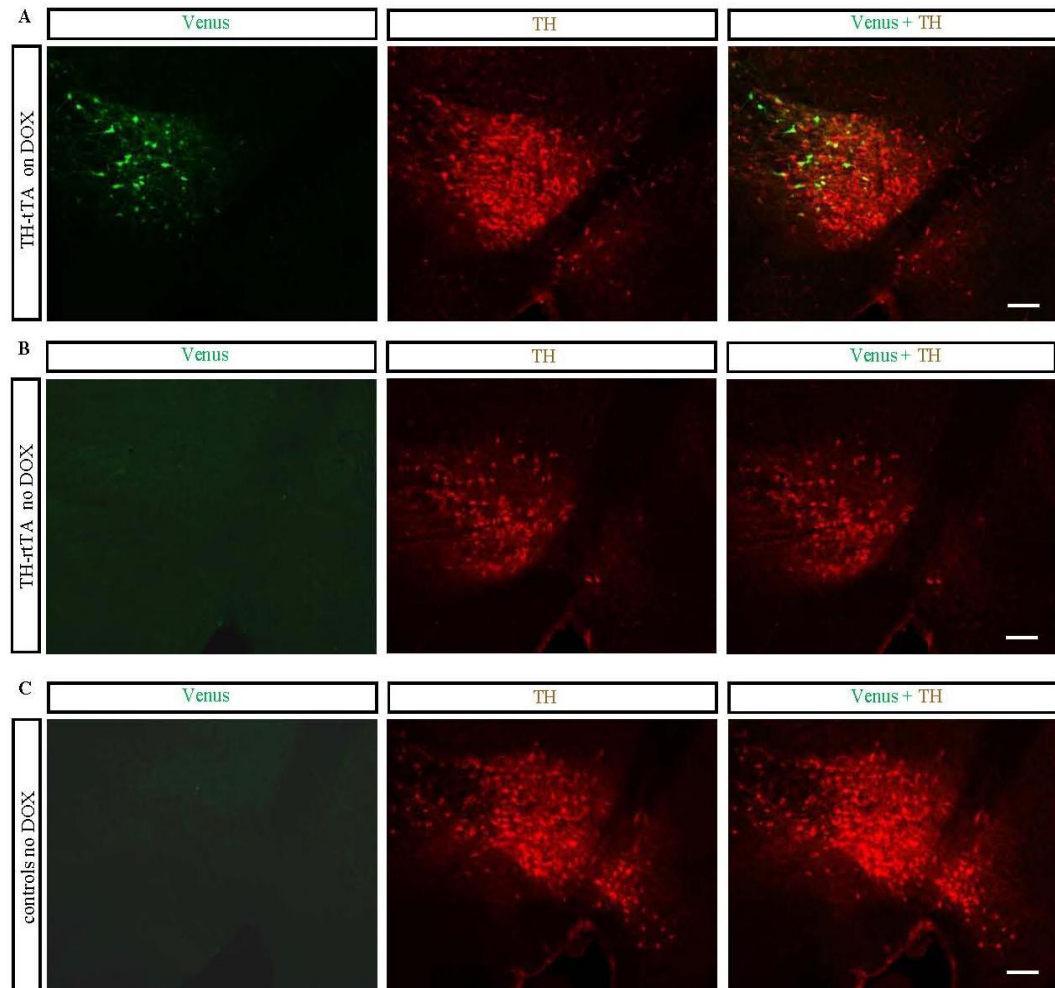
Figure 4.5 Cre-independent adult gene expression in DA neurons of TH-tTA and TH-rtTA mice using a AAV-tetO-Venus vector

(A-C) Confocal fluorescent pictures of Venus expression (green) in DA neurons co-stained for TH (red) in the SNpc of sagittal mouse brain sections 5 weeks after AAV-tetO-Venus virus injection. (A) TH-tTA mice were treated with DOX for 10 days before stereotactic injections until analysis to switch the system off. (B) TH-rtTA mice were here not DOX treated to keep

the system inactive. (C) Non-transgenic control mice were analyzed also 5 weeks after AAV-tetO-Venus virus injection. Scale bars: 250 μm.

4.1.3 Genetic deletion of dopaminergic cells in TH-tTA mice expressing diphtheria toxin-A

To confirm that TH-tTA mice can be efficiently used for regulated gene expression in the DA system, another experiment was performed. The TH-tTA/LC1 mice were crossed with R26dt-a mice to express the diphtheria toxin-a fragment (dt-a) in DA neurons. In triple transgenic TH-tTA/LC1/R26dt-a mice, the tTA protein activates in the absence of DOX Cre recombinase expression that causes the removal of a floxed transcriptional termination cassette in front of the dt-a gene encoded in the Rosa26 locus (Figure 4.6A). Expression of dt-a resulted in specific cell death in the target tissue. TH-tTA/LC1/Rosa26dt-a mice without DOX treatment died shortly after birth with 38% loss of DA cells in SNpc and 40% in VTA (Tillack thesis, 2013; Tillack *et al*., 2015). Whereas, mice parentally and postnatally treated with DOX for 6 weeks survived. Stereological quantification on SNpc and VTA of these mice 6 weeks and 14-30 weeks after removal of DOX using TH staining (Figure 4.6B) showed 18% loss of DA neurons in SNpc and 28% loss of DA neurons in VTA, 6 weeks after removal of DOX which is progressive to 32% for SNpc and 33% for VTA, 14-30 weeks after DOX removal (Figure 4.6C). This confirms of the tight control of the tet-system in TH-tTA/LC1/R26dt-a mice leading to an adult DA neuron loss.
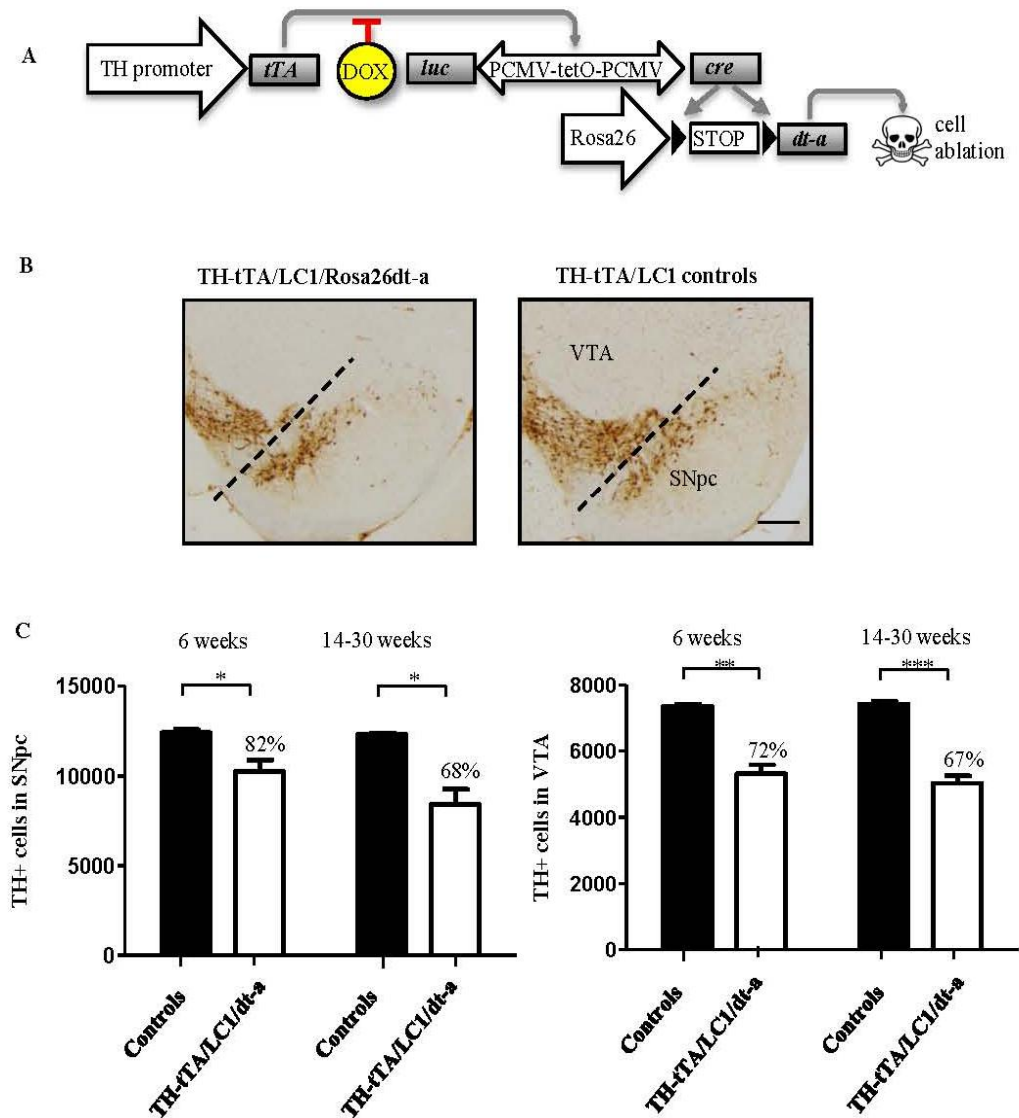
Figure 4.6 Loss of DA neurons in adult TH-tTA/LC1/Rosa26dt-a mice

(A) Scheme of diphteria toxin-a (dt-a) expression in TH-tTA/LC1/Rosa26dt-a mice. (B) TH stained coronal midbrain sections of adult TH-tTA/LC1/Rosa26dt-a mice and control mice raised with DOX till 6 weeks of age followed by 30 weeks without DOX. Scale bar = 500 µm. (C) Stereological quantification of TH-positive cells in the SNpc and VTA of adult TH-tTA/LC1/Rosa26dt-a and control mice raised with DOX till 6 weeks of age followed by 6 or 14-30 weeks without DOX. (n = 3, data are represented as mean +/- s.e.m.; * $p \leq 0.05$, ** $p \leq 0.01$, *** $p \leq 0.001$; Student´s t-test).

4.1.4 *In vivo* detection of bioluminescence in TH-tTA/LC1 and mice THrtTA/LC1 mice

In vivo visualization of the DA system using firefly luciferase expression from the LC1 construct is one of the features of TH-tTA/LC1 and TH-rtTA/LC1 mice (Tillack thesis, 2013; Tillack *et al*., 2015). This method allows us to detect bioluminescence signal originating from DA neurons without any surgical intervention and histological staining and monitor them over time. Karsten Tillack confirmed that administration of luciferase substrate D-luciferin in TH-tTA/LC1 mice without DOX treatment resulted in detection of bioluminescence signal in all openings of the skull, the nose, eyes and ears whereas no signal was detected in control mice (Tillack thesis, 2013; Tillack *et al*., 2015).

To evaluate the capability of TH-rtTA/LC1 mice comparable to TH-tTA/LC1 ones, bioluminescence imaging was done in the same paradigm for TH-tTA/LC1 mice. But this time to improve the bioluminescence imaging to detect even small signals in TH-tet system, a synthetic luciferin, CycLuc1 was applied (Evans *et al*., 2014). As reported recently, CycLuc1 enable us to image luciferase-expressing cells in the brains of living mice that could not be detected with D-luciferin, requiring less substrate and providing more intense and persistent light output. Thus using CycLuc1 in place of D-luciferin expands the scope of bioluminescence imaging and improves the sensitivity of this optical imaging method (Evans *et al*., 2014). It is confirmed that CycLuc1 signal peaked at 4– 5 min post-injection and then reached a steady signal that was up to 100-fold greater than that of D-luciferin, and remained for more than 60 min (Evans *et al*., 2014).

First, TH-tTA/LC1 mice without DOX treatment and TH-rtTA/LC1 mice with DOX treatment and their littermate's controls were anesthetized, shaved and i.p. injected with 100 μl of 5mM CycLuc1 in PBS. Luciferase activity was detected using an IVIS200 device and the picture overlaid with the normal light picture of the mouse to better determine the localization of the signal (Figures 4.7A and 4.7B). Next, mice were euthanized and the skin and skull were removed to reduce light scattering and absorbance for better detection. Brains were removed subsequently and cut sagittally.

A *in vivo* – luminescence- no fur | *post mortem* - no skull | *post mortem* - brain

TH-tTA/LC1 | control | ventral | sagittal

radiance [p/sec/cm²/sr]

1x10e4 — 9x10e4

B *in vivo* – luminescence no fur | *post mortem* - no skull | *post mortem* - brain

TH-rtTA/LC1 | control | ventral | sagittal

radiance [p/sec/cm²/sr]

1x10e4 — 9x10e4

C

TH-tTA/LC1 D-luciferin | TH-tTA/LC1 Cycluc1

Average Radiance [p/s/cm²/sr]

P=0.0293 *

D-luciferin | Cycluc1

TH-tTA/LC1

Total Flux [p/s]

P=0.0373 *

D-luciferin | Cycluc1

TH-tTA/LC1

D

TH-rtTA/LC1 D-luciferin | TH-rtTA/LC1 cycluc1

Average Radiance [p/s/cm²/sr]

n.s P=0.236

D-luciferin | Cycluc1

TH-rtTA/LC1

Total Flux [n/s1]

n.s. P=0.413

D-luciferin | Cycluc1

TH-rtTA/LC1

E

Day 0 | Day 7 | Day 14 | Day 42

radiance [p/sec/cm²/sr]

1x10e4 — 1x10e5

Radiance [p/s/cm²/sr]

Dox treatment

THrtTA/LC1

Control

0   7   14   21   28   35   42   49   days

73

Figure 4.7 *In vivo* detection and quantification of bioluminescence in TH-tTA/LC1 and TH-rtTA/LC1 mice using CycLuc1

> *In vivo* Bioluminescence signal with CycLuc1 substrate in anesthetised TH-tTA/LC1 (A) and TH-rtTA/LC1 (B) mice, after fur removal and in brain tissue of dead mice after removal of skull and in dissected brains. (C-D) Comparison of *in vivo* bioluminescence signals in TH-tTA/LC1 (C) and TH-rtTA (D) mouse receiving D-luciferin or CycLuc1 (n = 3, data are represented as mean +/- s.e.m., *p<0.05, Student´s t-test). (E) Temporal control of bioluminescence signal via DOX treatment in TH-rtTA/LC1 mice. Quantification of luciferase activity in anesthetised TH-rtTA/LC1 and LC1 control mice raised on DOX for 6 weeks and kept during adulthood without DOX. After initial measurement, mice were treated with DOX-containing food for 35 days and afterwards kept without DOX for further 14 days, n=3-8.

The origin of bioluminescence signals were mostly from the olfactory bulb and ventral midbrain and to a lower extent from the striatum and cerebellum (Figures 4.7A and 4.7B). Analyzing the bioluminescence light emitted from mice injected with CycLuc1 instead of D-luciferin showed a significantly stronger signal in the TH-tTA/LC1 and TH-rtTA/LC1 mice despite using 10 times less substrate (Figure 4.7C and D).

To confirm DOX regulation and inducibility of gene expression over time in TH-rtTA system, mice were raised on DOX for 6 weeks and then maintained without DOX during adulthood. These mice showed only a very weak bioluminescence activity that increased after 2 weeks on DOX to the maximal bioluminescence activity with faster kinetics compared to the TH-tTA/LC1 mice (Tillack *et al.,* 2015) and maintain a plateau phase when keeping them on DOX. Subsequently, fourteen days of treating mice without DOX resulted in efficient suppression of luciferase expression and a reduction of bioluminescence levels to the minimal level as before (Figure 4.7E). Thus, TH-rtTA/LC1 mice as well as TH-tTA/LC1 (Tillack *et al*., 2015) mice can be used for *in vivo* monitoring of the DA system over time and the bioluminescence signal can be improved using the new substrate CycLuc1. These results make it likely that TH-tTA/LC1 and TH-rtTA/LC1 mice can be used to follow degeneration and regeneration processes in the same mouse.

4.1.5 Multicolor labeling of dopaminergic cells by stereotactic injection of AAV-dual color Brainbow

Labeling and tracing of single DA neurons is essential for studying PD as innervations in nigrostriatal pathway are lost during this disease. It would also help to understand the developmental processes of the brain and basics of other neurodegenerative disorders. To test whether fluorescence is better than bioluminescence in TH-tet system and to trace different innervations areas, a virus-based combinatorial RGB labeling method for DA neurons and tracing their axons with three fluorophore encoding viruses AAV-LSL-XFP emitting red, yellow/green or blue light (RGB) after Cre mediated recombination has been established by Karsten Tillack in TH-tTA mice. Stereotactic injections of these constructs in the ventral midbrain of TH-tTA/LC1 resulted in specific labeling of DA neurons and their axons and dendrites up to the final innervation area such as the striatum in completely different colors five weeks after injection (Tillack thesis, 2013). So far we published only labeling of DA neurons in red using the AAV-LSL-mcherry vector (Tillack *et al*., 2015). Single DA cell tracing is easier in TH-tTA/LC1 mice compared to other DA cell specific Cre lines (e.g. DAT-Cre mice) due to the targeting of only 60% of the DA neurons which causes less DA cells to be labeled (Tillack *et al*., 2015). However, tracings were so far still only possible close to the cell body due to the still rather large number of labeled cells and sectioning through their axons. Treating the TH-tTA/LC1 mice with DOX and at the same time using a reduced number of viral particles might reduce the amount of labeled cells. Since in addition the color spectrum was not as broad as expected, we wanted to test recently developed alternative AAV vectors for multicolor labeling (Cai *et al*., 2013).

I tried the AAV-dual color Brainbow constructs - a newly improved "Brainbow" tool (Cai *et al*., 2013) - in our TH-tTA/LC1 mice treated transiently with DOX. In these AAV Brainbow constructs, farnesylated TagBFP and EYFP or mCherry and mTFP are placed in reverse orientation between mutant Lox sites (Figure 4.8A). Different fluorescent proteins are only expressed from the AAV-dual color Brainbow construct after Cre induced recombination/flipping with or without deletion of the cDNA for one fluorophore. Outcomes of these recombination events are eight different colors which can generate in combination with different copy numbers of the virus many additional colors (Figure 4.8B).
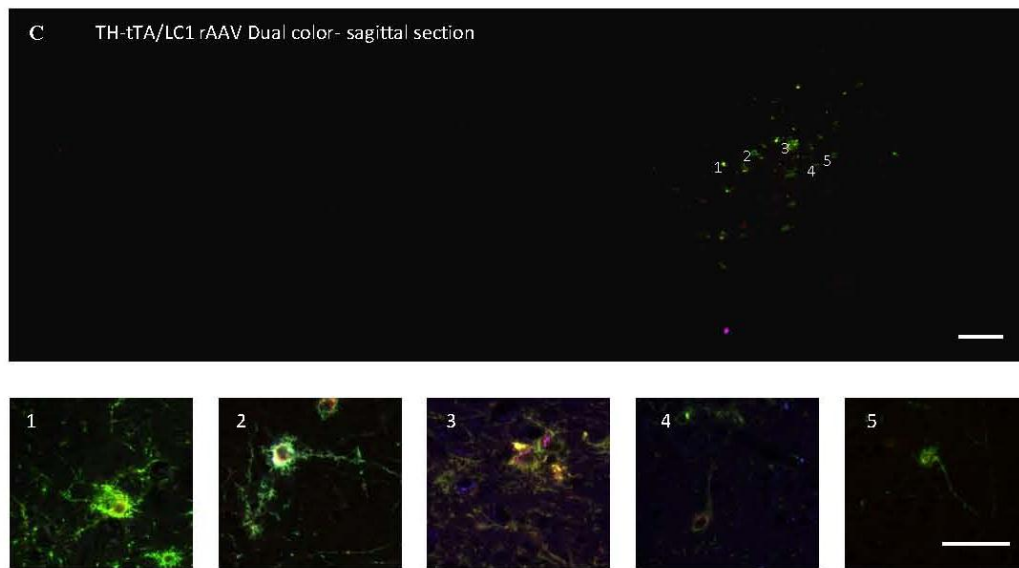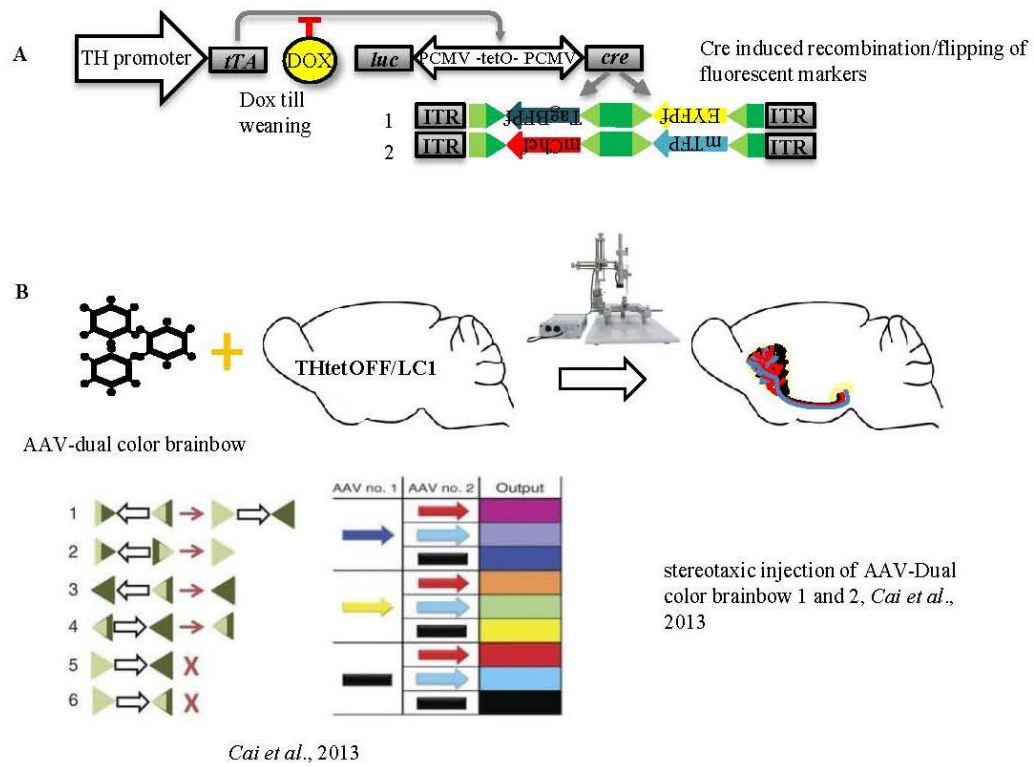
Figure 4.8 Visualization of dopaminergic neurons in mice using stereotactic injection of AAV-dual color Brainbow

(A) Genetic scheme of TH-tTA mice with AAV-dual color Brainbow used for labeling DA neurons. (B) Principle of single DA neuron labeling using TH-tTA/LC1 transgenic mice

stereotactic injected in the ventral midbrain with recombinant adeno-accociated virus encoding different fluorescent proteins (AAV-dual color Brainbow; Cai *et al.*, 2013). Different fluorescent proteins are only expressed from the AAV-dual color Brainbow construct after Cre induced recombination/flipping with or without deletion of the cDNA for one fluorophore. (C) Confocal images of sagittal midbrain of AAV injected mice Scale bars: 200 μm (C) and 20 μm (1-5).

AAV-dual color Brainbow constructs induced to the ventral midbrain of TH-tTA/LC1 mice through stereotactic injections (Figure 4.8B). TH-tTA/LC1 mice have been treated with DOX till 6 weeks of age to reduce the number of cells expressing the virus for improving single cell labeling. Five weeks after injections, mice were perfused and sagittal brain sections investigated by confocal microscope. Due to the application of DOX for 6 weeks in TH-tTA/LC1 mice only some of DA neurons in the midbrain were labeled after AAV-dual color Brainbow injection (Figure 4.8C). The few labeled DA cells which are mostly green in color (Figure 4.8C1-5) indicating preference of these viral vectors and/or the TH-tTA/LC1 mice for flipping/recombining specific lox site that leads to the green color. The axonal fiber bundles and terminals in the striatum didn't show a strong fluorescent expression.

These results show that DOX treatment of the TH-tTA/LC1 mice is beneficial to reduce the number of labeled DA neurons and that our RGB virus vector might allow generation of more colors and a better axonal labeling in DA neurons.

4.2 Inducible gene deletion and transient gene expression in TH-tTA mice as a model of Parkinson's disease

4.2.1 Induced deletion of the neurotrophic receptor Ret in TH-tTA mice

Many studies on animal models of PD have reported beneficial effects of GDNF on nigrostriatal DA neuron survival (d'Anglemont de Tassigny *et al*., 2015; Kramer and Liss, 2015) and stimulating its receptor Ret as a potential therapy for PD patients, although the molecular mechanism of this effect is still under debate (Aron and Klein, 2011; Barak *et al*., 2011; Kordower and Bjorklund, 2013).

Based on previous findings, mice which have had lost the neurotrophic receptor Ret showed an age-dependent DA neuron loss (Kramer *et al*., 2007). Two year old conditional Ret knockout mice in DA neurons showed a specific and progressive loss of DA cells in the SN (38%) and striatal innervations (63%) (Kramer *et al*., 2007). As TH-tTA mice showed tight suppression of prenatal and postnatal gene expression, this system was used to generate TH-tTA/LC1/Retlox and analyze Ret receptor loss specifically during adulthood (Tillack thesis, 2013). Considering the incomplete targeting of DA neurons in the TH-tTA mice, the amount of cell loss in 2 year old TH-tTA/LC1/Retlox mice was 15% for SNpc and 12% fiber loss in dorsal striatum whereas no loss for VTA cells and ventral innervations were observed /(Tillack thesis, 2013). Therefore, genetic deletion of Ret in TH-tTA mice led to a mild but significant loss of DA neurons and innervations of the SNpc which was comparable with constitutive conditional knockout mice. Thus, embryonic compensation does not play an important role for the observed phenotype in constitutive Ret knockout mice (Tillack thesis, 2013).

4.2.2 overexpression of human α-synuclein in TH-tTA mice

As α-synuclein is strongly linked to the pathogenesis of both familial and sporadic forms of PD (Polymeropoulos *et al*., 1997; Spillantini *et al*., 1997) and mutations in the gene locus are found in the common idiopathic form of PD (Satake *et al*., 2009; Simon-Sanchez *et al*., 2009; Stefanis, 2012), TH-tTA/tetO-synA53T mice were generated to express human α-synuclein protein with A53T missense mutation from the tet-responsive synA53T transgene (Lin *et al*., 2009) specifically in DA neurons to study the pathogenesis mechanisms of mutated α-synucleinA53T in PD (Tillack thesis, 2013).

In TH-tTA/tetO-synA53T mice, transgenic α-synuclein expression has been detected in the ventral midbrain, striatum and cerebellum as well as glomerular and the inner cell layers of the olfactory bulb and locus coeruleus (Tillack thesis, 2013). Co-staining of TH and human α-synuclein to quantify the efficiency of synA53T transgenic expression in DA neurons of the ventral midbrain in 3 months old TH-tTA/tetO-synA53T mice revealed 76% targeting of the SNpc and VTA. Using western blot, the level of transgenic α-synuclein protein expression was evaluated in the midbrain and striatum tissue lysates of 3 months old TH-tTA/tetO-synA53T mice and showed two fold overexpression of α-synuclein with the strongest signal detected in the striatum (Tillack thesis, 2013).

4.2.3 Translocation of α-synuclein into the nucleus in TH-tTA/tetO-synA53T mice

It has been shown that α-synuclein translocates into the nucleus and can bind histones which might lead to neurotoxicity and α-synuclein pathophysiology (Goers *et al*.,2003). α-synuclein mutations A30P and A53T that cause familial Parkinson's disease, exhibit increased nuclear targeting and toxicity (Kontopoulos *et al*., 2006).

It is also confirmed that posttranslational modifications to α-synuclein like phosphorylation at serine 129 (Ser129) might be critical in PD pathogenesis (Fujiwara *et al*., 2002; Chen *et al*., 2009). Phosphorylation at Ser129 has been reported to enhance α-synuclein toxicity both *in vivo* and *in vitro*, possibly by increasing the formation of α-synuclein aggregates (Fujiwara *et al*., 2002; Smith *et al*., 2005). Approximately 90% of α-synuclein deposited in LBs is phosphorylated at Ser129, whereas in the normal brain only 4% or less of total α-

synuclein is phosphorylated at this residue. This suggests that accumulation of Ser129-phosphorylated α-synuclein might lead to the formation of LBs and neuronal pathophysiology in Parkinson's disease (Sato *et al*., 2013).

To test whether in our TH-tTA/tetO-synA53T mice synA53T also translocates into the nucleus of DA neurons where it might mediate neurotoxicity, I stained sections with an antibody specific against phosphorylated serine 129 (Ser129) of human α-synuclein since this antibody does not cross-react with non-phosphorylated human α-synuclein proteins (Walker *et al*., 2013).

Fluorescent co-staining using antibodies against TH and phosphorylated α-synuclein (Ser129) antibodies on coronal midbrain sections in 3 months and 1 year old TH-tTA/tetO-synA53T mice showed phosphorylation of α-synuclein not only in the cytoplasm but also in the nucleus of a large numbers of α-synuclein expressed DA neurons (Figure 4.9B). No expression was observed in the control TH-tTA mice not expressing human α-synuclein (Figure 4.9B). This confirms that also in our TH-tTA/tetO-synA53T mice α-synuclein is translocated to the nucleus and could alter Ret expression.

To detect expression of human α-synuclein in the noradrenergic system in TH-tTA/tetO-synA53T mice, TH and human α-synuclein co-staining in the cerebellum sections of 2 year mutant TH-tTA/tetO-synA53T mice has been done and the quantification of TH/human α-synuclein positive cells in the locus coeruleus (LC) revealed 32% recombination efficacy. Considering incomplete targeting of TH-tTA mice and 17% quantified recombination efficacy in the LC of TH-tTA/LC1/Rosa26R (Tillack thesis, 2013), 32% targeting of LC in TH-tTA/tetO-synA53T mice make it an efficient tool to study also noradrenergic system as a PD model. However, more studies are required in young TH-tTA/tetO-synA53T mice to show that observed recombination efficacy is due to the targeting effect or spreading of α-synuclein in aged mice. Moreover, the same procedure in the TH-tTA/LC1/Retlox/tetO-synA53T will help to confirm the role of Ret loss in addition to the overexpression of human α-synuclein A53T in the noradrenergic system.
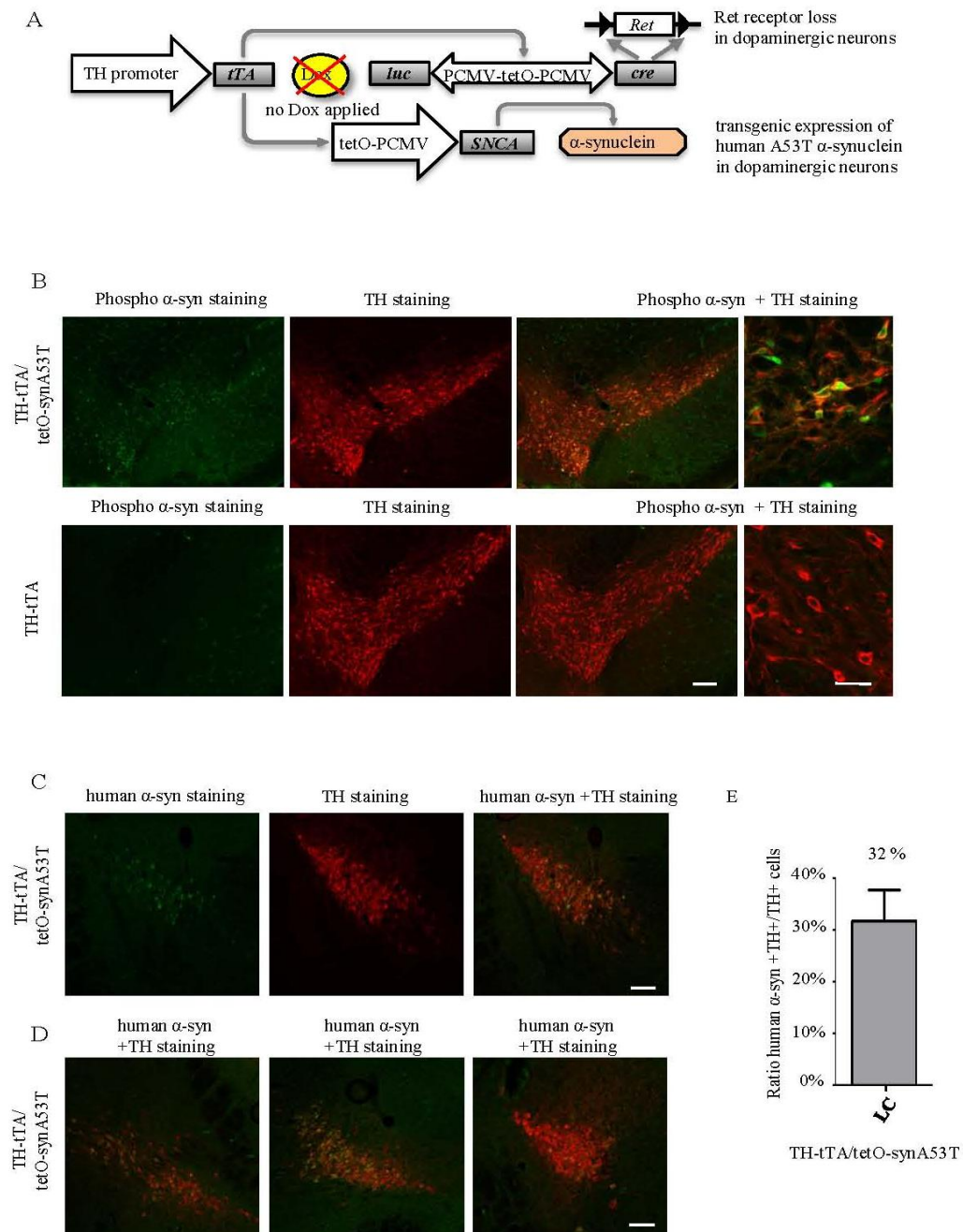
Figure 4.9 Expression of human α-synuclein A53T mutant protein in the nucleus of dopaminergic neurons of TH-tTA/tetO-synA53T mice

(A) Scheme of TH-tTA/LC1/Retlox/tetO-synA53T mice without DOX. (B) Confocal fluorescent pictures of Phosphorylated α-synuclein expression in coronal mouse brain sections stained for TH and for phosphorylated α-synuclein protein in TH-tTA/tetO-synA53T and TH-tTA control mice. Scale bars: 200 μm and 20 μm. (C-D) Confocal fluorescent

Images of human α-synuclein expression in LC co-stained with TH in TH-tTA/tetO-synA53T mice (C) and different example images of coronal sections stained for human α-synuclein and TH (D). Scale bars: 200μm. (E) Quantification of TH and human α-synuclein double positive cells in the LC to estimate recombination efficacy in noradrenergic system in the TH-tTA/tetO-synA53T mice (n = 3, data are represented as mean +/- s.e.m.).

4.2.4 Induced deletion of the neurotrophic receptor Ret and overexpression of human α-synuclein in TH-tTA mice

Investigations were also continued in the TH-tTA mice to observe the consequences of PD related α-synuclein expression in neurotrophically impaired DA neurons (Tillack thesis, 2013). Taking advantage from TH-tet system TH-tTA/LC1/Retlox/tetO-A53T were generated (Figure 4.9A) enabling us to trigger at the same time in the same cells gene deletion of the Ret receptor and on the other hand to express human α-synuclein protein with A53T missense mutation from the tet-responsive synA53T transgene (Lin *et al*., 2009) specifically in DA neurons (Tillack thesis, 2013).

4.2.5 Spreading of α-synuclein in TH-tTA/tetO-synA53T mice

Recent studies on neurodegenerative diseases with a central hallmark of formation and protein aggregation of α-synuclein especially PD suggest that α-synuclein may self-propagate, generating the "host to graft transmission" hypothesis, also called the "prion-like hypothesis" (Braak *et al.,* 2003; Kordower *et al*., 2008; Li *et al*., 2008; Recasens and Dehay, 2014a). Several *in vitro* and *in vivo* studies suggest that α-synuclein can undergo a toxic template conformational change and spread from cell to cell to initiate the formation of "LB–like aggregates" that might contribute to the pathogenesis and progression of PD (Desplats *et al*., 2009, Luk *et al*., 2012a, Luk *et al*., 2012b; Gelpi *et al*., 2014; Recasens and Dehay, 2014a).

To see whether spreading of α-synuclein takes place in TH-tTA/tetO-synA53T mice, co-staining with an antibody specifically recognizing human α-synuclein and another antibody recognizing both mouse and human α-synuclein (general α-synuclein) in mouse brain

sections from 2 year old TH-tTA controls, TH-tTA/tetO-synA53T, TH-tTA/LC1/Retlox and TH-tTA/LC1/Retlox/tetO-A53T mice was done. Neighbor sections co-stained with TH and Nissl to visualize DA neurons and cell bodies for exact detection of SNpc and VTA regions (Figure 4.10A and B). Using confocal microscopy, the spreading of α-synuclein in the SNpc and VTA of different groups of mice was determined. With the help of TH/Nissl staining the cells in the SNpc and VTA were traced and cells which showed no expressions of human α-synuclein but intense expression of general mouse α-synuclein in these regions were considered for spreading (Figure 4.10A and B). The mutated and misfolded form of human α-synuclein has been shown to be able to spread by exosomes or exocytosis to close neighboring cell bodies or postsynaptic cells connected by synpases (Schneider and Simons, 2013). Midbrain DA neurons of TH-tTA/tetO-synA53T mice which are not targeted by the genetic construct (around 40% of DA neurons) and therefore do not themselves express human α-synuclein might still show with time an enrichment of mouse α-synuclein. This might be explained by spreading since a small amount of transmitted misfolded human α-synuclein protein might be enough to induce misfolding and accumulation of mouse α-synuclein protein in neighboring cells that do not themselves express this toxic α-synuclein protein. Counting cells with enriched mouse α-synuclein but negative for a high amount of human α-synuclein in 2 year old TH-tTA/tetO-synA53T mice might give an indication if spreading might have taken place over time and if this number is higher compared to age mated control mice or younger TH-tTA/tetO-synA53T mice.

Obtained results from the quantification confirm one of the important neuropathology aspects of α-synuclein in PD which takes place in the TH-tTA/tetO-synA53T mouse model and Ret loss seems not to enhance spreading (Figure 4.10 C and D).

A | TH+ Nissl staining | Human α-synuclein staining | Mouse α-synuclein staining | Merged

TH-tTA/LC1 controls

TH-tTA/ tetO-synA53T

TH-tTA/LC1/ Retlox

TH-tTA/LC1/Retlox/ tetO-synA53T
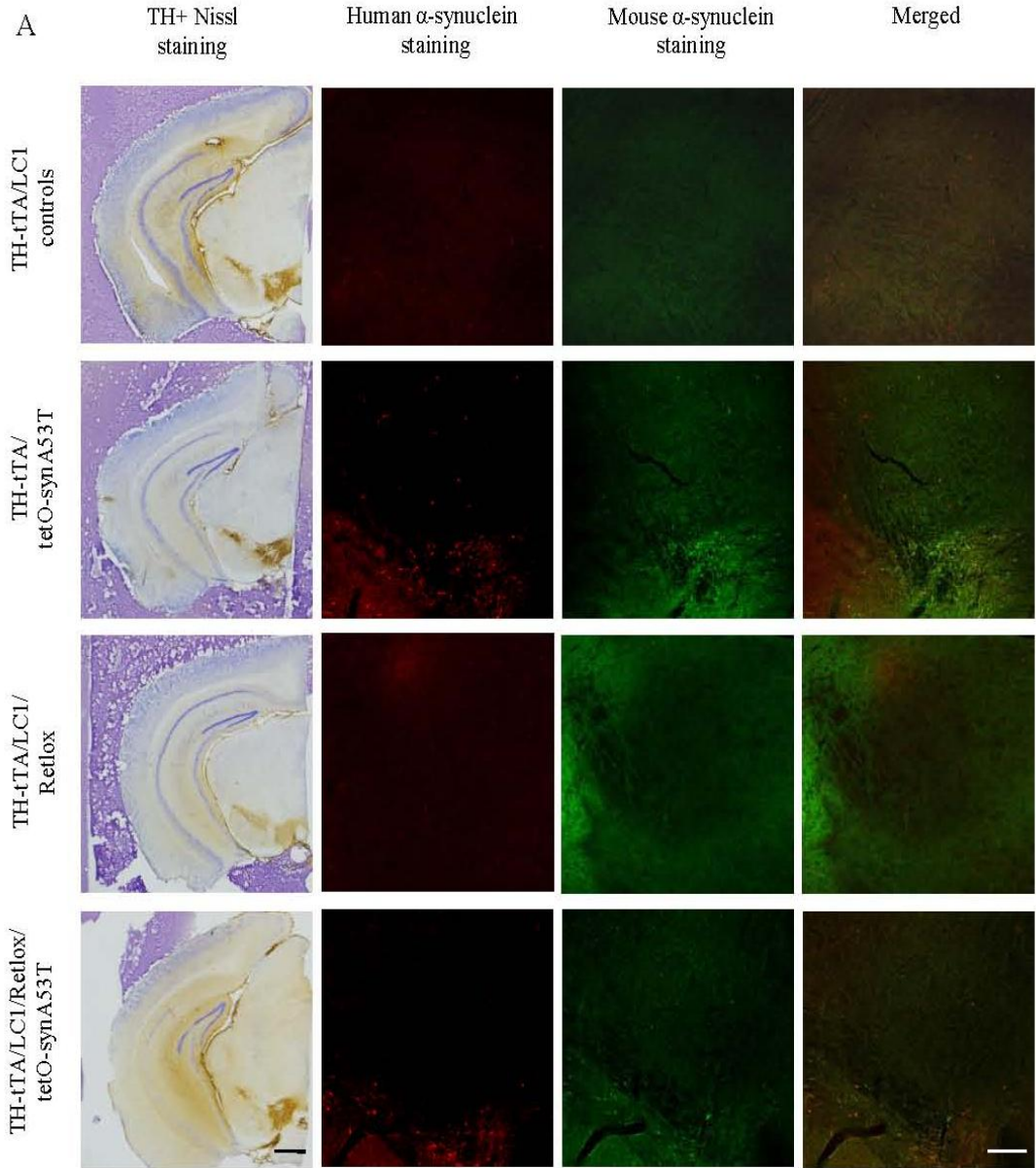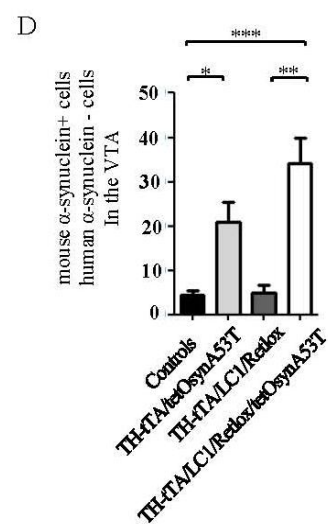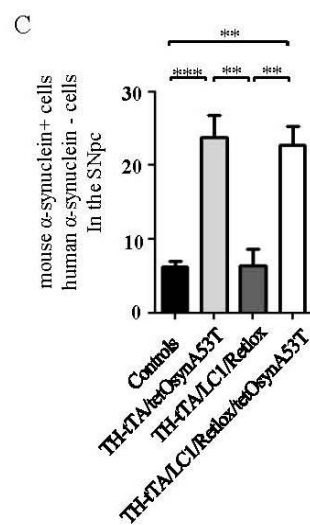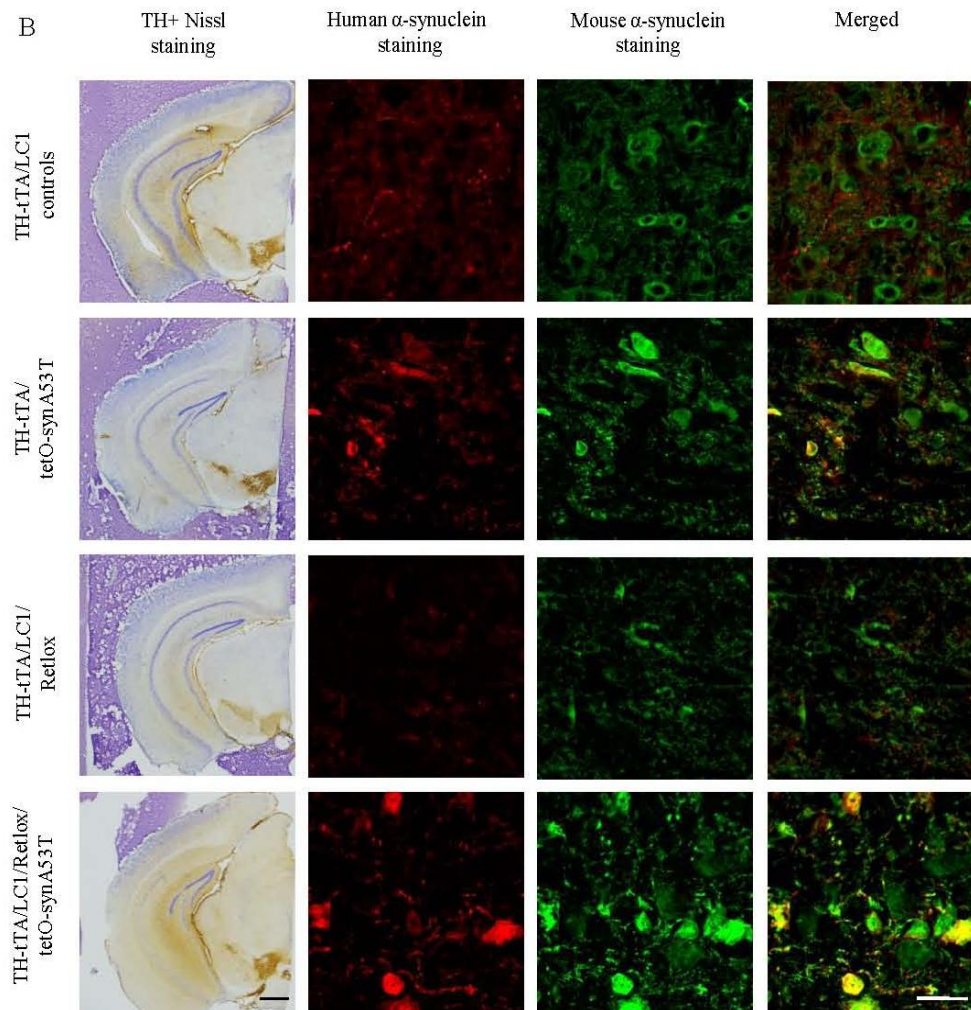
Figure 4.10 α-synuclein is spreading in synA53T transgenic mice

(A) Confocal images of human α-synuclein immunohistofluorescence staining in midbrain and zoom images (B) of 2 year old TH-tTA/LC1 controls, TH-tTA/tetO-synA53T, TH-tTA/LC1/Retlox and TH-tTA/LC1/Retlox/tetO-A53T mice co-stained with mouse α-synuclein shows spreading and prion like behavior of α-synuclein in TH-tTA/tetO-synA53T and TH-tTA/LC1/Retlox/tetO-A53T mice. Scale bar: 500 μm for TH+Nissl staining, 200 μm for human + mouse alphasynuclein staining and 20 μm for zoom images of human + mouse alphasynuclein staining. (C-D) Quantification of mouse α-synuclein positive cells in the SNpc (C) and VTA (D) shows spreading in TH-tTA/tetO-synA53T and TH-tTA/LC1/Retlox/tetO-A53T (n=3, data are represented as mean + s.e.m; * p≤0.05, ** p≤0.01, *** p≤0.001; One-way ANOVA, Tukey post-hoc test).

4.2.6 α-synuclein toxicity is enhanced in Ret deficient mice

To check whether deletion of neurotrophic Ret signaling and overexpression of human α-synuclein may lead to enhanced neurodegeneration, as well as verifying possible neurodegeneration in human α-synuclein overexpressed mice, four mouse groups including TH-tTA/tetO-A53T, TH-tTA/LC1/Retlox, TH-tTA/LC1/Retlox/tetO-A53T and TH-tTA/LC1 or TH-tTA controls were investigated at different ages. At the age of 3 months, there was no atypical behavior and no obvious histological alterations in the ventral midbrain and striatum visible in the four mouse lines supporting the idea that Ret loss and/or mild α-synuclein overexpression does not lead an early postnatal phenotype (Tillack thesis, 2013). To analyses a possible age-related phenotype, 1 year old mice were perfused. Histological quantification revealed only in TH-tTA/LC1/Retlox/tetO-synA53T mice a DA cell loss of 15% in the SNpc, 25% cell loss in the VTA, and a 15% DA innervation loss in the dorsal striatum and 21% loss in the ventral striatum. Dopamine levels were not significantly reduced but DOPAC levels were increased. In 1 year old TH-tTA/tetO-synA53T mice no cell loss but a significant 8-12% DA innervation loss and DOPAC increase in the striatum were observed (Tillack thesis, 2013). To investigate the progressive neurodegeneration, 2 year old mice sections were stained for TH to visualize DA neurons (Figure4.11A). Before starting stereological quantification of 2 Year old mice first the slides of TH stained midbrain sections from 1year old mice were obtained from Kartesn Tillack and counted for cell numbers in the SNpc and VTA (Figure 4.11B) to be constant in

analyzing data for 2 year old mice. Stereologicical quantification in 2 year old mice showed in TH-tTA/LC1/Retlox mice 18% loss only in the SNpc, in TH-tTA/tetO-synA53T mice 15% loss in SNpc and VTA, and an enhanced loss of 26% in the SNpc and 25% in the VTA of TH-tTA/LC1/Retlox/tetO-A53T mice (Figure4.11C). Despite the specificity of SNpc dopaminergic cell loss in TH-tTA/LC1/Retlox mice, TH-tTA/LC1/Retlox/tetO-A53T mice showed an enhanced neurodegeneration in both SNpc and VTA compared to TH-tTA/tetO-synA53T mice. To confirm that observed cell loss is not due to the lack of TH expression, midbrain sections stained for nissl and quantification results showed the same tendency of neuronal loss in the relevant groups as observed before with TH staining (Figure 4.11D).

Years ago it has been proposed that PD neurodegeneration is a dying-back process that begins in the striatal terminals (Hornykiewicz, 1998; Cheng *et al*., 2010). When measuring fiber density of TH positive axonal terminals in the striatum (Figure 4.11E and F),15%, 16% and 25% DA innervation loss was found in the dorsal striatum as well as 18%, 10% and 27% fiber loss in the ventral striatum of TH-tTA/tetO-synA53T, TH-tTA/LC-1/Retlox and TH-tTA/LC-1/Retlox/tetO-synA53T mice, respectively.

Besides neuronal and axonal loss, significant reduction of dopamine level and a tendency of increased DOPAC were both observed by HPLC in striatal tissue lysates of TH-tTA/tetO-synA53T mutant mice (Figure 4.11G), whereas no changes for levels of HVA was observed (Figure 4.11G).

Together these data show an enhanced neurodegeneration phenotype in TH-tTA/LC1/Retlox/tetO-synA53T mice, indicating a protective function of the neurotrophic receptor Ret against α-synuclein toxicity.
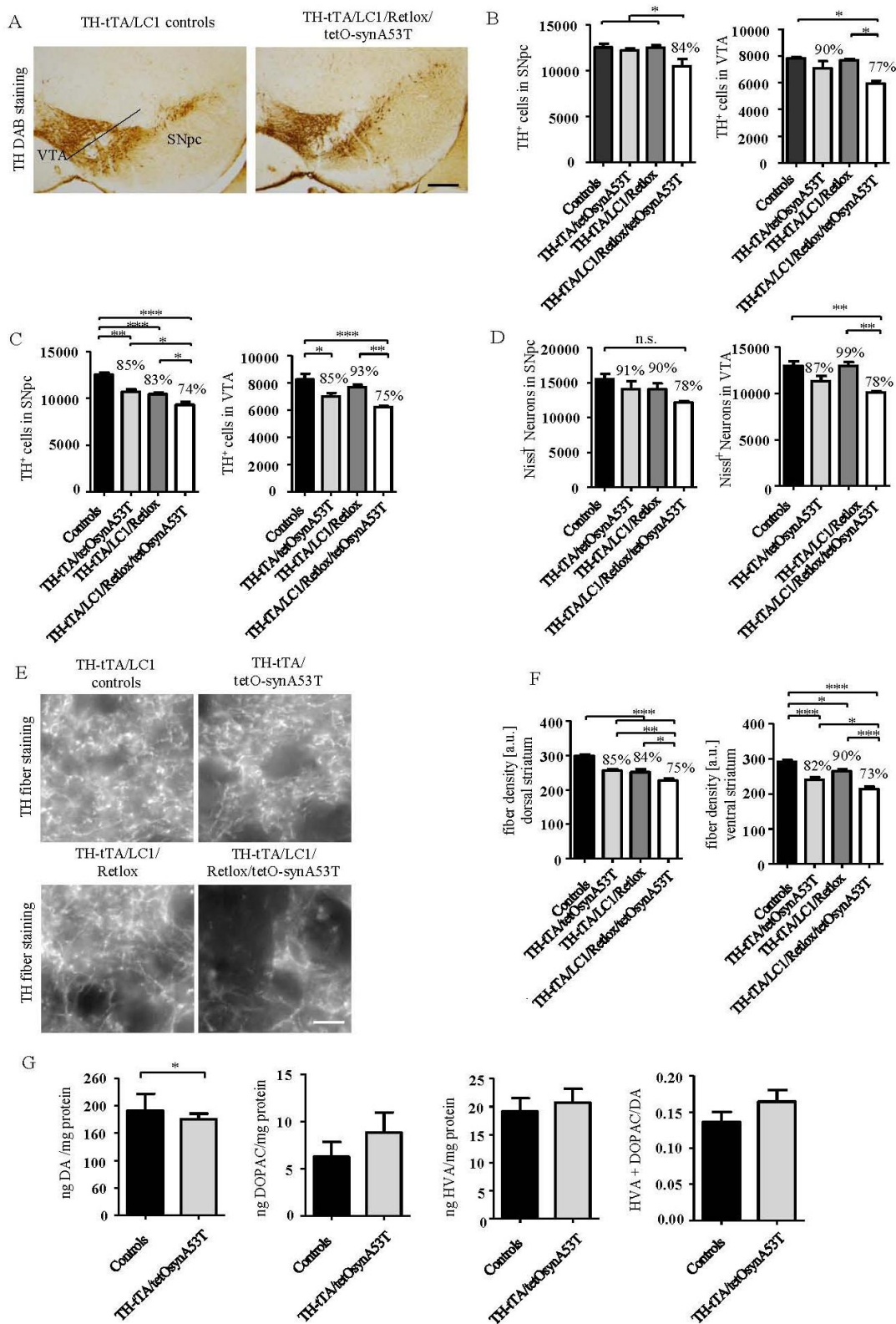
Figure 4.11 Alterations in the dopaminergic system of aged Ret mutant mice with transgenic human A53T α-synuclein expression

(A) Coronal midbrain sections of 2 year old TH-tTA control and TH-tTA/LC1/Retlox/tetO-A53T mice stained for TH to visualize DA neurons in the SNpc and the VTA. Scale bar: 200 μm. (B-D) Stereological quantification of TH positive cells in 1 Year old (B) and 2 Year old (C) and Nissl positive neurons (D) in the SNpc and VTA of TH-tTA control, TH-tTA/tetO-synA53T, TH-tTA/LC1/Retlox and TH-tTA/LC1/Retlox/tetO-A53T mice (n=4, data are represented as mean +/- s.e.m.,* p≤0.05, ** p≤0.01, *** p≤0.001; One-way ANOVA, Tukey post-hoc test). (E) Confocal fluorescent images of striatal sections of 2 year old TH-tTA control, TH-tTA/tetO-synA53T, TH-tTA/LC1/Retlox and TH-tTA/LC1/Retlox/tetO-A53T mice stained for TH to visualize DA fibers in dorsal striatum. Scale bar: 20 μm. (F) Density quantification of TH positive fibers in the dorsal and ventral striatum of 2 year old TH-tTA control, TH-tTA/tetO-synA53T, TH-tTA/LC1/Retlox and TH-tTA/LC1/Retlox/tetO-A53T mice (n=4,data are represented as mean +/- s.e.m., * p≤0.05, ** p≤0.01, *** p≤0.001; One-way ANOVA, Tukey post-hoc test). (G) Dopamine (DA) and DA metabolites in striatal brain lysates measured by HPLC in 2 year old mice. dihydroxyphenylalanine (DOPAC), homovanillic acid (HVA) (n=5, data are represented as mean +/- s.e.m.,* p≤0.05, Students t-test).

4.3 Mechanisms behind α-synuclein toxicity

4.3.1 Protein aggregation and reduced cell soma size in TH-tTA/tetO-synA53T mice

The primary pathologic features of PD are Lewy fibrils and Lewy bodies made up of aggregated α-synuclein. Histological techniques such as thioflavin S staining, can detect the presence of misfolded, amyloid and beta-sheet-rich material within the inclusions (Stefanis and Keller, 2006).

In order to address whether increased protein aggregation can be found in human α-synuclein overexpressing mice, thioflavin-S staining in midbrain sections of 2 year old mice was done (Figure 4.12A). Importantly, thioflavin-S positive staining and quantification of aggregates per mm^2 revealed a significant increase in the SNpc and VTA of TH-tTA/LC1/Retlox/tetO-synA53T mice whereas no changes could be observed in TH-tTA/tetO-synA53T and TH-tTA/LC1/Retlox (Figure 4.12B). These results indicate that deletion of Ret in α-synuclein A53T transgenic mice might enhance toxicity via impairing protein degradation or enhancing protein aggregation/accumulation resulting in an accelerated DA neuron degeneration phenotype.

To investigate whether alterations in Ret and α-synuclein also affect the soma size of the surviving DA neurons, the two-dimensional cell extension was measured in TH immunostained SNpc and VTA DA neuron of 2 year old mice using the nucleator probe of the StereoInvestigator software. Cell soma size in SNpc of TH-tTA/tetO-synA53T and TH-tTA/LC1/Retlox mice was significantly decreased - previously published for Ret deficient mice (Aron *et al*., 2010; Meka *et al*., 2015) but not for α-synuclein transgenic mice - and was more pronounced in TH-tTA/LC1/Retlox/tetO-synA53T mice (Figure 4.12C). The reduced TH soma size had a tendency to decrease in the VTA of TH-tTA/tetO-synA53T mice, but was significantly reduced when deletion of Ret added to the overexpression of human α-synuclein in mice (Figure 4.12C). The results confirm that α-synuclein toxicity is enhanced by deletion of Ret in mice.
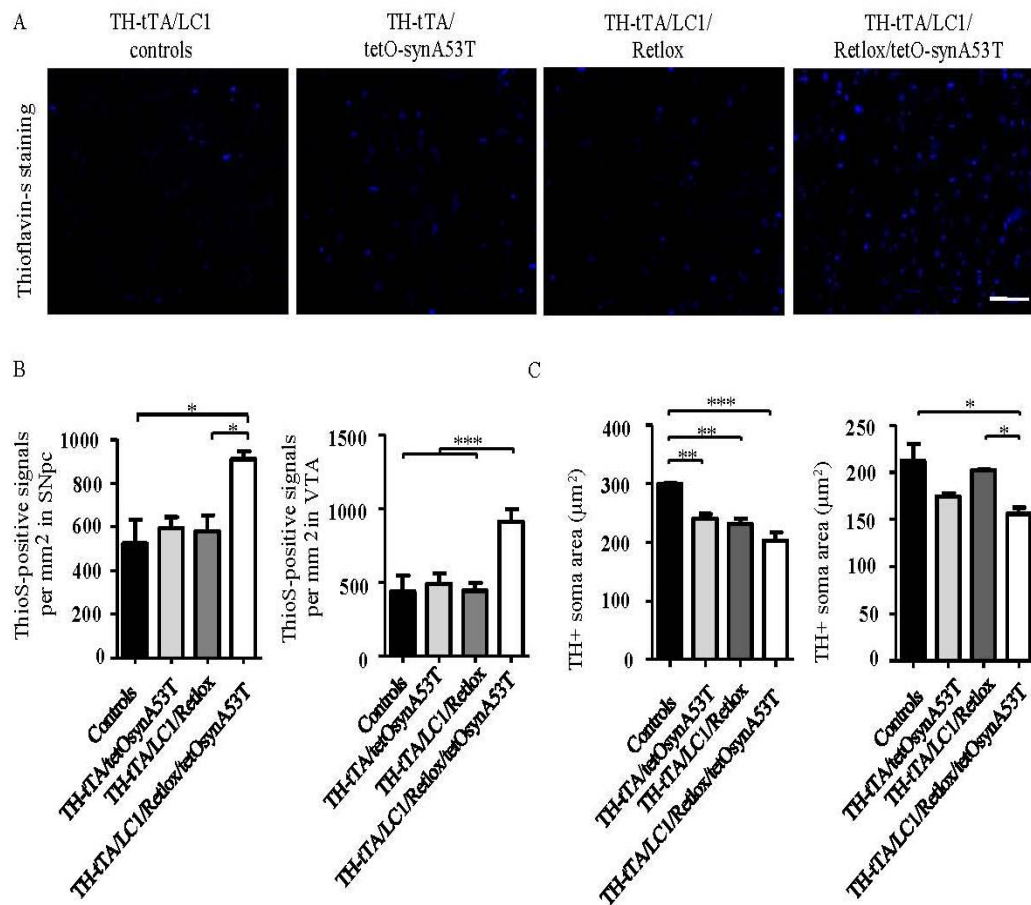
Figure 4.12 Alterations in the dopaminergic system and cell soma size of aged Ret mutant mice with transgenic human A53T α-synuclein expression

(A) Fluorescent images of coronal sections of 2 year old control, TH-tTA/tetO-synA53T, TH-tTA/LC1/Retlox and TH-tTA/LC1/Retlox/tetO-synA53T mice stained for thioflavin-S to visualize protein aggregation in the SNpc and the VTA. Scale bar: 200 µm. (B) Stereological quantification of thioflavin-S positive aggregates per mm^2 in the SNpc and VTA of 2 year old control, TH-tTA/tetO-synA53T, TH-tTA/LC1/Retlox and TH-tTA/LC1/Retlox/tetO-synA53T mice. (n=3-4). (C) Cell soma area measurements of SNpc and VTA TH positive neurons in 2 year old mice (n=4, data are represented as mean +/- s.e.m. * p≤0.05, ** p≤0.01, *** p≤0.001; One-way ANOVA, Tukey post-hoc test).

4.3.2 Cellular changes in the aged transgenic human A53T α-synuclein overexpressing mice

Besides aging, additional specific risk factors for PD are mitochondrial and gene dysfunctions relevant to energy metabolism (Phillipson, 2014). It has been reported by several studies that misfolded α-synuclein impairs complex I activity, ATP synthesis, and the mitochondrial membrane potential (Devi *et al*., 2008; Chinta *et al*., 2010; Dunning *et al*.,2013).

Thus, reduced cell size and dopamine levels observed in TH-tTA/tetO-synA53T mice might be explained by impaired energy supply due to misfolded α-synuclein. Therefore, I assessed mitochondria function in all mutant mice by measuring ATP levels and complex I activity. I found no alterations in total ATP levels in SN lysates of 1 year old (Figure 4.13A) and, 2 year old mutant mice (Figure 4.13B). Due to the lack of brain samples I analyzed only one year old TH-tTA/LC1/Retlox and TH-tTA/LC1/Retlox/tetO-synA53T mice but not 2 year old mice.

To have a look at respiratory chain activity, I assayed mitochondrial complex I activity in the enriched mitochondrial fractions from the SN of 1 year old TH-tTA/tetO-synA53T, TH-tTA/LC1/Retlox and TH-tTA/LC1/Retlox/tetO-synA53T mice performed. Surprisingly only the mitochondrial enriched fraction obtained from the SN of TH-tTA/tetO-synA53T and TH-tTA/LC1/Retlox mice showed a significant reduction of complex I activity while TH-tTA/LC1/Retlox/tetO-synA53T mice showed the same activity as TH-tTA control mice (Figure 4.13 C).

These observations suggest that Ret loss and human A53T α-synuclein overexpression decrease mitochondrial complex I activity without altering ATP production in mice. In double transgenic mice the mitochondrial complex I activity seems to be compensated by an unknown mechanism.
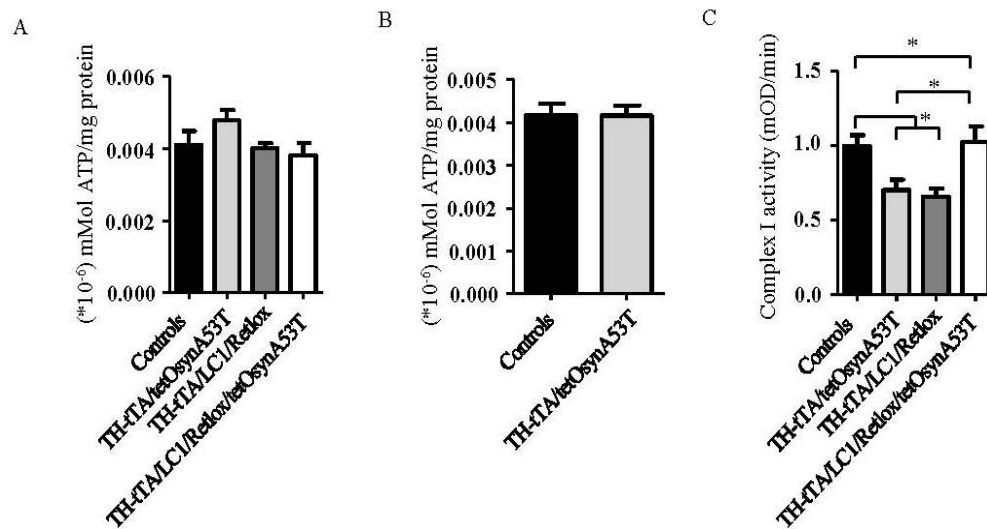
Figure 4.13 Cellular changes in the aged Ret mutant mice with transgenic human A53T α-synuclein expression.

(A-B) Total cellular ATP levels are measured in the SNpc of the mentioned genotypes in 1 year old (A) and 2 year old (B) mice. (A) (n=4-5, data are represented as mean +/- s.e.m.; One-way ANOVA, Tukey post-hoc test) (B) (n=5-6, data are represented as mean +/- s.e.m.; Students t-test) (C) Mitochondrial complex I activity in the SNpc of 1 year old mice showed a significant reduction in the TH-tTA/tetO-synA53T mice and TH-tTA/LC1/Retlox mice compared to age matched controls and TH-tTA/LC1/Retlox/tetO-synA53T mice (n = 7-12, data are represented as mean +/- s.e.m.; * p≤0.05; One-way ANOVA, Tukey post-hoc test).

4.3.3 Ret deletion in overexpressing human A53T α-synuclein transgenic mice enhanced gliosis and inflammation

Both microglia and astrocytes are activated during PD and some other neurodegenerative diseases, although the role of these resident immune cells of the brain in PD is still not clear (Dunning, 2013). In order to investigate the glia response in aged TH-tTA/tetO-synA53T and TH-tTA/LC1/Retlox mice, I stained striatal and midbrain sections from 2 year old mice for glial fibrillary acidic protein (GFAP) and ionized binding calcium adaptor molecule (Iba1) to visualize astrocytes and microglia, respectively (Figures 4.14A and 4.15A). I observed in the striatum of TH-tTA/tetO-synA53T mice a tendency of more astrocytes, while in TH-tTA/LC1/Retlox mice a clear gliosis could be detected - that was previously described (Kramer *et al.*, 2007) - and was further enhanced in TH-tTA/LC1/Retlox/tetO-synA53T mice (Figure 4.14B).

Iba1 staining in the SNpc revealed an enhanced inflammation in all transgenic mice compared to control mice while inflammation in VTA was more specific for TH-tTA/tetO-synA53T and TH-tTA/LC1/Retlox/tetO-synA53T mice where neurodegeneration takes place also in the VTA (Figure 4.15B). Iba1 positive microglial cells were further morphological categorized as resting, bushy or amoeboid. An increase in bushy microglia cells was found to be tightly correlated in all tissue with cell body loss (Figure 4.16A).

Taken together, in the striatum DA fiber loss correlated with gliosis while cell body loss in the SNpc and VTA generates an inflammation. It was shown previously already for Ret deficient mice that gliosis and inflammation is becoming significant in 2 year old mice as a consequence of the degeneration process already obvious in 1 year old mice (Kramer *et al.*, 2007).
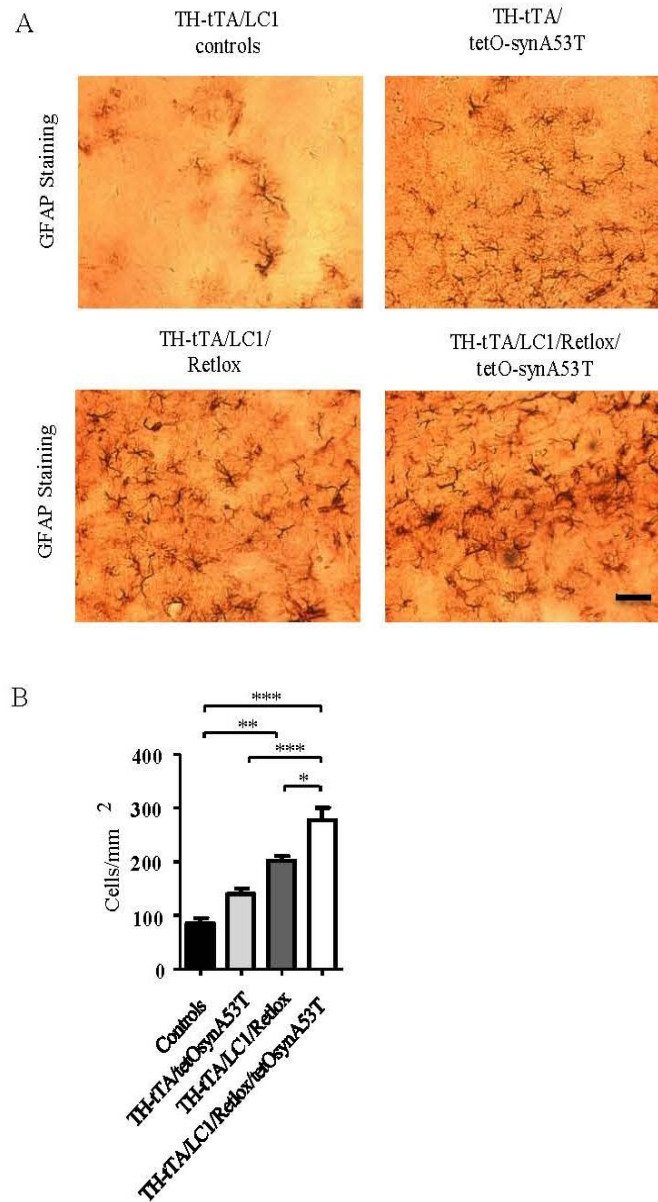
Figure 4.14 Gliosis accompanies DA neuronal fiber degeneration in the striatum of aged TH-tTA/LC1/Retlox and TH-tTA/LC1/Retlox/tetO-synA53T mice

(A) Representative images of coronal sections from 2 year old mice of the indicated genotypes stained with glial fibrillary acidic protein (GFAP) antibody showing astrocytes in the striatum (scale bar: 250 μm) (B) Quantifications of GFAP positive cells in the striatum of 2 year old mice of the indicated genotypes (n = 3, data are represented as mean +/- s.e.m.; * p≤0.05, ** p≤0.01, *** p≤0.001; One-way ANOVA, Tukey post-hoc test).
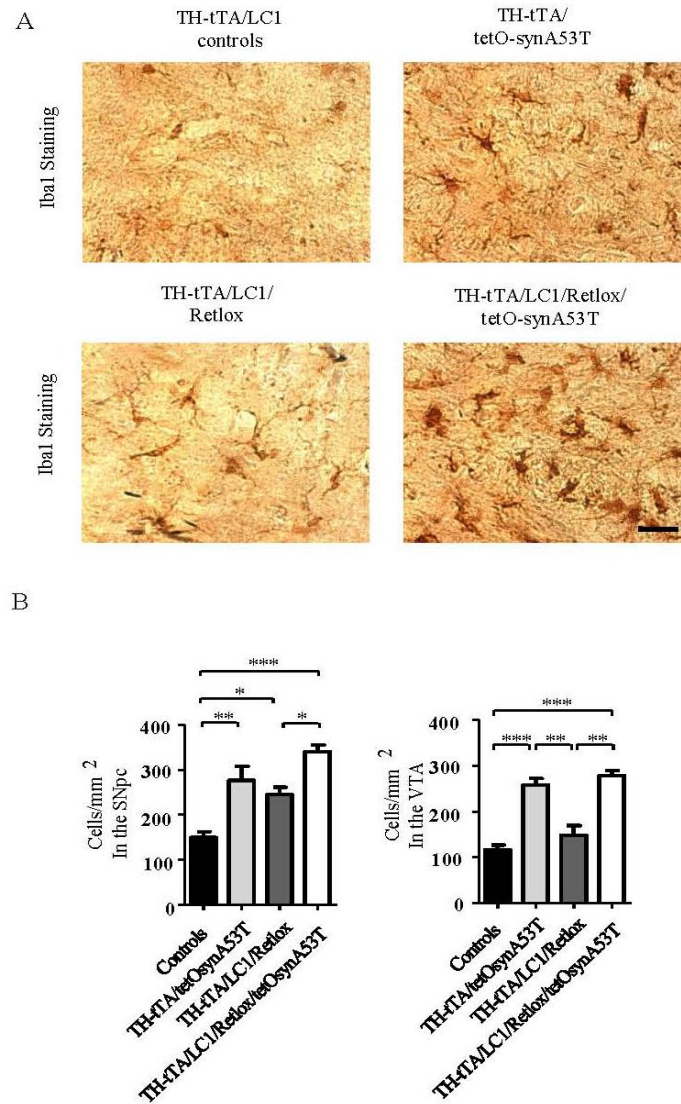
Figure 4.15 Inflammation accompanies DA neuronal degeneration in the SNpc and VTA of aged TH-tTA/tetO-synA53T, TH-tTA/LC1/Retlox and TH-tTA/LC1/Retlox/tetO-synA53T mice

(A) Representative images of coronal sections from 2 year old mice of the indicated genotypes stained with ionized binding calcium adaptor molecule (Iba1) antibody showing microglia in the SNpc (scale bar: 250 μm) (B) Quantifications of Iba1 positive cells in the SNpc and VTA of 2 year old mice of the indicated genotypes (n = 3, data are represented as mean +/- s.e.m.; * p≤0.05, ** p≤0.01, *** p≤0.001; One-way ANOVA, Tukey post-hoc test).
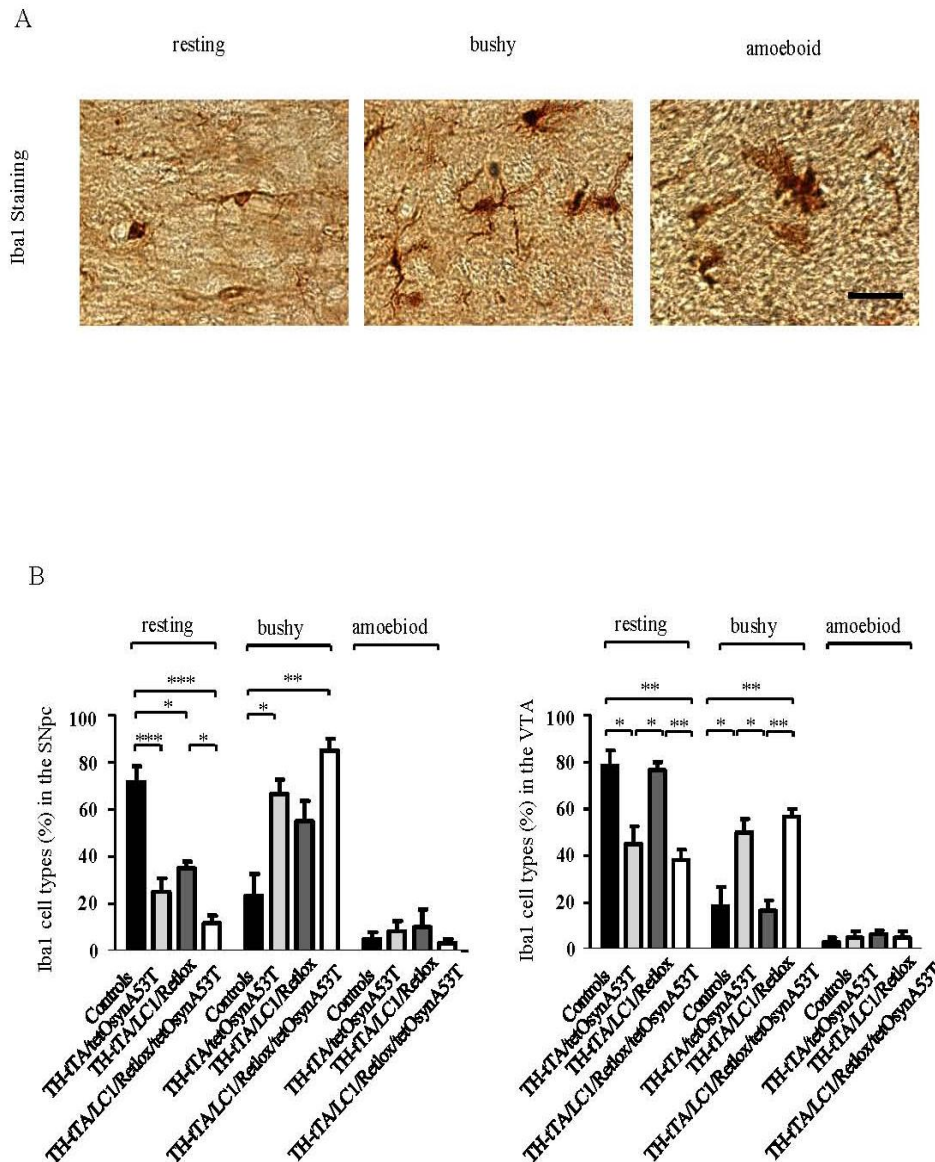
Figure 4.16 Inflammation accompanies DA neuronal degeneration in the SNpc and VTA of aged TH-tTA/tetO-synA53T, TH-tTA/LC1/Retlox and TH-tTA/LC1/Retlox/tetO-synA53T mice

(A) Representative images of resting, bushy and amoeboid microglial (Iba1) cell types in the SNpc of 2 year old mice (scale bar: 100 μm) (B) Quantifications of resting, bushy and amoeboid microglial (Iba1) cell types in the SNpc and VTA of 2 year old across the indicated genotypes (n = 3, data are represented as mean +/- s.e.m.; * p≤0.05, ** p≤0.01, *** p≤0.001; One-way ANOVA, Tukey post-hoc test).

97

4.3.4 Autophagy and mTOR signaling pathway are altered by overexpression of human A53T α-synuclein and deletion of Ret

Autophagy is crucial for maintaining homeostasis of the brain and removing protein aggregates (Lim *et al*., 2011). Accumulation of autophagosomes has been reported in the brains of patients with different neurodegenerative diseases such as PD patients (Rubinsztein *et al*., 2007). It has been shown that α-synuclein inclusions are preferred targets for p62-dependent autophagy (Watanabe *et al*., 2012) and p62 connects ubiquitinated proteins to LC3 for autophagic degradation (Pankiv *et al*., 2007; Lynch-Day *et al*., 2012). Therefore I examined the level of autophagic markers p62 and LC3 using immunohistofluorescence staining in midbrain sections of 2 year old mice (Figures 4.17A and 4.18A). Sections were co-stained for TH as dopaminergic marker and the signal intensity of these autophagic markers in the TH positive cells were measured using the ImageJ programm. P62 protein levels were significantly increased in the SNpc of TH-tTA/ tetO-synA53T, TH-tTA/LC1/Retlox and TH-tTA/LC1/Retlox/tetO-synA53T mice as well as in the VTA of TH-tTA/tetO-synA53T and TH-tTA/LC1/Retlox/tetO-synA53T mice (Figure 4.17B).

The same procedure was done in the same mice groups to measure LC3 protein level. However, this time the observed immunohistochemical signal was not in the SN or VTA but dorsal where the visual tegmental relay zone (VTRZ), parabrachial pigmented nucleus (PBP) and Red nucleus-parvicell part (RPC) might be localized. Because the staining was not strong enough to measure signal intensity in SNpc and VTA, I quantified the LC3 signal in the dorsal midbrain region (VTRZ, PBP and RPC areas) and found significantly increased LC3 protein levels in TH-tTA/tetO-synA53T and TH-tTA/LC1/Retlox mice and to a lesser extent in TH-tTA/LC1/Retlox/tetO-synA53T mice. Thus, increased autophagy marker expression in the midbrain suggest a block of the autophagy process in these cells correlated again with dopaminergic cell degeneration in the SNpc and VTA (Figure 4.11), and increased thioflavin-S positive protein accumulations (Figure 4.12).

Next I assessed the amount of phosphorylated ribosomal protein S6 (p-S6) in midbrain sections of 2 year old mice as a determinant of protein translation and cell size (Ruvinsky *et al*., 2005), as an inhibitor of autophagy (Blommaart *et al*., 1995) and as a possible marker of neurotrophic signaling including Ret receptor signaling (Decressac *et al*., 2012).
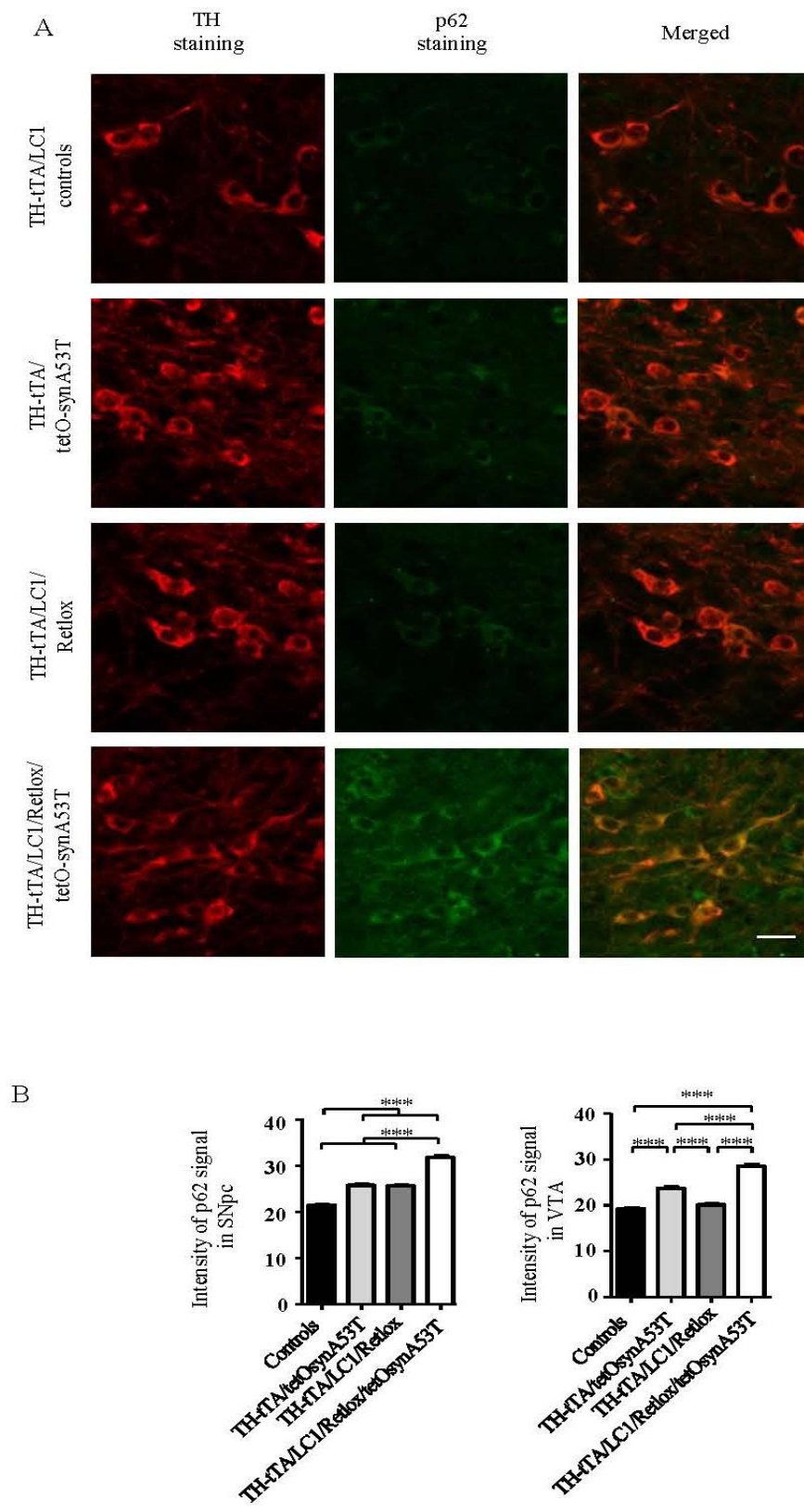
Figure 4.17 α-synuclein induced autophagic impairment in midbrain DA neurons

(A) Confocal images of p62 immunohistofluorescence staining of 2 year old control, TH-tTA/tetO-synA53T, TH-tTA/LC1/Retlox and TH-tTA/LC1/Retlox/tetO-synA53T mice co-stained with TH shows co-localization of p62 and TH. Scale bar: 20 µm. (B) Quantification of signal intensity in SNpc and VTA of relative mice group shows increased p62 level in TH-tTA/tetO-synA53T, TH-tTA/LC1/Retlox and TH-tTA/LC1/Retlox/tetO-synA53T mice compared to control group (n=3, data are represented as mean +/- s.e.m.; *** $p \leq 0.001$, One-way ANOVA, Tukey post-hoc test).

High amounts of p-S6 correlate with small cell size and high proliferation rates and are generated by S6 kinases that are activated by the Akt/mTOR complex. Co-staining of p-S6 with TH revealed enhanced p-S6 protein levels in both SNpc and VTA of the TH-tTA/LC1/Retlox/tetO-synA53T mice compared to control, TH-tTA/tetO-synA53T and TH-tTA/LC1/Retlox mice (Figure 4.19) correlating nicely with the reduced cell size observed in these double transgenic mice (Figure 4.12), increased p62 protein levels due to autophagy inhibition in these mice (Figure 4.17), but not with neurotrophic Ret signaling since Ret is deleted in these mice. Although p-S6 protein levels increase nicely in dopaminergic neurons after GDNF stimulation (Decressac *et al.*, 2012), these signals seem not to tightly correlate with the activation of the canonical GDNF receptor Ret. This might be explained by an alternative GDNF receptor which are also expressed in dopaminergic neurons and might mediate GDNF functions without the Ret receptor (Kramer and Liss, 2015).
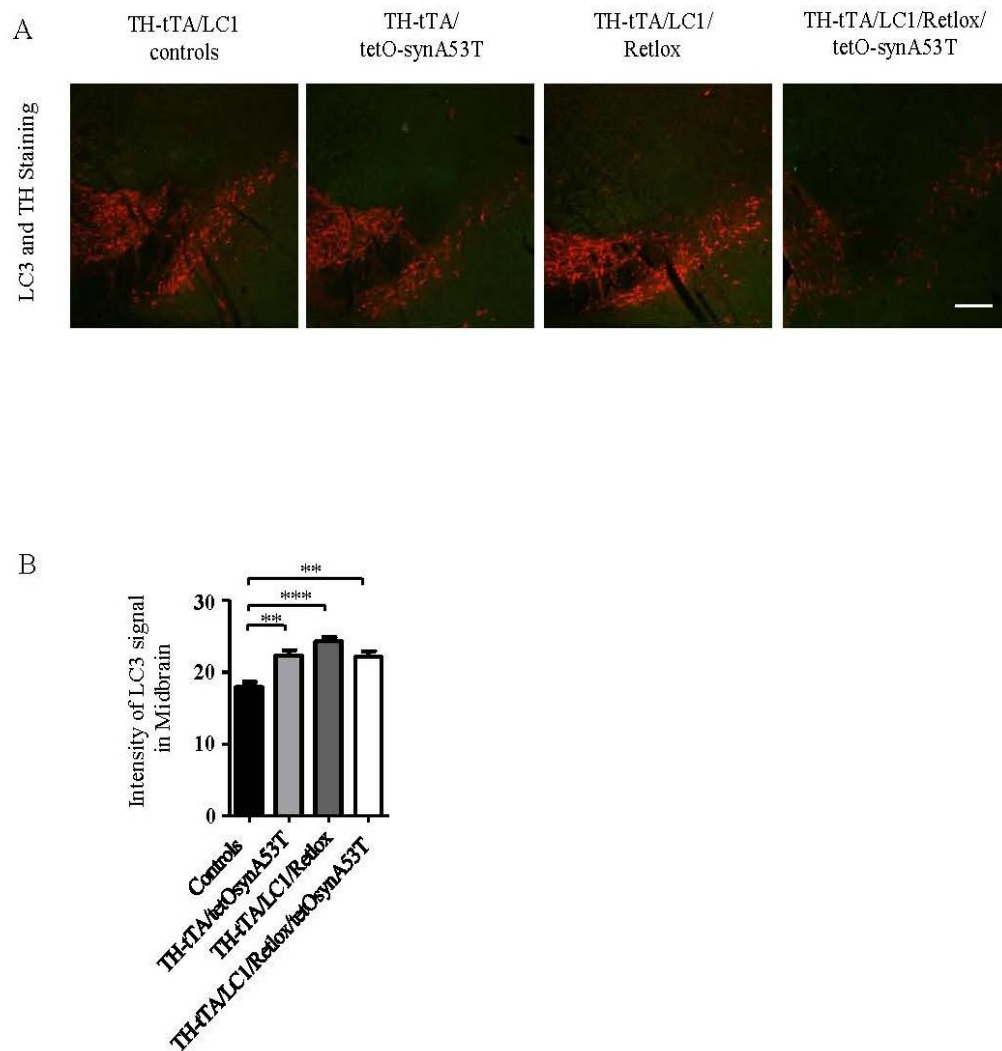
Figure 4.18 α-synuclein induced mitochondria-specific macroautophagy

(A) Double immunofluorescent staining for DA neurons (TH) and mitochondria marker (LC3) revealed neither co-localization of mitochondrial inclusions in SNpc nor obvious in VTA but in surrounding area. Scale bar: 200 µm (B) Quantification of signal intensity in midbrain of 2 year old control, TH-tTA/tetO-synA53T, TH-tTA/LC1/Retlox and TH-tTA/LC1/Retlox/tetO-synA53T mice shows increased LC3 level in TH-tTA/tetO-synA53T, TH-tTA/LC1/Retlox and TH-tTA/LC1/Retlox/tetO-synA53T mice compared to control group (n=1, data are represented as mean +/- s.e.m.; ** p≤0.01, *** p≤0.001, One-way ANOVA, Tukey post-hoc test).
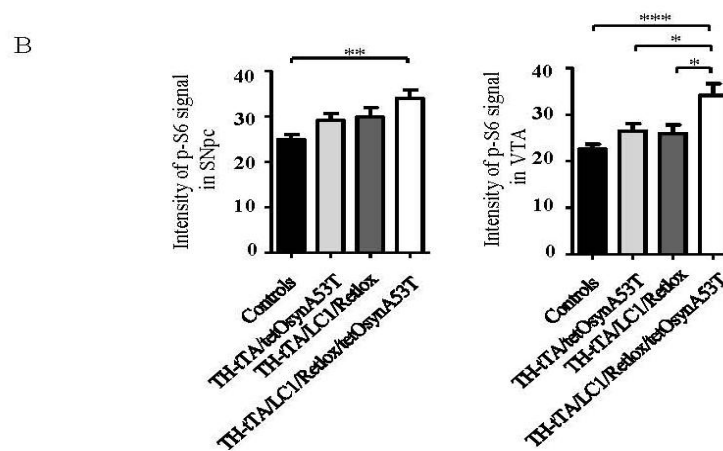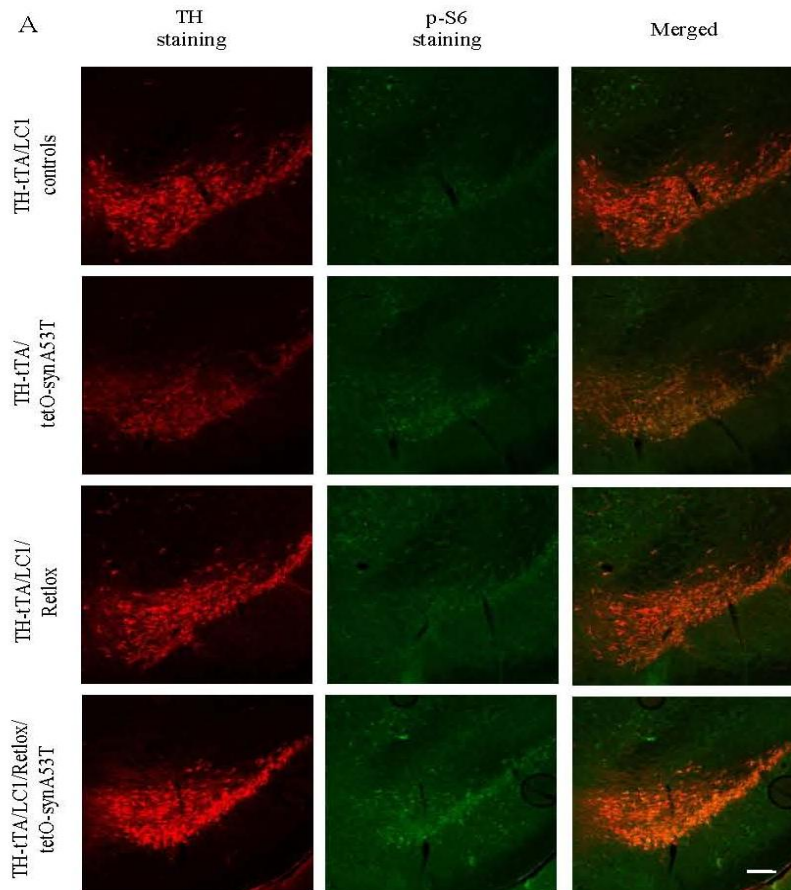
Figure 4.19 Phospho-S6 ribosomal protein -a marker for mTOR activity- is increased in TH-tTA/LC1/Retlox/tetO-synA53T mice

(A) Confocal images of p-S6 immunohistofluorescence staining of 2 year old control, TH-tTA/tetO-synA53T, TH-tTA/LC1/Retlox and TH-tTA/LC1/Retlox/tetO-synA53T mice co-

stained with TH shows co-localization of p-S6 and TH. Scale bar: 200 μm. (B) Quantification of signal intensity in SNpc and VTA of relative mice groups shows increased p-S6 level in TH-tTA/LC1/Retlox/tetO-synA53T mice compared to other group (n = 3, data are represented as mean +/- s.e.m.; * p≤0.05, ** p≤0.01, *** p≤0.001; One-way ANOVA, Tukey post-hoc test).

4.3.5 Mitophagy and mTOR signaling pathway is influenced by overexpression of human A53T α-synuclein

mTOR activation is crucial for protein translation, long-lasting synaptic plasticity cell survival via Akt, and autophagy (Tang *et al*., 2002; Cammalleri *et al*., 2003; Malagelada *et al*., 2008; canal *et al*., 2014), and mTOR deregulation has become a hallmark in neurodegenerative disorders (Tang *et al*., 2002; Cammalleri *et al*., 2003; Malagelada *et al*., 2008; canal *et al*., 2014).

A lot of molecules and proteins are involved in the regulation of macroautophagy from the early stages such as formation of phagophores, cargo recognition and mTOR signaling pathway until mitophagy takes place. Changes in the level of some of these mitophagy regulators have been profound in the brain of Parkinson's patients and in animal models of PD. Particularly important ones are include RTP801 (Malagelada *et al*., 2006), phosphorylated Akt (Malagelada *et al*., 2008), TOM40 (Bender *et al*., 2013), LAMP2A (Alvarez-Erviti *et al.,* 2010), and HSC-70 (Alvarez-Erviti *et al*., 2010), but there are many others. These changes might influence other cell signaling pathways, receptors and proteins such as GFRα1, Nurr1 and Ret (Decressac *et al*., 2012) and leads to neurodegeneration which can be detected by TH and DAT markers.

To further investigate the mechanisms by which α-synuclein causes toxicity in the cells and leads to neurodegeneration in TH-tTA/tetO-synA53T mice as well as to examine changes in the level of some proteins indicated in other studies, western blot analysis in two year old TH-tTA or LC1 control mice and TH-tTA/tetO-synA53T mice was done (Figures 4.20 and 4.21). The amount of the human α-synuclein, α-synuclein, GDNF, GFRα1, Ret, NCAM, Nurr1, TH, DAT, TOM20, TOM40, p-62, LC3, RTP801, S6, p-S6, Akt/Phospho-Akt, AMPK/Phospho-AMPK, mTOR/Phospho-mTOR(ser2448), mTOR/Phospho-

mTOR(ser2481) (Figure 4.21) and GFRα2, NDUF8B, NDUFA10, ATG9A, Girk2, HSC-70, LAMP2A, N-Cadherin, OPTN, Parkin, PINK, Syndecan3, S6, p-S6, Akt, Phospho-Akt, AMPK, Phospho-AMPK, mTOR, Phospho-mTOR(ser2448), Phospho-mTOR(ser2481), ULK1, Phospho-ULK1proteins (Figure 4.21) in the ventral midbrain of control and α-synuclein transgenic mice were measured and β-actin was used as a loading control.

The first obvious change was the level of human α-synuclein which was significantly increased to 4 fold from 2 fold in 3 months old mice, indicating a slow increase in the expression and accumulation of human α-synuclein in TH-tTA/tetO-synA53T mice model, which is in accordance to what happens in the Parkinson's patient with aging and progression of disease (Figure 4.20A). Accordingly, total levels of α-synuclein (human+mouse) increased (Figure 4.20A). In contrast to the data published by Decressac *et al*., 2012, there were no changes in the level of Nurr1 and Ret in TH-tTA/tetO-synA53T mice. TH showed a tendency to decrease, but was not significant as shown before by immunostaining (Figure 4.20A). This might be due to the more specific population targeted in staining rather than western blotting. TOM40 a membrane transport protein significantly increased as previously reported (Bender *et al*., 2013). A tendency toward an increase in the level of p-62 and significantly elevated LC3II protein level confirmed previous immunostaining findings (Figure 4.20A). RTP801 and phospho-mTOR(ser2481) protein levels were dramatically increased, whereas the levels of phospho-AMPK, phospho-AMPK/AMPK , phospho-mTOR(ser2448)/mTOR and ULK1 significantly decreased (Figures 4.20A and 4.21A). There were no further changes detected in levels of many other proteins, including GFRα2, NDUF8B, NDUFA10, ATG9A, Girk2, HSC-70, LAMP2A, N-Cadherin, OPTN, Parkin, PINK, Syndecan3, S6, p-S6, Akt and Phospho-Akt (Figure 4.21A).

In order to address the question of whether alterations in protein levels observed in 2 year old mice can already be detected at an earlier time point, 1 year old control, TH-tTA/tetO-synA53T, TH-tTA/LC1/Retlox and TH-tTA/LC1/Retlox/tetO-synA53T mice were analyzed by Western blotting concerning , the protein level of human α-synuclein, TOM40, p62, LC3, RTP801, AMPK, phosphor-AMPK, mTOR, phospho-mTOR(ser2448), phospho-mTOR(ser2481), ULK1 and phospho-ULK1 (Figure 4.23). Although, there were variations in the level of some of these proteins such as phospho-mTOR(ser2448), phospho-mTOR(ser2481) and mTOR, none of them were found to be significant (Figure 4.22B).

This supports the progressive nature of the neurodegeneration process in these mutant mice leading with aging to more profound alterations.

These results indicate that changes in the mitophagy pathway start in 1 year old mice. Presumably these changes later on lead to neurodegeneration by aging and progression of alteration in the proteins levels.
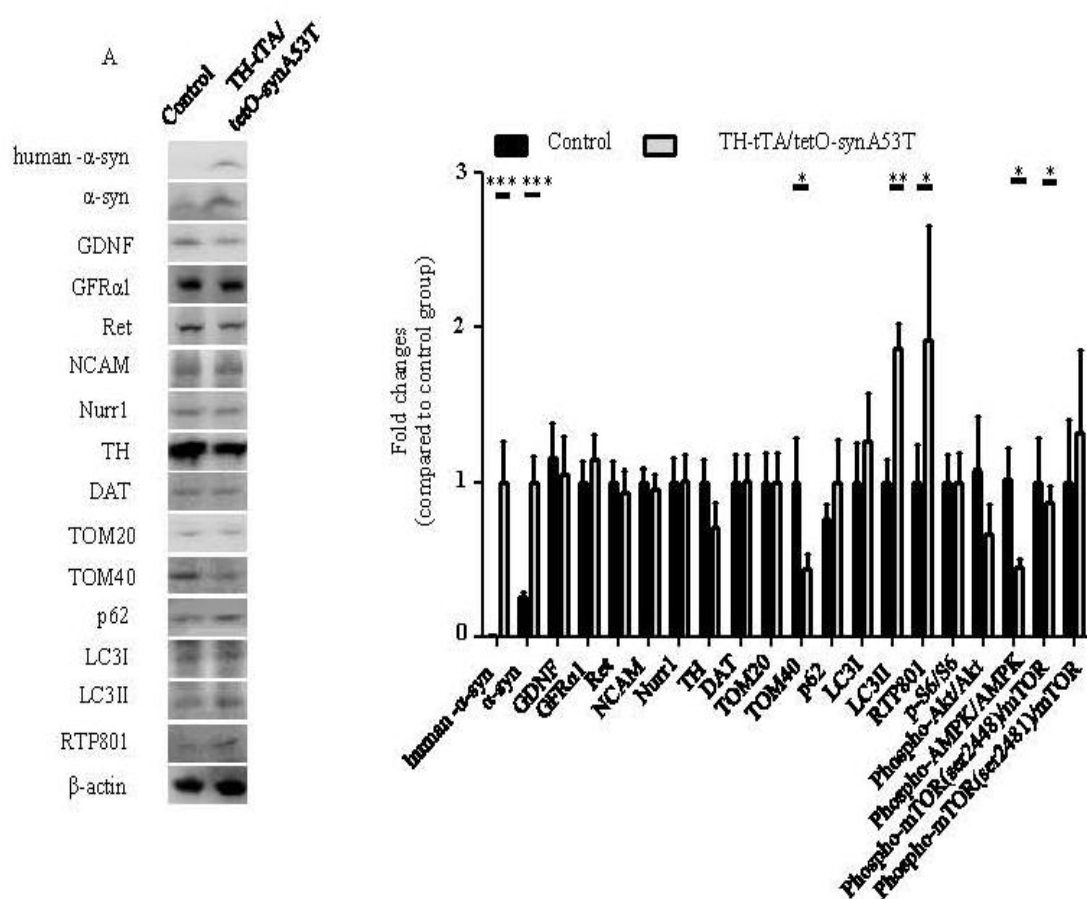
Figure 4.20 Alterations in 2 year old mice with DA neuron-specific human A53T α-synuclein overexpression

(A) The amount of the indicated proteins in the ventral midbrain of control and α-synuclein transgenic mice is measured by western blot analysis. β-actin was used as a loading control (n=6, data are represented as mean +/- s.e.m.; *p≤0.05, **p≤0.01 ***p≤0.001, Student´s t-test).
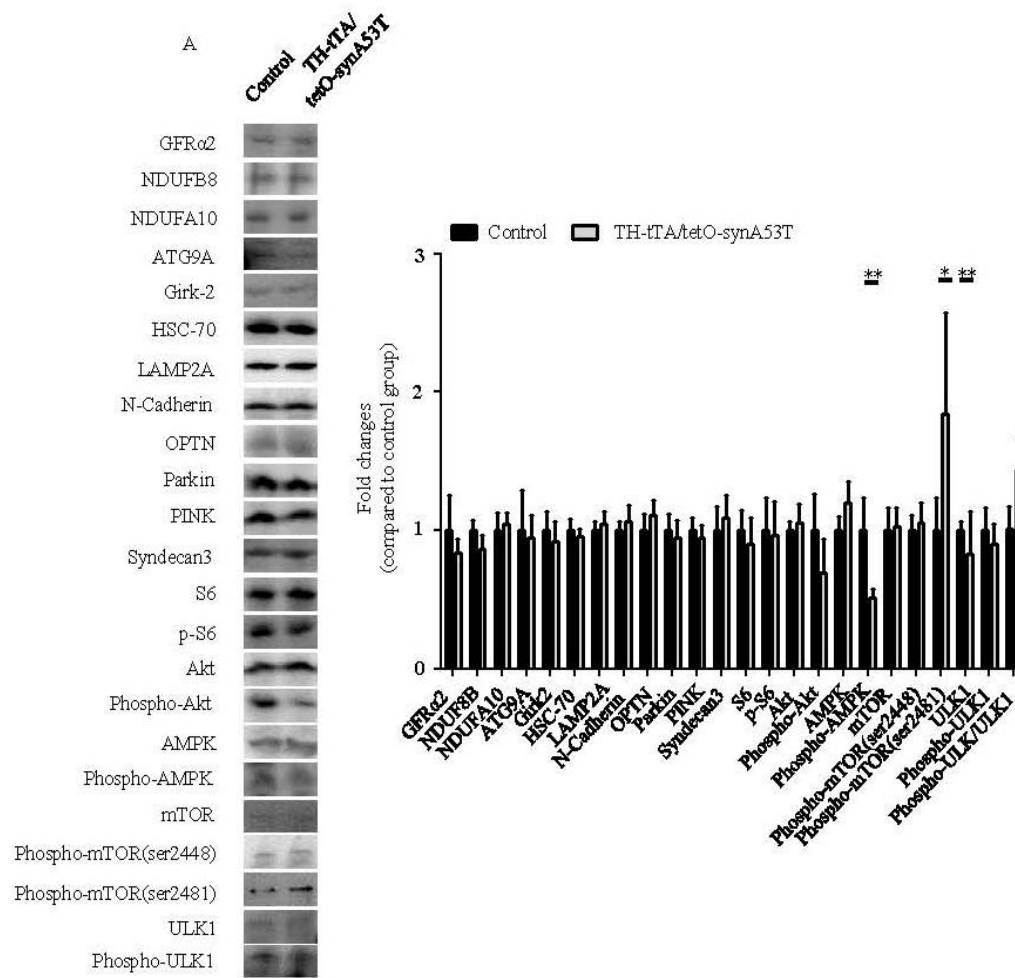
Figure 4.21 Alterations in 2 year old mice with DA neuron-specific human A53T α-synuclein overexpression

(A) The amount of the indicated proteins in the ventral midbrain of control and α-synuclein transgenic mice is measured by western blot analysis. β-actin was used as a loading control (n=6, data are represented as mean +/- s.e.m.; *p≤0.05, **p≤0.01, Student´s t-test).
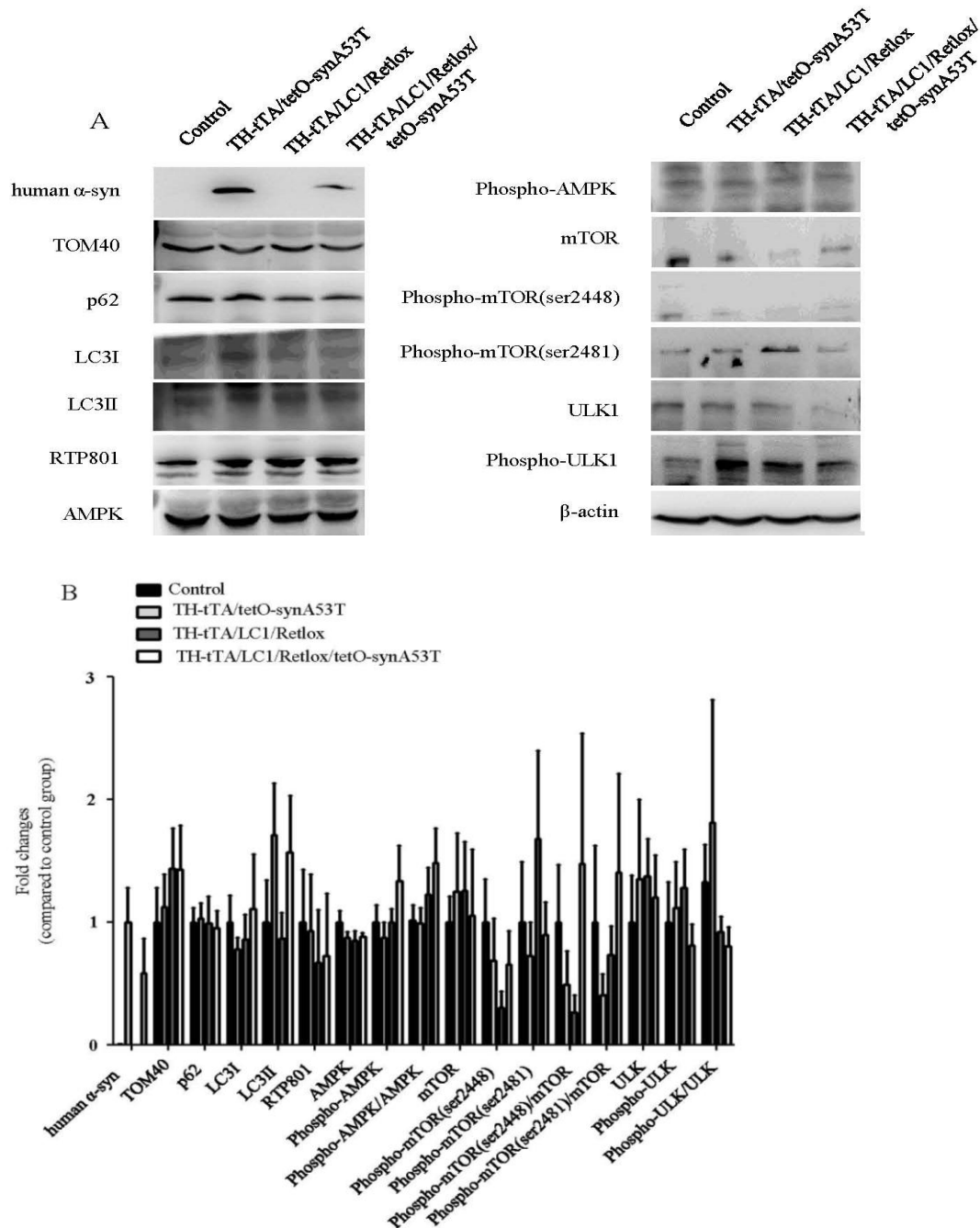
Figure 4.22 Alterations in 1 year old Ret mutant mice with transgenic human A53T α-synuclein overexpression

(A) The amount of the indicated proteins in the ventral midbrain of control, TH-tTA/tetO-synA53T, TH-tTA/LC1/Retlox and TH-tTA/LC1/Retlox/tetO-synA53T mice is measured by Western blot analysis. β-actin was used as a loading control (n=4, data are represented as mean +/- s.e.m.; *p≤0.05, **p≤0.01 ***p≤0.001, Oneway ANOVA, Tukey post-hoc test).

4.3.6 GDNF signaling can prevent mitochondrial fragmentation phenotype in human A53T α-synuclein overexpressing SH-SY5Y cells

In order to investigate how human α-synuclein and Ret influence mitochondrial function, first mitochondrial morphology in transfected SH-SY5Y cells was investigated. The mitochondrial network in SH-SY5Y cells was visualized by using MitoDsRed and mitochondria were classified into tubular or fragmented based on their length (Figure 4.23A). Mitochondrial fragmentation was increased after transfection with an α-synuclein A53T expression plasmid or Ret-specific siRNA from 20% in control siRNA-treated cells to 70-80% and further increased in Ret knock down+α-synucleinA53T overexpressing cells to 90% (Figure 4.23A and B). However, the mitochondrial fragmentation phenotype in SH-SY5Y cells overexpressing α-synuclein A53T could be completely rescued by treating the cells at the same time with the Ret receptor ligand GDNF and its co-receptor GFRα1 (Figure 4.23 A and B). Notably, the GDNF/GFRα1 treatment had no effect on α-synuclein A53T protein levels (Figure 2.23 D). The cell culture part was done by Eva Dürholt, a PhD student from Konstanze Winklhofer's lab (Figure 4.23).

To have a further look at the level of Ret, TOM40, p62 and LC3 proteins, cell lysates were loaded on SDS-PAGE gel and then transferred on PVDF membrane for immunodetection. Membranes were incubated with indicated antibodies and the protein levels were measured (Figure 4.24). No changes were detected in the level of TOM40 and p62 proteins, whereas slight increases in the level of Ret and LC3 in α-synuclein A53T and α-synucleinA53T+GDNF cells was observed (Figure 4.24). Increased protein levels of LC3 in α-synuclein A53T transfected cells is consistent with the increased LC3 protein levels in the midbrain of TH-tTA/tetO-synA53T mice but further increase of LC3 in α-synuclein A53T transfected cells treated with GDNF was not expected as well as increase in the level of Ret in α-synuclein A53T and α-synucleinA53T+GDNF transfected cells (Figure 4.24). These might be cell culture artifacts which further support the need to confirm cell culture *in vivo* in an animal model. However, the cell culture data support the *in vivo* mouse data that show an α-synuclein and Ret crosstalk on regulating autophagy - including mitophagy - to regulate mitochondrial integrity. We have shown here clearly that α-synuclein and Ret signaling converge on common targets such as mTOR and autophagy, but that α-synuclein seems not to directly alter Ret expression or signaling as proposed in earlier studies.
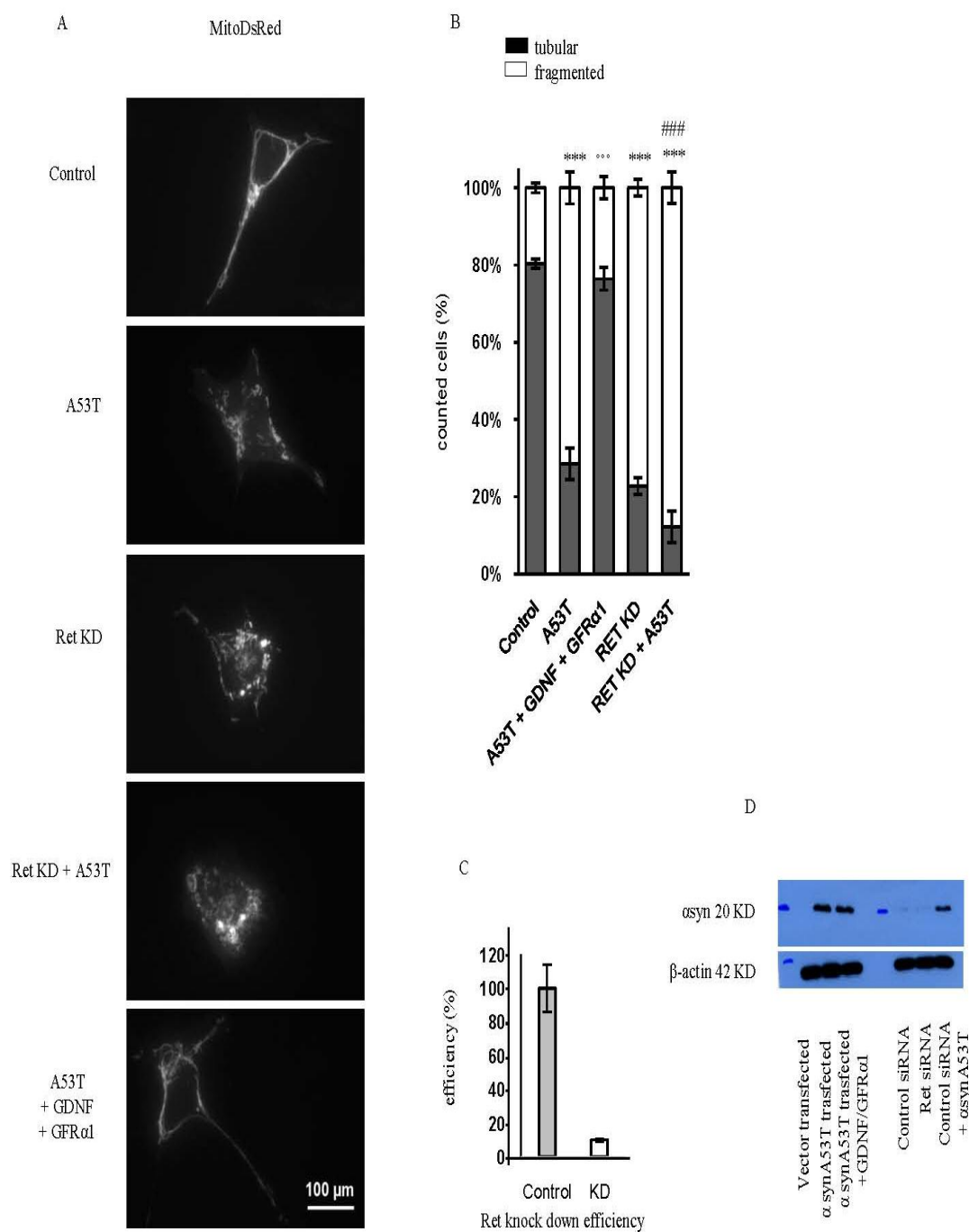
Figure 4.23 Mitochondrial fragmentation in α-synuclein A53T trasfected SH-SY5Y cells can be prevented by GDNF

(A) Representative images showing alterations in mitochondrial morphology after transfection with α-synuclein A53T and additional treatment with GDNF + GFRα1, also Ret

knock-down as indicated. MitoDsRed used as transfection control. (B) quantification of cells with tubular (white bar) or fragmented (grey bar) mithochondria from experiment showing a pronounced increase in cells with fragmented mitochondria due to α-synuclein, whereas this fragmentation can be rescued by GDNF + GFRα1 (data are represented as mean + s.e.m., ***p≤0.001, Control group compared to A53T, RetKD and RetKD+A53T groups. ###p≤0.001, RetKD+A53T group compared to A53T and RetKD groups. °°° p≤0.001, A53T+GDNF+GFR α1 group compared to A53T group. Oneway ANOVA, Tukey post-hoc test) (C) The graph showing qRT-PCR quantification of Ret knock-down efficiency. (D) Western blot image shows expression of α-synuclein A53T in cells. β-actin is shown as loading control.
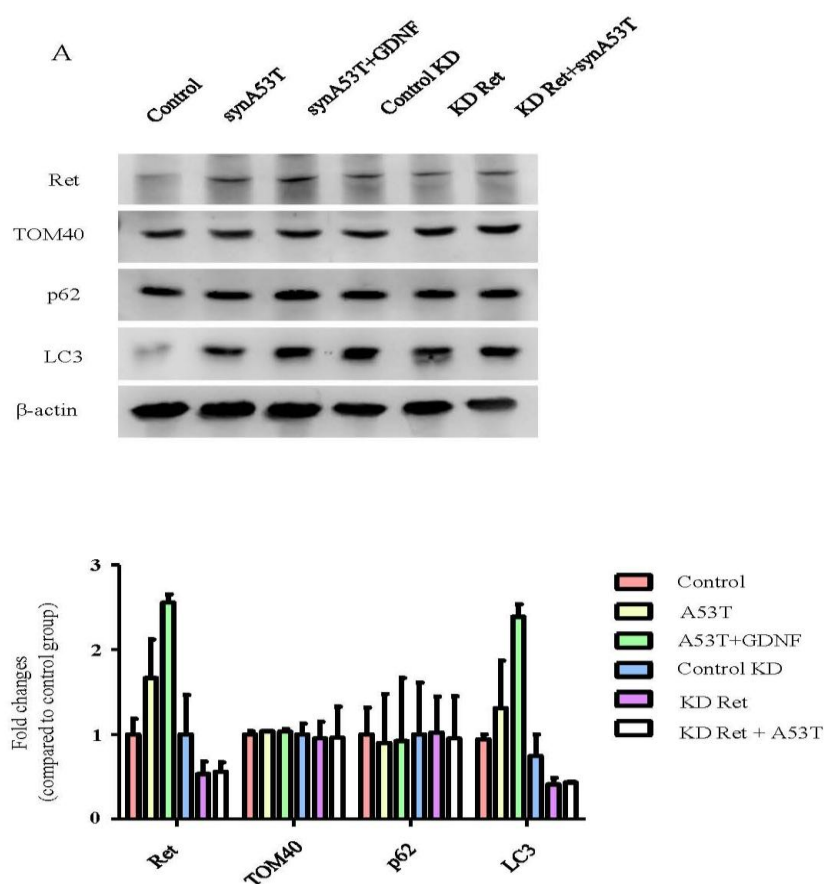
Figure 4.24 Alterations in α-synuclein A53T transfected SH-SY5Y cells

(A) The amount of the indicated proteins in the SH-SY5Y cells of control, α-synuclein A53T overexpression, α-synucleinA53T+GDNF overexpression, Control knock-down, Ret Knock-down, Ret knock-down+ α-synucleinA53T overexpression is measured by Western blot analysis. β-actin was used as a loading control (n=2, data are represented as mean +/- s.e.m, Oneway ANOVA, Tukey post-hoc test).

5. Discussion

5.1 Characterization of new TH-tet mouse lines specific for the dopaminergic system

5.1.1 Characterization of new TH-tTA and TH-rtTA mouse lines

The TH-tTA and TH-rtTA mice were generated to genetically target specifically mDA neurons, which are the most affected neurons in the pathology of PD, to assess cell-autonomic gene function in DA neurons without altering in addition neighboring or pre- or postsynaptic cells which can lead to secondary effects on DA neurons.

Three different groups have already generated transgenic mice in which the tet-system was used to target mDA neurons, but each of these published mouse lines has specific disadvantages such as low DAT levels and hyperactivity in a heterozygote DAT knockout mouse generated by a tTA knock-in into the endogenous DAT locus (Cagniard *et al*., 2006), tetracycline-dependent regulation loss in a TH-rtTA mouse line (Chinta *et al*., 2007), and not shown tetracycline-dependent regulation in a mouse line carrying a Pitx3-tTA construct (Lin *et al*., 2012). Therefore, our TH-tTA and TH-rtTA mouse lines have been established to overcome these limitations. An 8.9 kb fragment of the mouse TH 5' region including promoter and regulatory elements has been used to drive expression. When the tet-system is constitutively active during development and adulthood of the mouse (Figure 4.1, 4.2 and 4.3) this results in a broad activity of TH-tTA and TH-rtTA due to the wide TH expression in the CA neurons as well as in non-CA neurons (Baetge and Gershon, 1989; Jonakait *et al*., 1984; Teitelman *et al*., 1981). In TH-tTA/LC1/R26R and TH-rtTA/LC1/R26R mice expression was observed not only in the ventral midbrain but also in the cerebellum, hippocampus, thalamus, neocortex, pons, and olfactory bulb where TH promoter activity has been reported previously (Maskri *et al*., 2004; Min *et al*., 1994; Schimmel *et al*., 1999).

The expression levels in all expressing TH-tTA and TH-rtTA founders were approximately the same and quantification of LacZ and TH double positive cells showed an incomplete and mosaic targeting of mDA neurons (Figure 4.1, 4.2 and 4.3). How can the incomplete targeting in the TH-tTA and TH-rtTA mice be explained? Incomplete targeting of DA neurons was also reported by other studies in which transgenic mice were generated with the rat TH promoter (Gelman *et al*., 2003; Savitt *et al*., 2005). A comparison between the 5' region of rat and mouse reveals only a small

sequence difference indicating species specificity of some regulatory elements (Romano *et al*., 2005; Lenartowski and Goc, 2011). Transgenic mice carrying the Cre recombinase gene driven by a 9 kb rat TH promoter showed 80% co-localization of TH and Cre which is in a similar range as observed in TH-tet mouse lines with different target genes (Gelman *et al*., 2003; Savitt *et al*., 2005). Kelly and colleagues in 2006 used homologous recombination to generate a knock-in reporter mouse line in which the yellow fluorescent protein (YFP) replaced the first exon and intron of the TH gene (Kelly *et al*., 2006). YFP expression did not overlap completely with TH expression in this model, indicating that most likely the first intron of the TH gene contains *cis*-acting regulatory sequences which are important for accurate expression of TH (Kelly *et al*., 2006). Mosaic expression has been also reported in IRES knock-in mice expressing Cre-recombinase from the 3′-untranslated region of the endogenous TH gene (Lindeberg *et al*., 2004). Furthermore, in IRES mice the reporter construct showed significant difference in expression pattern. Use of the R26R reporter instead of cβ-LacZ reporter demonstrated a larger population of LacZ-expressing cells compared to sparse expression with the cβ-LacZ reporter (Lindeberg *et al*., 2004). Thus, an appropriate reporter construct itself is also an important factor for targeting since transgenic mouse lines do not express reporters homogeneously in DA neurons (Lindeberg *et al*., 2004). Insufficient expression of tTA and as a result insufficient activation of tet-responsive promoter activation (Böger and Gruss, 1999), differences in the genomic copy number and sites of integration (Robertson *et al*., 2002) could be additional reasons for the variation in the targeting level of transgene expression.

Although the incomplete and mosaic targeting in TH-tTA and TH-rtTA mice is a disadvantage for systemic approaches at the same time it can also be considered an advantage. In genetically mosaic animals somatic tissues have different genotypes, which allows to study cells and tissue in a wildtype surrounding (Lee *et al*., 1999). Mosaic expression can also be considered an advantage for electrophysiological studies where DA neurons with different genetic alterations (wildtype and mutated) can be compared *in vivo* in the same animal. MARCM (for mosaic analysis with a repressible cell marker) clones in the nervous system of *Drosophila melanogaster* has been successfully used to study mutant gene function in a wildtype background *in vivo* (Lee *et al*., 1999). In the "MARCM" system mutant cells but not heterozygous parents or homozygous wild type siblings are labeled (Lee *et al*., 1999). The newly established TH-tTA and TH-rtTA mice should allow a similar mosaic analysis in the nervous system of the mouse.

5.1.2 Genetic silencing of the LC1 and its independent targeting of adult DA neurons in TH-tTA and TH-rtTA mice

No induction of expression was observed in TH-rtTA/LC1/R26R mice if no DOX was administered from conception to adulthood as well as a reduced number of cells switched on expression in TH-tTA/LC1/R26R mice treated with DOX indicating difficulties to switch on the system during adulthood (Figure 4.1, 4.2 and 4.3). Similar observations have been reported previously by different research groups employing the tet-off system (Bejar *et al*., 2002; Lindeberg *et al*., 2002; Krestel *et al*., 2004). Prenatal treatment with DOX resulted in a slow reactivation, changed expression pattern and levels that failed to reach the original maximum value (Bejar *et al*., 2002; Lindeberg *et al*., 2002; Krestel *et al*., 2004). Also in tet-on mice difficulties in late gene activation has been reported (Chinta *et al*., 2007; Beard *et al*., 2006). This might be explained by epigenetic silencing of the inactive tet-responsive promoter in the mouse (Böger and Gruss, 1999; Kues *et al*., 2006; Palmiter and Brinster, 1986). To circumvent this problem, TH-tet mice were introduced to the tet-responsive promoter by injection of a rAAV vector as previously done by Zhu and colleagues (Zhu *et al*., 2007). Injection of AAV-tetO-Venus in the mouse brain which is independent of LC1 function activated by the tet-transactivator was successful and showed activation of both TH-tTA and TH-rtTA system (Figure 4.4 and 4.5). Therefore, silencing of tetO-constructs in the TH-tet mice can be overcome by viral injection in adult mice, indicating TH-tTA and TH-rtTA mice can be combined with different tetO-constucts and activate or inhibit gene expression at any time from embryogenesis to adulthood and even to seniority using DOX.

5.1.3 Genetic deletion of dopaminergic cells in TH-tTA mice expressing diphtheria toxin-A

The tight control of expression in the TH-tet system by applying DOX during development and after birth in TH-tTA mice is a clear genetic advantage to many other tet-systems previously described (Cagniard *et al*., 2006; Chinta *et al*., 2007; Lin *et al*., 2012). In this context using mosaic expression in the TH-tTA/LC1 mice and applying DOX allowed us to establish viable TH-tTA/LC1/Rosa26dt-a mice showing a progressive neurodegeneration in adult mice reaching to 30% of neuronal loss at the age

of 3-7 months (Figure 4.6). Whereas, applying DOX-free food in these mice resulted in the death of litters shortly after birth (Tillack *et al*., 2015) most likely due to the loss of noradrenergic neurons in the peripheral nervous system innervating the heart and resulting in developmental cardiovascular failure like in TH knockout mice (Kobayashi *et al*., 1995). TH knockout mice can be rescued by knocking-in TH into the noradrenergic-specific dopamine-β-hydroxylase locus (Zhou and Palmiter, 1995). Lethality in TH-tTA/LC1/Rosa26dt-a mice as a consequence of TH expressing noradrenergic cell loss is supported by data from DAT-Cre/Rosa26dt-a mice. They showed a reduced number of mDA neurons but are viable and have a normal motor behavior despite the DA cell loss of around 90% (Golden *et al*., 2013).

Here data showed that DA cell loss in TH-tTA/LC1/Rosa26dt-a mice transiently treated with DOX is less variable and is easier to generate compared to the commonly used injections of neurotoxins such as MPTP, 6-OHDA or rotenone to induce PD like pathology (Duty and Jenner, 2011). Thus, the inducible DA cell loss phenotype in TH-tTA/LC1/Rosa26dt-a mice might be a favorable alternative to test therapies for PD treatment.

5.1.4 *In vivo* detection of bioluminescence in TH-tTA/LC1 and THrtTA/LC1 mice

Because it would be a great advantage to monitor the progression of DA neuron degeneration in living mice, with the help of TH-tTA/LC1 mice a model that allows an *in vivo* bioluminescence (BLI) imaging of the DA system over time has been developed. The feasibility and kinetics of inducible gene expression in the adult TH-tTA/LC1 mice expressing the luciferase reporter enzyme has been shown previously with systemic application of the D-luciferin substrate (Tillack *et al*., 2015). I also confirmed the reversible gene activation with D-luciferin in TH-rtTA/LC1 mice (Figure 4.7). TH-rtTA/LC1 mice without DOX showed very weak luciferase signal (Figure 4.7) that might be explained by residual affinity of rtTA to tetO in the absence of DOX causing elevated background and basal activities of the target promoter or unspecific D-luciferase conversion (Urlinger *et al*., 2000). The luciferase signal in TH-rtTA mice increased 2 weeks after receiving DOX to a maximal level and decreased again to original level post 2 weeks after withdrawal of DOX (Figure 4.7). Comparing the data with TH-tTA mice revealed faster ON-kinetics in TH-rtTA mice but weaker signal,

even though the signal was strong enough to visualize the DA system. Lower basal activity and background signal observed in bioluminescence imaging of TH-rtTA/LC1 mice compared to the TH-tTA/LC1 mice might be due to the use of rtTA3G Tetracycline-Inducible Gene expression system which is the third generation of the most powerful and versatile inducible mammalian expression systems that offers significantly reduced background (Loew *et al*., 2010; Fan *et al*., 2012).

However, the sensitivity and the readout on the cellular level remained low. Several factors like optical properties of the substrate, expression level of the reporter gene, sensitivity of the device used for detection and the depth of labeled cells within the body affect the sensitivity of the imaging modality (Rice *et al*., 2001; Andrzejewska *et al*., 2015). The major problem of *in vivo* bioluminescence imaging is detection of cells placed deeper because the signal drops approximately tenfold for each 10 mm of tissue depth (Weissleder, 2001). To overcome the sensitivity problem, different efforts have been made to improve the optical properties of imaging probes. One of the recent innovations is developing new generations of synthetic luciferin substrates like CycLuc1 which has shown effectively improved signal intensity due to a better pharmacokinetics (Evans *et al*., 2014). To try to improve the bioluminescence signal in our TH-tet mice, I applied CycLuc1 (Evans *et al*., 2014) instead of D-luciferin which have been used previously (Figure 4.7).

Applying CycLuc1 significantly improved the bioluminescence signal - average radiance and light output - in TH-tTA/LC1 mice and to a lesser extent in TH-rtTA/LC1 mice by using 10 times less substrate (Figure 4.7). This data is consistent with data previously reported showing the efficient blood-brain-barrier cross of CycLuc1 in mice and a much better labeling of DA neurons using CycLuc1 compared to D-luciferin in mice carrying a DAT-Cre and Rosa26 floxed-stop luciferase reporter construct (Evans *et al*., 2014). The bioluminescence signal might be further improved by further enhancing the luciferase substrate signal intensity *in vivo* by for example red-shifting the signal (Mofford *et al*., 2015) or improving the luciferase processivity of the optimized CycLuc1 substrate (Harwood *et al*., 2011).

This data also suggest that, for expressing a gene for a short time period it might be an advantage to use the TH-rtTA mice, whereas for switching off a gene for a short time the TH-tTA mice might be preferred. The reasons are that (1) the tet-off systems shows a slower ON-kinetics (several weeks) compared to the tet-on system (several days), (2) this saves DOX-food costs, (3) long DOX-treatment times might result in an accumulation of DOX in the bones that is only slowly cleared after removal of DOX

from the food or water (Kistner *et al*., 1996; Gingrich and Roder, 1998; Xie *et al*., 1999). Using *in vivo* imaging in our TH-tet mice might allow to follow progressive degeneration and regeneration processes of the DA system over time in individual mice that would allow to (1) cut down the number of animals in longitudinal studies, (2) avoid inter-subject variability problems, (3) reduce the time for analysis dramatically by replacing or preceding a detailed histological analysis.

5.1.5 Multicolor labeling of dopaminergic cells by stereotactic injection of AAV-dual color Brainbow

There is a great interest to invent new methods to visualize synaptic circuits for detailed analysis of neuronal network architecture (Livet *et al*., 2007). Accordingly, sparse and random labeling of individual cells with different colors help to reveal the structure and function of individual neurons (Jefferis and Livet, 2012). Genetically labeling of neurons with multiple and distinct colors by using for example the Brainbow method represents a considerable improvement over current tracing techniques (Livet *et al*., 2007). The Brainbow method in mice has been adapted for *Drosophila melanogaster* to study the innervation patterns of neurons (Hampel *et al*., 2011), chick (Egawa *et al.,* 2013), and in zebrafish trigeminal sensory ganglion (Pan *et al*., 2011). Also zebrabow lines have been developed successfully for tissue-specific multicolor labeling (Pan *et al*., 2013). However, there was a little use of the original method in the mouse to trace neuronal connectivity outside the motoneurons and hippocampal system and the Brainbow mice did not express in DA neurons (Livet *et al*., 2007; Tillack thesis, 2013). Therefore, Cai and colleagues developed in 2013 mice with improved Brainbow transgenes which showed improved expression levels leading to multicolor spectral labeling of neuronal populations in numerous brain regions including cerebral cortex, brainstem, cerebellum, spinal cord and retina, although due to the use of the Thy1.2 promoter they were still not useful to label DA neurons (Cai *et al*., 2013).

Attempts to use Brainbow in the DA system of mouse brain by replacing the Thy1.2 promoter with the DA specific mouse TH promoter fragment or with the general CBA promoter followed by a stop cassette was also not successful and there was no strong expression of flourophores in all the generated mouse lines (Tillack thesis, 2013). Thus, as an alternative approach, rAAV vectors were designed encoding distinct XFPs behind a floxed STOP codon (LSL) which should allow a multicolor labeling of cells according

to the RGB scheme after Cre recombination (Figure 1.8) (Card *et al*., 2011; Weber *et al*., 2011; Tillack thesis, 2013). To label DA neurons, DA specific Cre mouse lines like TH-tTA/LC1 and DAT-Cre were stereotactic injected with a mix of three different fluorophores encoding AAV-LSL-XFP and evaluated 5 weeks later. Different fluorescently labeled DA neurons could be observed and showed to prove of principle (Figure 1.8) (Tillack thesis, 2013). However, there are still limitations to use this procedure for single cell tracings. First, the expression in this investigated time window seems not strong enough to visualize with certainty the complete axonal tree of a DA neuron, so that a longer time window and a higher virus concentration might be tried to increase the copy number and expression of the fluorophores (Tillack thesis, 2013). Second, as in the Brainbow approach also here the color saturation of the axon seems to alter with the distance to the soma, therefore the number of labeled cells might need to be reduced to allow better tracing for example by not completely activating Cre expression in all cells the TH-tTA/LC1 and TH-rtTA/LC1 with DOX (Livet *et al*., 2007; Cai *et al*., 2013; Tillack thesis, 2013).

In the meantime also different fluorophore-encoding rAAV viruses were published using Cre recombinase to activate fluorophore expression not by removing a floxed STOP cassette but be inversion of the fluorophore encoding cDNA (Cai *et al*., 2013). These Brainbow rAAV vectors are also using membrane tagged XFPs that might enhance axonal labeling (Cai *et al*., 2013). These Brainbow rAAV vectors obtained and then tested by stereotactic injection into the midbrain of TH-tTA/LC1 mouse employing different DOX treatment conditions (Figure 4.8). DOX was used to help to limit the number of reactivated mDA neurons for a successful sparse labeling.

As it is shown in the Figure 4.8, using DOX only very few cells got labeled which was one of the aims regarding single cell tracing, but most of the fluorescent cells were green in color. The reason that high diversity of color was not achieved might be that (1) infection of multiple AAV virions in one cell didn't happen or (2) there are preferred Cre-mediated recombination events leading to only one color (Cai *et al*., 2013; Weissman and Pan., 2015). Another problem is the lack of labeling of axonal fiber bundles and terminals in the striatum which might be due to a slow or inefficient transport of the membrane-bound fluorophores along the axons. That a DA axonal labeling is feasible has been shown with rAAV-LSL-XFP vectors in mice (Tillack thesis, 2013) and with pal GFP- or GFP-expressing Sindbis virus vectors in the rat brain where 8 neurons were traced in detail (Matsuda *et al*., 2009). Using our rAAV-LSL-XFP vectors it is observed that the labeling intensity and color saturation changes in the

long DA neuron axons towards the striatum, leading to a color change in the axons that make tracings in densely labeled areas difficult – as also described for the Brainbow constructs (Livet *et al*., 2007; Cai *et al*., 2013; Tillack thesis, 2013; Weissman and Pan., 2015). To optimize axonal tracing conditions in the DA systems further attention should be paid to the two main factors determining color diversity, the copy number of the fluorescent protein encoding transgene and the timing and level of Cre activity (Weissman and Pan., 2015). As a rule, more copies of the Brainbow DNA construct result in higher expression levels and more color combinations due to the mixture of more pigments (Weissman and Pan., 2015). However, a high level of DNA constructs present in cells may lead to reduced color diversity since all cells have all pigments (Cai *et al*., 2013). Taken together, for tracing of DA neurons our rAAV-LSL-XFP vectors in combination with the TH-tTA/LC1 mice seem currently to be the best tools and allow to optimize the copy number by adjusting the infection units of the virus and the Cre activity via the DOX regulated tet-system.

5.2 Inducible gene deletion and transient gene expression in TH-tTA mice as a model of Parkinson's disease

5.2.1 Induced deletion of the neurotrophic receptor Ret and overexpression of human α-synuclein in TH-tTA mice

After establishing and characterizing the new TH-tet system, the TH-tTA mice have been used to generate TH-tTA/LC1/Retlox mice that allowed by raising the mice on DOX to address the long standing question how far Ret is required for the maintenance of the adult DA system (Tillack thesis, 2013). The Ret recombination efficacy in mDA neurons in TH-tTA/LC1/Retlox mice reached about 40% and resulted in a 15% loss of neurons specifically in the SNpc and 12% innervation loss in the dorsal striatum (Figure 1.9). This confirms the mild but significant age dependent SN DA neuronal loss observed in conditional DAT-Cre Ret knockout mice (Kramer *et al*., 2007), and indicates no embryonic compensation in the DAT-Cre/Ret mice (Ibáñez *et al*., 2008) that could explain the discrepancy to GDNF deficient mice which were shown to have a very strong loss of DA neuron phenotype (Pascual *et al*., 2008) or no DA phenotype at all and α-synuclein (Tillack thesis, 2013; Kopra *et al*., 2015). Crossing Ret knockout mice with DJ-1 mice led to increased loss of DA neurons in the SNpc (Aron *et al*.,

2010) indicating Ret signals together with DJ-1, a chaperone protein mutated in some familiar forms of PD stimulate DA cell survival through the ERK signaling cascade (Aron *et al*., 2010). Also, double-deficient mice for Ret and parkin in mDA neurons showed an enhanced SN DA cell and striatal DA innervation loss when compared to the moderate degeneration in Ret deficient mice and no alterations in parkin-deficient mice (Meka *et al*., 2015).

This analysis is especially important since the previous efforts to generate a model for PD expressing mutant variants of α-synuclein with enhanced levels of DA neurodegeneration failed (Chesselet, 2008; Daher *et al*., 2009a; Lin *et al*., 2009; Nuber *et al.,* 2008) and even combination of α-synuclein mutant mice to other PD related proteins like parkin (von Coelln *et al*., 2006; Stichel *et al*., 2007) and DJ-1 (Ramsey *et al*., 2010) could not show any significant cell loss in the midbrain.

Here, the aim was to address in more detail the influence of Ret loss on α-synuclein toxicity. Therefore, TH-tTA/LC1/Retlox/tetO-A53T mice were generated enabling to trigger at the same time in the same DA neurons on one hand the deletion of the Ret receptor and on the other hand the overexpression of human A53T mutated α-synuclein protein. Investigations were also done in single transgenic TH-tTA/tetO-A53T mice with A53T missense mutation from the tet-responsive synA53T transgene (Lin *et al*., 2009) specifically in DA neurons (Tillack thesis, 2013). First I examined the level of human α-synuclein in these mice and I showed that α-synuclein amount accumulates to at least 4 times the wildtype levels in two year old TH-tTA/tetO-synA53T mice. TH-tTA/tetO-synA53T mice have been shown to mildly overexpress mutated α-synuclein from 2 fold in 3 months old mice (Figure 1.10 D-E) to 4 fold increasing by aging in 2 year old mice (Figure 4.20) similar to what is happening in the PD patients (Byers *et al*, 2011). This data could be more powerful than the data provided by stereotactic injections of toxins in the brain of rodents (Lo Bianco *et al*., 2004; Decressac *et al*, 2011; Decressac *et al*., 2012) which receive a high dose of toxic material at the same time and show also sign of injury not only due to the toxin but also side effects of the surgery and anxiety of the animals. Since even severely affected PD patients with a triplication of the α-synuclein encoding locus only express roughly the double amount of α-synuclein protein (Byers *et al*, 2011) our new α-synuclein transgenic mice seem to nicely recapitulate this α-synuclein expression level and are a good model to address α-synuclein toxicity and crosstalk with GDNF/Ret signaling.

In TH-tTA/tetO-synA53T mice 76% of DA neurons express at least the double amount of α-synuclein at 3 months of age (Figure 1.10 D and E) and the α-synuclein amount

accumulates to at least 4 times the wildtype levels in 2 year old mice (Figure 4.20). Karsten Tillack analyzed 1 year old mice and found neuronal loss in the SNpc and VTA and innervations loss in the striatum of 1 year old TH-tTA/LC1/Retlox/tetO-A53T mice as well as tendency of a decrease in the number of mDA neurons in TH-tTA/tetO-A53T mice (Figure 1.11). Here I investigated the 2 year time point and found that in two year old mice the progressive degeneration process lead in TH-tTA/tetO-synA53T mice to 15% DA cell loss in the SN and VTA, 15-18% DA innervation loss in the striatum (Figure 4.11 A-F) without significant increase in thioflavin S-positive protein inclusions (Figure 4.12 A-B). Also 15% total dopamine loss in the striatum of TH-tTA/tetO-synA53T mice (Figure 4.11G) was similar to what has been described in previous studies (Tofaris *et al*., 2006; Daher *et al*., 2009; Lin *et al*., 2012). These data is mostly comparable with a study using new line of tetracycline-regulated inducible transgenic mice that overexpressed the PD-related α-synuclein A53T missense mutation in the mDA neurons (Lin *et al*., 2012). Lin and colleagues in 2012 showed a robust and progressive loss of mDA neurons in the SNC and VTA of PITX3-IRES2-tTA/tetO-A53T mice. They observed 15% mDA neuron loss in the SNC of A53T mice at 1 month of age and 40% loss by the time the mice were 12 months, and there were no significant difference in the loss of mDA neurons between 12 and 20 months old in PITX3-IRES2-tTA/tetO-A53T mice (Lin *et al*., 2012). Although the neuroal loss in the mDA of our TH-tTA/tetO-synA53T mice has been shown but the time point that loss of DA neurons start is relatively late and different from what Lin and colleagues have been observed. The steady-state level of dopamine was also decreased in the striatum of 6 months old PITX3-IRES2-tTA/tetO-A53T mice which again happened late in our TH-tTA/tetO-synA53T mice. However, this late-onset of neurodegeneration is more similar to PD which is an age related disease.

5.2.2 α-synuclein translocation into the nucleus and spreading in TH-tTA/tetO-synA53T mice

The basic characterization of 3 months old TH-tTA/tetO-A53T mice revealed 76% recombination efficacy of human mutated α-synuclein A53T in the mDA neurons and 2 fold overexpression of α-synuclein with a strongest signal detected in the striatum (Figure 1.10) (Tillack thesis, 2013). Further investigation of two important features of α-synuclein including translocation into the nucleus and spreading which is believed to

play an important role in the pathogenesis of PD have been done in this study to confirm the potential mechanisms underlying α-synuclein pathophysiology. It is assumed that for inducing toxicity and pathophysiology of α-synuclein, translocation into the nucleus and binding with histones plays a vital role (Goers *et al*., 2003). Subsequently, staining for phosphorylated human α-synuclein (Ser129) which is the modified form of α-synuclein and most abundant in LBs and LNs that are observed most frequently in PD (Fujiwara *et al*., 2002; Anderson *et al*., 2006; Pe´rez-Revuelta *et al*., 2014), showed somal and nuclear localization of α-synuclein in TH-tTA/tetO-A53T mice (Figure 4.9 B). In accordance to our data other studies also showed α-synuclein phosphorylation at S129 in soma and nucleus in [A30P] αSYN transgenic mouse model that developed age-dependent impairment in fear conditioning behavior (Schell *et al*., 2009). Nuclear α-synuclein is suggested to enhance nigrostriatal degeneration (Kontopoulos *et al*., 2006). In a study by Decressac and colleagues in 2012, sections from AAV-α-synuclein injected rat (2 weeks survival) with sufficient expression level to induce progressive degeneration of DA neurons stained Immunofluorescence for α-synuclein phosphorylated on serine 129 (Ser129) showed prominent nuclear localization of α-synuclein in many DA neuronsthat nigral DA neurons (Decressac *et al*., 2012). They also showed that high expression of phospho-α-synuclein in the nucleus have reduced levels of DA marker VMAT2 and the survival-related transcription factor MEF2D which is in contrast to transduced DA cells with low nuclear expression of phospho-α-synuclein (Decressac *et al*., 2012).

If α-synuclein phosphorylation at Ser129 makes α-synuclein more or less toxic is still a matter of debate (Chen and Feany, 2005; Gorbatyuk *et al*., 2008; Yasuda, *et al*., 2013). α-synuclein phosphorylation at Ser129 is increased in parkin deficient mice but does not modulate DA neurodegeneration (Van Rompuy *et al*., 2015). In addition α-synuclein phosphorylation at Ser129 has been shown in melanoma cells to increase cell surface translocation along microtubule and vesicular release which might enhance spreading of α-synuclein (Lee *et al*., 2012). A study by Chen and Feany reported that phosphorylation at Ser129 is essential for α-synulein to have neuronal toxicity in a Drosophila model of PD (Chen and Feany, 2005). However, there exist also opposing reports. These reports come from studies on the neurotoxicity of the Ser129 phosphorylated α-synuclein in the viral vector-mediated rodent model of α-synuclein overexpression. It was shown that alteration of Ser129 to non-phosphorylated Ala resulted in enhanced (Gorbatyuk *et al*., 2008; Azeredo da Silveira *et al*., 2009) or unchanged toxicity of α-synuclein (McFarland *et al*., 2009) and alteration of Ser129 to a

phospho-mimetic Asp resulted in eliminated (Gorbatyuk *et al*., 2008; Azeredo da Silveira *et al*., 2009) or unchanged toxicity of α-synuclein (McFarland *et al*., 2009). Thus, if the Ser129 phosphorylation of α-synuclein has any effect on DA neurons it seems to be a protective one. Another study using viral vector-mediated delivery of parkin reported prevented DA neuronal loss induced by a chronic MPTP in mice (Yasuda *et al*., 2011). In this study the osmotic minipump-mediated MPTP infusion caused accumulation of the Ser129 phosphorylated α-synuclein in DA cells, which was enhanced by overexpression of parkin (Yasuda *et al*., 2011) which is in line with the report demonstrated that lentiviral-parkin attenuated α-synuclein-induced DA cell loss by increasing the number of the Ser129 phosphorylated α-synuclein positive inclusions in rats (Lo Bianco *et al*., 2004). These data suggest that the phosphorylation resulted in reduced toxicity of α-synuclein (Yasuda *et al*., 2011; Lo Bianco *et al*., 2004). Taken together, more examinations in primates might be required to prove if Ser129 phosphorylation of α-synuclein is protective or toxic.

Neuron-to-neuron transmission and spreading of α-synuclein is thought to be relevant to the slowly increasing LB and LN load in the brain during progression of human synucleinopathies involving more and more connected brain areas (Helwig *et al*., 2016). α-synuclein and tau pathology seem to start from the olfactory bulb and/or brain stem or even enteric nervous system and to progress into higher brain areas as described by the PD Braak stages (Braak *et al*., 2005; Visanji *et al*., 2013).

Recently, many animal models have been developed in an attempt to mimic PD like α-synuclein propagation and to investigate its relationship with protein aggregation and pathophysiology of PD. Based on that there are two experimental strategies to trigger long distance α-synuclein spreading in rodents. One method is direct injections of inoculations consisting of α-synuclein into the striatum and SNpc which resulted in accumulation and propagation of insoluble forms of the protein (Luk *et al*., 2012a, b; Mougenot *et al*., 2012; Masuda-Suzukake *el al*., 2013; Sacino *et al*., 2013; Recasens *et al*., 2014b; Peelaerts *et al*., 2015). The second method is based on injection of AAVs carrying human α-synuclein DNA into the rat vagus nerve which resulted in overexpression of human α-synuclein within medulla oblongata neurons connected to the rat vagus nerve and in a time dependent manner diffused and reached to the pontine, midbrain and finally forebrain regions (Ulusoy *et al*., 2013; Ulusoy *et al*., 2015). In contrast, if these preparations were injected into the brain of α-synuclein deficient mice no diffusion was observed (Blättler *et al*., 1997; Angot *et al*., 2010; Luk *et al*., 2012a; Mougenot *et al*., 2012; Recasens *et al*., 2014b). Although the propagation of α-

synuclein has been shown by injection methods still there is no transgenic mouse model showing α-synuclein propagation and pathophysiology without generating an injury which could artificially enhance α-synuclein spreading. Here this issue in our α-synuclein transgenic mice has been addressed and we could find also here spreading of α-synuclein accumulation to the neighboring cells in the midbrain regions of TH-tTA/tetO-A53T and TH-tTA/LC1/Retlox/tetO-A53T mice (Figure 4.10). This confirms that α-synuclein spreading is a naturally occurring process also in mice and further studies might be possible in our mice to investigate enhancing and inhibitory factors of α-synuclein spreading that could be helpful to slow down or prevent PD pathogenesis.

5.2.3 α-synuclein toxicity is enhanced in Ret deficient mice

Although we found the degree of SN DA neuron degeneration over time is very similar in mice deficient for Ret and in mice overexpressing α-synuclein, VTA DA neurons seem not to depend on Ret signaling for survival but are as vulnerable against α-synuclein overexpression, confirming previous results (Kramer *et al*., 2007; Lin *et al*.,2012).

TH-tTA/LC1/Retlox/tetO-synA53T mice at the age of 1 year have lost already 15% and 25% DA cells in the SN and in the VTA, respectively, and 15-20% of DA innervation in the striatum (Figure 1.11 A-D) (Tillack thesis, 2013). 2 year old TH-tTA/LC1/Retlox/tetO-synA53T mice showed a stronger DA system degeneration than the TH-tTA/tetO-synA53T and TH-tTA/LC1/Retlox mice leading to 25-26% DA cell loss, 25-27% DA innervation loss in the striatum (Figure 4.11 A-F). In addition, 2 year old TH-tTA/LC1/Retlox/tetO-synA53T mice also showed an enhanced protein inclusion phenotype in both SNpc and VTA (Figure 4.12 A-B), making these mice a rare genetic PD model presenting both hallmarks of the disease, age dependent protein accumulation and neurodegeneration of mDA neurons. So far only a few transgenic mouse models have been developed that express α-synuclein in DA neurons and recapitulate protein inclusions (Masliah *et al*., 2000; Rathke-Hartlieb *et al*, 2001; Tofaris *et al*., 2006) or DA cell loss (Richfield *et al*., 2002; Wakamatsu *et al*., 2008; Lin *et al*., 2012) but not both.

Interestingly in the α-synuclein challenged mice Ret signaling seems not only important for maintenance of SN DA neurons but also of VTA DA neurons which suggests not only an additive effect of α-synuclein and Ret signaling but a synergistic effect. Since deficiency of GDNF/Ret signaling enhances α-synuclein toxicity in SN and VTA DA

neurons in our mouse model, it can be conclude that the left over GDNF/Ret signaling components in α-synuclein overexpressing mice are still able to prevent stronger degeneration of neurons and axons and protein accumulation. This argues against the conclusion by Decressac *et al*. (Decressac *et al*., 2012) that α-synuclein accumulation interferes with GDNF/Ret signaling and makes PD patients unresponsive to GDNF therapy. Independent of a possible negative influence of α-synuclein accumulation on Ret expression – which is still a matter of debate (Hoffer and Hardy, 2011) – left over Ret seems able to be neuroprotective for DA neurons against α-synuclein toxicity. The Ret α-synuclein crosstalk is not only seen on mDA cell survival but also on securing DA cell size and volume. I could confirm previous data that have shown already a reduced SN DA cell size in mice lacking the Ret receptor (Aron *et al*., 2010; Meka *et al*., 2015) (Figure 4.12 C) and found in addition a so far not described reduced cell size in α-synuclein overexpressing SN and VTA DA neurons in 2 year old mice (Figure 4.12 C). Again, α-synuclein overexpressing and Ret loss together reduced the DA cell size in the SN and VTA further, supporting the notion that Ret signaling takes place even under α-synuclein overexpressing conditions and there is a synergistic effect of Ret and α-synuclein signaling.

5.2.4 Ret deletion in overexpressing human A53T α-synuclein transgenic mice enhanced gliosis and inflammation

As previously observed in Ret deficient mice (Kramer *et al*., 2007), in Ret and DJ-1 double deficient mice (Aron *et al*., 2010), in Ret and parkin double deficient mice (Meka *et al*., 2015), and in A53T α-synuclein overexpression model (Gu *et al*., 2010; Kurz *et al*., 2012), there is also in 2 year old α-synuclein transgenic mice and even more enhanced in Ret deficient mice overexpressing α-synuclein a gliosis in the striatum and inflammation in the SN region detectible which both seem to be a secondary consequence of the degeneration process.

Besides an increase of Iba-1 positive microglia cells there are more activated bushy microglia cells in TH-tTA/tetO-synA53T, TH-tTA/LC1/Retlox and more strongly in the TH-tTA/LC1/Retlox/tetO-synA53T mice (Figure 4.16) which are required for clearing the apoptotic SN and VTA DA neurons to prevent the accumulation of cellular debris to protect the neighboring healthy DA neurons and other cells from consequent harmful effects.

Astrocytes and microglial recruitment which also happens in the SNpc of PD patients brains (Teismann *et al.*, 2003) is most likely not the primary cause of DA neuron loss as it is observed only in aged mice but not in young mice (Kramer *et al*., 2007; Meka *et al*., 2015) but it accompanies the progressive neurodegeneration process observed in TH-tTA/tetO-synA53T, TH-tTA/LC1/Retlox and more strongly in the TH-tTA/LC1/Retlox/tetO-synA53T mice.

5.2.5 Influence of α-synuclein on GDNF/Ret signaling and its influence on the clinical GDNF trials in Parkinson's disease patients

GDNF/Ret signaling is an important modulator of DA midbrain neuron development and maintenance under both physiological and pathophysiological conditions such as PD (Kramer and Liss, 2015). GDNF and neurturin bind to GFRα1 and GFRα2, respectively and this complex then recruits other receptors, in particular Ret (Durbec *et al*., 1996b; Treanor *et al*., 1996; Trupp *et al*., 1996). GDNF also binds to NCAM (Paratcha *et al*., 2003; Chao *et al*., 2003; Cao *et al*., 2008), syndecan-3 (Bespalov *et al*., 2011), or N-cadherin (Zuo *et al*., 2013). Recent studies from the viral overexpressing α-synuclein rat model shows unchanged GFRα1 but reduced Ret, TH, DAT and Nurr1 protein levels (Decressac *et al*, 2012; Decressac *et al*, 2011; Lo Bianco *et al*, 2004). They showed intracellular response to GDNF blocked in DA neurons that overexpress α-synuclein due to the reduced expression of the transcription factor Nurr1 and its downstream target, the GDNF receptor Ret (Decressac *et al*, 2012) and highlighted the role of the Nurr1/Ret signaling pathway as a target of α-synuclein toxicity (Volakakis *et al*., 2015). Therefore, they claimed that GDNF and its close relative neurturin which are currently in clinical trials for neuroprotection in patients with PD is not functional as it also fails to protect nigral dopamine (DA) neurons against α-synuclein-induced neurodegeneration in animal models of PD (Decressac *et al*., 2012).

To examine if I could see the same changes in our mouse models I measured the level of GDNF, GFRα1, GFRα2, NCAM, Ret, Nurr1, TH, DAT and Girk2 proteins (Figures 4.20 − 4.21). Interestingly, I could not see any changes in the level of all mentioned proteins in 2 year TH-tTA/tetO-synA53T mice compared to age matched controls. This is in contrast to the data from the viral overexpressing α-synuclein rat model (Lo Bianco *et al*., 2004; Decressac *et al*., 2011; Decressac *et al*., 2012). Since so far no (Hoffer and Harvey, 2011) or only mild (Decressac *et al*., 2012) reductions of GDNF receptors were

found in PD patients this suggests that our slow progressive α-synuclein transgenic PD mouse model recapitulates these pathophysiological alterations in PD more closely than the viral α-synuclein overexpression model (Lo Bianco *et al*., 2004; Decressac *et al*., 2011; Decressac *et al*., 2012).

I assessed also the amount of phosphorylated ribosomal protein S6 (p-S6), which some laboratories use as a marker of neurotrophic GDNF/Ret signaling (Decressac *et al*., 2012). However, p-S6 is more a general indicator of protein translation and might correlate with cell size increase (Ruvinsky *et al*., 2005), inhibition of autophagy (Blommaart *et al*., 1995), and neuronal activity (Biever *et al*., 2015; Macedo *et al*., 2015) (Figures 4.20 - 4.21). I did not observe any difference in the level of S6 and p-S6 in TH-tTA/tetO-synA53T mice in contrast with the data from Decressac *et al*. that has been shown markedly reduced phosphorylated ribosomal protein S6 immunoreactivity in neurons overexpressing α-synuclein 2 weeks after injection of AAV in the striatum of rats (Decressac *et al*. 2012). Unexpectedly, immunostaining of p-S6 showed significant increase in 2 year old TH-tTA/LC1/Retlox/tetO-synA53T mice (Figure 4.19) which correlates with increased p62 protein levels and strong inhibition of autophagy in these mice as discussed below (Figures 4.17 and 4.20). The increased phospho-S6 levels in Ret deficient mice support the notion that phospho-S6 levels and GDNF/Ret signaling are not necessarily linked and caution has to be taken to use phosphor-S6 levels as readout for GDNF/Ret downstream signaling especially since GDNF can also signal through alternative receptors and S6 phosphorylation is induced by many signaling pathways (Decressac *et al*. 2012; Kramer and Liss, 2015; Biever *et al*., 2015; Macedo *et al*., 2015).

The lack of GDNF's protection effect in rats with viral overexpression of α-synuclein seems most likely due to the non-physiological and acute overexpression of α-synuclein and other technical problems and not due to the general lack of biological activity of GDNF in α-synuclein accumulating DA neurons (Hoffer and Harvey, 2011). Since in rats with viral overexpression of α-synuclein in the midbrain high viral overexpression of GDNF in the SN or striatum in a non-cell type specific manner has even been shown to reduce the TH staining in the striatum (Decressac *et al*, 2011), non-neuronal expression of lower amounts of GDNF or discontinuous delivery of GDNF is currently favored as application method of this neurotrophic factor (Tereshchenko *et al*, 2014). Thus, moderate stimulation of GDNF receptor Ret or its downstream signaling cascades are likely not only beneficial in our TH-tTA/tetO-synA53T mice but also in PD patients with α-synuclein accumulation as long as a critical number of DA neurons are still alive

or were replaced by cell therapy. Since clinical studies have shown that Ret ligands are safe and do not induce severe side effects, the major challenge seems to be to overcome the technical hurdles of delivering highly active Ret ligands to DA neurons and potentially to combine them with other drugs that target additional disease aspects (Aron and Klein, 2011; Kordower and Bjorklund, 2013). A clinical phase I gene therapy trial on PD patients with stereotactic injection of AAV encoded GDNF in the putamen on both brain sides has been conducted recently (UniQure) (Bartus *et al*., 2014) based on successful strategies used in several laboratories to treat PD animal models (Kirik *et al*., 2000b; Johnston *et al*., 2009; Eberling *et al*., 2009; Decressac *et al*., 2011). Using the stereotactic AAV-GDNF injection in patients the problem of GDNF delivery has been solved in this clinical trial. However, candidates for surgical treatment like deep-brain-stimulation in this trial have been selected from advanced PD patients (UniQure). In advanced PD the brains of these patients might have only very few DA neurons left on which GDNF is not able to induce survival and physiological function. Therefore, still this trial might not reveal a significant beneficial effect of GDNF such as the previous trials using direct GDNF protein infusion into the putamen, and accordingly a renewed, focused emphasis must be placed on advancing clinical efficacy by improving not only clinical trial design but also patient selection as well as developing better animal models to support clinical testing and most importantly moving forward—beyond the past limits (Bartus *et al*., 2014; Kramer 2015a; Kramer 2015b; Kramer and Liss 2015). Currently on going and future trials with GDNF in PD patients are hopefully better designed to be able to reveal the full potential of GDNF/Ret signaling in PD patients (Domanskyi *et al*., 2015).

5.2.6 α-synuclein and GDNF/Ret crosstalk on mitochondrial integrity

Since α-synuclein's negative effect on GDNF/Ret signaling is most likely not the DA cell death inducing mechanism, I investigated next mitochondrial integrity in our single and double transgenic mice.

α-synuclein protein has a noncanonical mitochondrial targeting sequence at its N-terminus and is indeed translocated to mitochondria in human fetal DA neuronal culture and postmortem normal brain tissues (Devi *et al*., 2008). The mitochondrial α-synuclein accumulation is enhanced in PD brains. α-synuclein interacts with complex I and interferes with its function, promoting the production of ROS (Devi *et al*., 2008; Yasuda *et al*., 2013). As a consequence, the activity and protein concentration of electron transport chain (ETC) complex I has been consistently shown to decrease in brains and

other tissues of PD patients (Schapira *et al*., 1989; Bindoff *et al*., 1989; Mann *et al*., 1994). The studies in α-synuclein knockout mice has confirmed that these mice are resistant to mitochondrial damage caused by complex I inhibitors, which generally result in a PD-like phenotype in mammals and rodents (Dauer *et al*., 2002; Klivenyi *et al*., 2006). I was also able to show in our TH-tTA/tetO-synA53T and TH-tTA/LC1/Retlox mice significant decrease in the complex I activity (Figure 4.13 C) similar to what has been observed before in heterozygous transgenic mice expressing wild type human α-synuclein under the regulatory control of the platelet-derived growth factor-b (PDGFb) promoter (Bender *et al*., 2013). In contrast to these mice which have been shown decreased energy production by ATP assay (Bender *et al*., 2013), I did not observe any changes in the ATP production in none of the mouse groups neither in 1 year nor in 2 year old mice (Figure 4.13 A-B). Surprisingly, in TH-tTA/LC1/Retlox/tetO-synA53T mice the mitochondrial complex I activity seems to be compensated by an unknown mechanism which partially might be explained by increased astrocyte population observed by GFAP staining in these mice.

Previously, in transgenic mice expressing wild type human α-synuclein has been shown that there are no changes in the complexes II, III and IV (Bender *et al*., 2013) – three of four membrane-bound complexes in the mitochondria- (Clayton, 1984) and only complex I showed the decrease in the subunit NDUFB8 (Bender *et al*., 2013). Due to the decrease in the level of complex I activity in our TH-tTA/tetO-synA53T which is in line with robust findings in human PD (Schapira *et al*., 1989), I have further looked at two subunits of this complex including NDUFB8 and NDUFA10 (Figure 4.21). In contrast to transgenic mice expressing wild type human α-synuclein which have a decrease in the level of NDUFB8 (Bender *et al*., 2013) I could not see any changes in both subunits NDUFB8 and NDUFA10 in our TH-tTA/tetO-synA53T (Figure 4.21). Thus the observed changes in the complex I activity in these mice might be due to the changes in other subunits which can be discovered in the future.

The Outer Mitochondrial Membrane – 40 kD (TOM40) protein is the key subunit of the TOM (Translocase of the Outer Membrane) complex which is the important part for many cytoplasmicaly synthesized mitochondrial proteins (Gottschalk *et al*., 2014). To date TOM40 is the only nuclear-encoded gene identified in genetic studies that likely contributes to late-onset Alzheimer's disease related mitochondria dysfunction and linked with Alzheimer's and PD (Gottschalk *et al*., 2014). Most of mitochondrial proteins are imported into mitochondria through the TOM complex, of which TOM40 is the central pore, mediating communication between the cytoplasm and the

mitochondrial interior (Gottschalk *et al*., 2014). Pathogenic proteins, such as α-synuclein, readily pass through the pore and cause toxic effects by directly inhibiting mitochondrial enzymes (Gottschalk *et al*., 2014). Therefore, TOM40 plays a central role in the mitochondrial dysfunction that underlies age-related neurodegenerative diseases (Gottschalk *et al*., 2014). By Western blotting I have confirmed that TOM40 is significantly decreased in TH-tTA/tetO-synA53T mice (Figure 4.20), similar to what has been reported for specific decrease in TOM40 protein levels both in mouse brain homogenates as well as in human midbrain samples which is inversely associated with α-synuclein accumulation (Bender *et al*., 2013). In contrast there were no changes in the level of pro-protein receptor for TOM complex "TOM20" in our TH-tTA/tetO-synA53T mice (Figure 4.20). This supports the notion that mitochondrial integrity is altered in our α-synuclein transgenic mice.

Cell culture experiments performed by Eva Dürholt, a PhD student in the lab of Konstanze Winklhofer, support a crosstalk of α-synuclein and GDNF/Ret on mitochondrial integrity. It has shown before (Butler *et al*., 2012) that α-synuclein A53T overexpression lead to mitochondrial fragmentation phenotype in SH-SY5Y cells which can be completely prevented by treating the cells with GDNF and soluble GFRα1– which possibly signals via the Ret receptor (Figure 4.23). These data suggest that GDNF/Ret signaling might prevents degeneration of DA neurons in TH-tTA/tetO-synA53T mice by maintaining proper mitochondrial function.

5.2.7 Autophagy is blocked by overexpression of human A53T α-synuclein and Ret loss and might contribute to the cell death phenotype

I searched further for molecular mechanisms which could explain the α-synuclein induced DA cell death phenotype which is strengthened in combination with Ret loss. The pathogenic mechanism by which α-synuclein aggregations leads to PD and progressive neuronal loss in SNpc is still not completely understood (Decressac *et al*., 2012). α-synuclein has been proposed previously to negatively influence autophagy and mitopahgy which has been discussed in details by separated markers below. Our model and how α-synuclein accumulation and Ret loss might lead to DA cell death in our mice through inhibition of autophagy and mTOR signaling is summarized in a schematic overview figure (Figure 5.1) and is supported by the data discussed below.

I took advantage of tissue sections and protein extracts from our 1 and 2 year old TH-tTA/tetO-synA53T and TH-tTA/LC1/Retlox/tetO-synA53T mice and looked at the level of different proteins claimed before by other studies to be important (Figures 4.17 - 4.22).

To understand the specific molecular events leading to α-synuclein dependent degradation of mDA neurons in our mouse model, I examined the protein levels of autophagy/lysosome degradation pathways by immunostaining and western blot analysis as its impairments in animal models of PD has been shown by several studies (Cuervo *et al*., 2004; Auluck *et al*., 2010; Dehay *et al*., 2010; Lin *et al*., 2012).

First I examined the level of p62 and LC3 proteins (Figures 4.17, 4.18 and 4.20). P62 is important for the initiation of pre-autophagosomal structures, which later bind to microtubule-associated protein 1 light chain 3 (LC3) to form autophagosome (Bjørkøy *et al*., 2005) and connects ubiquitinated proteins to LC3 for autophagic degredation (Pankiv *et al*., 2007). The accumulation of p62 is significantly elevated in the blockade of autophagy, therefore it is widely used as an autophagy marker (Lynch-Day *et al*., 2012). Western blot analysis showed significantly elevated levels of p62 in 2 year old TH-tTA/tetO-synA53T mice compared to the age matched controls (Figure 4.20). The observed increase in p62 protein levels is in accordance with the study by Lin and colleagues in 2012 which showed a similar increase of p62 expression in the midbrain homogenate of PITX3-tTA/tetO-synA53T transgenic mice (Lin *et al*., 2012). By immunostaining midbrain sections, I found also significant increase in the intensity level of p62 stained cells both in SNpc and VTA of 2 year TH-tTA/LC1/Retlox/tetO-synA53T mice which were more pronounced compared to TH-tTA/tetO-synA53T mice (Figure 4.17). While Ret loss increased p62 levels only in the SNpc, loss of Ret neurotrophic receptor in TH-tTA/tetO-synA53T mice significantly increases the p62 level further in the SN and VTA.

After the initiation of autophagy pathway, the elongation stage takes place and LC3-I protein is conjugated to the lipid phosphatidylethanolamine to form LC3-II, which localizes to the autophagosome membrane (Mizushima *et al*., 1998; Mizushima *et al*., 2003; Harris and Rubinsztein., 2012). LC3II remains bound to the inner and outer membrane of autophagosomes even after lysosomal fusion; therefore it is a good marker for autophagy (Harris and Rubinsztein, 2012). Since the number of autophagosomes in cells can increase with both autophagosome formation and blockade of autophagosomes breakdown (Metcalf *et al*., 2010; Ravikumar *et al*., 2010) the levels of LC3II do not necessarily reflect autophagic flux (Harris and Rubinsztein, 2012). Western blot

analysis of the midbrain homogenates of 2 year old TH-tTA/tetO-synA53T mice revealed significant increase in the level of LC3II but no changes in the level of LC3I protein (Figure 4.20) which could be an indication that autophagy is blocked and the lysosomal-mediated clearance of autophagosomes is impaired in these mice. Increased level of LC3II and no changes in the level of LC3I are also observed in a MPTP mouse model (Dehay *et al*., 2010), rotenone injected rat model of PD (Liu *et al*., 2015), and PD-derived cells confirmed the increase in basal steady-state levels of LC3-II (Sánchez-Danés *et al*., 2012) which is in accordance to our findings. In contrast, in another study on 1 month old A53T transgenic mice the level of LC3I was elevated and there was no obvious accumulation of LC3II (Lin *et al*., 2012). In addition, α-synuclein seemed to increase the intensity and size of LC3-positive puncta in the soma of mDA neurons from the PITX3- tTA/tetO-synA53T (Lin *et al*., 2012). Although I tried to show the effect of Ret receptor loss in TH-tTA/tetO-synA53T mice on the level of LC3 protein by immunohistochemistry, the intensity of staining was not strong enough for measuring the intensity of LC3 in the cells of SNpc and VTA (Figure 4.18). However, in the dorsal midbrain region above the SN and VTA I could see increased LC3 staining in the mutant mice. Autophagosomes fuse with the lysosomes for degradation and in this pathway lysosomal protein LAMP2 serves as an adaptor for the chaperone-mediated autophagy (CMA) pathway (Cuervo and Dice, 2000). Chaperone-mediated autophagy is dependent on the heat shock cognate 70 (HSC-70) protein and its binding to lysosomal-associated membrane protein 2A (LAMP2A) (Majeski and Dice, 2004; Alvarez-Erviti *et al*., 2010). HSC-70 chaperone recognizes lysosomal surface receptor A which is a highly specific subset of cytosolic proteins with a KFREQ motif that allows internalized for degredation by LAMP2A receptor (Majeski and Dice, 2004; Alvarez-Erviti *et al*., 2010). Previous work suggested that there might be reduced chaperone-mediated autophagy activity in PD brains with increased amount of oxidized protein and accumulation and aggregation of proteins in the SNpc (Alvarez-Erviti *et al*., 2010). In an *in vitro* model with increased α-synuclein levels LAMP2A levels were not altered (Alvarez-Erviti *et al*., 2010). But also increased chaperone mediated autophagy activity due to the increase in oxidative stress in PD SNpc and accumulation of oxidized protein was suggested (Owen *et al*., 1996; Kiffin *et al*., 2004) and in 1 and 18 months old PITX3- tTA/tetO-synA53T mice a significant increase in the density of LAMP2-positive puncta were observed in the soma of midbrain DA neurons (Lin *et al*., 2012). I examined the level of HSC-70 and LAMP2A by western blot analysis (Figure 4.21). However, I could not see any differences in the level of these proteins in our 2 year old

TH-tTA/tetO-synA53T mice consistent with the finding in PD patients. ATG9 is another important molecule in autophagy and one of the known transmembrane autophagy proteins which are required for autophagosome biogenesis (Winslow *et al.*, 2010). Depletion of ATG9 has been shown to inhibit autophagosome synthesis (Winslow and Rubinsztein, 2011), but ATG9 seems not affected by α-synuclein overexpression, however, ATG9 strans-Golgi network and LC3-positive vesicles altered (Winslow and Rubinsztein, 2011). ATG9 localizes to the trans-Golgi network and upon autophagy induction redistributes to the autophagosomes. Overexpression of α-synuclein results in decreased colocalization of ATG9 with the trans-Golgi network, LC3-positive vesicles and autophagosomes (Winslow and Rubinsztein, 2011).

To test whether ATG9 protein levels are altered in our TH-tTA/tetO-synA53T mice I measured the protein levels by Western blottings but found no alterations (Figure 4.21). We might be able to address the changes in the localization of ATG9 by double immunostaining with ATG9 and LC3 antibodies in the future.

5.2.8 mTOR signaling pathway is influenced by overexpression of human A53T α-synuclein and Ret loss and might explain the dopaminergic cell size and death phenotype

A master regulator of cellular metabolism and promoter of cell growth in response to environmental factors is the serine/threonine kinase mTOR (Mammalian Target Of Rapamycin), which plays a crucial role in regatively regulating autophagy and its degradation has been implicated in many human diseases (Kim and Guan., 2015), most importantly in neurodegenerative diseases (Laplante and Sabatini, 2012) including PD (Kiriyama and Nochi, 2015). Two distinct signaling complexes are formed by mTOR, mTOR complex 1 (mTORC1) and mTOR complex 2 (mTORC2) with specific substrate preferences and therefore elicit distinct downstream signaling events to modulate cellular function (Hoeffer and Klann, 2010; Kim and Guan, 2015). mTORC1 specifically binds to regulatory associated protein of mTOR (RAPTOR) (Hara *et al.*, 2002; Kim *et al.*, 2002; Sancak *et al.*, 2007; Vander Haar *et al.*, 2007; Thedieck *et al.*, 2007) and mTORC2 binds to the rapamycin-insensitive companion of mTOR (RICTOR) (Sarbassov *et al.*, 2004; Jacinto *et al.*, 2006; Frias *et al.*, 2006; Yang *et al.*, 2006; Pearce *et al.*, 2007; Thedieck *et al.*, 2007). Activation of mTORC1 regulates translation through S6K activation (Hoeffer and Klann, 2010). On the other hand

rapamycin can inhibit mTORC1 and the system goes through autophagy via activation of 4EBP signaling (Hoeffer and Klann, 2010). Phosphorylation at serine 2448 (mTORC1) and serine 2481 (mTORC2) can correlate with overall higher level of mTOR activity (Hoeffer and Klann, 2010). The tuberous sclerosis (TSC) tumor suppressor complex (TSC1/TSC2) negatively regulates mTORC1 and the growth factor/PI3K/Akt signaling pathway is upstream regulator of mTORC1 (Kim and Guan, 2015). Activation of Akt inhibits TSC1/2, a GTPase-activating protein (GAP) for the Ras homolog enriched in brain (Rheb) (Potter *et al*., 2002; Inoki *et al*., 2003a; Tee *et al*., 2003). Cellular stressors like low cellular energy levels inhibit mTORC1 activation by its sensor AMPK that is activated by a high AMP/ATP ratio and phosphorylates TSC2 which in turn increases the TSC1/2 GAP activity (Inoki *et al*., 2003b). AMPK also directly phosphorylates RAPTOR and this, results in a decrease activation of mTORC1 through allosteric inhibition (Gwinn *et al*., 2008). RTP801 protein (also known as REDD1) is encoded by the stress responsive gene DNA-damage-inducible transcript 4 (DDIT4) and rapidly upregulated under multiple cellular stresses such as hypoxia (Shoshani *et al*., 2002; Brugarolas *et al*., 2004), energy depletion (Sofer *et al*., 2005), and chemical molecules such as dopaminergic neurotoxins 6-OHDA, MPTP/MPP+ and rotenone (Malagelada *et al*., 2006). Thereby, low cellular oxygen levels also inhibit mTORC1 by upregulating RTP801which modulates TSC2 (Brugarolas *et al*., 2004; De Young *et al*., 2008).

Inhibition of mTORC1 results in increased ULK1/2 kinase activity in mammalian cells, while activated mTORC1 phosphorylates Ser758 (Ser757 in mouse) of ULK1 and prevents an essential aspect for ULK1 activation which is the interaction and phosphorylation of ULK1 by AMPK (Kim *et al*., 2011).

To find the effect of overexpression of human α-synuclein on mTOR signaling pathway, I have measured the levels of RTP801, Akt, phospho-Akt, AMPK, phospho-AMPK, ULK1, phospho-ULK1, mTOR, phospho-mTORC1 (ser2448) and, phospho-mTORC2 (ser2481) proteins in 2 year old TH-tTA/tetO-synA53T and control mice by western blot analysis (Figures 4.20 - 4.21).

The level of the pro-apoptotic RTP801 protein was dramatically increased in TH-tTA/tetO-synA53T mice (Figure 4.20) which so far has not been described in α-synuclein overexpressing conditions. Increased amounts of RTP801 have only been described in nigral neurons from both idiopathic PD, human brains or fibroblasts with mutated parkin, and parkin deficient mice (Malagelada *et al*., 2006; Romani-Aumedes *et al*, 2014). This finding underlines the crosstalk of α-synuclein with parkin which was

postulated after reduced α-synuclein toxicity was found in rodents overexpressing parkin (Petrucelli *et al.*, 2002; Lo Bianco *et al.*, 2004; Yamada *et al.*, 2005; Khandelwal *et al.*, 2010). RTP801 might be a parkin substrate and involved in the toxicity of parkin loss (Romani-Aumedes *et al.*, 2014).

In 2 year old TH-tTA/tetO-synA53T mice the level of phospho-mTORC1 (ser2448)/mTOR, phospho-mTORC2 (ser2481), phospho-AMPK/AMPK and ULK1 protein levels were significantly and phospho-Akt/Akt partially decreased which can lead to increased autophagy (Figures 4.20). In the experimental models of PD it has been proposed that in a first attempt to maintain cell function and viability stress-induced RTP801 elevation result in mTOR repression, but if the RTP801 upregulation is sustained, it leads to neuronal death by a sequential inhibition of mTOR and Akt (Canal *et al.*, 2014). Observation of upregulated RTP801 and diminished Akt phosphorylation in nigral neurons of PD brains also support this data and the proposed mechanism (Malagelada *et al.*, 2006; Romaní-Aumedesetal, 2014).

Reduced activity of AMPK in our mouse models is in accordance with studies showing that loss of AMPK activity strengthen neuronal loss and associated phenotypes in parkin and LRRK mutant flies of PD model (Ng *et al.*, 2012). AMPK collaborates with parkin in an efficient manner to guarantee the quality control of organelles (Hang *et al.*, 2015). Thus, AMPK activation may protect the neurons from death and play a survival role in PD (Rosso *et al.*, 2016).

mTORC2 activation via AGC family kinases including SGK1 and PKCα regulates cell survival, metabolism, and cytoskeletal organization (Kim and Guan, 2015). α-synuclein A53T reduces mTORC2 (ser2481) phosphorylation, this might explain the reduced cell soma size in our α-synuclein transgenic mice.

Mutations in phosphatase and tensin homolog (PTEN)-induced putative kinase 1 (PINK1) (Valente *et al.*, 2002; Valente *et al.*, 2004) and Parkin (Hattori *et al.*, 1998; Kitada *et al.*, 1998; Lucking *et al.*, 1998) were identified in early-onset Parkinson's disease and lead to Parkinsonism (Hardy, 2010). Parkin is an enzyme 3 (E3) ubiquitin ligase and in many outer mitochondrial membrane proteins Parkin-dependent ubiquitination sites have been identified (Sarraf *et al.*, 2013). PINK1 can phosphorylate ubiquitin and Parkin which results in the activation of Parkin (Kazlauskaite *et al.*, 2014; Koyano *et al.*, 2014; Wauer *et al.*, 2015). Furthermore, on depolarized mitochondria, PINK1 autophosphorylates and recruits Parkin to damaged mitochondria (Okatsu *et al.*, 2012). A recent study has shown that optineurin (OPTN) is necessary for PINK1-Parkin-dependent mitophagy (Lazarou *et al.*, 2015). OPTN phosphorylation by TANK-

binding kinase 1 (TBK1) enhances its binding ability to ubiquitinated outer mitochondrial membrane proteins and LC3 (Wild *et al*., 2011; Heo *et al*., 2015). Moreover, OPTN recruit autophagy-related proteins, such as ULK1 and LC3, to initiate autophagy (Lazarou *et al*., 2015). Thus, PINK1 and Parkin dysfunction results in the impairment of mitophagy in PD patients, which is regulated by OPTN (Kiriyama and Nochi, 2015).

Based on these findings, I further looked at the level of PINK1, Parkin and OPTN in 2 year TH-tTA/tetO-synA53T and in control mice (Figure 4.21). But I could not find any differences in the level of these proteins. This suggests a PINK1-Parkin-independent auto- and mitophagy pathway in our α-synuclein overexpression mice.

In summary, we can propose that α-synuclein overexpression and Ret loss in mice blocks autophagy, leads to mitochondrial defects and prevents signaling by the Akt and mTOR survival pathways. The combination of the molecular alterations described here can explain the observed age-dependent neurodegeneration phenotype of mDA neurons in our mice. The tight correlation of our findings with alterations found in tissue from PD patients suggest that our mouse model nicely recapitulate several cardinal features of PD. These include specific and age-dependent mDA neurodegeneration, protein aggregation, mitochondrial and autophagy defects. Therefore it might help to advance our understanding of the complex alterations leading to PD. In the long run this knowledge might help to develop an efficient treatment for PD which might prevent, slow down, hold or even reverse the observed pathological alterations.
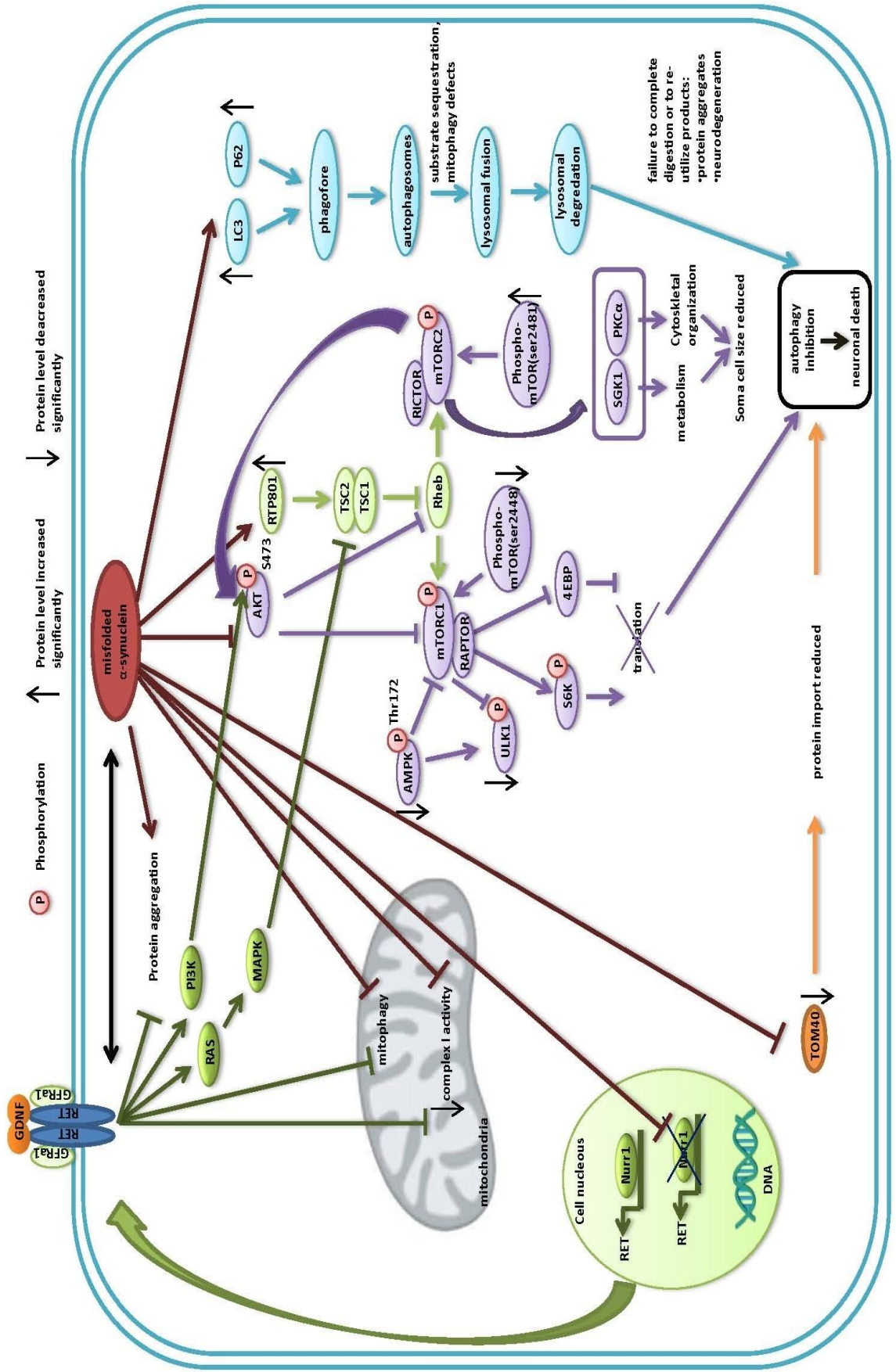
Figure 5.1 Schematic overview of α-synuclein mechanism in neurodegeneration

Overexpression of mutated α-synuclein A53T in TH-tTA/tetO-synA53T mice model resulted in α-synuclein oligomer formation and toxicity via perturbing major cell survival pathways. Misfolded α-synuclein A53T in our model increased the level of autophagy markers LC3 and p62. P62 is important for the initiation of pre-autophagosomal structures, which later binds to LC3 to form autophagosome and connects ubiquitinated proteins to LC3 for autophagic degredation. Loss of lysosome function might result in autophagosome accumulation, as autophagosomes do not fuse with dysfunctional lysosomes and the consequence is blockade of autophagy. In addition, α-synuclein A53T affect mammalian target of rapamycin (mTOR) signaling, a protein kinase involved in translation control and cell survival. mTOR includes two signaling complexes based on the unique compositions and substrates: mTORC1 and mTORC2. mTORC1 bound to the regulatory associated protein of mTOR (Raptor) and is sensitive to rapamycin. Activation of mTORC1 regulates translation through S6K activation. In another hand rapamycine can inhibit mTORC1 and the system goes through autophagy via the activation of 4EBP signaling. mTORC2 is resistant to rapamycin and bound to the rapamycin-insensitive companion of mTOR (Rictor). Downregulation of mTOR activity under stress conditions such as hypoxia or exposure to dopaminergic neurotoxins required the expression of RTP801 and an intactTSC1/TSC2 tumor suppressor complex. In these conditions, the stress responsive gene DNA-damage-inducible transcript 4 (DDIT4) rapidly encode and upregulates RTP801 protein. I have shown that RTP801 protein level is significantly increased that leads to inactivation of mTORC1. As a consequence the level of phospho-mTOR (ser2448)/mTOR, phospho-AMPK and ULK proteins significantly decreased that can lead to autophagy. As in the experimental models of PD has been proposed, in an attempt to maintain cell function and viability, stress-induced RTP801 elevation contributes to mTOR repression, but when the RTP801 upregulation is sustained, it leads to neuron cell death by a sequential inhibition of mTOR and Akt. mTORC2 regulates cell survival, metabolism, and cytoskeletal organization via AGC family kinases (SGK1 and PKCα). α-synuclein A53T affect mTORC2 as it is shown by phospho-mTOR(ser2481) and can be a possible mechanism for reduced cell soma size in our mice models. Moreover protein import TOM40 is significantly decreased. Complex I activity and mitophagy are also impaired in both overexpressed TH-tTA/tetO-synA53T and TH-tTA/LC1/Retlox mice and I have shown protein aggregation in TH-tTA/LC1/Retlox/tetO-synA53T mice. Staining the cells using phosphorylated alphasynuclein (ser129) antibody showed α-synuclein in the nucleus as well as in the cytosol, but no change in the level of Nurr1 and Ret protein levels in contrast to the data published by Decressac *et al* 2012. This data suggest that Ret is still functional in our slow progressive α-synuclein

transgenic PD mouse model which recapitulates these pathophysiological alterations in PD more closely than the viral α-synuclein overexpression model. Therefore GDNF therapy might still be beneficial for PD patients with accumulation of α-synuclein. Taken together, obtained data suggest impaired autophagy that leads to neuronal loss in our TH-tTA/tetO-synA53T and TH-tTA/LC1/Retlox/tetO-synA53T mice.

6. References

Abeliovich, A., Schmitz, Y., Farinas, I., Choi-Lundberg, D., Ho, W. H et al. (2000) 'Mice lacking α-synuclein display functional deficits in the nigrostriatal dopamine system' *Neuron* 25(1): 239–252.

Abeliovich, A., and Hammond, R. (2007): 'Midbrain dopamine neuron differentiation: Factors and fates' *Developmental Biology* 304(2): 447–454.

Adinoff, B. (2004): 'Neurobiologic Processes in Drug Reward and Addiction' *Harvard Review of Psychiatry* 12(6): 305–320.

Airaksinen, M. S., Titievsky, A., Saarma, M. (1999): 'GDNF family neurotrophic factor signaling: four masters, one servant?' *Molecular and Cell Neuroscience* 13(5): 313–325.

Airaksinen, M. S., and Saarma, M. (2002): 'The GDNF family: signalling, biological functions and therapeutic value' *Nature Reviews Neuroscience* 3(5): 383-394.

Alvarez-Erviti, L., Rodriguez-Oroz, M. C., Cooper, J. M., Caballero, C., Ferrer, I., Obeso, J, A, Schapira, A. H. (2010): 'Chaperone-Mediated Autophagy Markers in Parkinson Disease Brains' *Achieves of Neurology* 67(12):1464-1472.

Anders, J., Kjar, S., Ibanez, C. F. (2001): 'Molecular modeling of the extracellular domain of the RET receptor tyrosine kinase reveals multiple cadherin-like domains and a calcium-binding site' *Journal of Biological Chemistry* 276(38): 35808–35817.

Anderson, J. P., Walker, D. E., Goldstein, J. M., de Laat, R., Balducci, K., et al. (2006): 'Phosphorylation of Ser-129 is the dominant pathological modification of a-synuclein in familial and sporadic Lewy body disease' *Journal of Biological Chemistry* 281(40): 29739–29752.

Andrzejewska, A., Nowakowski, A., Janowski, M., Bulte, J. W., Gilad, A. A., Walczak, P., Lukomska, B. (2015): 'Pre- and postmortem imaging of transplanted cells' *International Journal of Nanomedicine* 10(1): 5543–5559.

Angot, E., Steiner, J. A., Hansen, C., Li, J. Y., Brundin, P. (2010): 'Are synucleinopathies prion-like disorders?' *The Lancet Neurology* 9(11):1128–1138.

Angot, E., Steiner, J. A., Lema Tomé, C. M., Ekström, P., Mattsson, B., Björklund, A., Brundin, P. (2012): 'Alpha-synuclein cell-to-cell transfer and seeding in grafted dopaminergic neurons in vivo' *PLoS One* 7(6):e39465.

Anwar, S., Peters, O., Millership, S., Ninkina, N., Doig, N., et al. (2011): 'Functional alterations to the nigrostriatal system in mice lacking all three members of the synuclein family' *The Journal of Neuroscience : The Official Journal of the Society for Neuroscience* 31(20): 7264–7274.

Arenas, E., Trupp, M., Åkerud, P. Ibañéz, C. F. (1995): 'GDNF prevents degeneration and promotes the phenotype of brain noradrenergic neurons in vivo' *Neuron* 15(6): 1465-1473.

Arighi, E., Borrello, M. G., Sariola, H. (2005): 'RET tyrosine kinase signaling in development and cancer' *Cytokine and Growth Factor Reviews* 16(4-5): 441–467.

Aron, L., Klein, P., Pham, T. T., Kramer, E.R., Wurst, W., Klein, R. (2010): 'Pro-survival role for Parkinson's associated gene DJ-1 revealed in trophically impaired dopaminergic neurons' *PLoS Biology* 8(4):e1000349.

Aron, L. and Klein, R. (2011): 'Repairing the parkinsonian brain with neurotrophic factors' *Trends in Neurosciences* 34(2): 88–100.

Asmus, S. E., Anderson, E. K., Ball, M. W., Barnes, B. A., Bohnen, A. M., et al. (2008): 'Neurochemical characterization of tyrosine hydroxylase-immunoreactive interneurons in the developing rat cerebral cortex' *Brain Research* 30(1222): 95-105.

Auluck, P. K., Caraveo, G., Lindquist, S. (2010): 'Alpha-synuclein: membrane interactions and toxicity in Parkinson's disease' *Annual Review of Cell and Developmental Biology* 26:211–233.

Azeredo da Silveira, S., Schneider, B. L., Cifuentes-Diaz, C., Sage, D., Abbas-Terki, T., Iwatsubo, T., Unser, M., Aebischer, P. (2009): 'Phosphorylation does not prompt, nor prevent, the formation of alpha-synuclein toxic species in a rat model of Parkinson's disease' *Human Molecular Genetics* 18(5): 872–887.

Baetge, G., Gershon, M. D. (1989): 'Transient catecholaminergic (TC) cells in the vagus nerves and bowel of fetal mice: relationship to the development of enteric neurons' *Developmental Biology* 132(1):189-211.

Bach, J-P., Ziegler, U., Deuschl, G., Dodel, R., Doblhammer-Reiter, G. (2011): 'Projected numbers of people with movement disorders in the years 2030 and 2050' *Movement Disorders* 26(12): 2286-2290.

Baker, H., Kobayashi, K., Okano, H., Saino-Saito, S. (2003a): 'Cortical and striatal expression of tyrosine hydroxylase mRNA in neonatal and adult mice' *Cellular and Molecular Neurobiology* 23(4-5): 507-518.

Baker, K. D., Shewchuk, L. M., Kozlova, T., Makishima, M., Hassell, A., et al. (2003b): 'The *Drosophila* orphan nuclear receptor DHR38 mediates an atypical ecdysteroid signaling pathway' *Cell* 113(6): 731–742.

Baron, U., Gossen, M., Bujard, H. (1997): 'Tetracycline-controlled transcription in eukaryotes: novel transactivators with graded transactivation potential' *Nucleic Acids Research* 25(14): 2723-2729.

Barak, S., Ahmadiantehrani, S., Kharazia, V. Ron, D. (2011): 'Positive autoregulation of GDNF levels in the ventral tegmental area mediates long-lasting inhibition of excessive alcohol consumption' *Translational psychiatry* 1: e60.

Barry, S. J. E., Gaughan, T. M., Hunter, R. (2012): 'Schizophrenia' *BMJ Clinical Evidence* 2012: 1007.

Bartus, R. T., Herzog, C. D., Chu, Y., Wilson, A., Brown, L., Siffert, J., Johnson E. M. Jr., Olanow, C. W., Mufson, E. J., Kordower, J. H. (2011): 'Bioactivity of AAV2-neurturin gene therapy (CERE-120): Differences between Parkinson's disease and nonhuman primate brains' *Movement Disorders* 26(1): 27–36.

Bartus, R. T., Weinberg, M. S., Samulski, R. J. (2014): 'Parkinson's Disease Gene Therapy: Success by Design Meets Failure by Efficacy' *Molecular Therapy* 22(3): 487–497.

Beard, C., Hochedlinger, K., Plath, K., Wutz, A., Jaenisch, R. (2006): 'Efficient method to generate single-copy transgenic mice by site-specific integration in embryonic stem cells' *Genesis* 44(1): 23–28.

Beitz, J. M. (2014): 'Parkinson's disease: a review' *Frontiers in Bioscience* S6, 65-74.

Beier, K.T., Steinberg, E. E., DeLoach, K. E., Xie, S., Miyamichi, K., Schwarz, L., Gao, X. J., Kremer, E. J., Malenka, R. C., Luo, L. (2015): 'Circuit architecture of VTA dopamine neurons revealed by systematic input-output mapping' *Cell* 162(3): 622–634.

Bejar, R., Yasuda, R., Krugers, H., Hood, K., Mayford, M. (2002): 'Transgenic calmodulin-dependent protein kinase II activation: dose-dependent effects on synaptic plasticity, learning, and memory' *Journal of Neuroscience* 22(13): 5719–5726.

Bender, A., Desplats, P., Spencer, B., Rockenstein, E., Adame, A., et al. (2013): 'TOM40 Mediates Mitochondrial Dysfunction Induced by α-Synuclein Accumulation in Parkinson's Disease' *PLoS ONE* 8(4): e62277.

Bentivoglio, M. and Morelli, M. (2005): *'The organisation and circuits of mesencephalic dopaminergic neurons and the distribution of dopamine receptors in the brain'* In: Handbook of Chemical Neuroanatomy. (Dopamine) Elsevier (21):1–107.

Benturquia, N., Courtin, C., Noble, F., and Marie-Claire, C. (2008): 'Involvement of D1 dopamine receptor in MDMA-induced locomotor activity and striatal gene expression in mice' *Brain Research* 1211: 1–5.

Bespalov, M. M., Sidorova, Y. A., Tumova, S., Ahonen-Bishopp, A., Magalhães, A. C., Kulesskiy, E., Paveliev, M., Rivera, C., Rauvala, H., Saarma, M. (2011): 'Heparan sulfate proteoglycan syndecan-3 is a novel receptor for GDNF, neurturin, and artemin' *Journal of Cell Biology* 192(1): 153-69.

Biever, A., Valjent, E., Puighermanal, E. (2015): 'Ribosomal Protein S6 Phosphorylation in the Nervous System: From Regulation to Function' *Frontiers in Molecular Neuroscience* 8: 75.

Bindoff, L. A., Birch-Machin, M., Cartlidge, N. E., Parker, W. D J.r., Turnbull, D. M. (1989): 'Mitochondrial function in Parkinson's disease' *The Lancet* 2(8653): 49.

Björklund, A., Kirik, D., Rosenblad, C., Georgievska, B., Lundberg, C., Mandel, R. J. (2000): 'Towards a neuroprotective gene therapy for Parkinson's disease: Use of adenovirus, AAV and lentivirus vectors for gene transfer of GDNF to the nigrostriatal system in the rat Parkinson model' *Brain Research* 886(1-2): 82–98.

Björklund, A. and Dunnett, S.B. (2007): 'Dopamine neuron systems in the brain: an update' *TRENDS in Neurosciences* 30(5): 194-202.

Bjørkøy, G., Lamark, T., Brech, A., Outzen, H., Perander, M., Overvatn, A., Stenmark, H., Johansen, T.(2005): 'p62/SQSTM1 forms protein aggregates degraded by autophagy and has a protective effect on huntingtin-induced cell death' *The Journal of Cell Biology* 171(4):603-614.

Blättler, T., Brandner, S., Raeber, A.J., Klein, M.A., Voigtländer, T., Weissmann, C., Aguzzi, A.(1997): 'PrP-expressing tissue required for transfer of scrapie infectivity from spleen to brain' *Nature* 389(6646): 69–73.

Blum, M. (1998): 'A null mutation in TGF-alpha leads to a reduction in midbrain dopaminergic neurons in the substantia nigra' *Nature Neuroscience* 1(5):374–377.

Böger, H., and Gruss, P. (1999): 'Functional determinants for the tetracycline-dependent transactivator tTA in transgenic mouse embryos' *Mechanisms of Development* 83(1-2): 141-153.

Bourdy, R. and Barrot, M. (2012): 'A new control center for dopaminergic systems: pulling the VTA by the tail' *Trends in Neurosciences* 35(11):681–690.

Bové, J., Prou, D., Perier, C., Przedborski, S. (2005): 'Toxin-Induced Models of Parkinson's Disease' *NeuroRx* 2(3): 484–494.

Braak, H., Del Tredici, K., Rub, U., de Vos, R. A., JansenSteur, E. N., Braak, E. (2003): 'Staging of brain pathology related to sporadic Parkinson's disease' *Neurobiology of Aging* 24(2): 197–211.

Braak, H., Rub, U., Jansen Steur, E. N., Del Tredici, K., de Vos, R. A. (2005): 'Cognitive status correlates with neuropathologic stage in Parkinson disease' *Neurology* 64(8): 1404–1410.

Brugarolas, J., Lei, K., Hurley, R. L., Manning, B. D., Reiling, J. H., et al. (2004): 'Regulation of mTOR function in response to hypoxia by REDD1 and the TSC1/TSC2 tumor suppressor complex' *Genes and Development* 18(23): 2893–2904.

Burré, J., Sharma, M., Tsetsenis, T., Buchman, V., Etherton, M., Südhof, T. C. (2010): 'α-Synuclein Promotes SNARE-Complex Assembly in vivo and in vitro' *Science (New York, N.Y.)* 329(5999): 1663–1667.

Butler, E. K., Voigt, A., Lutz, A. K., Toegel, J. P., Gerhardt, E., et al. (2012): 'The Mitochondrial Chaperone Protein TRAP1 Mitigates α-Synuclein Toxicity' *PLoS Genetics* 8(2): e1002488.

Byers, B., Cord, B., Nguyen, H. N., Schule, B., Fenno, L., Lee, P. C., Deisseroth, K., Langston, J. W., Pera, R. R., Palmer, T. D. (2011): 'SNCA triplication Parkinson's patient's iPSC-derived DA neurons accumulate alpha-synuclein and are susceptible to oxidative stress' *PLoS One* 6: e26159.

Cagniard, B., Beeler, J. A., Britt, J. P., McGehee, D. S., Marinelli, M., Zhuang, X. (2006): 'Dopamine scales performance in the absence of new learning' *Neuron* 51(5):541–7.

Calabresi, P., Picconi, B., Tozzi, A., Di Filippo, M. (2007): 'Dopamine- mediated regulation of corticostriatal synaptic plasticity' *Trends in Neurosciences* 30(5): 211–219.

Canal, M., Romaní-Aumedes, J., Martín-Flores, N., Pérez-Fernández, V., Malagelada, C. (2014): 'RTP801/REDD1: a stress coping regulator that turns into a troublemaker in neurodegenerative disorders' *Frontiers in Cellular Neuroscience* 8: 313.

Cammalleri, M., Lütjens, R., Berton, F., King, A. R., Simpson, C., Francesconi, W., Sanna, P. P. (2003): 'Time-restricted role for dendritic activation of the mTOR-p70^{S6K} pathway in the induction of late-phase long-term potentiation in the CA1' *Proceedings of the National Academy of Sciences of the United States of America* 100(24):14368–14373.

Card, J. P., Kobiler, O., McCambridge, J., Ebdlahad, S., Shan, Z., Raizade, M. H., Syed, A. F., Enquist, L. W. (2011): 'Microdissection of neural networks by conditional reporter expression from a Brainbow herpesvirus' *Proceedings of the National Academy of Sciences of the United States of America* 108(8): 3377-3382.

Carlsson, A., Falck, B., Hillarp, N. A. (1962): 'Cellular localization of brain monoamines' *Acta Physiologica Scandinavica Supplementum* 56(196): 1–28.

Cao, J. P., Wang, H. J., Yu, J. K., Yang, H., Xiao, C. H. and Gao, D. S. (2008): 'Involvement of NCAM in the effects of GDNF on the n eurite outgrowth in the dopamine neurons' *Neuroscience Research* 61(4): 390-397.

Chao, C. C., Ma, Y. L., Chu, K. Y. Lee, E. H. (2003): 'Integrin alphav and NCAM mediate the effects of GDNF on DA neuron survival, outgrowth, DA turnover and motor activity in rats' *Neurobiology of Aging* 24(1): 105-116.

Chen, L., and Feany, M. B. (2005): 'Alpha-synuclein phosphorylation controls neurotoxicity and inclusion formation in a *Drosophila* model of Parkinson disease' *Nature Neuroscience* 8(5): 657–663.

Chen, L., Periquet, M., Wang, X., Negro, A., McLean, P. J., Hyman, B. T., Feany, M. B. (2009): 'Tyrosine and serine phosphorylation of alpha-synuclein have opposing effects on neurotoxicity and soluble oligomer formation' *Journal of Clinical Investigation* 119(11): 3257–3265.

Chen, S., Zhang, X. J., Xie, W. J., Qiu, H. Y., Liu, H., Le, W. D. (2015): 'A new VMAT-2 inhibitor NBI-641449 in the treatment of huntington disease' *CNS Neuroscience & Therapeutics* 21(8): 662–671.

Cheng, H-C., Ulane, C. M., Burke, R. E. (2010): 'Clinical Progression in Parkinson's Disease and the Neurobiology of Axons' *Annals of Neurology* 67(6): 715–725.

Chesselet, M.F. (2008): 'In vivo alpha-synuclein overexpression in rodents: a useful model of Parkinson's disease?' *Experimental Neurology* 209(1): 22-27.

Chinta, S. J., Kumar, M. J., Hsu, M., Rajagopalan, S., Kaur, D., et al. (2007): 'Inducible alterations of glutathione levels in adult dopaminergic midbrain neurons result in nigrostriatal degeneration' *Journal of Neuroscience* 27(51): 13997–4006.

Chinta, S. J., Mallajosyula, J. K., Rane, A., Andersen, J. K., (2010): 'Mitochondrial alpha-synuclein accumulation impairs complex I function in dopaminergic neurons and results in increased mitophagy in vivo' *Neuroscience Letters* 486(3): 235-239.

Choi-Lundberg, D. L., Lin, Q., Chang, Y. N., Chiang, Y. L., Hay, C. M., Mohajeri, H., Davidson, B. L., Bohn, M. C. (1997): 'Dopaminergic neurons protected from degeneration by GDNF gene therapy' *Science* 275(5301): 838–841.

Chou, K. (2016): 'Clinical manifestations of Parkinson Disease' UpToDate. Retrieved on 7/22/2013 from www.uptodate.com.

Chu, Y., Le, W., Kompoliti, K., Jankovic, J., Mufson, E. J., Kordower, J. H. (2006): 'Nurr1 in Parkinson's disease and related disorders' *The Journal of Comparative Neurology*, 494(3), 495–514.

Conway, K. A., Lee, S. J., Rochet, J. C., Ding, T. T., Williamson, R. E., Lansbury, P. T. Jr. (2000): 'Acceleration of oligomerization, not fibrillization, is a shared property of both α-synuclein mutations linked to early-onset Parkinson's disease: Implications for pathogenesis and therapy' *Proceedings of the National Academy of Sciences* 97(2): 571–576.

Costanzo, M., and Zurzolo, C. (2013): 'The cell biology of prion-like spread of protein aggregates: mechanisms and implication in neurodegeneration' *Biochemical Journal* 452(1):1-17.

Clayton, D.A. (1984): 'Transcription of the mammalian mitochondrial genome' *Annual review of biochemistry* 53: 573–594.

Craenenbroeck, K. V., Bosscher, K. D., Berghe, W. V., Vanhoenacker, P., Haegeman, G. (2006): 'Role of glucocorticoids in dopamine-related neuropsychiatric disorders' *Molecular and Cellular Endocrinology* 245(1-2): 10–22.

Cuervo, A. M., Stefanis, L., Fredenburg, R., Lansbury, P. T., Sulzer, D. (2004): 'Impaired degradation of mutant alpha-synuclein by chaperone-mediated autophagy' *Science* 305(5688): 1292–1295.

D' Anglemont de Tassigny, X., Pascual, A., López-Barneo, J. (2015): 'GDNF-based therapies, GDNF-producing interneurons, and trophic support of the dopaminergic nigrostriatal pathway Implications for Parkinson's disease' *Frontiers in Neuroanatomy* 9:10.

Dackis, C. A., Gold, M. S. (1985): 'New concepts in cocaine addiction: the dopamine depletion hypothesis' *Neuroscience Biobehavioral Reviews* 9(3):469–477.

Daher, J. P. L, Ying, M., Banerjee, R., McDonald, R. S., Dumas Hahn, M., Yang, L., Beal, M. F., Thomas, B., Dawson, V. L., Dawson, T. D., Moore, D. J (2009): 'Conditional transgenic mice expressing C-terminally truncated human α-synuclein (αSyn119) exhibit reduced striatal dopamine without loss of nigrostriatal pathway dopaminergic neurons' *Molecular Neurodegeneration* 4:34.

Dahlström, A., and Fuxe, K. (1964): 'Evidence for the existence of monoamine-containing neurons in the central nervous system. I. Demonstration of monoamines in the cell bodies of brain stem neurons. *Acta Physiologica Scandinavica Supplementum* 232: 1–55.

Daubner, S. C., Le, T., Wang, S. (2011): 'Tyrosine Hydroxylase and Regulation of Dopamine Synthesis' *Archives of Biochemistry and Biophysics* 508(1): 1–12.

Dauer, W., Kholodilov, N., Vila, M., Trillat, A. C., Goodchild, R., et al. (2002): 'Resistance of alpha-synuclein null mice to the parkinsonian neurotoxin MPTP' *Proceedings of the National Academy of Sciences of the United States of America* 99(22): 14524–14529.

Dauer, W., and Przedborski, S. (2003): 'Parkinson's Disease: Mechanisms and Models' *Neuron* 39(6): 889-909.

de Graaf, E., Srinivas, S., Kilkenny, C., D'Agati, V., Mankoo, B. S., Costantini, F. Pachnis, V. (2001): 'Differential activities of the RET tyrosine kinase receptor isoforms during mammalian embryogenesis' *Genes* and *Development* 15(18): 2433-2444.

de Lau, L.M., Schipper, C. M. A., Hofman, A., Koudstaal, P. J., Breteler, M. M. (2005): 'Prognosis of Parkinson disease: risk of dementia and mortality: the Rotterdam Study' *Achieves of Neurology* 62(8):1265-1269.

Decressac, M., Ulusoy, A., Mattsson, B., Georgievska, B., Romero-Ramos, M., Kirik, D., Bjorklund, A. (2011): 'GDNF fails to exert neuroprotection in a rat alpha-synuclein model of Parkinson's disease' *Brain* 134(pt 8): 2302-2311.

Decressac, M., Kadkhodaei, B., Mattsson, B., Laguna, A., Perlmann, T., Bjorklund, A. (2012): 'alpha-Synuclein-induced down-regulation of Nurr1 disrupts GDNF signaling in nigral dopamine neurons' *Science translational medicine* 4(163): 163-156.

Decressac, M., Volakakis, N., Björklund, A., Perlmann, T. (2013): 'NURR1 in Parkinson disease—from pathogenesis to therapeutic potential' *Nature Reviews Neurology* 9(11): 629-636.

Dehay, B., Bové, J., Rodríguez-Muela, N., Perier, C., Recasens, A., Boya, P., Vila, M. (2010): 'Pathogenic Lysosomal Depletion in Parkinson's Disease' *The Journal of Neuroscience* 30(37):12535–12544.

Deister, C. and Schmidt, C. E. (2006): 'Optimizing neurotrophic factor combinations for neurite outgrowth' *Journal of Neural Engineering* 3(2):172-179.

Deleidi, M., and Gasser, T. (2013): 'The role of inflammation in sporadic and familial Parkinson's disease' *Cellular and Molecular Life Sciences* 70(22): 4259-4273.

Desplats, P., Lee, H-J., Bae, E-J., Patrick, C., Rockenstein, E., et al. (2009): 'Inclusion formation and neuronal cell death through neuron-to-neuron transmission of α-synuclein' *Proceedings of the National Academy of Sciences of the United States of America* 106(31): 13010–13015.

Devi, L., Raghavendran, V., Prabhu, B. M., Avadhani, N. G., Anandatheerthavarada, H. K. (2008): 'Mitochondrial Import and Accumulation of α-Synuclein Impair Complex I in Human Dopaminergic Neuronal Cultures and Parkinson Disease Brain' *The Journal of Biological Chemistry* 283(14): 9089–9100.

DeYoung, M. P., Horak, P., Sofer, A., Sgroi, D., Ellisen, L. W. (2008): 'Hypoxia regulates TSC1/2-mTOR signaling and tumor suppression through REDD1-mediated 14-3-3 shuttling' *Genes and Development* 22(2):239–251.

Dickson, D. W. (2012): 'Parkinson's Disease and Parkinsonism: Neuropathology' *Cold Spring Harbor Perspectives in Medicine* 2(8): a009258.

Domanskyi, A., Saarma, M., Airavaara, M. (2015): 'Prospects of neurotrophic factors for Parkinson's disease: comparison of protein and gene therapy' *Human Gene Therapy* 26(8): 550–559.

Dunning, C. J., George, S., Brundin, P. (2013): 'What's to like about the prion-like hypothesis for the spreading of aggregated alpha-synuclein in Parkinson disease?' *Prion* 7(1): 92-97.

Durbec, P. L., Larsson-Blomberg, L. B., Schuchardt, A., Costantini, F., Pachnis, V. (1996a): 'Common origin and developmental dependence on c-ret of subsets of enteric and sympathetic neuroblasts' *Development* 122(1): 349–358.

Durbec, P., Marcos-Gutierrez, C. V., Kilkenny, C., Grigoriou, M., Wartiowaara, K., et al. (1996b): 'GDNF signalling thro ugh the Ret receptor tyrosine kinase' *Nature* 381(6585): 789-793.

Duty, S., Jenner, P. (2011): 'Animal models of Parkinson's disease: a source of novel treatments and clues to the cause of the disease' *British journal of pharmacology* 164(4):1357–91.

Eberling J. L., Jagust, W. J., Christine, C. W., Starr, P., Larson, P., Bankiewicz, K. S., Aminoff, M. J. (2008): 'Results from a phase I safety trial of hAADC gene therapy for Parkinson disease' *Neurology* 70(21): 1980–1983.

Egawa, R., Hososhima, S., Hou, X., Katow, H., Ishizuka, T., Nakamura, H., Yawo, H. (2013): 'Optogenetic Probing and Manipulation of the Calyx-Type Presynaptic Terminal in the Embryonic Chick Ciliary Ganglion' *PLoS ONE* 8(3): e59179.

Eggert, K., Schlegel, J., Oertel, W., Würz, C., Krieg, J. C., Vedder, H. (1999): 'Glial cell line-derived neurotrophic factor protects dopaminergic neurons from 6-hydroxydopamine toxicity in vitro' *Neuroscience Letters* 269(3): 178–182.

Elbaz, A., Bower, J. H., Peterson, B. J., Maraganore, D. M., McDonnell, S. K., Ahlskog, J. E., Schaid, D. J., Rocca, W. A. (2003): 'Survival study of Parkinson disease in Olmsted county, Minnesota' *Achieves of Neurology* 60(1): 91-96.

Emmanoulidou, E., Stefanis, L., Vekrellis, K. (2010a): 'Specific cell-derived soluble α-synuclein oligomers are degraded by the 26S proteasome and impair its function' *Neurobiology of Aging* 31(6): 953–968.

Falck, B., Hillarp, N. A., Thieme, G., Torp, A. (1962): 'Fluorescence of catecholamines and related compounds condensed with formaldehyde' *Journal of Histochemistry and Cytochemistry* 10: 348–354.

Fan, X., Petitt, M., Gamboa, M., Huang, M., Dhal, S., Druzin, M. L., Wu, J. C., Chen-Tsai, Y., Nayak, N. R. (2012): 'Transient, Inducible, Placenta-Specific Gene Expression in Mice' *Endocrinology* 153(11): 5637–5644.

Fisher, C. E., Michael, L., Barnett, M. W. Davies, J. A. (2001): 'Erk MAP kinase regulates branching morphogenesis in the developing mouse kidney' *Development* 128(21): 4329-4338.

Frias, M. A., Thoreen, C. C., Jaffe, J. D., Schroder, W., Sculley, T., Carr, S. A., Sabatini, D. M. (2006): 'mSin1 is necessary for Akt/PKB phosphorylation, and its isoforms define three distinct mTORC2s' *Current Biology* 16(18):1865–1870.

Fornai, F., Schlüter, O. M., Lenzi, P., Gesi, M., Ruffoli, R., et al. (2005): 'Parkinson-like syndrome induced by continuous MPTP infusion: Convergent roles of the ubiquitin-proteasome system and α-synuclein' *Proceedings of the National Academy of Sciences of the United States of America* 102(9): 3413–3418.

Fuji, T., Sakai, M., Nagatsu, I. (1994): 'Immunohistochemical demonstration of expression of tyrosine hydroxylase in cerebellar Purkinje cells of the human and mouse' *Neurosceince letters* 165(1-2): 161-163.

Fujiwara, H., Hasegawa, M., Dohmae, N., Kawashima, A., Masliah, E., Goldberg, M. S., Shen, J., Takio, K., Iwatsubo, T. (2002): 'alpha-Synuclein is phosphorylated in synucleinopathy lesions' *Nature Cell Biology* 4(2): 160–164.

Fukuda, K., Kiuchi, K. Takahashi, M. (2002): 'Novel mechanism of regulation of Rac activity and lamellipodia formation by RET tyrosine kinase' *Journal of Biological Chemi*stry 277(21): 19114-19121.

Galleguillos, D., Fuentealba, J. A., Gómez, L. M., Saver, M., Gómez, A., Nash, K., Burger, C., Gysling, K., Andrés, M. E. (2010): 'Nurr1 regulates RET expression in dopamine neurons of adult rat midbrain' *Journal of Neurochemistry* 114(4): 1158–1167.

Gash, D. M., Zhang, Z., Ovadia, A., Cass, W. A, Yi, A., Simmerman, L., Russell, D., Martin, D., Lapchak, P. A., Collins, F., Hoffer, B. J., Gerhardt, G. A. (1996): 'Functional recovery in parkinsonian monkeys treated with GDNF' *Nature* 380(6571): 252–255.

Gazewood, J., Richards, D., Clebak, K. (2013): 'Parkinson Disease: An update' *American Family Physician* 87(4):267-273.

Gelman, D. M., Noain, D., Avale, M. E., Otero, V., Low, M. J., Rubinstein, M. (2003): 'Transgenic mice engineered to target Cre/loxP-mediated DNA recombination into catecholaminergic neurons' *Genesis* 36(4):196–202.

Gelpi, E., Navarro-Otano, J., Tolosa, E., Gaig, C., Compta, Y., Rey, M. J., Martí, M. J., Hernández, I., Valldeoriola, F., Reñé, R., Ribalta, T. (2014): 'Multiple organ involvement by alpha-synuclein pathology in Lewy body disorders' *Movement Disorders* 29(8): 1010–1018.

George, J. M. (2002): 'The synucleins' *Genome Biology* 3(1): reviews3002.1–reviews3002.6.

George, J. M., Jin, H., Woods, W. S., Clayton, D. F. (1995): 'Characterization of a novel protein regulated during the critical period for song learning in the zebra finch' *Neuron* 15(2): 361–372.

Gerfen, C. R., Herkenham, M., Thibault, J. (1987): 'The neostriatal mosaic. II. patch-directed and matrix-directed mesostriatal dopaminergic and non-dopaminergic systems' *Journal of Neuroscience* 7(12): 3915–3934

German, D.C., Schlusselberg, D. S., Woodward, D. J. (1983) 'Three-dimensional computer reconstruction of midbrain dopaminergic neuronal populations:from mouse to man' *Journal of Neural Transmission* 57(4):243–254.

Gingrich, J. R., and Roder, J. (1998): 'Inducible gene expression in the nervous system of transgenic mice. *Annual Review of Neuroscience* 21:377–405.

Gill, S. S., Patel, N. K., Hotton, G. R., O'Sullivan, K., McCarter, R., Bunnage, M., Brooks, D. J., Svendsen, C. N., Heywood, P. (2003): 'Direct brain infusion of glial cell line-derived neurotrophic factor in Parkinson disease' *Nature Medicine* 9(5): 589–595.

Goers, J., Manning-Bog, A. B., McCormack, A. L., Millett, I. S., Doniach, S., Di Monte, D. A., Uversky, V. N., Fink, A. L. (2003): 'Nuclear localization of alpha-synuclein and its interaction with histones' *Biochemistry* 42(28):8465-8471.

Golden, J. P., DeMaro, J. A., Knoten, A., Hoshi, M., Pehek, E., Johnson, E. M., Gereau, R.W., Jain, S. (2013): 'Dopamine-Dependent Compensation Maintains Motor Behavior in Mice with Developmental Ablation of Dopaminergic Neurons' *The Journal of Neuroscience 33*(43): 17095–17107.

Gorbatyuk, O. S., Li, S., Sullivan, L. F., Chen, W., Kondrikova, G., Manfredsson, F. P., et al. (2008): 'The phosphorylation state of Ser-129 in human α-synuclein determines neurodegeneration in a rat model of Parkinson disease' *Proceedings of the National Academy of Sciences of the United States of America 105*(2): 763–768.

Gossen, M., and Bujard, H. (1992): 'Tight control of gene expression in mammalian cells by tetracycline-responsive promoters' *Proceedings of the National Academy of Sciences of the United States of America* 89(12): 5547–5551.

Gossen, M., Freundlieb, S., Bender, G., Muller, G., Hillen, W., Bujard, H. (1995): 'Transcriptional activation by tetracyclines in mammalian cells' *Science* 268(5218): 1766–1769.

Gossen, M., and Bujard, H. (2002): 'Studying gene function in eukaryotes by conditional gene inactivation' *Annual Review of Genetics* 36: 153–173.

Gottschalk, W. K., Lutz, M. W., He, Y. T., Saunders, A. M., Burns, D. K., Roses, A. D., Chiba-Falek, O. (2014): 'The Broad Impact of TOM40 on Neurodegenerative Diseases in Aging' *Journal of Parkinson's disease and Alzheimer's disease* 1(1):12.

Greenamyre, J. T., Betarbet, R., Sherer, T. B. (2003): 'The rotenone model of Parkinson's disease: genes, environment and mitochondria' *Parkinsonism and Related Disorders* 9(2): S59–S64.

Greten-Harrison, B., Polydoro, M., Morimoto-Tomita, M., Diao, L., Williams, et al. (2010): 'αβγ-Synuclein triple knockout mice reveal age-dependent neuronal dysfunction' *Proceedings of the National Academy of Sciences of the United States of America* 107(45): 19573–19578.

Grondin, R., Zhang, Z., Yi, A., Cass, W. A., Maswood, N., Andersen, A. H., Elsberry, D. D., Klein, M. C., Gerhardt, G. A., Gash, D. M. (2002): 'Chronic, controlled GDNF infusion promotes structural and functional recovery in advanced parkinsonian monkeys' *Brain* 125(pt 10): 2191–2201.

Gschwind, A., Fischer, O. M., Ullrich, A. (2004): 'The discovery of receptor tyrosine kinases: targets for cancer therapy' *Nature Reviews Cancer* 4 (5): 361–370.

Gu, X.L., Long, C.X., Sun, L., Xie, C., Lin, X., Cai, H. (2010): 'Astrocytic expression of Parkinson's disease-related A53T alpha-synuclein causes neurodegeneration in mice' *Molecular Brain* 3:12.

Gwinn, D. M., Shackelford, D. B., Egan, D. F., Mihaylova, M. M., Mery, A., Vasquez, D. S., Turk, B. E., Shaw, R. J. (2008): 'AMPK phosphorylation of raptor mediates a metabolic checkpoint' *Molecular Cell* 30(2):214–226.

Hampel, S., Chung, P., McKellar, C. E., Hall, D., Looger, L. L., Simpson, J. H. (2011): 'Drosophila Brainbow: a recombinase-based fluorescent labeling technique to subdivide neural expression patterns' *Nature Methods* 8(3): 253–259.

Hang, L., Thundyil, J., Lim, K. L. (2015): 'Mitochondrial dysfunction and Parkinson disease: a Parkin-AMPK alliance in neuroprotection' *Annals of the New York Academy of Sciences* 1350(1): 37–47.

Hara, K., Maruki, Y., Long, X., Yoshino, K., Oshiro, N., Hidayat, S., Tokunaga, C., Avruch, J,. Yonezawa, K. (2002): 'Raptor, a binding partner of target of rapamycin (TOR), mediates TOR action' *Cell* 110(2):177–189.

Hardy, J. (2010): 'Genetic Analysis of Pathways to Parkinson Disease' *Neuron* 68(2): 201–206.

Harwood, K. R., Mofford, D. M., Reddy, G. R., Miller, S. C. (2011): 'Identification of mutant firefly luciferases that efficiently utilize aminoluciferins' *Chemistry and Biology* 18(12): 1649–1657.

Hattori, N., Kitada, T., Matsumine, H., Asakawa, S., Yamamura, Y., et al. (1998): 'Molecular genetic analysis of a novel Parkin gene in Japanese families with autosomal recessive juvenile parkinsonism: Evidence for variable homozygous deletions in the Parkin gene in affected individuals' *Annals of Neurology* 44(6): 935–941.

Hegarty, S. V., Sullivan, A. M., O'Keeffe, G. W. (2013): 'Midbrain dopaminergic neurons: A review of the molecular circuitry that regulates their development' *Developmental Biology* 379(2): 123–138.

Hely, M. A., Morris, J. G., Traficante, R., Reid, W. G., O'Sullivan, D. J., Williamson, P. M. (1999): 'The Sydney multicentre study of Parkinson''s disease: progression and mortality at 10 years' *Journal of Neurology, Neurosurgery and Psychiatry* 67(3):300-307.

Helwig, M., Klinkenberg, M., Rusconi, R., Musgrove, R. E., Majbour, N. K., El-Agnaf, O. M., Ulusoy, A., Di Monte, D. A. (2016): 'Brain propagation of transduced a-synuclein involves non-fibrillar protein species and is enhanced in a-synuclein null mice' *Brain* 139(pt 3); 856–870.

Henderson, C. E., Phillips, H. S., Pollock, R. A., Davies, A. M., Lemeulle, C., Armanini, M., Simmons, L., Moffet, B., Vandlen, R. A. Rosenthal, A. (1994): 'GDNF: A potent survival factor for motoneurons present in peripheral nerve and muscle' *Science* 266(5187): 1062-1064.

Heo, J-M., Ordureau, A., Paulo, J. A., Rinehart, J., Harper, J. W. (2015): 'The PINK1-PARKIN Mitochondrial Ubiquitylation Pathway Drives a Program of OPTN/NDP52 Recruitment and TBK1 Activation to Promote Mitophagy' *Molecular Cell* 60(1): 7–20.

Hobson, P., Holden, A., Meara, J. (1999): 'Measuring the impact of Parkinson's disease with the Parkinson's Disease Quality of Life questionnaire' *Age and Ageing* 28(4):341-346.

Hoeffer, C.A., and Klann, E. (2010): 'mTOR signaling: at the crossroads of plasticity, memory and disease' *Trends Neuroscience* 33(2):67-75.

Hoffer, B. J., and Harvey, B. K. (2011): 'Is GDNF beneficial in Parkinson disease?' *Nature Reviews Neurology* 7(11): 600-602.

Hökfelt, T., Martensson. R., Björklund, A., Kleinau, S., Goldstein, M. (1984): '*Distributional of tyrosine hydroxylaseimmunoreactive neurons in the rat brain'* In: Handbook of Chemical Neuroanatomy. (Classical Transmitters in the CNS, Part I) Elsevier (2): 277–379.

Hoglinger, G.U., Alvarez-Fischer, D., Arias-Carrion, O., Djufri, M., Windolph, A., Keber, U., Borta, A., Ries, V., Schwarting, R. K. W., Scheller, D., Oertel, W. H. (2015): 'A new dopaminergic nigro-olfactory projection' *Acta Neuropathologica* 130(3): 333–348.

Hornykiewicz, O. (1998): 'Biochemical aspects of Parkinson's disease' *Neurology* 51(2 Suppl 2): S2–S9.

Hou, J. G., Lin, L. F., Mytilineou, C. (1996): 'Glial cell line-derived neurotrophic factor exerts neurotrophic effects on dopaminergic neurons in vitro and promotes their survival and regrowth after damage by 1-methyl-4- phenylpyridinium' *Journal of Neurochemistry* 66(1): 74–82.

Huse, D. M., Schulman, K., Orsini, L., Castelli-Haley, J., Kennedy, S., Lenhart, G. (2005): 'Burden of illness in Parkinson's disease' *Movement Disorders* 20(11):1449-1454.

Ibáñez, C. F. (2008): 'Catecholaminergic neuron survival: getting hooked on GDNF' *Nature Neuroscience* 11: 735–736.

Inoki, K., Li, Y., Xu, T., Guan, K.L. (2003a): 'Rheb GTPase is a direct target of TSC2 GAP activity and regulates mTOR signaling' *Genes and Development* 17(15): 1829–1834.

Inoki, K., Zhu, T., Guan, K. L. (2003b): 'TSC2 mediates cellular energy response to control cell growth and survival' *Cell* 115(5): 577–590.

Jacinto, E., Facchinetti, V., Liu, D., Soto, N., Wei, S., Jung, S. Y., Huang, Q., Qin, J., Su, B. (2006): 'SIN1/MIP1 maintains rictor-mTOR complex integrity and regulates Akt phosphorylation and substrate specificity' *Cell* 127(1):125–137.

Jain, S., Naughton, C. K., Yang, M., Strickland, A., Vij, K., Encinas, M., Golden, J., Gupta, A., Heuckeroth, R., Johnson, E. M. Jr., Milbrandt, J. (2004): 'Mice expressing a dominant-negative Ret mutation phenocopy human Hirschsprung disease and delineate a direct role of Ret in spermatogenesis' *Development* 131(21): 5503–5513.

Jain, S. (2011): 'Multi-organ autonomic dysfunction in Parkinson Disease' *Parkinsonism and Related Disorders* 17(2): 77-83.

Jankovic, J., Hurtig, H., Dashe, J. (2016): 'Etiology and pathogenesis of Parkinson Disease' UpToDate. from www.uptodate.com.

Jefferis, G. S., Livet, J. (2012)**:** 'Sparse and combinatorial neuron labelling' *Current Opinion in Neurobiology* 22(1):101-10.

Jhou, T. C., Good, C. H., Rowley, C. S., Xu, S., Wang, H., Burnham, N. W., Hoffman, A. F., Lupica, C. R., Ikemoto, S. (2013): 'Cocaine Drives Aversive Conditioning via Delayed Activation of Dopamine-Responsive Habenular and Midbrain Pathways' *The Journal of Neuroscience* 33(17): 7501–7512.

Jiang, C., Wan, X., He, Y., Pan, T., Jankovic, J., Le, W. (2005): 'Age-dependent dopaminergic dysfunction in Nurr1 knockout mice' *Experimental Neurology* 191(1): 154–162.

Johnston, L. C., Eberling, J., Pivirotto, P., Hadaczek, P., Federoff, H. J., Forsayeth, J., Bankiewicz, K.S. (2009): 'Clinically relevant effects of convection-enhanced delivery of AAV2-GDNF on the dopaminergic nigrostriatal pathway in aged rhesus monkeys' *Human Gene Therapy* 20(5): 497–510.

Jonakait, G. M., MArkey, K. A, Goldstein, M., Black, I. B. (1984): 'Transient expression of selected catecholaminergic traits in cranial sensory and dorsal root ganglia of the embryonic rat' *Developmental Biology* 101(1): 51-60.

Jones, H. M., Pilowsky, L. S. (2002): 'Dopamine and antipsychotic drug action revisited' *British Journal of Psychiatry* 181: 271–275.

Juárez-Olguín, H., Calderón´Guzmán, D., Hernández García, E., Barragán Mejía, G. (2016): 'The Role of Dopamine and Its Dysfunction as a Consequence of Oxidative Stress' *Oxidative Medicine and Cellular Longevity* 2016(2016): 1-14.

Kadkhodaei, B., Ito, T., Joodmardi, E., Mattsson, B., Rouillard, C., Carta, M., Muramatsu, S., Sumi-Ichinose, C., Nomura, T., Metzger, D., Chambon, P., Lindqvist, E., Larsson, N. G., Olson, L., Björklund, A., Ichinose, H., Perlmann, T. (2009): 'Nurr1 is required for maintenance of maturing and adult midbrain dopamine neurons' *Journal of Neuroscience* 29(50): 15923–15932.

Kadkhodaei, B., Alvarsson, A., Schintu, N., Ramsköld, D., Volakakis, N., et al. (2013): 'Transcription factor Nurr1 maintains fiber integrity and nuclear-encoded mitochondrial gene expression in dopamine neurons' *Proceedings of the National Academy of Sciences of the United States of America* 110(6): 2360–2365.

Kahle, P. J. (2008): 'α-Synucleinopathy models and human neuropathology: Similarities and differences' *Acta Neuropathologica* 115(1): 87–95.

Kaplan, D. R. and Miller, F. D. (2000): 'Neurtrophin signal transduction in the nervous system' *Current Opinion in Neurobiology* 10(3): 381-391.

Kazlauskaite, A., Kondapalli, C., Gourlay, R., Campbell, D. G., Ritorto, M. S., Hofmann, K., Alessi, D. R., Knebel, A., Trost, M., Muqit, M. M. (2014): 'Parkin is activated by PINK1-dependent phosphorylation of ubiquitin at Ser65' *Biochemical Journal* 460(1): 127–139.

Kelly, B. B., Hedlund, E., Kim, C., Ishiguro, H., Isacson, O., Chikaraishi, D. M., Kim, K. S., Feng, G. (2006): 'A tyrosine hydroxylase-yellow fluorescent protein knock-in reporter system labeling dopaminergic neurons reveals potential regulatory role for the first intron of the rodent tyrosine hydroxylase gene' *Neuroscience* 142(2): 343–354.

Kempster, P. A., Hurwitz, B., Lees., A. J. (2007): 'A New Look at James Parkinson's Essay on the Shaking Palsy' *Neurology* 69(5): 482-485.

Khandelwal, P. J., Dumanis, S. B., Feng, L. R., Maguire-Zeiss, K., Rebeck, G., Lashuel, H. A., & Moussa, C. E. (2010): 'Parkinson-related parkin reduces α-Synuclein phosphorylation in a gene transfer model' *Molecular Neurodegeneration* 5: 47.

Kholodilov, N. G., Neystat, M., Oo, T. F., Lo, S. E., Larsen, K. E., Sulzer, D., Burke, R. E. (1999): 'Increased expression of rat synuclein in the substantia nigra pars compacta identified by mRNA differential display in a model of developmental target injury' *Journal of Neurochemistry* 73(6): 2586–2599.

Kiffin. R., Christian, C., Knecht, E., Cuervo, A. M. (2004): 'Activation of chaperone-mediated autophagy during oxidative stress' *Molecular Biology of the Cell* 15(11):4829-4840.

Kim, D. H., Sarbassov, D. D., Ali, S. M., King, J. E., Latek, R. R., Erdjument-Bromage, H., Tempst, P., Sabatini, D. M. (2002): 'mTOR interacts with raptor to form a nutrient-sensitive complex that signals to the cell growth machinery' *Cell* 110(2):163–175.

Kim, J., Kundu, M., Viollet, B., Guan, K. L. (2011): 'AMPK and mTOR regulate autophagy through direct phosphorylation of Ulk1' *Nature Cell Biology* 13(2):132–141.

Kim, Y. C., Guan, K-L. (2015): 'mTOR: a pharmacologic target for autophagy regulation' *Journal of Clinical Investigation.* 125(1):25–32.

Kircher, T. T., and Thienel, R. (2006): '*Functional brain imaging of symptoms and cognition in schizophrenia'* The Boundaries of Consciousness. Amsterdam: Elsevier. p.302. ISBN 0-444-52876-8.

Kirik, D., Rosenblad, C., Björklund, A. (2000a): 'Preservation of a functional nigrostriatal dopamine pathway by GDNF in the intrastriatal 6-OHDA lesion model depends on the site of administration of the trophic factor' *European Journal of Neuroscience* 12(11): 3871–3882.

Kirik, D., Rosenblad, C., Bjorklund, A., Mandel, R. J. (2000b): 'Long-term rAAV-mediated gene transfer of GDNF in the rat Parkinson's model: intrastriatal but not intranigral transduction promotes functional regeneration in the lesioned nigrostriatal system' *Journal of Neuroscience* 20(12): 4686–4700.

Kiriyama, Y., and Nochi, H. (2015): 'The Function of Autophagy in Neurodegenerative Diseases' *International Journal of Molecular Science* 16(11): 26797–26812.

Kistner, A., Gossen, M., Zimmermann, F., Jerecic, J., Ullmer, C., et al. (1996): 'Doxycycline-mediated quantitative and tissue-specific control of gene expression in transgenic mice' *Proceedings of the National Academy of Sciences of the United States of America* 93(20): 10933–8.

Kitada, T., Asakawa, S., Hattori, N., Matsumine, H., Yamamura, Y., Minoshima, S., Yokochi, M., Mizuno, Y., Shimizu, N. (1998): 'Mutations in the parkin gene cause autosomal recessive juvenile parkinsonism' *Nature* 392(6676): 605–608.

Klein, C., and Westenberger, A. (2012): 'Genetics of Parkinson's Disease' *Cold Spring Harbor Perspectives in Medicine* 2(1):a008888.

Klivenyi, P., Siwek, D., Gardian, G., Yang, L., Starkov, A., et al. (2006): 'Mice lacking alpha-synuclein are resistant to mitochondrial toxins' *Neurobiology Disease* 21(3): 541–548.

Knowles, P. P., Murray-Rust, J., Kjaer, S., Scott, R. P., Hanrahan, S., Santoro, M., Ibáñez, C. F., McDonald, N. Q. (2006): 'Structure and chemical inhibition of the RET tyrosine kinase domain' *Journal of Biological Chemistry* 281(44): 33577–33587.

Kobayashi, K., Morita, S., Sawada, H., Mizuguchi, T., Yamada, K., Nagatsu, I., Hata, T., Watanabe, Y., Fujita, K., Nagatsu, T. (1995): 'Targeted disruption of the tyrosine hydroxylase locus results in severe catecholamine depletion and perinatal lethality in mice' *Journal of Biological Chemistry* 270(45):27235-27243.

Kokaia, Z., Airaksinen, M. S., Nanobashvili, A., Larsson, E., Kujamäki, E., Lindvall, O., Saarma, M. (1999): 'GDNF family ligands and receptors are differentially regulated after brain insults in the rat' *European Journal of Neuroscience* 11(4): 1202-1216.

Konradi, C., Heckers, S. (2003): 'Molecular aspects of glutamate dysregulation: implications for schizophrenia and its treatment' *Pharmacology and Therapeutics* 97(2): 153–179.

Kontopoulos, E., Parvin, J. D., Feany, M. B. (2006): 'α-synuclein acts in the nucleus to inhibit histone acetylation and promote neurotoxicity' *Human Molecular Genetics* 15(20): 3012–3023.

Koob, G. F., Moal, M. (2001): 'Drug addiction, dysregulation of reward, and allostasis' *Neuropsychopharmacology* 24(2): 97–129.

Kopra, J., Vilenius, C., Grealish, S., Härma, M.-A., Varendi, K., Lindholm, J., et al. (2015): 'GDNF is not required for catecholaminergic neuron survival *in vivo*' *Nature Neuroscience* 18(3): 319–322.

Kordower, J. H., Chu, Y., Hauser, R. A., Freeman, T. B., Olanow, C. W. (2008): 'Lewybody-like pathology in long-term embryonic nigral transplants in Parkinson's disease' *Nature Medicine* 14(5): 504–506.

Kordower, J. H., Bjorklund, A. (2013): 'Trophic factor gene therapy for Parkinson's disease' *Movement Disorders* 28(1): 96-109.

Kowsky, S., Pöppelmeyer, C., Kramer, E. R., Falkenburger, B. H., Kruse, A., Klein, R., Schulz, J. B. (2007): 'RET signaling does not modulate MPTP toxicity but is required for regeneration of dopaminergic axon terminals' *Proceedings of the National Academy of Sciences of the United States of America* 104(50): 20049–20054.

Koyano, F., Okatsu, K., Kosako, H., Tamura, Y., Go, E., et al. (2014): 'Ubiquitin is phosphorylated by PINK1 to activate parkin' *Nature* 510(7503): 162–166.

Kramer, E. R., Aron, L., Ramakers, G. M. J., Seitz, S., Zhuang, X., Beyer, K., Smidt, M. P., Klein, R. (2007): 'Absence of Ret Signaling in Mice Causes Progressive and Late Degeneration of the Nigrostriatal System' *PLoS Biology* 5(3): e39.

Kramer, E. R., and Liss, B. (2015): 'GDNF-Ret signaling in midbrain dopaminergic neurons and its implication for Parkinson disease' *FEBS Letters* 589(24 Pt A): 3760-3772.

Kramer, E. R. (2015): 'The neuroprotective and regenerative potential of parkin and GDNF/Ret signaling in the midbrain dopaminergic system' *Neural Regeneration Research* 10(11): 1752–1753.

Kramer, E. R. (2015): 'Crosstalk of parkin and Ret in dopaminergic neurons' *Oncotarget* 6(18): 15704–15705.

Krestel, H. E., Shimshek, D. R., Jensen, V., Nevian, T., Kim, J., et al. (2004): 'A genetic switch for epilepsy in adult mice' *Journal of Neuroscience* 24(46): 10568–10578.

Krüger, R., Kuhn, W., Müller, T., Woitalla, D., Graeber, M., Kösel, S., Przuntek, H., Epplen, J. T., Schöls, L., Riess, O. (1998): 'Ala30Pro mutation in the gene encoding alpha-synuclein in Parkinson's disease' *Nature Genetics* 18(2):106-108.

Kues, W. A., Schwinzer, R., Wirth, D., Verhoeyen, E., Lemme, E., Herrmann, D., Barg-Kues, B., Hauser, H., Wonigeit, K., Niemann, H. (2006): 'Epigenetic silencing and tissue independent expression of a novel tetracycline inducible system in double-transgenic pigs' *FASEB Journal* 20(8): 1200–1202.

Kurz, A., May, C., Schmidt, O., Müller, T., Stephan, C., Meyer, H.E., Gispert, S., Auburger, G., Marcus, K. (2012): 'A53T-alpha-synuclein-overexpression in the mouse nigrostriatal pathway leads to early increase of 14-3-3 epsilon and late increase of GFAP' *Journal of Neuronal Transmission* 119(3):297-312.

Lammel, S., Lim, B. K., Ran, C., Huang, K. W., Betley, M. J., Tye, K. M., Deisseroth, K., Malenka, R.C. (2012): 'Input-specific control of reward and aversion in the ventral tegmental area' *Nature* 491(7423): 212–217.

Lane, E., and Dunnett, S. (2008): 'Animal models of Parkinson's disease and L-dopa induced dyskinesia: how close are we to the clinic?' *Psychopharmacology* 199(3): 303–312.

Lang, A. E., Gill, S., Patel, N. K., Lozano, A., Nutt, J. G. (2006): 'Randomized controlled trial of intraputamenal glial cell line-derived neurotrophic factor infusion in Parkinson disease' *Annals of Neurology* 59(3): 459–466.

Laplante, M., Sabatini, D.M. (2012): 'mTOR signaling in growth control and disease' *Cell* 149(2): 274–293.

Laruelle, M., Abi-Dargham, A., van Dyck, C. H., Gil, R., D'Souza, C. D., et al. (1996): 'Single photon emission computerized tomography imaging of amphetamine-induced dopamine release in drug-free schizophrenic subjects' *Proceedings of the National Academy of Sciences of the United States of America* 93(17): 9235–9240.

Lazarou, M., Sliter, D. A., Kane, L. A., Sarraf, S. A.,Wang, C., Burman, J. L., Sideris, D. P., Fogel, A. I., Youle, R. J. (2015): 'The ubiquitin kinase PINK1 recruits autophagy receptors to induce mitophagy' *Nature* 524(7565): 309–314.

Le, W., Conneely, O. M., He, Y., Jankovic, J., Appel, S. H. (1999): 'Reduced Nurr1 expression increases the vulnerability of mesencephalic dopamine neurons to MPTP-induced injury' *Journal of Neurochemistry* 73(5): 2218–2221.

Lee, T., and Luo, L. (1999): 'Mosaic analysis with a repressible cell marker for studies of gene function in neuronal morphogenesis' *Neuron* 22(3):451–61.

Lemmon, M. A., Schlessinger, J. (2010): 'Cell signaling by receptor tyrosine kinases' *Cell* 141(7): 1117–1134.

Lerner, T. N., Shilyansky, C., Davidson, T. J., Evans, K. E., Beier, K. T., Zalocusky, K. A., Crow, A. K., Malenka, R. C., Luo, L., Tomer, R., Deisseroth, K. (2015): 'Intact-brain analyses reveal distinct information carried by SNc dopamine subcircuits' *Cell* 162(3): 635–647.

Lew, M. (2007): 'Overview of Parkinson's Disease' *Pharmacotherapy* 27(12 Pt 2): 155S-160S.

Lenartowski, R., and Goc, A. (2011): 'Epigenetic, transcriptional and posttranscriptional regulation of the tyrosine hydroxylase gene' *International Journal of Developmental Neuroscience* 29(8):873-83.

Li, J. Y., Englund, E., Holton, J. L., Soulet, D., Hagell, P., et al. (2008): 'Lewy bodies in grafted neurons in subjects with Parkinson's disease suggest host- to-graft disease propagation' *Nature Medicine* 14(5): 501–503.

Lim, J., Kim, H. W., Youdim, M. B., Rhyu, I. J., Choe, K. M., Oh, Y. J. (2011): 'Binding preference of p62 towards LC3-ll during dopaminergic neurotoxin-induced impairment of autophagic flux' *Autophagy* 7(1): 51-60.

Lin, L. F., Doherty, D. H., Lile, J. D., Bektesh, S. Collins, F. (1993): 'GDNF: a glial cell line-derived neurotrophic factor for midbrain dopaminergic neurones' *Science* 260(5111): 1130-1132.

Lin, X., Parisiadou, L., Gu, X.L., Wang, L., Shim, H., Sun, L., Xie, C., Long, C.X., Yang, W.J., Ding, J., Chen, Z.Z., Gallant, P.E., Tao-Cheng, J.H., Rudow, G., Troncoso, J.C., Liu, Z., Li, Z., Cai, H. (2009): 'Leucine-rich repeat kinase 2 regulates the progression of neuropathology induced by Parkinson's-disease-related mutant alpha-synuclein' *Neuron* 64(6):807-27.

Lin, X., Parisiadou, L., Sgobio, C., Liu, G., Yu, J., et al. (2012): 'Conditional expression of Parkinson's disease related mutant alpha-synuclein in the midbrain dopaminergic neurons causes progressive neurodegeneration and degradation of transcription factor nuclear receptor related 1' *Journal of Neuroscience* 32(27):9248–9264.

Lindeberg, J., Mattsson, R., Ebendal, T. (2002): 'Timing the doxycycline yields different patterns of genomic recombination in brain neurons with a new inducible Cre transgene' *Journal of Neuroscience Research* 68(2): 248–253.

Lindeberg J., Usoskin, D., Bengtsson, H., Gustafsson, A., Kylberg, A., et al. (2004): 'Transgenic expression of Cre recombinase from the tyrosine hydroxylase locus' *Genesis* 40(2):67–73.

Lindholm, P., and Saarma, M. (2010): 'Novel CDNF/MANF family of neurotrophic factors' *Developmental Neurobiology* 70(5): 360-71.

Liu, B., Sun, J., Zhang, J., Mao, W., Ma, Y., Li, S., Cheng, X., Lv, C. (2015): 'Autophagy-related protein expression in the substantia nigra and eldepryl intervention in rat models of Parkinson's disease' *Brain Research* 1625:180-8.

Livet, J., Weissman, T.A., Kang, H., Draft, R.W., Lu, J., Bennis, R.A., Sanes, J.R., Lichtman, J.W. (2007): 'Transgenic strategies for combinatorial expression of fluorescent proteins in the nervous system' *Nature* 450(7166): 56-62.

Lo Bianco, C., Deglon, N., Pralong, W., Aebischer, P. (2004): 'Lentiviral nigral delivery of GDNF does not prevent neurodegeneration in a genetic rat model of Parkinson's disease' *Neurobiology of Disease* 17(2): 283-289.

Lo Bianco, C., Schneider, B. L., Bauer, M., Sajadi, A., Brice, A., Iwatsubo, T., & Aebischer, P. (2004): 'Lentiviral vector delivery of parkin prevents dopaminergic degeneration in an α-synuclein rat model of Parkinson's disease' *Proceedings of the National Academy of Sciences of the United States of America* 101(50): 17510–17515.

Loew, R., Heinz , N., Hampf, M., Bujard, H., Gossen, M. (2010): 'Improved Tet-responsive promoters with minimized background expression' *BMC Biotechnology* 10: 81.

López-Pérez, S. J., Morales-Villagr´an, A., Medina-Ceja, L. (2015): 'Effect of perinatal asphyxia and carbamazepine treatment on cortical dopamine and DOPAC levels' *Journal of Biomedical Science* 22:14.

Louis, E.D., Marder, K., Cote, L., Tang, M., Mayeux, R. (1997): 'Mortality from Parkinson disease' *Achieves of Neurology* 54(3):260-264.

Lucking, C. B., Abbas, N., Durr, A., Bonifati, V., Bonnet, A. M., de Broucker, T., De Michele, G., Wood, N. W., Agid, Y., Brice, A. (1998): 'Homozygous deletions in parkin gene in European and North African families with autosomal recessive juvenile parkinsonism' *The Lancet* 352(9137): 1355–1356.

Luk, K. C., Kehm, V. M., Zhang, B., O'Brien, P., Trojanowski, J. Q., Lee, V. M. (2012a): 'Intracerebral inoculation of pathological α-synuclein initiates a rapidly progressive neurodegenerative α-synucleinopathy in mice' *Journal of Experimental Medicine* 209(5): 975–86.

Luk, K.C., Kehm, V., Carroll, J., Zhang, B., O'Brien, P., et al. (2012b): 'Pathological α-synuclein transmission initiates Parkinson-like neurodegeneration in nontransgenic mice' *Science (New York, N.Y.)* 338(6109): 949–53.

Luo, Y., Wang, Y., Kuang, S. Y., Chiang, Y. H., Hoffer, B. (2010): 'Decreased level of Nurr1 in heterozygous young adult mice leads to exacerbated acute and long-term toxicity after repeated methamphetamine exposure' *PLoS ONE* 5: e15193.

Lynch-Day, M. A., Mao, K., Wang, K., Zhao, M., Klionsky, D. J. (2012): 'The Role of Autophagy in Parkinson's Disease' *Cold Spring Harbor Perspectives in Medicine* 2(4): a009357.

Lynd-Balta, E. and Haber, S.N. (1994): 'The organization of midbrain projections to the striatum in the primate: sensorimotor-related striatum versus ventral striatum' *Neuroscience* 59(3): 625–640.

Macedo, D., Tavares, L., McDougall, G. J., Miranda, H. V., Stewart, D., Ferreira, R. B. et al. (2015): '(Poly)phenols protect from alpha-synuclein toxicity by reducing oxidative stress and promoting autophagy' *Human Molecular Genetics* 24(6): 1717-1732.

MacPhee, G., and Stewart, D. (2001): 'Parkinson's Disease' *Reviews in Clinical Gerontology* 11(1): 33-49.

Majeski, A. E., Dice, J. F. (2004): 'Mechanisms of chaperone-mediated autophagy' *International Journal of Biochemistry and Cell Biol*ogy 36(12): 2435-2444.

Malagelada, C., Jin, Z. H., Greene, L. A. (2008): 'RTP801 Is Induced in Parkinson's Disease and Mediates Neuron Death by Inhibiting Akt Phosphorylation/Activation' *The Journal of Neuroscience* 28(53): 14363–14371.

Malagelada, C., Ryu, E. J., Biswas, S. C., Jackson-Lewis, V., Greene, L. A. (2006): 'RTP801 is elevated in Parkinson brain substantia nigral neurons and mediates death in cellular models of

Parkinson's disease by a mechanism involving mammalian target of rapamycin inactivation' *Journal of Neuroscience* 26(3): 9996– 10005.

Malcolm, R., Kajdasz, D. K., Herron, J., Anton, R. F., Brady, K. T. (2000): 'A double-blind, placebo-controlled outpatient trial of pergolide for cocaine dependence. *Drug and Alcohol Dependence* 60(2):161–8.

Manié, S., Santoro, M., Fusco, A., Billaud, M. (2001): 'The RET receptor: function in development and dysfunction in congenital malformation' *Trends in Genetics* 17(10): 580-589.

Mann, V. M., Cooper, J. M., Daniel, S. E., Srai, K., Jenner, P., et al. (1994): 'Complex I, iron, and ferritin in Parkinson's disease substantia nigra' *Annals of Neurology* 36(6): 876–881.

Marks, W. J. Jr., Bartus, R. T., Siffert, J., Davis, C. S., Lozano, A., et al. (2010): 'Gene delivery of AAV2- neurturin for Parkinson's disease: a doubleblind, randomised, controlled trial' *The Lancet Neurology* 9(12): 1164–1172.

Maroteaux, L., Campanelli, J. T., Scheller, R. H. (1988): 'Synuclein: A neuron-specific protein localized to the nucleus and presynaptic nerve terminal' Journal of Neuroscience 8(8): 2804–2815.

Maroteaux, L., and Scheller, R. H. (1991): 'The rat brain synucleins; family of proteins transiently associated with neuronal membrane' *Molecular Brain Research* 11(3-4): 335–343.

Maskri, L., Zhu, X., Fritzen, S., Kühn, K., Ullmer, C., Engels, P., Andriske, M., Stichel, C. C., Lübbert, H. (2004): 'Influence of different promoters on the expression pattern of mutated human alpha-synuclein in transgenic mice' *Neurodegenerative Diseases* 1(6):255-265.

Masliah, E., Rockenstein, E., Veinbergs, I., Mallory, M., Hashimoto, M., Takeda, A., Sagara, Y., Sisk, A., Mucke, L. (2000): 'Dopaminergic loss and inclusion body formation in alpha-synuclein mice: implications for neurodegenerative disorders' *Science* 287(5456): 1265-1269.

Masuda, M., Miura, M., Inoue, R., Imanishi, M., Saino-Saito, S., Takada, M., Kobayashi, K., Aosaki, T. (2011): 'Postnatal development of tyrosine hydroxylase mRNA-expressing neurons in mouse neostriatum' *European Journal of Neuroscience* 34(9): 1355-1367.

Masuda-Suzukake, M., Nonaka, T., Hosokawa, M., Oikawa, T., Arai, T., et al. (2013): 'Prion-like spreading of pathological α-synuclein in brain' *Brain* 136(pt 4): 1128–1138.

Matsuda, W., Furuta, T., Nakamura, K. C., Hioki, H., Fujiyama, F., et al. (2009): 'Single nigrostriatal dopaminergic neurons form widely spread and highly dense axonal arborizations in the neostriatum' *Journal of Neuroscience* 29(2): 444–453.

McFarland, N. R., Fan, Z., Xu, K., Schwarzschild, M. A., Feany, M. B., Hyman, B. T., McLean, P. J, (2009): 'Alpha-synuclein S129 phosphorylation mutants do not alter nigrostriatal toxicity in a rat model of Parkinson disease' *Journal of Neuropathology and Experimental Neurology* 68(5): 515–524.

Meka, D.P., Müller-Rischart, A.K., Nidadavolu, P., Mohammadi, B., Motori, E., et al. (2015): 'Parkin cooperates with GDNF/RET signaling to prevent dopaminergic neuron degeneration' *The Journal of Clinical Investigation* 125(5):1873-1885.

Meng, X., Lindahl, M., Hyvönen, M. E., Parvinen, M., de Rooij, D. G., Hess, M. W., Raatikainen-Ahokas, A., Sainio. K, Rauvala, H., Lakso, M., Pichel, J. G., Westphal, H., Saarma, M., Sariola, H. (2000): 'Regulation of cell fate decision of undifferentiated spermatogonia by GDNF' *Science* 287(5457): 1489–1493.

Metcalf, D. J., García-Arencibia, G., Hochfeld, W. E., Rubinsztein, D. C. (2012): 'Autophagy and misfolded proteins in neurodegeneration' *Experimental Neurology* 238(1):22-28.

Mijatovic, J., Airavaara, M., Planken, A., Auvinen, P., Raasmaja, A., Piepponen, T. P., Costantini, F., Ahtee, L., Saarma, M. (2007): 'Constitutive Ret activity in knock-in multiple endocrine neoplasia type B mice induces profound elevation of brain dopamine concentration via enhanced synthesis and increases the number of TH-positive cells in the substantia nigra' *Journal of Neuroscience* 27(18): 4799–4809.

Min, N., Joh, T. H., Kin, K. S., Peng, C., Son, J. H. (1994): '5′ Upstream DNA sequence of the rat tyrosine hydroxylase gene directs high-level and tissue-specific expression to catecholaminergic neurons in the central nervous system of transgenic mice' *Molecular Brain Research* 27(2): 281-289.

Miller, D. W., Hague, S. M., Clarimon, J., Baptista, M., Gwinn- Hardy, K., Cookson, M. R., Singleton, A. B. (2004): 'α-Synuclein in blood and brain from familial Parkinson disease with SNCA locus triplication' *Neurology* 62(10): 1835–1838.

Mizushima, N., Sugita, H., Yoshimori, T., Ohsumi, Y. (1998): 'A new protein conjugation system in human. The counterpart of the yeast Apg12p conjugation system essential for autophagy' *Journal of Biological Chemistry* 273(51): 33889–33892.

Mizushima, N., Kuma, A., Kobayashi, Y., Yamamoto, A., Matsubae, M., Takao, T., Natsume, T., Ohsumi. Y., Yoshimori, T. (2003): 'Mouse Apg16L, a novel WD-repeat protein, targets to the autophagic isolation membrane with the Apg12–Apg5 conjugate' *Journal of Cell Science* 116(pt 9): 1679–1688.

Mofford, D. M., Adams, S. T., Reddy, G. S. K. K., Reddy, G. R., Miller, S. C. (2015): 'Luciferin Amides *Enable in Vivo* Bioluminescence Detection of Endogenous Fatty Acid Amide Hydrolase Activity' *Journal of the American Chemical Society* 137(27): 8684–8687.

Money, K. M., and Stanwood, G. D. (2013): 'Developmental origins of brain disorders: roles for dopamine' 7(260): 1-14.

Mori, F., Tanji, K., Yoshimoto, M., Takahashi, H., Wakabayashi, K. (2002a): 'Demonstration of α-synuclein immunoreactivity in neuronal and glial cytoplasm in normal human brain tissue using proteinase K and formic acid pretreatment' *Experimental Neurology* 176(1): 98–104.

Mori, F., Tanji, K., Yoshimoto, M., Takahashi, H., Wakabayashi K. (2002b): 'Immunohistochemical comparison of α- and β-synuclein in adult rat central nervous system' *Brain Research* 941(1-2): 118–126.

Mougenot, A. L., Nicot, S., Bencsik, A., Morignat, E., Verche`re, J., et al. (2012): 'Prion-like acceleration of a synucleinopathy in a transgenic mouse model' *Neurobiology of Aging* 33(9): 2225–2228.

Murphy, D. D., Rueter, S. M., Trojanowski, J. Q., Lee, V. M. (2000): 'Synucleins are developmentally expressed, and α-synuclein regulates the size of the presynaptic vesicular pool in primary hippocampal neurons' *Journal of Neuroscience* 20(9): 3214–3220.

Nerius, M., Fink, A., Doblhammer-Reiter, G. (2015): 'Parkinson's Disease in Germany: Prevalence, Incidence and Mortality Based on Health Claims Data' *Rostock Discussion Paper* 32:1-21.

Nestler, E. J. (2013): 'Cellular basis of memory for addiction' *Dialogues in Clinical Neuroscience* 15(4): 431–443.

Ng, C. H., Guan, M. S., Koh, C., Ouyang, X., Yu, F., Tan, E. K., O'Neill, S. P., Zhang, X., Chung, J., Lim, K. L. (2012): 'AMP kinase activation mitigates dopaminergic dysfunction and mitochondrial abnormalities in Drosophila models of Parkinson's disease' *Journal of Neuroscience* 32(41):14311-14317.

Nieoullon, A., and Coquerel, A. (2003): 'Dopamine: a key regulator to adapt action, emotion, motivation and cognition' *Current Opinion in Neurology* 16(2): S3–S9.

Nuber, S., Petrasch-Parwez, E., Winner, B., Winkler, J., von Hörsten, S., Schmidt, T., Boy, J., Kuhn, M., Nguyen, H. P., Teismann, P., Schulz, J. B., Neumann, M., Pichler, B. J., Reischl, G., Holzmann, C., Schmitt, I., Bornemann, A., Kuhn, W., Zimmermann, F., Servadio, A., Riess, O. (2008): 'Neurodegeneration and motor dysfunction in a conditional model of Parkinson's disease' *Journal of Neuroscience* 28(10): 2471-2484.

Nutt, J. G., Burchiel, K. J., Comella, C. L., Jankovic, J., Lang, A. E., et al. (2003): 'Randomized, double-blind trial of glial cell line-derived neurotrophic factor (GDNF) in PD' *Neurology* 60(1): 69–73.

Obeso, J. A., Rodríguez-Oroz, M. C., Benitez-Temino, B., Blesa, F. J., Guridi, J., Marin, C., Rodriguez, M. (2008): 'Functional organization of the basal ganglia: therapeutic implications for Parkinson's disease' *Movement Disorders* 23(3): S548–559.

Okatsu, K., Oka, T., Iguchi, M., Imamura, K., Kosako, H., et al. (2012): 'PINK1 autophosphorylation upon membrane potential dissipation is essential for Parkin recruitment to damaged mitochondria' *Nature Communications* 3(1016).

Olanow, C. W., and Brundin, P. (2013): 'Parkinson's disease and alpha synuclein: is Parkinson's disease a prion-like disorder?' *Movement Disorders* 28(1):31-40.

Owen, A. D., Schapira, A. H., Jenner, P., Marsden, C. D. (1996): 'Oxidative stress and Parkinson's Disease' *Annals of the New York Academy of Sciences* 786: 217-223.

Pachnis, V., Mankoo, B., Costantini, F. (1993): 'Expression of the c-ret proto-oncogene during mouse embryogenesis' *Development* 119(4): 1005–1017.

Pakkenberg, B., Moller, A., Gundersen, H. J., MouritzenDam, A., Pakkenberg, H. (1991): 'The absolute number of nerve cells in substantia nigra in normal subjects and in patients with

Parkinson's disease estimated with an unbiased stereological method' *Journal of Neurology Neurosurgery and Psychiatry* 54(1): 30–33.

Palacino, J. J., Sagi, D., Goldberg, M. S., Krauss, S., Motz, C., Wacker, M., Klose, J., Shen, J. (2004): 'Mitochondrial dysfunction and oxidative damage in parkin-deficient mice' *The Journal of Biological Chemistry* 279(18): 18614–18622.

Palmiter, R. D., and Brinster, R. L. (1986): 'Germ-line transformation of mice' *Annual Review of Genetics* 20: 465-499.

Pan, T., Zhu, W., Zhao, H., Deng, H., Xie, W., Jankovic, J., Le, W. (2008): Nurr1 deficiency predisposes to lactacystin-induced dopaminergic neuron injury in vitro and in vivo. *Brain Research* 1222: 222–229.

Pan, Y. A., Freundlich, T., Weissman, T. A., Schoppik, D., Wang, X. C., et al. (2013): 'Zebrabow: multispectral cell labeling for cell tracing and lineage analysis in zebrafish' *Development (Cambridge, England)* 140(13): 2835–2846.

Pankiv, S., Clausen, T. H., Lamark, T., Brech, A., Bruun, J. A., Outzen, H., Overvatn, A., Bjorkoy, G., Johansen, T. (2007): 'p62/SQSTM1 binds directly to Atg8/LC3 to facilitate degradation of ubiquitinated protein aggregates by autophagy' *Journal of Biological Chemistry* 282(33): 24131–24145.

Paratcha, G., Ledda, F., Ibanez, C.F. (2003): 'The neural cell adhesion molecule NCAM is an alternative signaling receptor for GDNF family ligands' *Cell* 113(7): 867-79.

Pascual, A., Hidalgo-Figueroa, M., Piruat, J. I., Pintado, C. O., Gómez-Díaz, R., López-Barneo, J. (2008): 'Absolute requirement of GDNF for adult catecholaminergic neuron survival' *Nature Neuroscience* 11(7): 755–761.

Pascual, A., Hidalgo-Figueroa, M., Gutierrez, F., Lopez-Barneo, J., Bonilla, S. (2012): 'GDNF Is Predominantly Expressed in the PV+ Neostriatal Interneuronal Ensemble in Normal Mouse and after Injury of the Nigrostriatal Pathway' *Journal of Neuroscience* 32(3), 864–872.

Paxinos, G., and B.J. Franklin's, K. (2005): '*The Mouse Brain in Stereotaxic Coordinates*' Academic Press

Pearce, L. R., Huang, X., Boudeau, J., Pawłowski, R., Wullschleger, S., Deak, M., Ibrahim, A. F. M., Gourlay, R., Magnuson, M. A., Alessi, D. R. (2007): 'Identification of Protor as a novel Rictor-binding component of mTOR complex-2' *Biochemical Journal* 405(3):513–522.

Peelaerts, W., Bousset, L., Van der Perren, A., Moskalyuk, A., Pulizzi, R., Giugliano, M., Van den Haute, C., Melki, R., Baekelandt, V. (2015): 'α-Synuclein strains cause distinct synucleinopathies after local and systemic administration' *Nature* 522(7556): 340–344.

Pérez-Revuelta, B. I., Hettich, M. M., Ciociaro, A., Rotermund, C., Kahle, P. J., Krauss, S., Di Monte, D. A. (2014): 'Metformin lowers Ser-129 phosphorylated *α*-synuclein levels via mTOR-dependent protein phosphatase 2A activation' *Cell Death and Disease* 5(5): e1209.

Perlmann, T., and Jansson, L. (1995): 'A novel pathway for vitamin A signaling mediated by RXR heterodimerization with NGFI-B and NURR1' *Genes and Development* 9(7): 769–782.

Petrucelli, L., O'Farrell, C., Lockhart, P. J., Baptista, M., Kehoe, K., Vink, L., Choi, P., Wolozin, B., Farrer, M., Hardy, J., Cookson, M. R. (2002): 'Parkin protects against the toxicity associated with mutant alpha-synuclein: proteasome dysfunction selectively affects catecholaminergic neurons' *Neuron* 36(6):1007-19.

Phillipson, O. T. (2014): 'Management of the aging risk factor for Parkinson's disease' *Neurobiology of Aging* 35(4): 847-857.

Polymeropoulos, M. H., Lavedan, C., Leroy, E., Ide, S. E., Dehejia, A., et al. (1997): 'Mutation in the alpha-synuclein gene identified in families with Parkinson's disease' *Science* 276(5321): 2045–2047.

Potashkin, J. A., Blume, S. R., Runkle. N. K. (2011): 'Limitations of Animal Models of Parkinson's Disease' *Parkinson's Disease* 2011 (ID 658083): 7 pages.

Postuma, R., Gagnon, J., Montplaisir, J. (2010): 'Clinical prediction of Parkinson's Disease: Planning for the age of neuroprotection' *Journal of Neurology* 81(9): 1008-1013.

Potter, C. J., Pedraza, L. G., Xu, T. (2002): 'Akt regulates growth by directly phosphorylating Tsc2' *Nature Cell Biology* 4(9):658–665.

Prensa, L. and Parent, A. (2001): 'The nigrostriatal pathway in the rat: a single-axon study of the relationship between dorsal and ventral tier nigral neurons and the striosome/matrix striatal compartments' *Journal of Neuroscience* 21(18), 7247–7260.

Ramsey, C. P., Tsika, E., Ischiropoulos, H., Giasson, B. I. (2010): 'DJ-1 deficient mice demonstrate similar vulnerability to pathogenic Ala53Thr human α-syn toxicity' *Human Molecular Genetics* 19(8):1425-1437.

Rathke-Hartlieb, S., Kahle, P. J., Neumann, M., Ozmen, L., Haid, S., Okochi, M., Haass, C., Schulz, J. B. (2001): 'Sensitivity to MPTP is not increased in Parkinson's disease-associated mutant alpha-synuclein transgenic mice' *Journal of Neurochemistry* 77(4): 1181-1184.

Rasheed, N., and Alghasham, A. (2012): 'Central Dopaminergic Systemand Its Implications in Stress-Mediated Neurological Disorders and Gastric Ulcers: Short Review' *Advances in Pharmacological Sciences* 2012(182671): 1-11.

Ravikumar, B., Sarkar, S., Davies, J. E., Futter, M., Garcia-Arencibia, M., Green-Thompson, Z.W., et al. (2010): 'Regulation of mammalian autophagy in physiology and pathophysiology' *Physiological Reviews* 90(4): 1383–1435.

Recasens, A., and Dehay, B. (2014a): 'Alpha-synuclein spreading in Parkinson's disease' *Frontiers in Neuroanatomy* 8: 159.

Recasens, A., Dehay, B., Bove´, J., Carballo-Carbajal, I., Dovero, S., et al. (2014b): 'Lewy body extracts from Parkinson disease brains trigger α-synuclein pathology and neurodegeneration in mice and monkeys' *Annals of Neurology* 75(3): 351–362.

Reichmann, H. (2016): 'Modern treatment in Parkinson's disease, a personal approach' *Journal of Neural Transmission* 123(1):73–80.

Rice, B. W., Cable, M. D., Nelson, M. B. (2001): 'In vivo imaging of light-emitting probes' *Journal of Biomedical Optics* 6(4): 432–440.

Richfield, E. K., Thiruchelvam, M. J., Cory-Slechta, D. A., Wuertzer, C., Gainetdinov, R. R., Caron, M. G., Di Monte, D. A., Federoff, H. J. (2002): 'Behavioral and neurochemical effects of wild-type and mutated human alpha-synuclein in transgenic mice' *Experimental Neurology* 175(1): 35-48.

Rideout, H. J., Dietrich, P., Savalle, M., Dauer, W. T., Stefanis, L. (2003): 'Regulation of α-synuclein by bFGF in cultured ventral midbrain dopaminergic neurons' *Journal of Neurochemistry* 84(4): 803–813.

Robertson, A., Perea, J., Tolmachova, T., Thomas, P. K., Huxley, C (2002): 'Effects of mouse strain, position of integration and tetracycline analogue on the tetracycline conditional system in transgenic mice' *Gene* 282(1-2): 65-74.

Romano, G., Suon, S., Jin, H., Donaldson, A. E., Iacovitti, L. (2005): 'Characterization of Five Evolutionary Conserved Regions of the Human Tyrosine Hydroxylase (TH) Promoter: Implications for the Engineering of a Human TH Minimal Promoter Assembled in a Self-Inactivating Lentiviral Vector System' *Journal of cellular physiology* 204(2):666-677.

Romaní-Aumedes, J., Canal, M., Martín-Flores, N., Sun, X., Pérez-Fernández, V., et al. (2014): 'Parkin loss of function contributes to RTP801 elevation and neurodegeneration in Parkinson's disease. *Cell Death and Disease* 5(8):e1364.

Rosso, P., Fioramonti, M., Fracassi, A., Marangoni, M., Taglietti, V., Siteni, S., Segatto, M. (2016): ˈAMPK in the central nervous system: physiological roles and pathological implications' *Research and Reports in Biology* 2016(7): 1-13.

Rubinsztein, D. C., Gestwicki, J. E., Murphy, L. O., Klionsky, D. J. (2007): 'Potential therapeutic applications of autophagy' *Nature Reviews Drug Discovery* 6(4): 304-312.

Sacino, A. N., Brooks, M., McGarvey, N. H., McKinney, A. B., Thomas, M. A., et al. (2013): 'Induction of CNS α-synuclein pathology by fibrillar and non-amyloidogenic recombinant α-synuclein. *Acta Neuropathologica Communications* 1: 38.

Sancak, Y., Thoreen, C. C., Peterson, T. R., Lindquist, R. A., Kang, S. A., Spooner, E., Carr, S. A., Sabatini, D. M. (2007): 'PRAS40 is an insulin-regulated inhibitor of the mTORC1 protein kinase' *Molecular Cell* 25(6): 903–915.

Sánchez-Danés, A., Richaud-Patin, Y., Carballo-Carbajal, I., Jiménez-Delgado, S., Caig, C., et al. (2012): 'Disease-specific phenotypes in dopamine neurons from human iPS-based models of genetic and sporadic Parkinson's disease' *EMBO Molecular Medicine* 4(5): 380-395.

Santoro, M., Carlomagno, F., Melillo, R.M., Fusco, A. (2004a): 'Dysfunction of the RET receptor in human cancer' *Cellular and Molecular Life Sciences* 61(23): 2954–2964.

Santoro, M., Melillo, R. M, Carlomagno, F., Vecchio, G., Fusco, A. (2004b): 'Minireview: RET: normal and abnormal functions' *Endocrinology* 145(12): 5448–5451.

Sarbassov, D. D., Ali, S. M., Kim, D. H., Guertin, D. A., Latek, R. R., Erdjument-Bromage, H., Tempst, P., Sabatini, D. M. (2004): 'Rictor, a novel binding partner of mTOR, defines a rapamycin-insensitive and raptor-independent pathway that regulates the cytoskeleton. *Current Biology* 14(14):1296–1302.

Sariola, H., and Saarma, M. (2003): 'Novel functions and signalling pathways for GDNF' *Journal of Cell Science* 116(pt 19): 3855-3862.

Sarkar, C., Basu, B., Chakroborty, D., Dasgupta, P. S., Basu, S. (2010): 'The immunoregulatory role of dopamine: an update' *Brain, Behavior, and Immunity* 24(4): 525–528.

Sarraf, S. A., Raman, M., Guarani-Pereira, V., Sowa, M. E., Huttlin, E. L., Gygi, S. P., Harper, J. W. (2013): 'Landscape of the PARKIN-dependent ubiquitylome in response to mitochondrial depolarization' *Nature* 496(7445): 372–376.

Satake, W., Nakabayashi, Y., Mizuta, I., Hirota, Y., Ito, C., et al. (2009): 'Genome-wide association study identifies common variants at four loci as genetic risk factors for Parkinson's disease' *Nature Genetics* 41(12):1303-1307.

Satoh, J., and Suzuki, K. (1990): 'Tyrosine hydroxylase-immunoreactive neurons in the mouse cerebral cortex during the postnatal period' *Developmental Brain Research* 53(1): 1-5.

Sato, H., Kato, T., Arawaka, S. (2013): 'The role of Ser129 phosphorylation of α-synuclein in neurodegeneration of Parkinson's disease: a review of in vivo models' *Reviews in Neuroscience* 24(2): 115-123.

Savitt, J. M., Jang, S. S., Mu, W., Dawson, V. L., Dawson, T. M. (2005): 'Bcl-x is required for proper development of the mouse substantia nigra' *Journal of Neuroscience* 25(29): 6721–6728.

Sauer, H., Rosenblad, C., Bjorklund, A. (1995): 'Glial cell line-derived neurotrophic factor but not transforming growth factor beta 3 prevents delayed degeneration of nigral dopaminergic neurons following striatal 6-hydroxydopamine lesion' *Proceedings of the National Academy of Sciences of the United States of America* 92(19): 8935–8939.

Schapira, A. H., Cooper, J. M., Dexter, D., Jenner, P., Clark, J.B., et al. (1989): 'Mitochondrial complex I deficiency in Parkinson's disease' *The Lancet* 1(8649): 1269.

Schimmel, J.J., Crews, L., Roffler-Tarlov, S., Chikaraishi, D.M. (1999): '4.5 kb of the rat tyrosine hydroxylase 5′ flanking sequence directs tissue specific expression during development and contains consensus sites for multiple transcription factors' *Molecular Brain Research* 74(1-2):1–14.

Schlessinger, J. (2000): 'Cell signaling by receptor tyrosine kinases' *Cell* 103(2): 211–225.

Schneider, A., Simons, M. (2013): 'Exosomes: vesicular carriers for intercellular communication in neurodegenerative disorders' *Cell and Tissue Research* 352(1):33-47.

Schönig, K., Schwenk, F., Rajewsky, K., Bujard, H. (2002): 'Stringent doxycycline dependent control of CRE recombinase in vivo' *Nucleic Acids Research* 30(23): e134.

Schrag, A., Jahanshahi, M., Quinn, N. (2000): 'How does Parkinson's disease affect quality of life? A comparison with quality of life in the general population' *Movement Disorders* 15(6):1112-1118.

Schell, H., Hasegawa, T., Neumann, M., Kahle, P. J. (2009): 'Nuclear and neuritic distribution of serine-129 phosphorylated α-synuclein in transgenic mice' *Neuroscience* 160(4): 796–804.

Schmitt, K. C., Rothman, R. B., Reith, M. E. (2013): 'Nonclassical pharmacology of the dopamine transporter: atypical inhibitors, allosteric modulators, and partial substrates' *Journal of Pharmacology and Experimental Therapeutics* 346(1): 2–10.

Schuchardt, A., D'Agati, V., Larsson-Blomberg, L., Costantini, F., Pachnis, V. (1994): 'Defects in the kidney and enteric nervous system of mice lacking the tyrosine kinase receptor Ret' *Nature* 367(6461): 380–383.

Scott, R. P. (2002): *'Signal transduction mechanisms mediated by the GDNF family ligands and receptors'* PhD thesis, Karolinska Institute, Stockholm.

Sherer, T. B., Fiske, B. K., Svendsen, C. N., Lang, A. E., Langston, J. W. (2006): 'Crossroads in GDNF therapy for Parkinson's disease' *Movement Disorders* 21(2): 136–141.

Shoshani, T., Faerman, A., Mett, I., Zelin, E., Tenne, T., et al. (2002): 'Identification of a novel hypoxia-inducible factor 1- responsive gene, RTP801, involved in apoptosis' *Molecular and Cellular Biology* 22(7): 2283–2293.

Shoptaw, S., Kintaudi, P.C., Charuvastra, C., Ling, W. (2002): 'A screening trial of amantadine as a medication for cocaine dependence' *Drug and Alcohol Dependence* 66(3):217–24.

Simón-Sánchez, J., Schulte, C., Bras, J. M., Sharma, M., Gibbs, J. R., et al. (2009): 'Genome-wide association study reveals genetic risk underlying Parkinson's disease. *Nature Genetics* 41(12):1308-1312.

Singleton, A. B., Farrer, M., Johnson, J., Singleton, A., Hague, S., et al. (2003): 'α-Synuclein locus triplication causes Parkinson's disease' *Science* 302(5646): 841.

Slaney, T. R., Mabrouk, O. S., Porter-Stransky, K. A., Aragona, B. J., Kennedy, R. T. (2013): 'Chemical gradients within brain extracellular space measured using low flowpush-pull perfusion sampling in vivo' *ACS Chemical Neuroscience* 4(2) 321–329.

Smith, W. W., Margolis, R. L., Li, X., Troncoso, J. C., Lee, M. K., Dawson, V. L., Dawson, T. M., Iwatsubo, T., Ross, C. A. (2005): 'Alpha-synuclein phosphorylation enhances eosinophilic cytoplasmic inclusion formation in SH-SY5Y cells' *The Jornal of Neuroscience* 25(23):5544–5552.

Smidt, M. P., and Burbach, J. P. (2007): 'How to make a mesodiencephalic dopaminergic neuron' *Nature Reviews Neuroscience* 8(1): 21–32.

Soares, B. G., Lima, M. S., Reisser, A. A., Farrell, M. (2001): 'Dopamine agonists for cocaine dependence' *Cochrane Database of Systematic Reviews* 2003(2):CD003352.

Sofer, A., Lei, K., Johannessen, C. M., Ellisen, L. W. (2005): 'Regulation of mTOR and cell growth in response to energy stress by REDD1' *Molecular and Cellular Biology* 25(14): 5834–5845.

Spillantini, M. G., Schmidt, M. L., Lee, V. M., Trojanowski, J. Q., Jakes, R., Goedert, M. (1997): 'Alpha-synuclein in Lewy bodies' *Nature* 388: 839–40.

Stefanis, L., and Keller, J. N. (2006): '*The Proteasome in Neurodegeneration*' inclusion formation and dissolution following proteosomal inhibition in neuronal cells. Springer.

Stefanis, L. (2012): 'α-Synuclein in Parkinson's Disease' *Cold Spring Harbor Perspectives in Medicine*, 2(2), a009399.

Stichel, C. C., Zhu, X. R., Bader, V., Linnartz, B., Schmidt, S., Lübbert, H. (2007): 'Mono- and double-mutant mouse models of Parkinson's disease display severe mitochondrial damage' *Human Molecular Genetics* 16(20): 2377-2393.

Stine, S. M., Krystal, J. H., Kosten, T. R., Charney, D. S. (1995): 'Mazindol treatment for cocaine dependence' *Drug and Alcohol Dependence* 39(3): 245–252.

Surguchov, A. (2008): 'Molecular and cellular biology of synucleins' *International Review of Cell and Molecular Biology* 270: 225-317.

Suri, C., Fung, B. P., Tischler, A. S., Chikaraishi, D. M. (1993): 'Catecholaminergic cell lines from the brain and adrenal glands of tyrosine hydroxylase-SV40 T antigen transgenic mice' *Journal of Neuroscience* 13(3): 1280-1291.

Takahashi, M., Ritz, J., Cooper, G. M. (1985): 'Activation of a novel human transforming gene, ret, by DNA rearrangement' *Cell* 42(2): 581–588.

Takahashi, M. (2001): 'The GDNF/RET signaling pathway and human diseases' *Cytokine and Growth Factor Reviews* 12(4): 361–373.

Tan, E. K., Chung, H., Zhao, Y., Shen, H., Chandran, V. R., Tan, C., Teoh, M. L., Yih, Y., Pavanni, R., Wong, M. C. (2003): 'Genetic analysis of Nurr1 haplotypes in Parkinson's disease' *Neuroscience Letters* 347(3): 139–142.

Tanaka, M., Xiao, H., Kiuchi, K. (2002): 'Heparin facilitates glial cell line-derived neurotrophic factor signal transduction' *NeuroReport* 13(15): 1913- 1916.

Tang, S. J., Reis, G., Kang, H., Gingras, A-C., Sonenberg, N., Schuman, E. M. (2002): 'A rapamycin-sensitive signaling pathway contributes to long-term synaptic plasticity in the hippocampus' *Proceedings of the National Academy of Sciences of the United States of America* 99(1): 467–472.

Tee, A. R., Manning, B. D., Roux, P. P., Cantley, L. C., Blenis, J. (2003) 'Tuberous sclerosis complex gene products, Tuberin and Hamartin, control mTOR signaling by acting as a GTPase-activating protein complex toward Rheb' *Current Biology* 13(15):1259–1268.

Teitelman, G., Gershon, M. D., Rothman, T. P., Joh, T. H., Reis, D. J. (1981): 'Proliferation and distribution of cells that transiently express a catecholaminergic phenotype during development in mice and rats' *Developmental Biology* 86(2): 348-355.

Teismann, P., Tieu, K., Cohen, O., Choi, D-K., Wu, D. C., Marks, D., Vila, M., Jackson-Lewis, V., Przedborski, S. (2003): 'Pathogenic role of glial cells in Parkinson's disease. *Movement Disorders* 18(2): 121–129.

Tereshchenko, J., Maddalena, A., Bahr, M., Kugler, S. (2014): 'Pharmacologically controlled, discontinuous GDNF gene therapy restores motor function in a rat model of Parkinson's disease' *Neurobiology of Disease* 65: 35-42.

Terzioglu, M., and Galter, D. (2008): 'Parkinson's disease: genetic versus toxin-induced rodent models' *FEBS Journal* 275(7): 1384–1391.

Thedieck, K., Polak, P., Kim, M. L., Molle, K. D., Cohen, A., Jenö, P., et al. (2007): 'PRAS40 and PRR5-like protein are new mTOR interactors that regulate apoptosis' *PLoS One* 2(11):e1217.

Thiruchelvam, M. J., Powers, J. M., Cory-Slechta, D. A., Richfield, E. K. (2004): 'Risk factors for dopaminergic neuron loss in human α-synuclein transgenic mice' *European Journal of Neuroscience* 19(4): 845–854.

Tillack, Karsten (2013): New approaches to genetically modify and visualize dopaminergic neurons in mice (Thesis) Germany: Berlin.

Tofaris, G. K., Garcia Reitbock, P., Humby, T., Lambourne, S. L., O'Connell, M., et al. (2006): 'Pathological changes in dopaminergic nerve cells of the substantia nigra and olfactory bulb in mice transgenic for truncated human alpha-synuclein (1-120): implications for Lewy body disorders' *Journal of Neuroscience* 26(15): 3942-3950.

Tofaris, G. K., and Spillantini, M. G. (2007): 'Physiological and pathological properties of alpha-synuclein' *Cellular and Molecular Life Sciences* 64(17): 2194-201.

Tomac, A., Lindqvist, E., Lin, L. F., Ogren, S. O., Young, D., Hoffer, B. J., Olson, L. (1995): 'Protection and repair of the nigrostriatal dopaminergic system by GDNF in vivo' *Nature* 373(6512): 335–339.

Treanor, J. J., Goodman, L., de Sauvage, F., Stone, D. M., Poulsen, K. T., et al. (1996): 'Characterization of a multicomponent receptor for GDNF' *Nature* 382(6586): 80-83.

Trupp, M., Arenas, E., Fainzilber, M., Nilsson, A. S., Sieber, B. A., Grigoriou, M., Kilkenny, C., Salazar-Grueso, E., Pachnis, V., Arumäe, U. (1996): 'Functional receptor f or GDNF encoded by the c-ret proto- oncogene' *Nature* 381(6585): 785-789.

Trupp, M., Belluardo, N., Funakoshi, H., Ibañéz, C. F. (1997): 'Complementary and overlapping expression of glial cell line-derived neurotrophic factor (GDNF), cret proto-oncogene, and gdnf receptor-alpha indicates multiple mechanisms of trophic actons in the adult rat CNS' *Journal of Neuroscience* 17(10): 3554-3567.

Tsui-Pierchala, B. A., Ahrens, R. C., Crowder, R. J., Milbrandt, J. Johnson, E. M., Jr (2002a): 'The long and short isoforms of RET function as independent signaling complexes' *Journal of Biological Chemistry* 277(37): 34618-34625.

Tsui-Pierchala, B. A., Milbrandt, J. Johnson, E. M. (2002b): 'NGF utilizes c-RET via a novel GFL-independent, inter-RTK signaling mechanism to maintain the trophic status of mature sympathetic neurons' *Neuron* 33(2): 261-273.

Uéda, K., Fukushima, H., Masliah, E., Xia, Y., Iwai, A., Yoshimoto, M., Otero, D. A., Kondo, J., Ihara, Y., Saitoh, T. (1993): 'Molecular cloning of cDNA encoding an unrecognized component of amyloid in Alzheimer disease' *Proceedings of the National Academy of Sciences of the United States of America* 90(23): 11282–11286.

Ulusoy, A., Rusconi, R., Pérez-Revuelta, B. I., Musgrove, R. E., Helwig, M., Winzen-Reichert, B., Di Monte, A. D. (2013): 'Caudo-rostral brain spreading of α-synuclein through vagal connections' *EMBO Molecular Medicine* 5(7): 1051–1059.

Ulusoy, A., Musgrove, R. E., Rusconi, R., Klinkenberg, M., Helwig, M., Schneider, A., Di Monte, D. A. (2015): 'Neuron-to-neuron α-synuclein propagation *in vivo* is independent of neuronal injury' *Acta Neuropathologica Communications*, 3: 13.

Ungless, M. A., and Grace, A. A. (2012): 'Are you or aren't you? Challenges associated with physiologically identifying dopamine neurons' *Trends in Neurosciences* 35(7): 422–430.

Urlinger, S., Baron, U., Thellmann, M., Hasan, M. T., Bujard, H., Hillen, W. (2000): 'Exploring the sequence space for tetracycline-dependent transcriptional activators: Novel mutations yield

expanded range and sensitivity' *Proceedings of the National Academy of Sciences of the United States of America*, 97(14): 7963–7968.

Valente, E. M., Brancati, F., Caputo, V., Graham, E. A., Davis, M. B., et al. (2002): 'PARK6 is a common cause of familial parkinsonism' *Neurological Sciences* 23(Suppl 2): 117–118.

Valente, E. M., Abou-Sleiman, P. M., Caputo, V., Muqit, M. M., Harvey, K., et al. (2004): 'Hereditary early-onset Parkinson's disease caused by mutations in PINK1' *Science* 304(5674): 1158–1160.

Vander Haar, E., Lee, S. I., Bandhakavi, S., Griffin, T. J., Kim, D. H. (2007): 'Insulin signalling to mTOR mediated by the Akt/PKB substrate PRAS40' *Nature Cell Biology* 9(3): 316–323.

Van Rompuy, A.-S., Oliveras-Salvá, M., Van der Perren, A., Corti, O., Van den Haute, C., & Baekelandt, V. (2015): 'Nigral overexpression of alpha-synuclein in the absence of parkin enhances alpha-synuclein phosphorylation but does not modulate dopaminergic neurodegeneration' *Molecular Neurodegeneration* 10: 23.

Vila, M., Vukosavic, S., Jackson-Lewis, V., Neystat, M., Jakowec, M., Przedborski, S. (2000): 'α-Synuclein up-regulation in substantia nigra dopaminergic neurons following administration of the parkinsonian toxin MPTP' *Journal of Neurochemistry* 74(2): 721–729.

Visanji, N. P., Brooks, P. L., Hazrati, L.-N., Lang, A. E. (2013): 'The prion hypothesis in Parkinson's disease: Braak to the future' *Acta Neuropathologica Communications* 1: 2.

Volakakis, N., Tiklova, K., Decressac, M., Papathanou, M., Mattsson, B., Gillberg, L., Nobre, A., Björklund, A., Perlmann, T. (2005): 'Nurr1 and Retinoid X Receptor Ligands Stimulate Ret Signaling in Dopamine Neurons and Can Alleviate α-Synuclein Disrupted Gene Expression' *The Journal of Neuroscience* 35(42): 14370 –14385.

Volkow, N. D., Fowler, J. S., Wang, G. J., Goldstein, R. Z. (2002): 'Role of dopamine, the frontal cortex and memory circuits in drug addiction: insight from imaging studies' *Neurobiology of Learning and Memory* 78(3):610–624.

Volman, S. F., Lammel, S., Margolis, E. B., Kim, Y., Richard, J. M., Roitman, M. F. Lobo, M. K. (2013): 'New insights into the specificity and plasticity of reward and aversion encoding in the mesolimbic system' *Journal of Neurosciences* 33(45): 17569–17576.

von Coelln, R., Thomas, B., Andrabi, S. A., Lim, K. L., Savitt, J. M., Saffary, R., Stirling, W., Bruno, K., Hess, E. J., Lee, M. K., Dawson, V. L., Dawson, T. M. (2006): 'Inclusion body formation and neurodegeneration are parkin independent in a mouse model of alpha-synucleinopathy' *Journal of Neuroscience* 26(14):3685-96.

Wakamatsu, M., Ishii, A., Iwata, S., Sakagami, J., Ukai, Y., et al. (2008): 'Selective loss of nigral dopamine neurons induced by overexpression of truncated human alpha-synuclein in mice' *Neurobiology of Aging* 29(4): 574-585.

Waldmeier, P., Bozyczko-Coyne, D., Williams, M., Vaught, J. L. (2006): 'Recent clinical failures in Parkinson's disease with apoptosis inhibitors underline the need for a paradigm shift in drug discovery for neurodegenerative diseases' *Biochemical Pharmacology* 72(10): 1197–1206.

Walker, D. G., Lue, L. F., Adler, C. H., Shill, H. A., Caviness, J. N. et al. (2013): 'Changes in Properties of Serine 129 Phosphorylated α-Synuclein with Progression of Lewy Type Histopathology in Human Brains' *Experimental neurology* 240:190-204.

Wallén, A. A., Castro, D. S., Zetterström, R. H., Karlén, M., Olson, L., Ericson, J., Perlmann, T. (2001): 'Orphan nuclear receptor Nurr1 is essential for Ret expression in midbra dopamine neurons and in the brain stem' *Molecular and Cellular Neuroscience* 18(6): 649–663.

Wang, Z., Benoit, G., Liu, J., Prasad, S., Aarnisalo, P., Liu, X., Xu, H., Walker, N. P., Perlmann, T. (2003): 'Structure and function of Nurr1 identifies a class of ligand-independent nuclear receptors' *Nature* 423(6939): 555–560.

Wang, Y., Shi, M., Chung, K. A., Zabetian, C. P., Leverenz, J. B. et al. (2012): 'Phosphorylated α-Synuclein in Parkinson's Disease'. *Science Translational Medicine* 4(121):121ra20.

Wang, X. (2013): 'Structural studies of GDNF family ligands with their receptors—Insights into ligand recognition and activation of receptor tyrosine kinase RET' *Biochimica et Biophysica Acta* 1834(10): 2205–2212.

Watanabe, Y., Tatebe, H., Taguchi, K., Endo, Y., Tokuda, T., Mizuno, T., Nakagawa, M., Tanaka, M. (2012): 'p62/SQSTM1-Dependent Autophagy of Lewy Body-Like α-Synuclein Inclusions' *PLoS ONE* 7(12): e52868.

Wauer, T., Simicek, M., Schubert, A., Komander, D. (2015): 'Mechanism of phospho-ubiquitin-induced PARKIN activation' *Nature* 524(7565): 370–374.

Weber, K., Thomaschewski, M., Warlich, M., Volz, T., Cornils, K., Niebuhr, B., Täger, M., Lütgehetmann, M., Pollok, J.M., Stocking, C., Dandri, M., Benten, D., Fehse, B. (2011): 'RGB marking facilitates multicolor clonal cell tracking' *Nature Medicine* 17(4):504–509.

Weissleder, R. (2001): 'A clearer vision for in vivo imaging' *Nature Biotechnology* 19(4):316–317.

Weissman, T. A., & Pan, Y. A. (2015): 'Brainbow: New Resources and Emerging Biological Applications for Multicolor Genetic Labeling and Analysis' *Genetics* 199(2): 293–306.

Whetten-Goldstein, K., Sloan, F., Kulas, E., Cutson, T., Schenkman, M. (1997): 'The burden of Parkinson's disease on society, family, and the individual' *Journal of American Geriatrics Society* 45(7): 844–849.

Wild, P., Farhan, H., McEwan, D. G., Wagner, S., Rogov, V. V., Brady, N. R., Richter, B., Korac, J., Waidmann, O., Choudhary, C., et al. (2011): 'Phosphorylation of the autophagy receptor optineurin restricts Salmonella growth' *Science* 333(6039): 228–233.

Winslow, A. R., Chen, C. W., Corrochano, S., Acevedo-Arozena, A., Gordon, D. E., Peden, A. A., Lichtenberg, M., Menzies, F. M., Ravikumar, B., Imarisio, S., Brown, S., O'Kane, C. J., Rubinsztein, D. C. (2010): 'α-Synuclein impairs macroautophagy: implications for Parkinson's disease' *The Journal of Cell Biology* 190(6): 1023–1037.

Winslow, A. R., Rubinsztein, D. C. (2011): 'The Parkinson disease protein α-synuclein inhibits autophagy' *Autophagy*. 7(4):429-431.

Withers, G. S., George, J. M., Banker, G. A., Clayton, D. F. (1997): 'Delayed localization of synelfin (synuclein, NACP) to presynaptic terminals in cultured rat hippocampal neurons' *Developmental Brain Research* 99(1): 87–94.

Xie, W., Chow, L. T., Paterson, A. J., Chin, E., Kudlow, J. E. (1999): 'Conditional expression of the ErbB2 oncogene elicits reversible hyperplasia in stratified epithelia and up-regulation of TGFalpha expression in transgenic mice' *Oncogene* 18(24): 3593–3607.

Yamada, M., Mizuno, Y., Mochizuki, H. (2005): 'Parkin gene therapy for alpha-synucleinopathy: a rat model of Parkinson's disease' *Human genetic therapy* 16(2): 262-270.

Yang, Q., Inoki, K., Ikenoue, T., Guan, K. L. (2006): 'Identification of Sin1 as an essential TORC2 component required for complex formation and kinase activity' *Genes and Development* 20(20):2820–2832.

Yang, L., Beal, M. F. (2011): 'Determination of neurotransmitter levels in models of Parkinson's disease by HPLC-ECD' *Methods in Molecular Biology* 793: 401-415.

Yao, S. C., Hart, A. D., Terzella, M. J. (2013): 'An evidence-based osteopathic approach to Parkinson disease' *Osteopathic Family Physician* 5(3): 96–101.

Yasuda, T., Hayakawa, H., Nihira, T., Ren, Y. R., Nakata, Y., Nagai, M., Hattori, N., Miyake, K., Takada, M., Shimada, T., Mizuno, Y., Mochizuki, H. (2011): 'Parkin-mediated protection of dopaminergic neurons in a chronic MPTP-minipump mouse model of Parkinson disease' *Journal of Neuropathology and Experimental Neurology* 70(8): 686–697.

Yasuda, T., Nakata, Y., Mochizuki, H. (2013): 'α-Synuclein and Neuronal Cell Death' *Molecular Neurobiology 47*(2): 466–483.

Yavich, L., Tanila, H., Vepsäläinen, S., Jäkälä, P. (2004): 'Role of α-Synuclein in Presynaptic Dopamine Recruitment' *Journal of Neuroscience* 24(49):11165–11170.

Ylikoski, J., Pirvola, K., Virkkala, J., Suvanto, P., Liang, X.-Q., Magal, E., Altschuler, R., Miller, J. M., Saarma, M. (1998): 'Guinea pig auditory neurons are protected by glial cell line-derived growth factor from degeneration after noise trauma' *Hearing Research* 124(1-2): 17-26.

Zarranz, J. J., Alegre, J., Gómez-Esteban, J. C., Lezcano, E., Ros, R, et al. (2004): 'The new mutation, E46K, of alpha-synuclein causes Parkinson and Lewy body dementia' *Annals of Neurology* 55(2):164-173.

Zetterström, R. H., Solomin, L., Jansson, L., Hoffer, B. J., Olson, L., Perlmann, T. (1997): 'Dopamine neuron agenesis in Nurr1-deficient mice' *Science* 276(5310): 248–250.

Zhou, Q. Y., and Palmiter, R. D. (1995): 'Dopamine-deficient mice are severely hypoactive, adipsic, and aphagic' *Cell* 83(7):1197–1209.

Zhou, X., Vink, M., Klaver, B., Berkhout, B., Das, A. T. (2006): 'Optimization of the Tet-On system for regulated gene expression through viral evolution' *Gene Theraoy* 13(19):1382-1390.

Zhu, P., Aller, M. I., Baron, U., Cambridge, S., Bausen, M., et al. (2007): 'Silencing and Un-silencing of Tetracycline-Controlled Genes in Neurons' *PLoS ONE* 2(6): e533.

Zuo, T., Qin, J. Y., Chen, J., Shi, Z., Liu, M., Gao, X. Gao, D. (2013): 'Involvement of N-cadherin in the protective effect of glial cell line-derived neurotrophic factor on dopaminergic neuron damage' *International Journal of Molecular Medicine* 31(3): 561-568.

Appendices

Abbreviations

AA	Amino acid
AAAH	Aromatic amino acid hydroxylase
AADC	L-amino acid decarboxylase
AAV	Adeno-associated virus
ALDH	Aldehyde dehydrogenase
AMP	Adenosine monophosphate
AMPK	AMP-activated protein kinase
AR	Autosomal recessive
ARTN	Artemin
ATG9A	Autophagy Related 9A
ATP	Adenosine triphosphate
BLI	Bioluminescence imaging
BSA	Bovine serum albumin
CA	Catecholaminergic
Ca2+	Calcium
CBA	Chicken-β-actin/CMV-minimal fusion promoter
CLD	Cadherin-like domain
CNS	Central nervous system
COMT	Catechol-O-methyl transferase
DA	Dopaminergic
DAB	Di-amino-benzidine
DAT	Dopamine transporter
DMSO	Dimethyl sulfoxide
DNA	Deoxy ribose nucleic acid
dNTP	Deoxyribonucleotide triphosphate
DOPAC	3,4-Dihydroxyphenylacetic acid
DOPAL	3,4-dihydroxyphenylacetaldehyde
Dox	Doxycycline
dt	Dorsal tier
DT-A	Diphtheria toxin-A
E.Coli	Escherichia Coli
ECD	Extra Cellular Domain

ECL	Enhanced chemiluminescence
ECM	Extracellular matrix
EDTA	Ethylenediaminetetraacetic acid
e.g.	Example given
EGTA	Ethylene glycol tetraacetic acid
ER	Estrogen receptor
ERK	Extracellular signal-regulated kinases
et al.	And others
FGF8	Fibroblast growth factor 8
GDNF	Glial cell line-derived neurotrophic factor
GFAP	Glial fibrillary acidic protein
GFLs	Glial cell line-derived neurotrophic factor family ligands
GFP	Green fluorescent protein
GFRα	GDNF family receptor-α
GIRK2	G protein-activated inward rectifier potassium channel 2
GPI	Glycosyl phosphatidylinositol
h α-synuclein	human α-synuclein
hCMV	human cytomegalovirus
Hsc-70	heat shock cognate 70
HPLC	High-performance liquid chromatography
HRP	Horse radish peroxidase
HVA	Homovanillic acid
Iba1	Inonized calcium binding adaptor protein 1
KDa	Kilodalton(s)
ko	Knockout
LAMP2A	Lysosome-associated membrane protein 2
LB	Lewy Body
LC	Locus Coeruleus
LC3	Microtubule-associated protein light chain 3
L-DOPA	L-3,4-dihydroxyphenylalanine
Lmx1	LIM homeobox transcription factor 1
LN	Lewy neurites
LRRK2	Leucine-rich repeat kinase 2
MAO	Monoamine oxidase
MAPK	Mitogen-activated protein kinase
MEN2	Multiple endocrine neoplasia 2
mDA	Midbrain dopaminergic

min	Minute(s)
MPP	1-methyl-4-phenylpyridinium
MPTP	1-Methyl-4-Phenyl-1,2,3,6-Tetrahydropyridine
mRNA	Messenger ribonucleic acid
mTOR	mammalian target of rapamycin
3-MT	3-methoxytyramine
NA	Noradrenergic
NCAM	Neural cell adhesion molecule
N-Cadherin	neuronales Cadherin
NDUF10	NADH:ubiquinone oxidoreductase subunit 10
NDUFB8	NADH:ubiquinone oxidoreductase subunit B8
NE	Norepinephrine
NGF	Nerve growth factor
NMDA	N-methyl-D-aspartate receptor
NRTN	Neurturin
n.s.	Non-significant (p>0.05, Student's t-test)
NT	Neurotrophin
Nurr1	Nuclear receptor-related 1
6-OHDA	6-hydroxydopamine
OPTN	Optineurin
PBS	Phosphate buffered saline
PCR	Polymerase chain reaction
PD	Parkinson's disease
PFA	Paraformaldehyde
PDVF	Polyvinylidenfluorid
pH	Potential hydrogen
PI3K	Phosphoinositide-3 kinase
PINK1	PTEN homolog-induced putative kinase 1
Pitx3	Paired-like homeodomain transcription factor 3
PSPN	Persephin
PTEN	Phosphatase and tensin homolog
R26R	ROSA 26 Locus
rAAV	Recombinant adeno-associated virus
Rac	Ras-related C3 botulinum toxin substrate
Ret	Rearranged during transfection
RGB	Red Green Blue
ROS	Reactive oxygen species

RRF	retrorubral field
RTK	Receptor tyrosine kinase
RXR	retinoid X receptor
SDS-PAGE	Sodium dodecyl sulfate polyacrylamide gel electrophoresis
Shh	Sonic hedgehog
SNARE	soluble N-ethylmaleimide-sensitive-factor attachment receptor
SN	Substantia nigra
SNpc	Substantia nigra pars compacta
SZ	Schizophrenia
TAE buffer	Tris/Acetic acid/EDTA buffer
TBS	Tris buffered saline
TBS-T	Tris-Buffered Saline and Tween 20
Tet-system	Tetracycline-regulated system
Tet-OFF	Tetracycline-regulated OFF
Tet-ON	Tetracycline-regulated ON
TetR	Tet repressor protein
TFP	Teal fluorescence protein
TGF	Transforming growth factor
TH	Tyrosine hydroxylase
Thy	Thymocyte differentiation antigen
T_m	Melting temperature
TRE	tTA responsive promoter element
TOM	translocase of outer membrane
(r)tTA	(reverse) tetracycline controlled transactivator protein
VMAT	Vesicular monoamine transporter
VAMP2	Vesicle-associated membrane protein 2
vg	viral genomes
vt	ventral tier
VTA	Ventral tegmental area
WPRE	woodchuck hepatitis post-transcriptional regulatory element
wt	Wild type
6-OHDA	6-hydroxydopamine
ºC	Degree centigrade
μ	Micro
%	Percent
Δ	Truncated

List of Figures

Introduction

Results

List of Tables

Matherials

Methods

An Efficient and Versatile System for Visualization and Genetic Modification of Dopaminergic Neurons in Transgenic Mice

Karsten Tillack[☯]**, Helia Aboutalebi**[☯]**, Edgar R. Kramer***

Development and Maintenance of the Nervous System, Center for Molecular Neurobiology, University Medical Center Hamburg-Eppendorf, Hamburg, Germany

☯ These authors contributed equally to this work.
* kramer@zmnh.uni-hamburg.de

Abstract

Background & Aims

The brain dopaminergic (DA) system is involved in fine tuning many behaviors and several human diseases are associated with pathological alterations of the DA system such as Parkinson's disease (PD) and drug addiction. Because of its complex network integration, detailed analyses of physiological and pathophysiological conditions are only possible in a whole organism with a sophisticated tool box for visualization and functional modification.

Methods & Results

Here, we have generated transgenic mice expressing the tetracycline-regulated transactivator (tTA) or the reverse tetracycline-regulated transactivator (rtTA) under control of the tyrosine hydroxylase (TH) promoter, TH-tTA (tet-OFF) and TH-rtTA (tet-ON) mice, to visualize and genetically modify DA neurons. We show their tight regulation and efficient use to overexpress proteins under the control of tet-responsive elements or to delete genes of interest with tet-responsive Cre. In combination with mice encoding tet-responsive luciferase, we visualized the DA system in living mice progressively over time.

Conclusion

These experiments establish TH-tTA and TH-rtTA mice as a powerful tool to generate and monitor mouse models for DA system diseases.

Introduction

The DA system in the brain is essential for mental and physical health as it controls many basic processes including movement, memory, motivation and emotion. Alterations in the DA system can lead to diseases such as Parkinson's disease, schizophrenia, attention-deficit

hyperactivity disorder and drug addiction [1]. The ability to temporarily regulate gene expression in DA neurons would greatly advance the field since it would allow the separation of developmental and adult gene functions, the induction of genetically neurodegenerative, neuroprotective or regenerative processes, and the labelling and monitoring of DA neurons over time during development and aging.

In the last decade several Cre expressing mice have been generated to delete genes of interest in DA neurons using promoters of different genes. They include genes such as TH [2–4], the first and rate-limiting enzyme for dopamine synthesis and highly expressed in DA neurons from early embryonic day 9–10 onwards throughout life [5], dopamine transporter (DAT) [6–10], required for dopamine re-uptake into DA neurons and expressed from embryonic day 9, and Pitx3 [11], a transcription factor involved in DA neurons differentiation. Moreover, even mice with estrogen-regulated Cre under the control of the DAT [12], Pitx-3 [13], or TH promoter [14] were generated for temporarily controlled gene deletions. In these mice, Cre recombinase is fused to a truncated estrogen receptor (CreER) and Cre activation can be regulated with the estrogen receptor antagonist, tamoxifen, which enables translocation of CreER into the nucleus where it can trigger recombination [15]. However, the use of the CreER system is frequently hampered by leakiness, female infertility during tamoxifen treatment, and unexpected toxicity of tamoxifen in the presence of the CreER construct [15–18]. In addition, Cre-mediated recombination is an irreversible event, allowing one to switch genes of interest on or off only once, which prevents switching back and forth between the on and off state.

To overcome this limitation, we established transgenic mice using the tet-system [19, 20] that expresses the tetracycline-dependent transactivator (tTA) or the reverse tetracycline-dependent transactivator (rtTA) under control of mouse TH gene promoter elements. In the tet-OFF system, tTA binds and activates the associated tetO promoter in the absence of tetracycline or its derivative doxycycline (DOX). In the tet-ON mice, rtTA binds and activates the tetO promoter in the presence of DOX. Here, we show that in TH-tTA and TH-rtTA mice, tTA and rtTA are expressed in the midbrain DA system and their activity is tightly regulated by DOX. We used these mice to genetically delete DA neurons and to detect and continuously monitor changes of the DA system over time in living mice. These experiments establish TH-tTA and TH-rtTA mice as an excellent tool for genetically modulating and visualizing the DA system in mice.

Materials and Methods

Transgenic mice

All procedures were performed in accordance with the German and European Animal Welfare Act and approved by the Hamburg State Authority for Health and Consumer Protection (BGV Hamburg, license 31/11; 28/12). All surgery was performed under anesthesia, and all efforts were made to minimize suffering. To obtain tissue for histology, mice were anesthetized by intraperitoneal injection of Ketamine (240mg/kg) and Xylazine (30mg/kg) and subsequently transcardially perfused with buffer and fixative. For stereotactic injection and *in vivo* imaging, isoflurane anesthesia was used in combination with buprenorphine (0,05mg/kg) and carprofen (5mg/kg) analgesia for the stereotactic injection. Surgical anesthesia was ensured by the absence of any nociceptive responses to tail and toe-pinching. Mice not needed for histology were sacrificed by cervical dislocation.

Mice were housed under constant conditions at 22°C and 40–50% humidity in a 12 h light/dark cycle with free access to food and water. Doxycycline (DOX) was administered to mice with the drinking water (2 mg ml-1) plus 5% sucrose or food pellets (200 mg kg-1).

To generate the TH-tTA mice, the tTA2S encoding sequence from pUHT61-1 was cloned by PCR downstream of a 8.9 kilobase mouse TH promoter fragment in pBS-SK(-)-TH-Cre (W. Wurst, Helmholtz Center Munich, Germany) digested with SmaI and XbaI to linearize the vector and to release the Cre coding sequence (Fig 1, S1 Fig). To generate the TH-rtTA mice, rtTA3G was PCR cloned from pUC57 (GenScript USA Inc.) with primers encoding restriction sites for XmaI at the ends and cloned into XmaI digested pBS-TH-tTA2S to release tTA2S. TH-tTA2S and TH-rtTA3G expression cassettes were released from the pBS vector backbone by SalI digestion and purified by agarose DNA gel electrophoresis for pronucleus injection into C57BL/6JxCBA F1 hybrid zygotes. Positive founders were identified by PCR genotyping using the following primers: gTH2f- AGAACTCGGGACCACCAGCTTG, gTH2r- CACTTTAGCC CCGTCGCGATG and backcrossed to C57BL6 mice. Depending on the founder, the TH-tTA and TH-rtTA mice can be officially called C57BL/6-Tg(TH-tTA2S)1 to 4 and C57BL/6-Tg (TH-rtTA3G)1 to 5, respectively.

LC1 mice [21], Rosa26R reporter mice [22] and ROSA26-dt-a mice [23] were described previously (Figs 1–6).

Stereotactic injections of recombinant AAV vectors

The pAAV-tetO-Venus vector was generated by PCR amplification of the tetO sequence fused with the cytomegalovirus (CMV) minimal promoter from pUHD10-3 [24] with primers encoding restriction sites for XbaI 5' and NheI 3'. The PCR product was cloned into pAAV-hsyn1-Venus [25] substituting the synapsin promoter sequence with the tetO promoter after XbaI and NheI digestion (Fig 2). The AAV-LSL-mcherry DNA using the cytomegalovirus enhancer/chicken beta actin (CBA) promoter was published previously [26].

Before recombinant AAV production, inverted terminal repeat sequences of all rAAV vectors were checked by SmaI digestion. The production of rAAV2/5 vectors was conducted at the Vector Core Facility of the UKE using standard protocols. Typical titers used for *in vivo* transductions in this study were 10^{13} vg ml-1. For substantia nigra injections, glass pipettes were used attached to a 10 µl syringe and an automatic pump at coordinates: bregma: -3.15 mm, lateral: 1.2 mm, ventral: 4.2 mm. A volume of 1 µl virus solution was injected at a rate of 0.2 µl per minute. Injection pipette was left in place for additional 5 minutes before retraction. Adult mice (2–12 months) were maintained after stereotactic injection with the AAV vectors in the ON state for the indicated time points (5 weeks in Fig 2 and 1 to 6 weeks in Fig 4) before fluorescent protein expression was investigated. Some TH-tTA/LC1 mice were treated with DOX-containing food after stereotactic injection as indicated (see Fig 4).

Histological and immunohistochemical stainings

Mouse brain tissue processing and stainings were conducted as described before [27]. A mouse anti-TH antibody (1:1000; Acris #22941) was used for immunostaining of DA neurons. DAB stainings were mounted in aqueous mounting medium and fluorescent stainings or transgenic sections were mounted in anti-fading reagent (Fluoromount G).

To stain for β-galactosidase activity, sections were first incubated in 0.5% EGTA (v/v), 20 mM MgCl$_2$ solution in PBS at room temperature for 15 min and subsequently washed 3 times in washing buffer (2.5 mM MgCl$_2$, 0.02% (v/v) Tween 20 in PBS) for 10 min each at room temperature. Sections were stained in X-gal solution in the dark at 37°C for 1 to 24 h depending on the level of β-galactosidase activity. The chromatic reaction was stopped by incubation in 4% PFA on ice for 10 min, followed by washing 3 times in PBS for 10 min at room temperature. Sections were mounted in aqueous mounting medium.
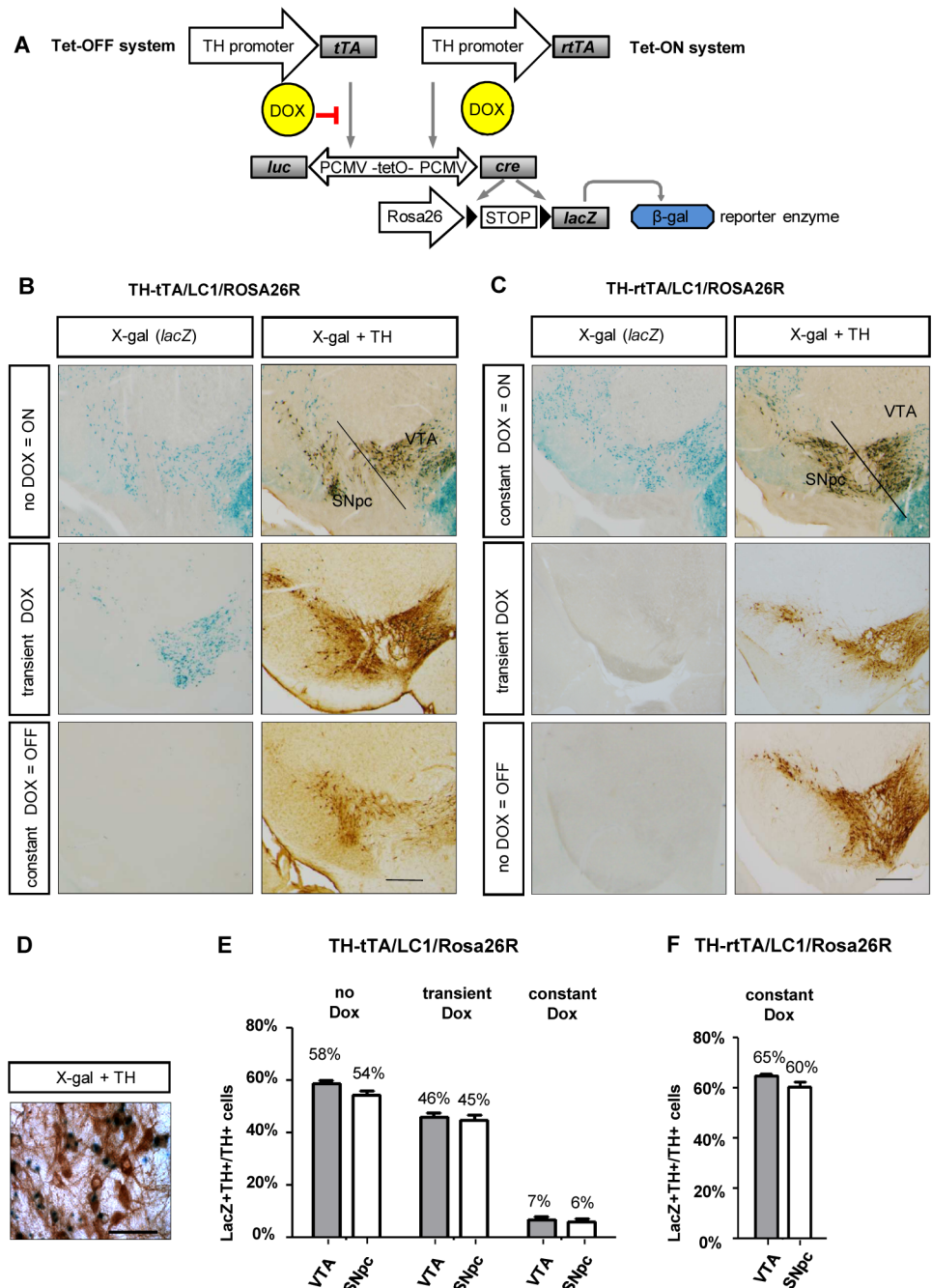
Fig 1. Specificity, inducibility and efficacy of gene expression in TH-tTA/LC1/Rosa26R and TH-rtTA/ LC1/Rosa26R mice. (A) Genetic scheme of DOX-regulated reporter gene expression in TH-tTA and TH-rtTA mice crossed with LC1 and Rosa26R reporter mice. **(B and C)** Coronal midbrain brain sections with substantia nigra pars compacta (SNpc) and ventral tegmental area (VTA) DA neurons of TH-tTA/LC1/ Rosa26R (B) and TH-rtTA/LC1/Rosa26R (C) mice raised with or without doxycycline (DOX) or transiently with DOX to have the system switched off during development (TH-tTA mice treated with DOX during pre- and postnatal development till 6 weeks of age; TH-rtTA mice raised without DOX) and on during analysis (TH- tTA mice from the age of 6 weeks without DOX; TH-rtTA mice from the age of 6 weeks with DOX). Sections were stained for β-galactosidase activity with X-gal to visualize cells with activated tet-system. Adjacent sections were X-gal stained and co-stained with tyrosine hydroxylase (TH) antibodies and DAB substrate (brown) to mark DA neurons. **(D)** Zoom in picture of TH and lacZ double positive cells in the SNpc. **(E and F)** Quantification of TH and lacZ double positive cells (LacZ+TH+) in the SNpc and VTA to estimate recombination efficacy in DA neurons (TH+) of animals treated constantly (constant DOX), transiently

(transient DOX) or without DOX (no DOX) in the tet-OFF (E) and tet-ON mice (F). mean + s.e.m.; n = 3. Scale bars: 500 μm (B and C), 50 μm (D).
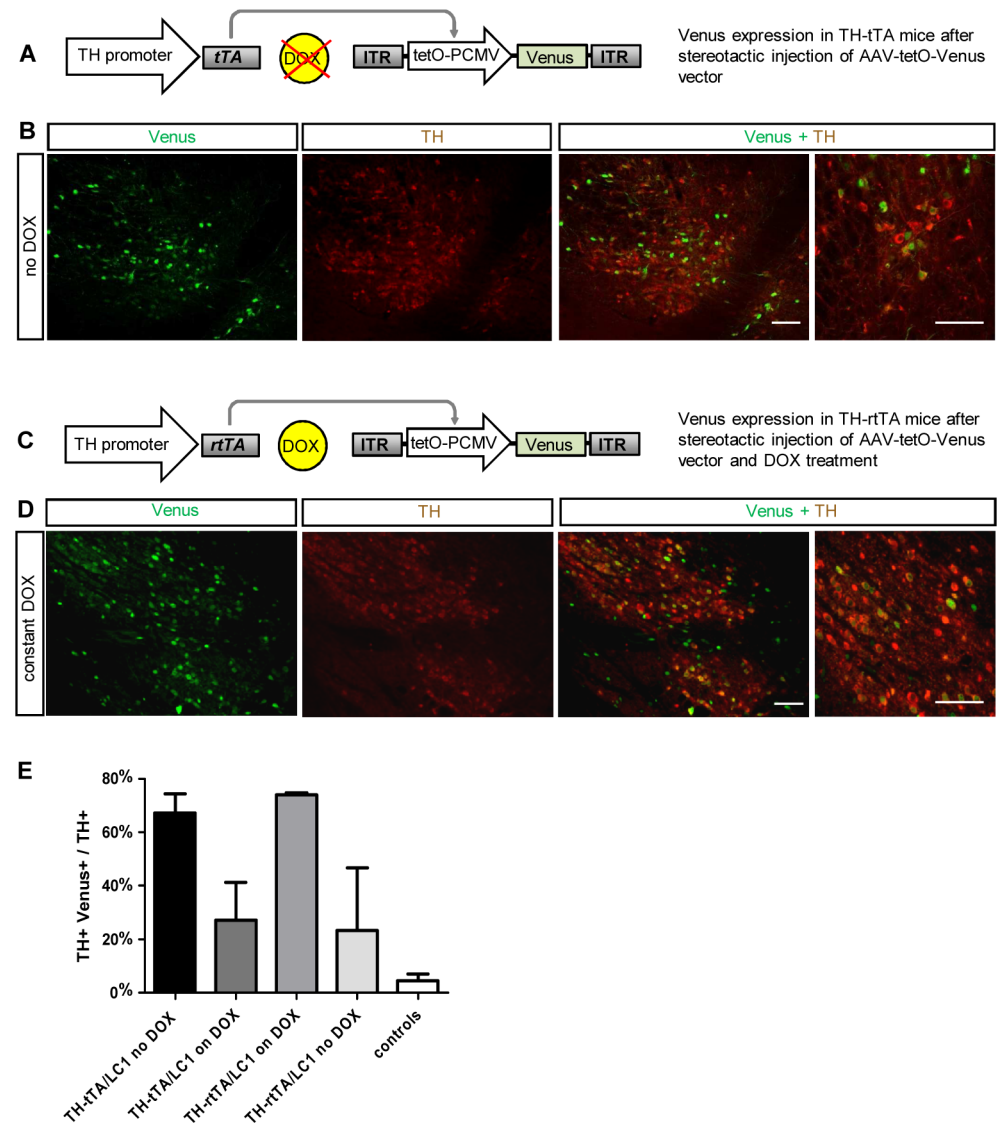
Fig 2. Cre independent adult gene expression in DA neurons of TH-tTA and TH-rtTA mice using a AAV-tetO-Venus vector. (A) Scheme of fluorescent DA neuron labelling in non-DOX treated TH-tTA mice stereotactically injected with AAV-tetO-Venus vector in the ventral midbrain. **(B)** Confocal fluorescent pictures of Venus expression (green) in DA neurons co-stained for tyrosine hydroxylase (TH; red) in the substantia nigra pars compacta (SNpc) of sagittal TH-tTA mouse brain sections. **(C)** Scheme of fluorescent DA neuron labeling in DOX-treated TH-rtTA mice stereotactically injected with AAV-tetO-Venus vector in the ventral midbrain. **(C)** Scheme of fluorescent DA neuron labelling in DOX-treated TH-rtTA mice stereotactically injected with AAV-tetO-Venus vector in the ventral midbrain. **(D)** Confocal fluorescent pictures of Venus expression in DA neurons co-stained for TH in the substantia nigra pars compacta (SNpc) of sagittal TH-rtTA mouse brain sections. **(E)** Quantification reveals that in the ON-state 67% and 73% and in the OFF-state 27% and 23% of TH+ cells are also Venus-positive in TH-tTA and TH-rtTA mice, respectively. In non-transgenic mice (controls) only 5% of TH+ cells were also Venus-positive. n = 3–5. Scale bars: 250 μm and in high magnification picture 50 μm.
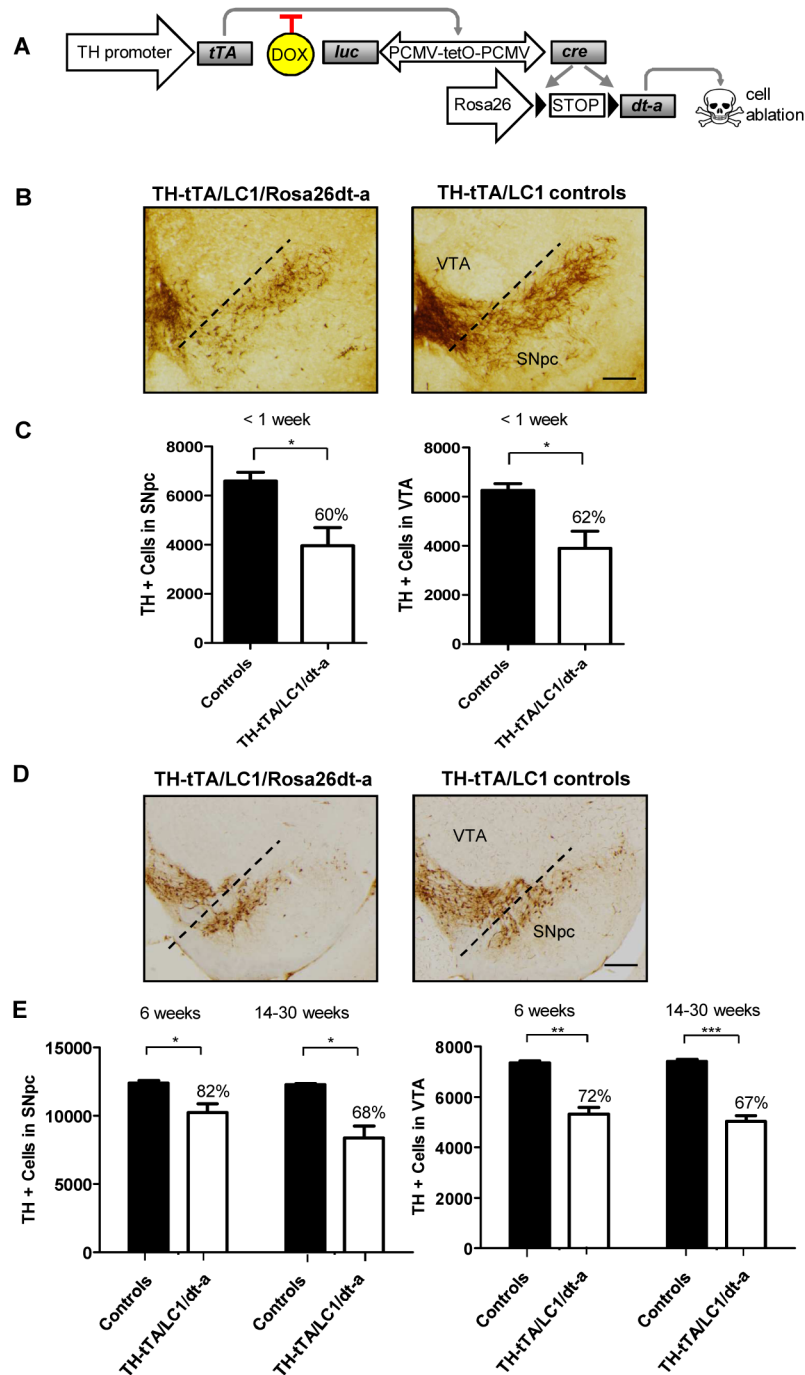
Fig 3. Loss of DA neurons in newborn and adult TH-tTA/LC1/Rosa26dt-a mice. (A) Scheme of diphteria toxin-a (dt-a) expression in TH-tTA/LC1/Rosa26dt-a mice. (B) Coronal midbrain sections of newborn TH-tTA/LC1/Rosa26dt-a mice and control mice, both stained for tyrosine hydroxylase (TH) to visualize DA neurons of the substantia nigra pars compacta (SNpc) and ventral tegmental area (VTA). No DOX was applied. Scale bar = 50 μm. (C) Stereological quantification of TH-positive cells in the SNpc and VTA of newborn TH-tTA/LC1/Rosa26dt-a and control mice without DOX treatment. (D) TH stained coronal midbrain sections of adult TH-tTA/LC1/Rosa26dt-a mice and control mice raised with DOX until 6 weeks of age followed by 30 weeks without DOX. Scale bar = 500 μm. (E) Stereological quantification of TH-positive cells in the SNpc and VTA of adult TH-tTA/LC1/Rosa26dt-a and control mice raised with DOX until 6 weeks of age followed by 6 or 14–30 weeks without DOX. mean + SEM, *p < 0.05, **p < 0.01, ***p < 0.001 Student´s t-test, n = 3.

doi:10.1371/journal.pone.0136203.g003
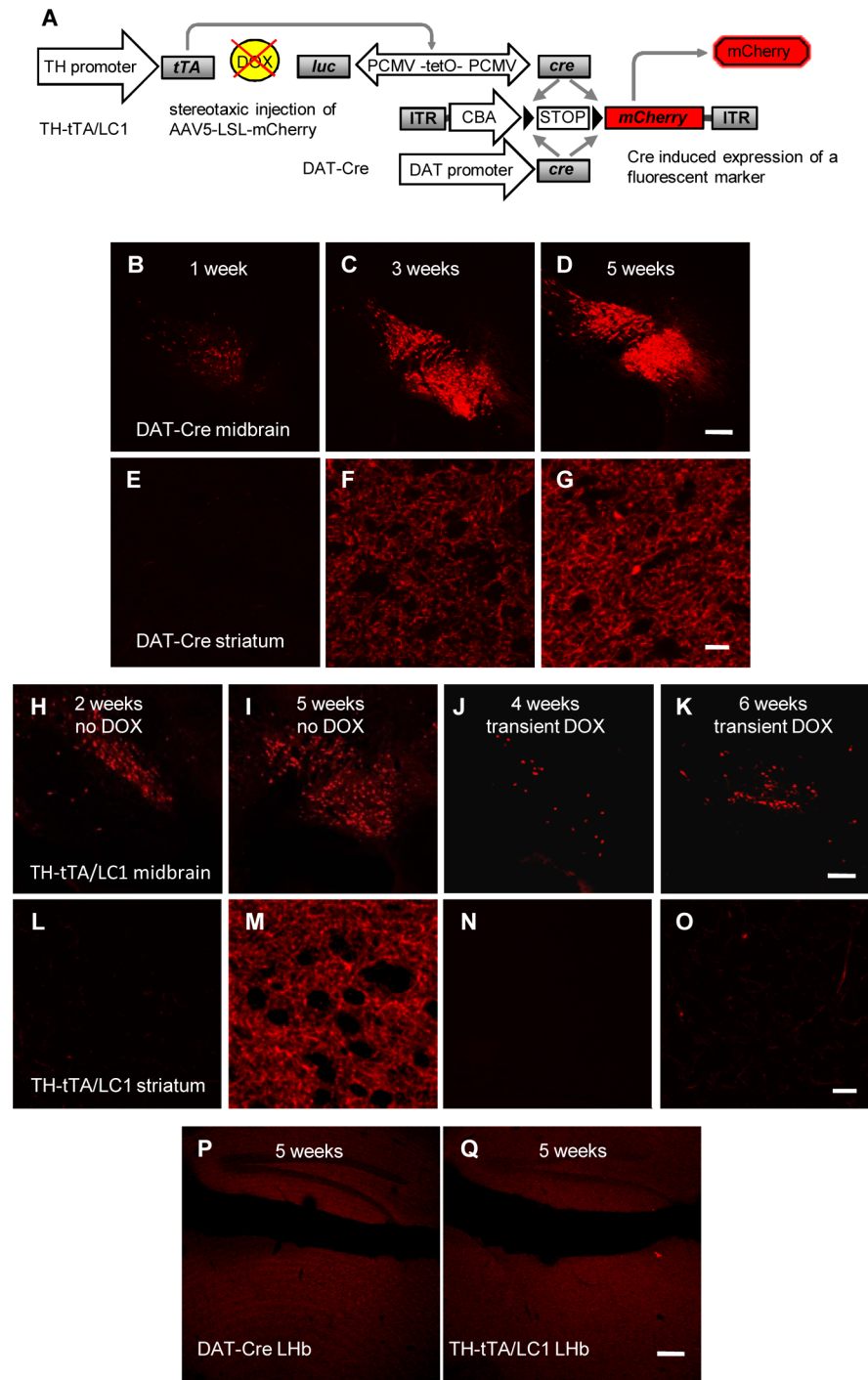
Fig 4. Efficient fluorescent labeling of DA neurons and their axons in AAV-LSL-mCherry injected DA neuron-specific Cre mice. (A) Scheme for specific fluorescent labeling of DA neuron in mice expressing a DA neuron-specific Cre and stereotaxic injected in the mindbrain with a recombinant AAV vector expressing mCherry after a floxed STOP codon. **(B-G)** Fluorescent mCherry expression in DA cells of the midbrain (B-D) and DA fibers in the striatum (E-G) in sagittal sections of stereotaxic injected DAT-Cre mice. Expression was evaluated 1 (B,E), 3 (C,F) and 5 weeks (D,G) after injection. After 1 week, no expression could be detected in DA fibers of the striatum. Expression in DA fibers was saturated 5 weeks after injection. Scale bars = 200 μm (B-D); 20 μm (E-G). **(H-O)** Fluorescent mCherry expression in DA cells of the midbrain (H-K) and DA fibers in the striatum (L-O) after stereotaxic injection of TH-tTA/LC1 mice. Fluorescent expression was evaluated at the indicated time points in mice raised without DOX. Some mice were kept on DOX-containing food after the

virus injection until analyzed (J, K, N, O). Scale bars = 200 μm (H-K); 20 μm (L-O). **(P and Q)** No fluorescent mCherry expression was detected in the lateral habenula (LHb) of AAV-LSL-mCherry injected DAT-Cre (P) and TH-tTA/LC1 (Q) mice after 5 weeks. Scale bars = 200 μm.

doi:10.1371/journal.pone.0136203.g004
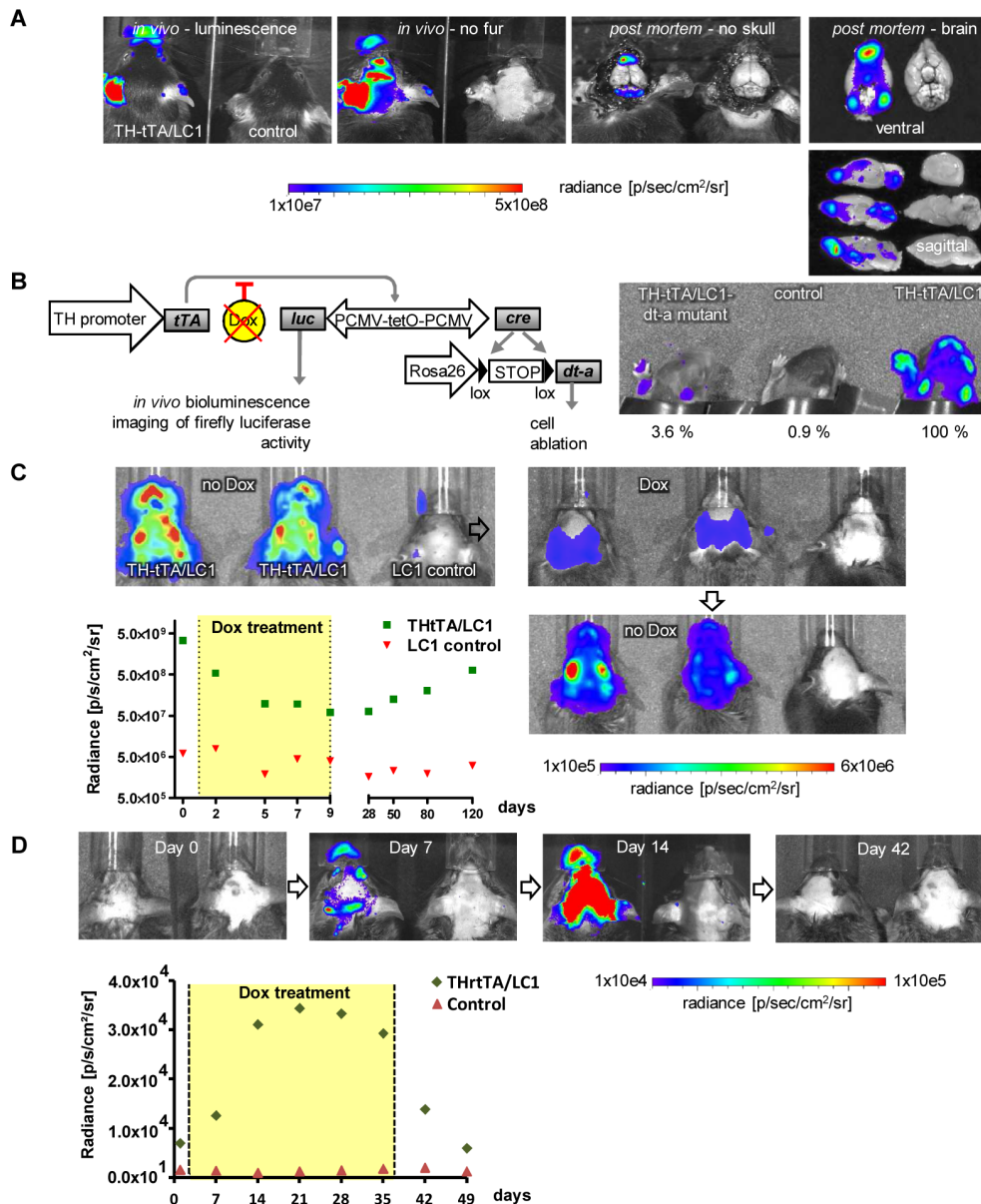
Fig 5. _In vivo_ bioluminescence imaging of DA neurons in TH-tTA/LC1 and TH-rtTA/LC1 mice. (A) Detection of luciferase activity in anesthetised TH-tTA/LC1 and LC1 control mice after fur removal and in brain tissue of dead mice after removal of the skull and dissection of brains using an IVIS200 _in vivo_ imaging device (Calipers Co.). **(B)** Comparison of the _in vivo_ bioluminescence signals in P3 TH-tTA/LC1 mouse pups expressing diphteria toxin A (dt-a) with TH-tTA/LC1 control mice and LC1 mice without luciferase expression. The radiance [p/sec/cm2/sr] RAW data luminescence signal intensity is shown in percentage compared to the maximal signal in the TH-tTA/LC1 control mice. **(C)** Temporal control of bioluminescence signal via DOX treatment in TH-tTA/LC1 mice. Quantification of luciferase activity in anesthetised TH-tTA/LC1 and LC1 control mice. After initial measurement, mice were treated with DOX in the drinking water (2 mg/ml) for 8 days and afterwards kept without DOX for further 111 days. Bioluminescence was again measured at the indicated time points, n = 3. **(D)** Temporal control of bioluminescence signal via DOX treatment in TH-rtTA/LC1 mice. Quantification of luciferase activity in anesthetised TH-rtTA/LC1 and LC1 control mice raised on DOX for 6 weeks and kept during adulthood without DOX. After initial measurement, mice were treated with DOX-containing food for 35 days and afterwards kept without DOX for further 14 days, n = 3–8.

doi:10.1371/journal.pone.0136203.g005
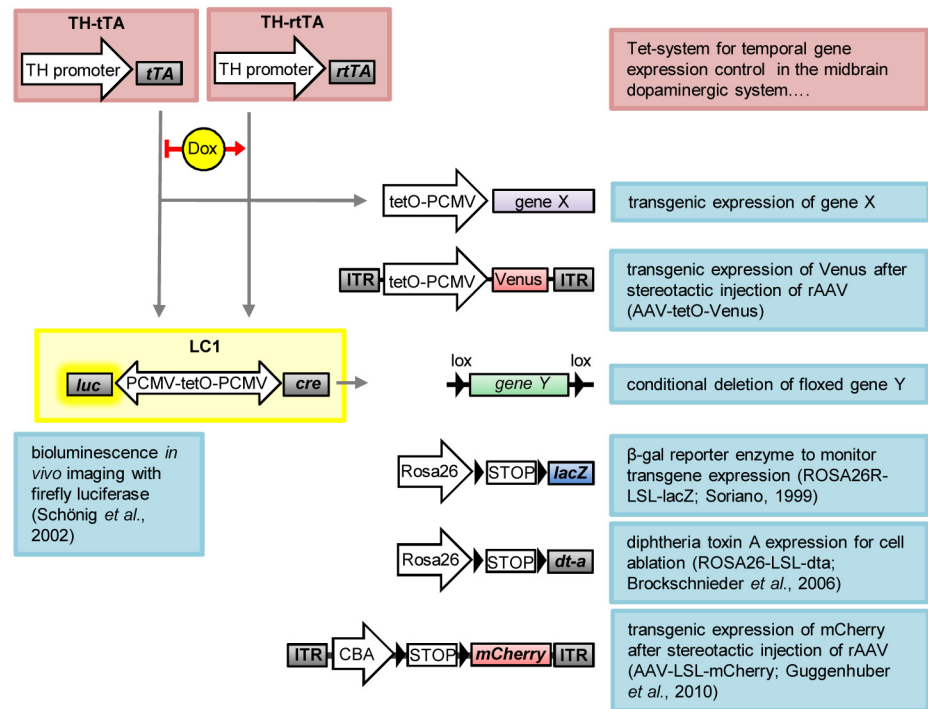
Fig 6. Schematic overview of utilized transgenic mice and recombinant AAV (rAAV) constructs. TH-tTA and TH-rtTA mice express, under the tyrosine hydroxylase (TH) promoter, the tetracycline-regulated transactivator protein (tTA) or the reverse tetracycline-regulated transactivator protein (rtTA) in dopaminergic (DA) neurons. tTA binds to the tetracycline operon (tetO) in the absence of doxycycline (DOX) and rtTA binds in the presence of DOX, driving transient expression of gene X, for example the fluorescent protein Venus from a recombinant AAV vector (AAV-tetO-Venus), or luciferase and Cre from the LC1 construct. The LC1 encodes a luciferase enzyme, which can be used for bioluminescence *in vivo* imaging, and the Cre recombinase for deleting gene Y or removing floxed STOP codons (LSL). Cre is used here as a genetic switch to activate, from the ROSA locus, either expression of the reporter gene lacZ (encoding β-galactosidase) to visualize transgene expression or to activate expression of diphtheria toxin protein A (dt-a) to selectively induce cell death of DA neurons. Here we use Cre also to activate expression of the fluorescent protein mCherry from AAV-LSL-mCherry.

doi:10.1371/journal.pone.0136203.g006

Conventional microscopy

Transmitted light images were acquired using a SZX16 stereo microscope equipped with a DP72 camera and cellSens Entry 1.4.1 imaging software (Olympus). DAB stained sections and fluorescent cells were imaged with an epifluorescent upright microscope Axio Imager.M1 (Zeiss, Goettingen, Germany) equipped with an automated stage (Ludl MAC 6000 system), Hamamatsu camera C8484 and Axiovision software 4.8. Fluorescent sections were imaged with a Leica TCS SP2 confocal microscope system with 10x (0.3 NA) and 63x (oil 1.32 NA) objectives or Zeiss LSM 700 Confocal microscope system with 10x (0.25 NA) and 40x (oil 1.3 NA) objectives. Confocal images were acquired by using a 514-nm Argon line for Venus or a 561-nm photodiode laser for mCherry. Image stack were maximally projected and contrast and intensity levels were uniformly adjusted using ImageJ (NIH).

Quantifications

Stereological countings were performed on 30 μm coronal serial sections analyzing every sixth section for the SNpc and VTA. This was done using an oil immersion 63x objective, a counting frame of 50 x 50 μm, and a grid size of 100 x 100 μm, as described previously [27] using the

optical fractionator method of the StereoInvestigator software 8.0 (MicroBrightField). To quantify lacZ positive and TH positive cells (Fig 1) we counted at least 2 representative 30 μm serial coronal sections. Venus positive and TH positive cells (Fig 2) were quantified in at least 3 representative 50 μm serial sagittal sections per mouse (every forth section) by applying a binary mask and the "Analyze Particles" function in ImageJ (NIH).

In vivo bioluminescence imaging

Bioluminescence *in vivo* imaging was performed on adult mice (2–12 months in Fig 5A, 5C and 5D) and non DOX treated P3 mice (Fig 5B) by using the IVIS 200 system and Living Image 3.2 software (Perkin Elmer) according to manufacturer´s instructions. For bioluminescence imaging, mice were i.p. injected with D-luciferin aqueous solution (15 mg ml^{-1}; 4.5 mg per 30g of bodyweight).

Statistical analysis

Data are expressed as means + s.e.m. The statistical analyses were performed with GraphPad Prism 5.0 (GraphPad Software) using two-tailed, unpaired Student´s t-test or ANOVA, followed by Tukey´s post hoc test to compare group means. In all analyses, p-values smaller than 0.05 were considered statistically significant.

Results

Generation and basic characterization of TH-tTA and TH-rtTA mice

To develop a tet-OFF and a tet-ON system for DA neurons of the mouse, we cloned the tTA2S or rtTA3G transactivator encoding sequences downstream of an 8.9 kilobase promoter fragment of the mouse TH gene and generated transgenic mice by pronuclear injections (Fig 1; S1 Fig). We generated 12 TH-tTA founder mice of which 9 founders went germline and 9 TH-rtTA founders of which 8 went germline. The founders were functionally characterized by crossing them with LC1 mice [21] and with Rosa26R reporter mice [22] (Fig 1A).

In the triple-transgenic TH-tTA/LC1/Rosa26R mice, the tTA transactivator-induced Cre recombinase expression from the LC1 transgene triggered the deletion of a STOP cassette in front of the LacZ gene, encoding the reporter enzyme β-galactosidase, in the Rosa26 locus. Using X-gal staining, we could detect β-galactosidase activity in midbrain DA neurons in 4 of the 9 TH-tTA founder lines (founder 1 in Fig 1B; founder 2–4 in S2 Fig). 5 founder lines did not show any lacZ expression. The four TH-tTA founder lines showed no difference in the expression pattern without DOX and no obvious physiological or behavioral abnormalities (data not shown).

To switch the tet-system permanently ON in TH-rtTA/LC1/Rosa26R mice, the parents were fed DOX-containing food before pregnancy and their offspring were kept on DOX until analysis. 5 founders showed X-gal staining under these conditions and were similar with regards to expression and physiology (founder 1 in Fig 1C; founder 2–5 in S3 Fig).

To analyze the expression of TH-tTA and TH-rtTA mice in midbrain DA neurons, we performed a co-staining of X-gal with an immunohistochemical TH staining and quantified the double-positive cells. In the TH-tTA/LC1/Rosa26R mice, 54% of substantia nigra pars compacta (SNpc) DA neurons and 58% of ventral tegmental area (VTA) DA neurons were also X-gal labeled (Fig 1D and 1E). TH-rtTA/LC1/Rosa26R mice showed 60% of SN and 65% of VTA DA neurons also positive for X-gal (Fig 1F). Thus, there seems to be an incomplete targeting of midbrain DA neurons in our TH-tet mice, as previously described for other Cre mice using the TH promoter [2–4]. This might be on one hand a disadvantage for systemic approaches, but

on the other hand an advantage to enable investigation of targeted and non-targeted DA neurons in the same mice, which is preferred for example in electrophysiological studies.

Besides expression in DA neurons of the VTA and SNpc, DA neurons in the arcuate nuclei and retrorubral field and noradrenergic cells of the locus coeruleus (LC) were stained, too (S4 and S5 Figs). TH expression has been described not only in catecholaminergic neurons, such as DA and noradrenergic neurons, but also transiently or permanent in many other cells inside and outside the nervous system. Transient TH protein expression during development in the absence of catecholamine synthesis has been reported in rodents for example in some interneurons of the cortex [28, 29], mesospiny neurons in the striatum [30] and Purkinje cells of the cerebellum [31]. Also the accessory, deeper layer and periglomerular cells of the olfactory bulb express TH protein during development [1, 32]. However, in adult mice TH protein expression is no longer detectable in these cell populations, although they continue to express TH mRNA [33]. As a consequence, X-gal staining was observed in the TH-tTA/LC1/Rosa26R and TH-rtTA/LC1/Rosa26R mice with the tet-system constantly active in many distinct brain regions such as the cerebellum, pons, striatum, hippocampus, cortex, thalamus, and lateral midbrain (Fig 1B, S4 and S5 Figs). Also, the extent of expression in the different tissues was variable, ranging from activity in all Purkinje cells of the cerebellum and all medium spiny neurons in the striatum to only mosaic, sporadic activation in pyramidal cells in the hippocampus and cortex (S4 and S5 Figs).

In the SNpc and VTA region of TH-tTA/LC1/Rosa26R and TH-rtTA/LC1/Rosa26R mice raised with constitutive active tet-system, more than 60% of X-gal positive cells were also stained with antibodies against TH. Similarly, in transiently DOX treated TH-tTA/LC1/Rosa26R mice, more than 90% of X-gal positive cells were stained (S2B and S3B Figs). Therefore, these cells were considered to be DA neurons. The X-gal-positive cells negative for TH protein expression might be due to cells that only express TH mRNA and no TH protein [34–36] (as described earlier) or cells expressing TH only during development and not adulthood (see next two chapters) (S2B and S2C, S3B and S3C Figs). The endogenous TH enzyme starts to be expressed in the mouse ventral midbrain at embryonic day E9-10 [37, 38] soon after the identification of the first midbrain DA neurons by the expression of the retinoic acid–synthesizing enzyme Aldh1a1 and before DA neurons are functionally connected to their postsynaptic partners [5]. Thus, our TH-tet mice permit targeting of DA neurons very early on during development and requires tight regulation of the tet-system if they are used to alter expression during a later developmental phase, e.g. during adulthood.

Regulation of gene expression in TH-tTA and TH-rtTA mice

To test the regulation of the tet-system in the TH-tTA and TH-rtTA mice, we first tried to switch off the tet-system completely by constantly feeding TH-tTA/LC1/Rosa26R mice with DOX-containing food or feeding TH-rtTA/LC1/Rosa26R mice with non DOX-containing food. This resulted in very few X-gal positive cells in the ventral midbrain DA system (Fig 1B and 1C). This suggests that there is a tight regulation of the transcriptional activity in both TH-tet mice under these conditions with little leakage.

Next, we wanted to know if we could switch gene expression on or off ad libitum. Therefore, we transiently fed TH-tTA/LC1/Rosa26R mice with DOX until they were 6 weeks of age followed by 6 weeks without DOX before analysis. This protocol enabled us to specifically label X-gal positive DA neurons in the midbrain of 12 week old mice (Fig 1A and 1C, S2B Fig). By applying transient DOX treatment, we targeted in TH-tTA/LC1/Rosa26R mice around 40% of midbrain DA neurons (Fig 1E). To test the tet-system inducibility in TH-rtTA/LC1/Rosa26R mice, we raised them without DOX and started with the DOX treatment at 6 weeks of age for

at least 6 additional weeks. However, no X-gal stained cells were observed (Fig 1C). The reduced number of responding DA neurons after DOX treatment in TH-tTA/LC1/Rosa26R mice, as well as the lack of DOX response of adult TH-rtTA/LC1/Rosa26R mice, might be due to genetic silencing of the LC1 construct that prevents re-activation, as previously described [39, 40].

LC1 independent targeting of adult DA neurons in TH-tTA and TH-rtTA mice

In order to overcome possible genetic silencing of the LC1 construct in TH-rtTA/LC1 mice, we generated an AAV vector expressing the fluorescent protein Venus directly under the control of the tetO promoter (AAV-tetO-Venus). Before virus production, we tested the AAV-tetO--Venus DNA construct in HEK293-T cells co-transfected with a tTA expression vector and found a DOX-dependent expression of Venus (S6 Fig). Subsequently, the AAV-tetO-Venus virus vector was stereotactically injected in the SN of adult non-DOX treated TH-tTA mice and DOX-treated TH-rtTA (Fig 2). We investigated 5 weeks after injection the expression of Venus in the mouse midbrain DA neurons visualized by TH antibody staining. In TH-tTA/ AAV-tetO-Venus mice, 67% of DA neurons were also Venus-positive (Fig 2A, 2B and 2E). With DOX treatment 10 days before AAV-tetO-Venus injection, we observed only 27% of Venus-positive DA neurons in TH-tTA mice (Fig 2E, S7 Fig). In DOX-treated TH-rtTA/AAV-tetO-Venus mice, 73% of DA neurons were expressing Venus, while only 23% expressed Venus without DOX (Fig 2C–2E, S7 Fig). In non-transgenic control mice, AAV-tetO-Venus injection resulted in only 5% of Venus-positive DA neurons, which was comparable with background expression seen in AAV-tetO-Venus transfected HEK293-T cells (Fig 2E, S6 and S7 Figs). This result confirms that it is possible to induce the tet-system in TH-rtTA mice with a transient postnatal DOX treatment. Furthermore, it provides evidence that in both transgenic mouse lines, the TH-tTA and TH-rtTA mice, the tet-system can efficiently activate expression from virally provided and tetO regulated genes of interest during adulthood.

Genetic deletion of DA neurons in TH-tTA mice

We made use of our TH-tTA mice to generate a genetic mouse model with reduced number of DA neurons. To do this, we replaced the Rosa26R with the Rosa26dt-a transgene in the triple-transgenic mice that, in the absence of DOX, induced cell death by the expression of diphtheria toxin-A [23] (Fig 3A). TH-tTA/LC1/Rosa26dt-a mice without DOX died shortly after birth in the first postnatal week and lost around 40% of midbrain DA neurons in the SNpc and VTA (Fig 3B and 3C).

The mice survived until adulthood if transiently treated with DOX during embryogenesis and early postnatal development until 6 weeks of age. We stereologically quantified the number of DA neurons in mice 6 weeks and between 14 to 30 weeks after removal of DOX and found 18 to 32% less DA neurons in the SNpc and 28 to 33% less DA neurons in the VTA, respectively (Fig 3D and 3E). This supports the tight regulation of the tet-system in our TH-tTA mice and the possibility to generate, with this approach, a genetic adult-onset DA system neurodegeneration mouse model.

Fluorescent labeling of adult DA neurons in TH-tTA mice

Our next goal was to test the TH-tet mice for developing an efficient system for fluorescently labeling DA neuron cell bodies and axons for fast assessment of the DA fiber density in the striatum and possibly axonal tracing experiments. The currently available fluorescent DA neuron marker mice, such as the TH-GFP [41, 42], Pitx3-GFP [43] or DAT-GFP [44] mice efficiently

label the DA cell bodies, but only weakly label the DA innervation in the target fields. This includes the striatum, which is important to investigate in the DA system degeneration or regeneration experiments related to PD. This is most likely due to the low copy number of fluorescent protein encoding cDNAs in the transgenic mice and the very long and manifold brunched axons of DA neurons.

Since the stereotactic injection of the AAV-tetO-Venus vector in the TH-tTA and TH-rtTA mice did not efficiently label the complete axonal network of DA neurons, we tried to enhance the fluorescent signal by using the Cre-lox system. We stereotactically injected adult TH-tTA/LC1 mice in the SNpc with an AAV-LSL-mCherry virus construct, that uses the strong cytomegalovirus enhancer/chicken beta actin (CAG) promoter followed by a floxed STOP codon (LSL) and the mCherry expression cassette [26] (Fig 4A). As an alternative DA neuron-specific Cre mouse line, we also injected DAT-Cre mice with the same AAV-LSL-mCherry virus [7] (Fig 4A). In both mouse lines the STOP codon was efficiently removed in midbrain DA neurons and allowed to label them with mCherry (Fig 4B–4O). To determine the minimal time required to label DA axons in the striatum, we analyzed the mice 1, 2, 3, 4, 5 and 6 weeks after virus injection. We found that 1 week was sufficient to label a few cell bodies, but after 5 weeks there was a strong fluorescent staining of midbrain DA neurons and of the DA fibers in the striatum for both AAV-LSL-mCherry injected mouse lines, DAT-Cre (Fig 4B–4G) and TH-tTA/LC1 mice (Fig 4H, 4I, 4L and 4M). In both Cre lines injected with AAV-LSL-mCherry, DAT-Cre and TH-tTA/LC1 mice, we did not observe labeled fibers in the lateral habenula (LHb), which is still an open question in the field (Fig 4P and 4Q) [34–36, 45, 46]. Treating the TH-tTA/LC1 mice after viral injection for 4 or 6 weeks with DOX strongly reduced the amount of labeled cells in the midbrain and the fiber staining in the striatum (Fig 4J, 4K, 4N and 4O). Together with the previous experiments this shows the tight regulation of the tet-system in our TH-tTA mice during adulthood. These data suggests that the combination of TH-tTA/LC1 mice with the AAV-LSL-mCherry virus is an excellent approach to efficiently label TH expressing neurons and their axons in their target fields such as the striatum.

In vivo bioluminescence imaging of the DA system in TH-tTA and TH-rtTA mice

To be able to visualize and monitor the DA system in living mice over time, we made use of luciferase expression from the LC1 construct in our TH-tTA/LC1 mice. Systemic application of the D-luciferin substrate allowed us to detect a bioluminescence signal through all openings of the skull, the nose, ears and eyes of the double transgenic mice, but no signal in single transgenic mice (Fig 5A). Removing the black fur improved the detection of the *in vivo* signal through the skull directly above the brain (Fig 5A). Removing the skin and skull post mortem enabled us to detect the luminescence signal directly above the specific brain regions with TH expression, such as the olfactory bulb, the midbrain and the cerebellum, without further scattering of the signal (Fig 5A). Further dissection of the brain showed that the bioluminescence signal arises from the TH-positive cells already detected in the TH-tTA/LC1/ROSA26R mice with lacZ staining (Fig 1). The specificity of the *in vivo* signal was confirmed in TH-tTA/LC1/Rosa26dt-a mice, in which the signal was strongly diminished (Fig 5B). This is consistent with the view that almost all the cells, in which LC1 was active and led to luciferase and Cre expression, died due to the Cre-mediated diphtheria toxin-A expression. Treating shaved TH-tTA/LC1 mice for 8 days with DOX-containing food continuously reduced the *in vivo* bioluminescence signal, consistent with a down regulation of luciferase in the mice (Fig 5C). Subsequently, the bioluminescence signal increased slowly again when the mice were on DOX-free food (Fig 5C). In TH-rtTA/LC1 mice raised on DOX for 6 weeks and maintained without DOX during

adulthood, we could show reversible gene activation during adulthood with faster ON-kinetics compared to the TH-tTA/LC1 mice (Fig 5D). TH-rtTA/LC1 mice without DOX showed only a very weak luciferase signal that increased after 2 weeks on DOX to the maximal luciferase signal and decreased again to the original levels 2 weeks after withdrawal from DOX (Fig 5D).

Thus, the bioluminescence signal in TH-tTA/LC1 and TH-rtTA/LC1 mice allows *in vivo* monitoring of the integrity and gene expression activity of the DA system, and might therefore be applied to follow degeneration and regeneration processes of the DA system over time in the same mouse.

Discussion

The TH-tTA and TH-rtTA mouse lines described enable targeting of midbrain DA neurons with high efficiency during all developmental stages, show a tight DOX-dependent regulation and therefore can be used for a multitude of applications (Fig 6). We have shown that the TH-tTA and TH-rtTA mice are an excellent tool for regulating gene expression in midbrain DA neurons. They can be used to overexpress or delete genes of interest and they can be combined with the Cre-lox recombination system (Figs 1–6). Therefore, our TH-tTA and TH-rtTA mouse lines permit studying, for example, the loss of function phenotype of genes in the adult DA system that lead to embryonic lethality or possible activation of compensatory mechanisms during development, which might mask their function during adulthood. In addition, we show that the TH-tet mice can be efficiently used to visualize DA neurons and their innervation fluorescently in the brain (Figs 2 and 4). Furthermore, they can be used to monitor the DA system *in vivo* as an entity over the whole life time of a mouse and therefore allow following alterations progressively over time (Fig 5).

In 2004, the first ratTH-rtTA2S-M2 construct was generated and successfully used in HEK293 cells and in the dopaminergic cell line MN9D [47]. However, three groups have only recently generated transgenic mice in which the tet-system was targeted to midbrain DA neurons [48, 49]. In the first mouse line, a tTA knock-in was created into the endogenous DAT locus, which generates a heterozygote DAT knockout mouse showing low DAT levels and hyperactivity [50]. In a second line, a TH-rtTA mouse line, tetracycline-dependent regulation was subsequently lost [49](data not shown). In the third mouse line, carrying a Pitx3-tTA construct, tetracycline-dependent regulation has not yet been shown [48]. To preserve our functional tet-system mouse lines for the research community, we immediately conserved them by sperm freezing.

The TH-tTA and TH-rtTA mice can be combined with many different tetO-constructs at the same time and used to activate or inhibit gene expression during embryogenesis, adulthood and in aging mice since DOX is rapidly taken up into cells, shows low toxicity and penetrates the placenta and the blood-brain barrier [51–53]. Silencing of tetO-constructs in the mouse can be overcome, as shown here, by administering it at specific time points, for example, by electroporation of DNA in embryos or by viral injections in adult mice. If a gene should only be expressed for a short time period, the rapid inducible tet-ON system might be preferred. However, if a gene should only be switched off for a short time period the use of the tet-OFF system might be an advantage and can save DOX-food costs. In order to decide between each system, it is worthwhile mentioning that the tet-OFF systems shows a slower ON-kinetics (several weeks) compared to the tet-ON system (several days), as shown also in our *in vivo* luciferase experiment. Furthermore, long DOX-treatment times might lead to an accumulation of DOX in the bone that is only slowly cleared after removal of DOX from the food or water [51–53].

The mosaic or incomplete targeting of DA neurons in our mouse TH promoter-driven system seems to be a common issue and has already been reported for transgenic mice generated

with the rat TH promoter [2, 4]. This seems to be the case even in mice with the transgene knocked into the endogenous mouse TH locus behind an internal ribosomal entry sequence (IRES) [3]. Besides the TH promoter specific features this appears to be at least in part also due to the reporter construct used as viral vectors and transgenic mice do not express their encoded reporter homogeneously in DA neurons [3]. In addition, we did not find any fluorescently labeled DA neurons when we crossed the TH-tTA/LC1 mice with Ai9 tdTomato reporter mice [54] (data not shown). This is surprising, because Ai9 mice use like the Rosa26R and Rosa26dt-a mice the Rosa locus for tdTomato expression [22]. Yet, Ai9 mice labeled DA neurons nicely when crossed with DAT-Cre mice [54](data not shown). Despite this, more research is needed to better understand the underlying biology of this phenomenon. The mosaic targeting can also be an advantage for some experiments. In studies where DA cells with different genetic alterations need to be compared *in vivo* in the same environment—for example, in electrophysiological studies—the partial targeting of DA neurons in the TH-tTA mice will turn out to be a very helpful condition, much like the MARCM clones in *Drosophila melanogaster* that turned out to be an excellent tool to study *in vivo* gene function in the wildtype background of flies [55]. The mosaic expression in the TH-tTA/LC1 mice allowed us to establish viable TH-tTA/LC1/Rosa26dt-a mice showing a very reproducible and progressive DA system degeneration in young adult mice reaching in 3–7 month old mice 30% of DA neuron loss. The DA system degeneration in TH-tTA/LC1/Rosa26dt-a mice is less variable and cumbersome to generate compared to the commonly used injections of neurotoxins such as MPTP, 6-OHDA or rotenone to generate PD animal models [56]. Therefore, the inducible DA system degeneration phenotype in TH-tTA/LC1/Rosa26dt-a mice might be a favorable alternative to test cell and tissue replacement therapies for the treatment of PD.

The neonatal lethality in TH-tTA/LC1/Rosa26dt-a mice is most likely due to the loss of noradrenergic neurons in the peripheral nervous system innervating for example the heart. This view is supported by the findings that DAT-Cre/Rosa26dt-a mice also show a reduced number of midbrain DA neurons but are viable and show a normal motor behavior despite the DA cell loss of around 90% [57]. In addition, TH deficiency in mice has been shown to be embryonal lethal apparently due to cardiovascular failure [58] and the lethality can be rescued by knocking-in TH into the noradrenergic-specific dopamine-β-hydroxylase locus [59]. DOX treatment of TH-tTA/LC1/Rosa26dt-a mice during development prevents postnatal lethality and allows deleting dopaminergic neurons during adulthood.

To enable the unbiased fluorescent detection of DA neuron axonal branches and to allow *in vivo* detection of the fluorescently labeled DA system in our TH-tet mice, we made use of a Cre-mediated expression of mCherry from an AAV vector (AAV-LSL-mCherry). We show as a proof of principle that for this purpose the AAV5-LSL-mCherry virus can be used in combination with both mouse lines expressing Cre recombinase in DA neurons, the DAT-Cre and the TH-tTA/LC1 mice. The advantage of the TH-tTA/LC1 mice becomes apparent if you want to label DA neurons in which genetic alterations should not only be induced by Cre recombinase events but also by the tet-O promoter enabling reversible gene activation.

Recently, the approach to characterize in more detail the VTA cell population innervating the LHb to promote reward led to the finding that different TH and DAT promoter driven Cre mice label in combination with different AAV viruses, distinct VTA neurons [34–36, 45, 46]. In summary, three different TH promoter driven Cre lines seem to have targeted neurons which innervate the LHb, express TH, GAD and VGlut2 mRNA [46], but do not express TH protein, and have electrophysiological properties like GABAergic and glutamatergic neurons. In addition, one identical DAT-Cre mouse line was used by two groups in combination with two different AAV reporter constructs. One group reported targeting of VTA neurons innervating the LHb, the other group not [35, 36]. We have detected no DA innervation of the LHb

from the midbrain with our AAV-LSL-mCherry virus in the same DAT-Cre mouse line used before and in our TH-tTA/LC1 mice. Taken together these results support the idea that not only the Cre expressing mouse line but also the transgenic or viral reporter construct dramatically influences the outcome of targeting and that the outcome of a specific combination of Cre and reporter is so far not predictable.

We can imagine that combining several AAV-LSL-XFP viruses encoding different fluorescent proteins (XFP) might allow labeling and tracing single DA neurons in almost unique colors. This could facilitate the detailed analysis of the heterogeneous population of DA neurons [1, 60] for which only 8 neurons have been traced in detail from the rat brain and none from the mouse brain [61]. Further experiments are needed to test this hypothesis in detail.

We provide here the proof of principle that *in vivo* imaging of the DA system in our TH-tet mice is feasible using bioluminescence signals. *In vivo* imaging might allow detecting progressive degeneration and regeneration processes of the DA system over time in individual mice and therefore might be suitable for testing drugs for their beneficial or detrimental effect. This method should allow cutting down the number of animals in longitudinal studies and should avoid inter-subject variability problems. Since the *in vivo* measurement takes only seconds to minutes, it might reduce the time for analysis dramatically and can replace or precede a detailed histological analysis. The special resolution and signal intensity of the *in vivo* signal might be further improved by replacing the skull with a glass plate, using more sensitive bioluminescence substrates such as Cycluc1 [62], and by switching for bioluminescence imaging to a red-shifted luciferase variant [63].

In the future, TH-tet mice might also be used for altering and monitoring acute DA cell physiology by combining them with Ca2+ imaging and optogenetic tools, such as in AAV-LSL-channelrhodopsin or halorhodopsin vectors and the KENGE-tet system, using knockin-mediated enhanced gene expression by improved tetracycline-controlled gene induction to express a highly light-sensitive channelrhodopsin-2 mutant at levels sufficient to drive the activities in different cells [64, 65].

With the TH-tTA and TH-rtTA mice we generated a versatile tet-system available to genetically modify the DA system of the mouse for studying *in vitro* and *in vivo* DA neuron development and maintenance, physiology and pathophysiology, and biochemical or histological alterations. The establishment of the tet-OFF and tet-ON system in mouse DA neurons enlarged our tool kit for more sophisticated and fine-tuned manipulations of the DA system that should help to increase our knowledge about this complex and fascinating system and might shed more light on the etiology and possible treatments of human diseases such as PD, schizophrenia and drug addiction.

Supporting Information

S1 Fig. Schematic overview of transgenic TH-tTA mice. (A) Scheme of the TH-tTA DNA construct: transcription of the tetracycline transactivator protein tTA is controlled by a 8.9 kb mouse genomic fragment upstream of the AUG start codon of the tyrosine hydroxylase (TH) coding sequence. **(B)** Agarose gel analysis of the TH-tTA fragment isolated from the SalI cut plasmid used for pronucleus injection (PI) into C57Bl/6J single cell embryos to generate transgenic mice. 1: GeneRuler 1kb DNA ladder; 2: TH-tTA DNA fragment of around 12 kb. **(C)** Principle of the Tet-OFF system: tTA protein is expressed via the TH-tTA construct and binds in the absence of doxycycline (DOX) to the tet-responsive promoter (*tetO*) and activates gene of interest expression.
(TIF)

S2 Fig. Specificity, inducibility and efficacy of gene expression in additional TH-tTA founders after crossing them with LC1 and Rosa26R mice. (A) Coronal midbrain brain sections with SNpc and VTA DA neurons of TH-tTA/LC1/Rosa26R for founders 2, 3, and 4, respectively. Mice were raised without (no) DOX, with (constant) DOX or with DOX until the age of 6 weeks followed by 6 weeks without (transient) DOX. Sections were stained for beta-galactosidase activity with X-gal to visualize cells with activated tTA, LC1 and ROSA26 locus. Scale bars: 500 µm. (B) Ratio of lacZ and TH double positive cells to all lacZ positive cells in the SNpc and VTA in TH-tTA/LC1/Rosa26R without or transient DOX treatment as indicated. (C) lacZ positive cells in the VTA, SNpc and ventral midbrain without VTA and SNpc in non DOX treated TH-tTA/LC1/Rosa26R mice.
(TIF)

S3 Fig. Specificity, inducibility and efficacy of gene expression in additional TH-rtTA founders after crossing them with LC1 and Rosa26R mice. (A) Coronal midbrain brain sections with SNpc and VTA DA neurons of TH-rtTA/LC1/Rosa26R for founders 2, 3, 4, and 5, respectively. Mice were raised with (constant) DOX, without (no) DOX, or transiently without DOX until the age of 6 weeks followed by 6 weeks with (transient) DOX. Sections were stained for beta-galactosidase activity with X-gal to visualize cells with activated rtTA, LC1 and ROSA26 locus. Scale bars: 500 µm. (B) Ratio of lacZ and TH double positive cells to all lacZ positive cells in the SNpc and VTA in TH-rtTA/LC1/Rosa26R with constant DOX treatment. (C) lacZ positive cells in the VTA, SNpc and ventral midbrain without VTA and SNpc in constantly DOX treated TH-rtTA/LC1/Rosa26R mice.
(TIF)

S4 Fig. Specificity, inducibility and efficacy of gene expression outside midbrain DA neurons in adult mice of TH-tTA founder 1 after crossing with LC1 and Rosa26R mice. Coronal mouse brain sections stained with X-gal to visualize β-galactosidase expression in TH-tTA/LC1/Rosa26R mice without (A, C, E, G) or transient DOX (B, D, F, H). Broad lacZ expression was detected in mice without DOX treatment in the cerebellum and pons (A), in the striatum (C), the olfactory bulb (E), the hippocampus and different layers of the cortex (G). Mice transiently treated with Dox during development till 6 weeks after birth and evaluated 6 weeks later showed still X-gal staining in the cerebellum (B) but not anymore in the pons (B), the striatum (D), hippocampus and cortex (H). Scale bars: 200 µm (A-H), blowup 500 µm (A-D). (I) Quantification of TH+ lacZ+ double positive cells in the locus coeruleus of TH-tTA/LC1/Rosa26R mice without DOX revealed 17% targeted noradrenergic neurons.
(TIF)

S5 Fig. Specificity and efficacy of gene expression outside midbrain DA neurons in adult mice of TH-rtTA founder 1 after crossing with LC1 and Rosa26R mice. Coronal mouse brain sections stained with X-gal to visualize β-galactosidase expression in TH-rtTA/LC1/Rosa26R mice with DOX. Broad lacZ expression was detected in the cerebellum and pons (A), hippocampus (B), striatum (C), in different layers of the cortex (B and C) and the olfactory bulb (D). Scale bars: 200 µm (A and C), blowup 500 µm (A-D).
(TIF)

S6 Fig. Transfection of new pAAV-tetO-Venus DNA construct in HEK293-T cells. Cells were transfected with the following DNA constructs and analyzed 48 hours later for Venus expression: (A) pUHD61-1-tTA vector encoding tTA under a CMV promoter; (B) pAAV-tetO-Venus vector encoding Venus under the tetO promoter; and (C) co-transfection of both pUHD61-1-tTA and pAAV-tetO-Venus vector. Scale bar: 200 µm.
(TIF)

S7 Fig. Cre-independent adult gene expression in DA neurons of TH-tTA and TH-rtTA mice using a AAV-tetO-Venus vector. (A-C) Confocal fluorescent pictures of Venus expression (green) in DA neurons co-stained for TH (red) in the substantia nigra pars compacta (SNpc) of sagittal mouse brain sections 5 weeks after AAV-tetO-Venus virus injection. TH-tTA mice were treated with DOX for 10 days before streotactic injections until analysis to switch the system off (A). TH-rtTA mice were here not DOX treated to keep the system inactive (B). Non-transgenic control mice were analyzed also 5 weeks after AAV-tetO-Venus virus injection (C). Scale bars: 250 μm.
(TIF)

Acknowledgments

Author Contributions

Conceived and designed the experiments: ERK. Performed the experiments: KT HA ERK. Analyzed the data: KT HA ERK. Contributed reagents/materials/analysis tools: KT HA ERK. Wrote the paper: KT HA ERK.

References

1. Bjorklund A, Dunnett SB. Dopamine neuron systems in the brain: an update. Trends Neurosci. 2007; 30(5):194–202. Epub 2007/04/06. doi: S0166-2236(07)00067-7 [pii] doi: 10.1016/j.tins.2007.03.006 PMID: 17408759.

2. Gelman DM, Noain D, Avale ME, Otero V, Low MJ, Rubinstein M. Transgenic mice engineered to target Cre/loxP-mediated DNA recombination into catecholaminergic neurons. Genesis. 2003; 36(4):196–202. doi: 10.1002/gene.10217 PMID: 12929090.

3. Lindeberg J, Usoskin D, Bengtsson H, Gustafsson A, Kylberg A, Soderstrom S, et al. Transgenic expression of Cre recombinase from the tyrosine hydroxylase locus. Genesis. 2004; 40(2):67–73. Epub 2004/09/29. doi: 10.1002/gene.20065 PMID: 15452869.

4. Savitt JM, Jang SS, Mu W, Dawson VL, Dawson TM. Bcl-x is required for proper development of the mouse substantia nigra. J Neurosci. 2005; 25(29):6721–8. Epub 2005/07/22. doi: 25/29/6721 [pii] doi: 10.1523/JNEUROSCI.0760-05.2005 PMID: 16033881.

5. Wurst W, Prakash N. Genetic Control of Meso-diencephalic Dopaminergic Neuron Development in Rodents. In: Iversen LL, IS D., Dunnett SB, Bjorklund A, editors. Dopamine Handbook: Oxford University Press; 2010. p. 141–59.

6. Backman CM, Malik N, Zhang Y, Shan L, Grinberg A, Hoffer BJ, et al. Characterization of a mouse strain expressing Cre recombinase from the 3' untranslated region of the dopamine transporter locus. Genesis. 2006; 44(8):383–90. Epub 2006/07/26. doi: 10.1002/dvg.20228 PMID: 16865686.

7. Zhuang X, Masson J, Gingrich JA, Rayport S, Hen R. Targeted gene expression in dopamine and serotonin neurons of the mouse brain. J Neurosci Methods. 2005; 143(1):27–32. Epub 2005/03/15. doi: S0165-0270(04)00350-4 [pii] doi: 10.1016/j.jneumeth.2004.09.020 PMID: 15763133.

8. Ekstrand MI, Terzioglu M, Galter D, Zhu S, Hofstetter C, Lindqvist E, et al. Progressive parkinsonism in mice with respiratory-chain-deficient dopamine neurons. Proc Natl Acad Sci U S A. 2007; 104(4):1325–30. doi: 10.1073/pnas.0605208103 PMID: 17227870; PubMed Central PMCID: PMC1783140.

9. Turiault M, Parnaudeau S, Milet A, Parlato R, Rouzeau JD, Lazar M, et al. Analysis of dopamine transporter gene expression pattern—generation of DAT-iCre transgenic mice. FEBS J. 2007; 274 (14):3568–77. Epub 2007/06/15. doi: EJB5886 [pii] doi: 10.1111/j.1742-4658.2007.05886.x PMID: 17565601.

10. Parlato R, Rieker C, Turiault M, Tronche F, Schutz G. Survival of DA neurons is independent of CREM upregulation in absence of CREB. Genesis. 2006; 44(10):454–64. Epub 2006/09/19. doi: 10.1002/dvg.20236 PMID: 16981198.

11. Smidt MP, von Oerthel L, Hoekstra EJ, Schellevis RD, Hoekman MF. Spatial and temporal lineage analysis of a Pitx3-driven Cre-recombinase knock-in mouse model. PLoS One. 2012; 7(8):e42641. doi: 10.1371/journal.pone.0042641 PMID: 22870339; PubMed Central PMCID: PMC3411649.

12. Engblom D, Bilbao A, Sanchis-Segura C, Dahan L, Perreau-Lenz S, Balland B, et al. Glutamate receptors on dopamine neurons control the persistence of cocaine seeking. Neuron. 2008; 59(3):497–508. Epub 2008/08/15. doi: S0896-6273(08)00582-5 [pii] doi: 10.1016/j.neuron.2008.07.010 PMID: 18701074.

13. Qiu HY, Guo C, Cheng XW, Huang Y, Xiong ZQ, Ding YQ. Pitx3-CreER mice showing restricted Cre expression in developing ocular lens and skeletal muscles. Genesis. 2008; 46(6):324–8. Epub 2008/06/11. doi: 10.1002/dvg.20399 PMID: 18543300.

14. Rotolo T, Smallwood PM, Williams J, Nathans J. Genetically-directed, cell type-specific sparse labeling for the analysis of neuronal morphology. PLoS One. 2008; 3(12):e4099. Epub 2009/01/01. doi: 10.1371/journal.pone.0004099 PMID: 19116659.

15. Hayashi S, McMahon AP. Efficient recombination in diverse tissues by a tamoxifen-inducible form of Cre: a tool for temporally regulated gene activation/inactivation in the mouse. Dev Biol. 2002; 244(2):305–18. Epub 2002/04/12. doi: 10.1006/dbio.2002.0597 S0012160602905972X [pii]. PMID: 11944939.

16. Takebayashi H, Usui N, Ono K, Ikenaka K. Tamoxifen modulates apoptosis in multiple modes of action in CreER mice. Genesis. 2008; 46(12):775–81. Epub 2008/12/24. doi: 10.1002/dvg.20461 PMID: 19105217.

17. Schmidt-Supprian M, Rajewsky K. Vagaries of conditional gene targeting. Nat Immunol. 2007; 8 (7):665–8. Epub 2007/06/21. doi: ni0707-665 [pii] doi: 10.1038/ni0707-665 PMID: 17579640.

18. Forni PE, Scuoppo C, Imayoshi I, Taulli R, Dastru W, Sala V, et al. High levels of Cre expression in neuronal progenitors cause defects in brain development leading to microencephaly and hydrocephaly. J Neurosci. 2006; 26(37):9593–602. Epub 2006/09/15. doi: 26/37/9593 [pii] doi: 10.1523/JNEUROSCI.2815-06.2006 PMID: 16971543.

19. Traykova-Brauch M, Schonig K, Greiner O, Miloud T, Jauch A, Bode M, et al. An efficient and versatile system for acute and chronic modulation of renal tubular function in transgenic mice. Nat Med. 2008; 14 (9):979–84. doi: 10.1038/nm.1865 PMID: 18724376; PubMed Central PMCID: PMC3446847.

20. Schonig K, Freundlieb S, Gossen M. Tet-Transgenic Rodents: a comprehensive, up-to date database. Transgenic Res. 2013; 22(2):251–4. doi: 10.1007/s11248-012-9660-9 PMID: 23180363; PubMed Central PMCID: PMC3591533.

21. Schonig K, Schwenk F, Rajewsky K, Bujard H. Stringent doxycycline dependent control of CRE recombinase in vivo. Nucleic Acids Res. 2002; 30(23):e134. Epub 2002/12/06. PMID: 12466566.

22. Soriano P. Generalized lacZ expression with the ROSA26 Cre reporter strain. Nat Genet. 1999; 21 (1):70–1. Epub 1999/01/23. doi: 10.1038/5007 PMID: 9916792.

23. Brockschnieder D, Pechmann Y, Sonnenberg-Riethmacher E, Riethmacher D. An improved mouse line for Cre-induced cell ablation due to diphtheria toxin A, expressed from the Rosa26 locus. Genesis. 2006; 44(7):322–7. Epub 2006/06/23. doi: 10.1002/dvg.20218 PMID: 16791847.

24. Gossen M, Freundlieb S, Bender G, Muller G, Hillen W, Bujard H. Transcriptional activation by tetracyclines in mammalian cells. Science. 1995; 268(5218):1766–9. PMID: 7792603.

25. Shevtsova Z, Malik JM, Michel U, Bahr M, Kugler S. Promoters and serotypes: targeting of adeno-associated virus vectors for gene transfer in the rat central nervous system in vitro and in vivo. Exp Physiol. 2005; 90(1):53–9. doi: 10.1113/expphysiol.2004.028159 PMID: 15542619.

26. Guggenhuber S, Monory K, Lutz B, Klugmann M. AAV vector-mediated overexpression of CB1 cannabinoid receptor in pyramidal neurons of the hippocampus protects against seizure-induced excitoxicity. PLoS One. 2010; 5(12):e15707. Epub 2011/01/05. doi: 10.1371/journal.pone.0015707 PMID: 21203567.

27. Kramer ER, Aron L, Ramakers GM, Seitz S, Zhuang X, Beyer K, et al. Absence of Ret signaling in mice causes progressive and late degeneration of the nigrostriatal system. PLoS Biol. 2007; 5(3):e39. Epub 2007/02/15. doi: 1544-9173-5-3-e39 [pii] doi: 10.1371/journal.pbio.0050039 PMID: 17298183; PubMed Central PMCID: PMC1808500.

28. Asmus SE, Anderson EK, Ball MW, Barnes BA, Bohnen AM, Brown AM, et al. Neurochemical characterization of tyrosine hydroxylase-immunoreactive interneurons in the developing rat cerebral cortex. Brain Res. 2008; 1222:95–105. doi: 10.1016/j.brainres.2008.05.053 PMID: 18589406; PubMed Central PMCID: PMC2576998.

29. Satoh J, Suzuki K. Tyrosine hydroxylase-immunoreactive neurons in the mouse cerebral cortex during the postnatal period. Brain Res Dev Brain Res. 1990; 53(1):1–5. PMID: 1972039.

30. Masuda M, Miura M, Inoue R, Imanishi M, Saino-Saito S, Takada M, et al. Postnatal development of tyrosine hydroxylase mRNA-expressing neurons in mouse neostriatum. Eur J Neurosci. 2011; 34 (9):1355–67. doi: 10.1111/j.1460-9568.2011.07873.x PMID: 22004548.

31. Fujii T, Sakai M, Nagatsu I. Immunohistochemical demonstration of expression of tyrosine hydroxylase in cerebellar Purkinje cells of the human and mouse. Neurosci Lett. 1994; 165(1–2):161–3. Epub 1994/ 01/03. PMID: 7912416.

32. Min N, Joh TH, Kim KS, Peng C, Son JH. 5' upstream DNA sequence of the rat tyrosine hydroxylase gene directs high-level and tissue-specific expression to catecholaminergic neurons in the central nervous system of transgenic mice. Brain Res Mol Brain Res. 1994; 27(2):281–9. Epub 1994/12/01. PMID: 7898312.

33. Baker H, Kobayashi K, Okano H, Saino-Saito S. Cortical and striatal expression of tyrosine hydroxylase mRNA in neonatal and adult mice. Cellular and molecular neurobiology. 2003; 23(4–5):507–18. PMID: 14514011.

34. Stamatakis AM, Jennings JH, Ung RL, Blair GA, Weinberg RJ, Neve RL, et al. A unique population of ventral tegmental area neurons inhibits the lateral habenula to promote reward. Neuron. 2013; 80 (4):1039–53. doi: 10.1016/j.neuron.2013.08.023 PMID: 24267654; PubMed Central PMCID: PMC3873746.

35. Lammel S, Steinberg EE, Foldy C, Wall NR, Beier K, Luo L, et al. Diversity of transgenic mouse models for selective targeting of midbrain dopamine neurons. Neuron. 2015; 85(2):429–38. doi: 10.1016/j. neuron.2014.12.036 PMID: 25611513.

36. Stuber GD, Stamatakis AM, Kantak PA. Considerations when using cre-driver rodent lines for studying ventral tegmental area circuitry. Neuron. 2015; 85(2):439–45. doi: 10.1016/j.neuron.2014.12.034 PMID: 25611514; PubMed Central PMCID: PMC4303766.

37. Diporzio U, Zuddas A, Cosenzamurphy DB, Barker JL. Early Appearance of Tyrosine-Hydroxylase Immunoreactive Cells in the Mesencephalon of Mouse Embryos. Int J Dev Neurosci. 1990; 8(5):523– 32. WOS:A1990EC81300002. PMID: 1980787

38. Kawano H, Ohyama K, Kawamura K, Nagatsu I. Migration of Dopaminergic-Neurons in the Embryonic Mesencephalon of Mice. Dev Brain Res. 1995; 86(1–2):101–13. doi: 10.1016/0165-3806(95)00018-9 WOS:A1995RC41800011.

39. Zhu P, Aller MI, Baron U, Cambridge S, Bausen M, Herb J, et al. Silencing and un-silencing of tetracycline-controlled genes in neurons. PLoS One. 2007; 2(6):e533. Epub 2007/06/21. doi: 10.1371/journal. pone.0000533 PMID: 17579707.

40. Oyer JA, Chu A, Brar S, Turker MS. Aberrant epigenetic silencing is triggered by a transient reduction in gene expression. PLoS One. 2009; 4(3):e4832. doi: 10.1371/journal.pone.0004832 PMID: 19279688; PubMed Central PMCID: PMC2654015.

41. Sawamoto K, Nakao N, Kobayashi K, Matsushita N, Takahashi H, Kakishita K, et al. Visualization, direct isolation, and transplantation of midbrain dopaminergic neurons. Proc Natl Acad Sci U S A. 2001; 98(11):6423–8. Epub 2001/05/17. doi: 10.1073/pnas.111152398 111152398 [pii]. PMID: 11353855.

42. Donaldson AE, Marshall CE, Yang M, Suon S, Iacovitti L. Purified mouse dopamine neurons thrive and function after transplantation into brain but require novel glial factors for survival in culture. Mol Cell Neurosci. 2005; 30(1):108–17. doi: 10.1016/j.mcn.2005.06.004 PMID: 16024255; PubMed Central PMCID: PMC1949425.

43. Zhao S, Maxwell S, Jimenez-Beristain A, Vives J, Kuehner E, Zhao J, et al. Generation of embryonic stem cells and transgenic mice expressing green fluorescence protein in midbrain dopaminergic neurons. Eur J Neurosci. 2004; 19(5):1133–40. Epub 2004/03/16. doi: 10.1111/j.1460-9568.2004.03206.x EJN3206 [pii]. PMID: 15016072.

44. Zhou W, Lee YM, Guy VC, Freed CR. Embryonic stem cells with GFP knocked into the dopamine transporter yield purified dopamine neurons in vitro and from knock-in mice. Stem cells. 2009; 27(12):2952– 61. doi: 10.1002/stem.216 PMID: 19750538.

45. Root DH, Mejias-Aponte CA, Qi J, Morales M. Role of glutamatergic projections from ventral tegmental area to lateral habenula in aversive conditioning. J Neurosci. 2014; 34(42):13906–10. doi: 10.1523/ JNEUROSCI.2029-14.2014 PMID: 25319687; PubMed Central PMCID: PMC4198536.

46. Root DH, Mejias-Aponte CA, Zhang S, Wang HL, Hoffman AF, Lupica CR, et al. Single rodent mesohabenular axons release glutamate and GABA. Nat Neurosci. 2014; 17(11):1543–51. doi: 10.1038/nn. 3823 PMID: 25242304.

47. Gardaneh M, O'Malley KL. Rat tyrosine hydroxylase promoter directs tetracycline-inducible foreign gene expression in dopaminergic cell types. Brain Res Mol Brain Res. 2004; 126(2):173–80. doi: 10. 1016/j.molbrainres.2004.04.008 PMID: 15249141.

48. Lin X, Parisiadou L, Sgobio C, Liu G, Yu J, Sun L, et al. Conditional expression of Parkinson's disease-related mutant alpha-synuclein in the midbrain dopaminergic neurons causes progressive neurodegeneration and degradation of transcription factor nuclear receptor related 1. J Neurosci. 2012; 32 (27):9248–64. doi: 10.1523/JNEUROSCI.1731-12.2012 PMID: 22764233; PubMed Central PMCID: PMC3417246.

49. Chinta SJ, Kumar MJ, Hsu M, Rajagopalan S, Kaur D, Rane A, et al. Inducible alterations of glutathione levels in adult dopaminergic midbrain neurons result in nigrostriatal degeneration. J Neurosci. 2007; 27 (51):13997–4006. doi: 10.1523/JNEUROSCI.3885-07.2007 PMID: 18094238.

50. Cagniard B, Beeler JA, Britt JP, McGehee DS, Marinelli M, Zhuang X. Dopamine scales performance in the absence of new learning. Neuron. 2006; 51(5):541–7. doi: 10.1016/j.neuron.2006.07.026 PMID: 16950153.

51. Xie W, Chow LT, Paterson AJ, Chin E, Kudlow JE. Conditional expression of the ErbB2 oncogene elicits reversible hyperplasia in stratified epithelia and up-regulation of TGFalpha expression in transgenic mice. Oncogene. 1999; 18(24):3593–607. doi: 10.1038/sj.onc.1202673 PMID: 10380881.

52. Kistner A, Gossen M, Zimmermann F, Jerecic J, Ullmer C, Lubbert H, et al. Doxycycline-mediated quantitative and tissue-specific control of gene expression in transgenic mice. Proc Natl Acad Sci U S A. 1996; 93(20):10933–8. PMID: 8855286; PubMed Central PMCID: PMC38261.

53. Gingrich JR, Roder J. Inducible gene expression in the nervous system of transgenic mice. Annu Rev Neurosci. 1998; 21:377–405. doi: 10.1146/annurev.neuro.21.1.377 PMID: 9530501.

54. Madisen L, Zwingman TA, Sunkin SM, Oh SW, Zariwala HA, Gu H, et al. A robust and high-throughput Cre reporting and characterization system for the whole mouse brain. Nat Neurosci. 2009; 13(1):133–40. Epub 2009/12/22. doi: nn.2467 [pii] 10.1038/nn.2467. PMID: 20023653. doi: 10.1038/nn.2467

55. Lee T, Luo L. Mosaic analysis with a repressible cell marker for studies of gene function in neuronal morphogenesis. Neuron. 1999; 22(3):451–61. PMID: 10197526.

56. Duty S, Jenner P. Animal models of Parkinson's disease: a source of novel treatments and clues to the cause of the disease. British journal of pharmacology. 2011; 164(4):1357–91. doi: 10.1111/j.1476-5381.2011.01426.x PMID: 21486284; PubMed Central PMCID: PMC3229766.

57. Golden JP, Demaro JA 3rd, Knoten A, Hoshi M, Pehek E, Johnson EM Jr., et al. Dopamine-dependent compensation maintains motor behavior in mice with developmental ablation of dopaminergic neurons. J Neurosci. 2013; 33(43):17095–107. doi: 10.1523/JNEUROSCI.0890-13.2013 PMID: 24155314; PubMed Central PMCID: PMC3807031.

58. Zhou QY, Quaife CJ, Palmiter RD. Targeted disruption of the tyrosine hydroxylase gene reveals that catecholamines are required for mouse fetal development. Nature. 1995; 374(6523):640–3. doi: 10.1038/374640a0 PMID: 7715703.

59. Zhou QY, Palmiter RD. Dopamine-deficient mice are severely hypoactive, adipsic, and aphagic. Cell. 1995; 83(7):1197–209. PMID: 8548806.

60. Lammel S, Hetzel A, Hackel O, Jones I, Liss B, Roeper J. Unique properties of mesoprefrontal neurons within a dual mesocorticolimbic dopamine system. Neuron. 2008; 57(5):760–73. Epub 2008/03/18. doi: S0896-6273(08)00107-4 [pii] doi: 10.1016/j.neuron.2008.01.022 PMID: 18341995.

61. Matsuda W, Furuta T, Nakamura KC, Hioki H, Fujiyama F, Arai R, et al. Single nigrostriatal dopaminergic neurons form widely spread and highly dense axonal arborizations in the neostriatum. J Neurosci. 2009; 29(2):444–53. Epub 2009/01/16. doi: 29/2/444 [pii] doi: 10.1523/JNEUROSCI.4029-08.2009 PMID: 19144844.

62. Evans MS, Chaurette JP, Adams ST Jr., Reddy GR, Paley MA, Aronin N, et al. A synthetic luciferin improves bioluminescence imaging in live mice. Nat Methods. 2014; 11(4):393–5. doi: 10.1038/nmeth.2839 PMID: 24509630; PubMed Central PMCID: PMC4026177.

63. Loening AM, Wu AM, Gambhir SS. Red-shifted Renilla reniformis luciferase variants for imaging in living subjects. Nat Methods. 2007; 4(8):641–3. doi: 10.1038/nmeth1070 PMID: 17618292.

64. Tanaka KF, Matsui K, Sasaki T, Sano H, Sugio S, Fan K, et al. Expanding the repertoire of optogenetically targeted cells with an enhanced gene expression system. Cell reports. 2012; 2(2):397–406. doi: 10.1016/j.celrep.2012.06.011 PMID: 22854021.

65. Smedemark-Margulies N, Trapani JG. Tools, methods, and applications for optophysiology in neuroscience. Frontiers in molecular neuroscience. 2013; 6:18. doi: 10.3389/fnmol.2013.00018 PMID: 23882179; PubMed Central PMCID: PMC3713398.

Supplementary Figure 1.

A

B

C

Supplementary Figure 2.

A

	TH-tTA founder 2	TH-tTA founder 3	TH-tTA founder 4
no DOX			
transient DOX			
constant DOX			

B

no DOX

transient DOX

C

no DOX
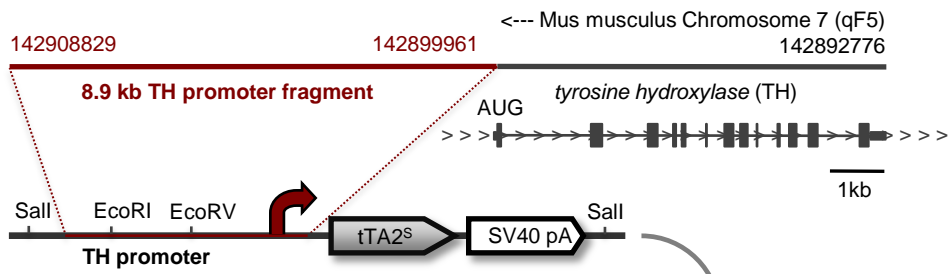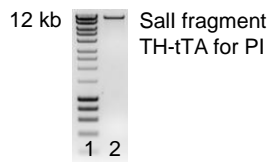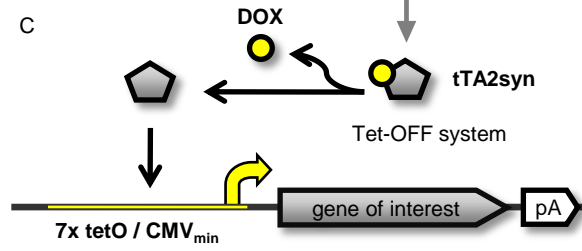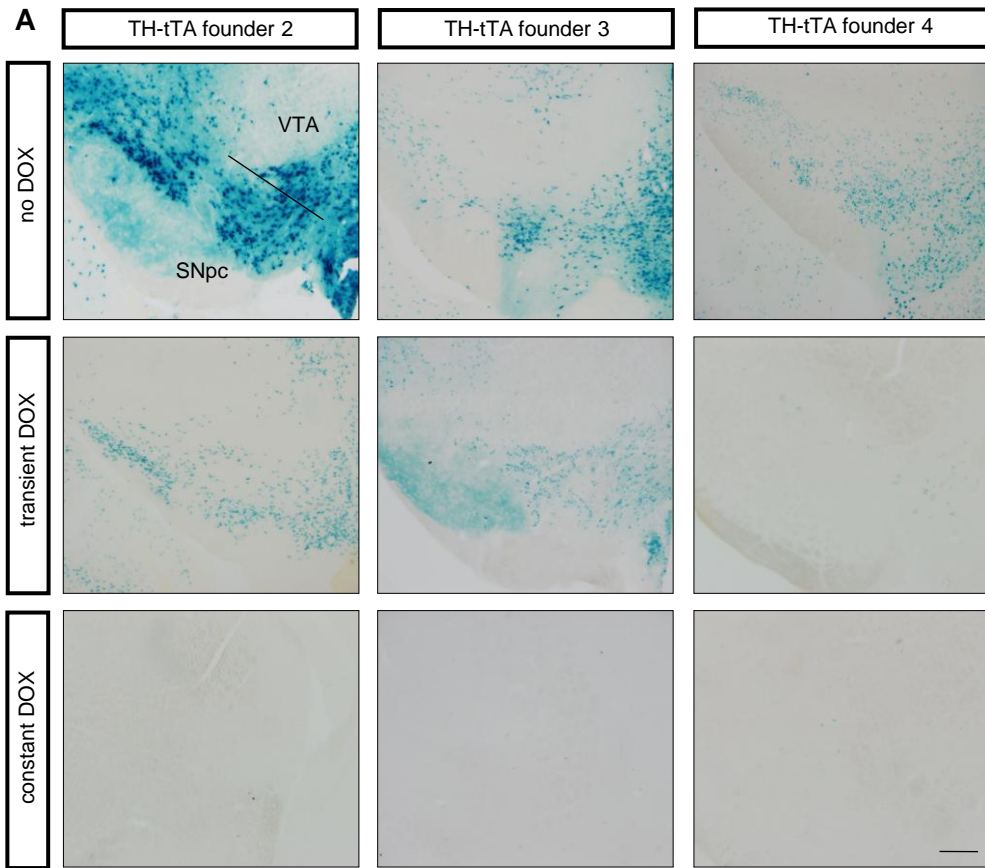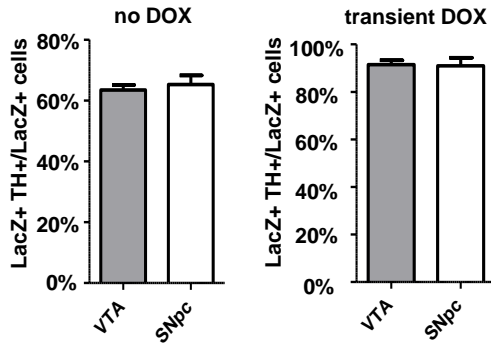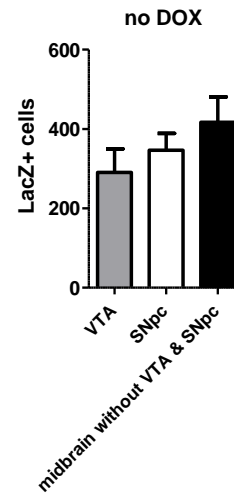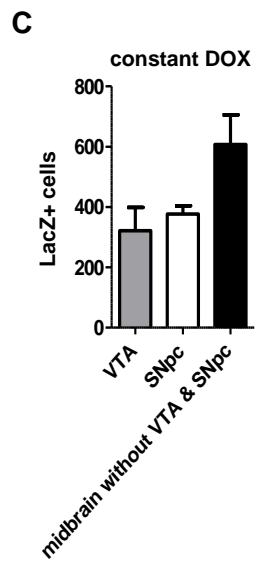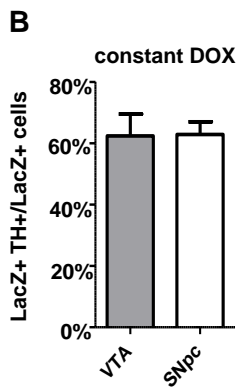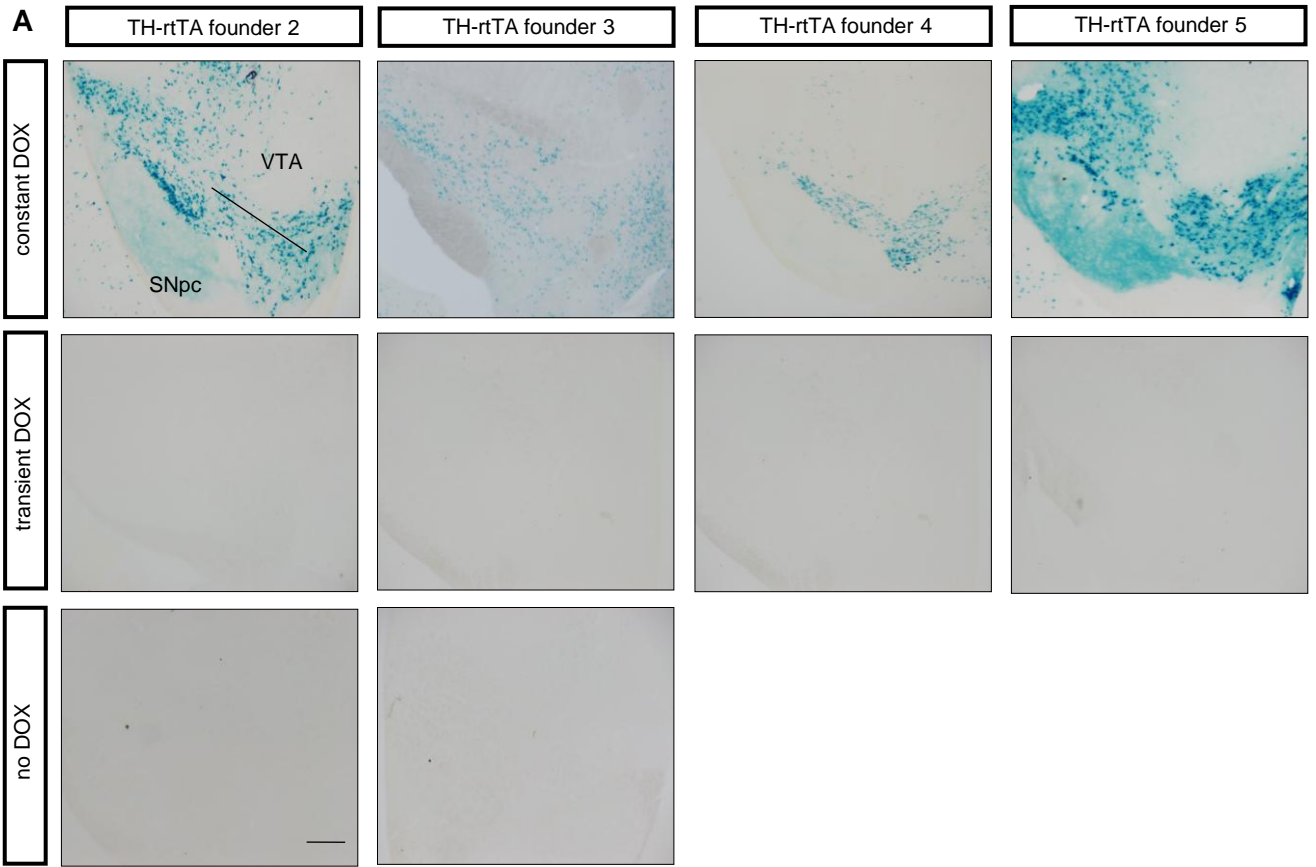
Supplementary Figure 4.
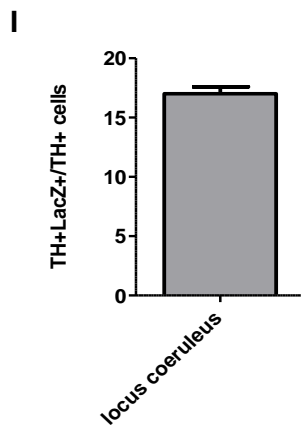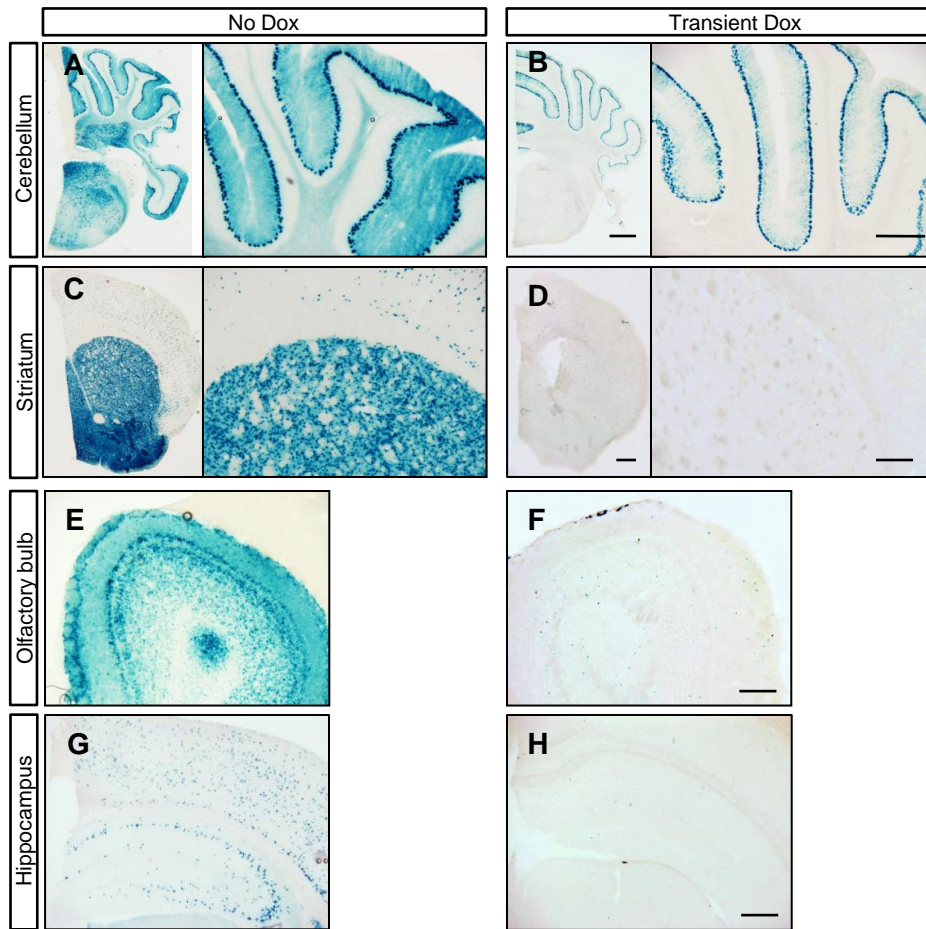
Supplementary Figure 5.

Supplementary Figure 6.

pUHD61-1-tTA	pAAV-tetO-Venus	pUHD61-1-tTA + pAAV-tetO-Venus

Supplementary Figure 7.

	Venus	TH	Venus + TH
A TH-tTA on DOX			
B TH-rtTA no DOX			
C controls no DOX			